Analyse mathématique de modèles de dynamique des populations : équations aux dérivées partielles paraboliques et équations intégro-différentielles

Jimmy Garnier

Aix*Marseille université

École doctorale en Mathématiques et Informatiques de Marseille ED 184

Analyse mathématique de modèles de dynamique des populations : équations aux dérivées partielles paraboliques et équations intégro-différentielles

THÈSE

présentée et soutenue publiquement le 18 Septembre 2012

pour l'obtention du

Doctorat de l'université d'Aix-Marseille

(spécialité Mathématiques Appliquées)

par

Jimmy GARNIER

Composition du jury

Rapporteurs :	M. Odo DIEKMANN	
	M. Benoît PERTHAME	
Examinateurs :	M. Henri BERESTYCKI	
	M. François HAMEL	Directeur
	M. Alain RAPAPORT	
	M. Jean Michel ROQUEJOFFRE	
	M. Lionel ROQUES	Directeur

Unité de Biostatistique et Processus Spatiaux (BioSP) – UR 546

Biostatistique BIOSP & Processus Spatiaux

INRA

Mis en page avec la classe thloria.

à Sandra, Naïs et Élouane.

Table des matières

Table des figures

Première partie

Introduction générale

1 Contexte scientifique

Cette thèse porte sur l'analyse mathématique de problèmes d'évolution nonlinéaires et plus précisément sur l'étude de modèles de réaction-dispersion. La forme générale de ces équations de réaction-dispersion est la suivante :

$$\frac{\partial u}{\partial t}(t,x) = \mathcal{D}(u)(t,x) + f(x,u(t,x)),\ t>0,\ x\in\mathbb{R}. \tag{1}$$

Ces équations interviennent dans des domaines très variés comme la combustion [27, 189, 194], la chimie [32], la biologie ou l'écologie [103, 70, 135]. Elles modélisent généralement l'évolution d'entités qui interagissent entre elles et se déplacent. En particulier, dans le domaine de la dynamique des populations ou la génétique des populations, la quantité $u(t,x)$ représente la densité de population à l'instant t et à la position x. Le terme de réaction $f(x,u)$ correspond au taux de croissance de la population. Il permet de modéliser les interactions entre les individus et les caractéristiques de l'habitat ou du milieu. Ce terme de réaction dépend d'une part de la densité u et d'autre part du milieu dans lequel évolue la population au travers de la variable d'espace x. Le mouvement des individus est décrit grâce à l'opérateur de dispersion $\mathcal{D}$. Suivant le mode de déplacement des individus, cet opérateur sera local ou non-local.

L'objectif de la thèse est de comprendre l'influence du terme de réaction f, de l'opérateur de dispersion $\mathcal{D}$, et de la donnée initiale u_0 sur la propagation des solutions u de l'équation de réaction-dispersion (1).

Nous nous intéresserons principalement à deux types d'équations de réaction-dispersion : les équations de *réaction-diffusion* et les *équations intégro-différentielles*. Les équations de réaction-diffusion sont des équations aux dérivées partielles paraboliques nonlinéaires. L'opérateur de dispersion $\mathcal{D}$ est un opérateur différentiel elliptique du second ordre. Les premières équations de réaction-diffusion du type

$$\frac{\partial u}{\partial t}(t,x) = \frac{\partial^2 u}{\partial x^2}(t,x) + f(u(t,x)),\ t>0,\ x\in\mathbb{R}, \tag{2}$$

ont été introduites à la fin des années 30 dans les articles de Fisher [72] et Kolmogorov, Petrovsky, et Piskunov [112], pour des modèles de génétique des populations.

Dans ces premiers modèles, la nonlinéarité f est indépendante de la variable d'espace x. Le milieu est dit *homogène*. Dans ce cas homogène, nous considérons des nonlinéarités f régulières, $f\in C^1([0,1])$, et s'annulant en 0 et 1

$$f(0) = f(1) = 0.$$

Les fonctions $p_- \equiv 0$ et $p^+ \equiv 1$ sont alors des *états stationnaires* de l'équation (2). En outre, les nonlinéarités étudiées vérifient l'une des trois propriétés suivantes :

(A) Monostable : f est de type *monostable* si

$$f'(0)>0, \quad f'(1)<0 \quad \text{et} \quad f>0 \text{ sur }]0,1[.$$

Dans ce cas, le terme de croissance $f(u)$ est toujours strictement positif sur $]0,1[$. L'exemple le plus classique de terme monostable est $f(u) = u(1-u)(1+au)$, avec $a\geq 0$. Si $a\leq 1$, le taux de croissance par individu $f(u)/u$ (défini par $f'(0)$ en $u=0$) est décroissant sur l'intervalle $[0,1]$ ce qui correspond à un terme de réaction du type KPP, pour Kolmogorov, Petrovsky, et Piskunov [112] (voir figure 1(a)).

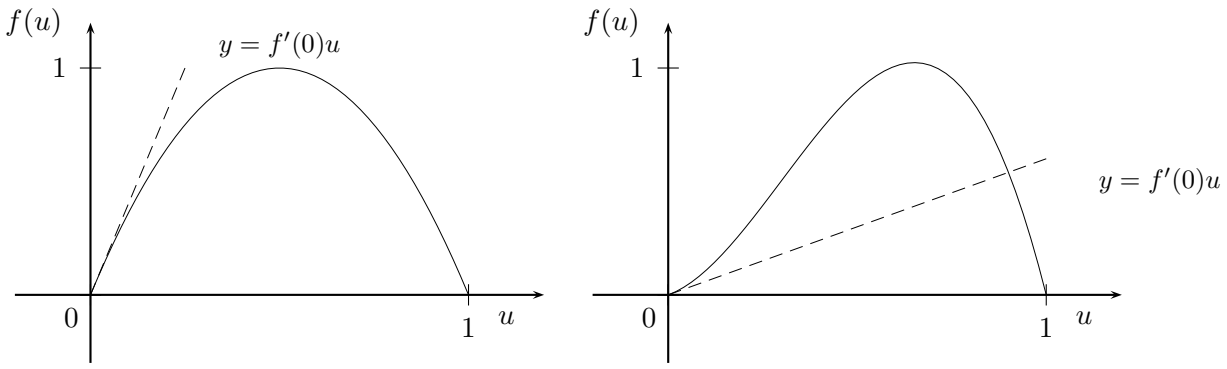

(a) Nonlinéarité KPP (b) Nonlinéarité monostable à effet Allee faible

FIGURE 1 – Nonlinéarités de type monostable (A)

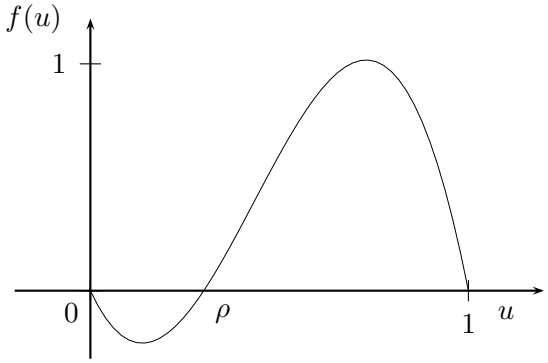

FIGURE 2 – Nonlinéarité de type bistable (B)

Par contre, si $a > 1$, le maximum du taux de croissance par individu n'est plus atteint en $u = 0$. En écologie, ceci correspond à un effet Allee faible [175](voir figure 1(b)).

(B) Bistable : f est de type *bistable* si

$$\int_0^1 f(s)\,ds > 0, \quad f'(0) < 0, \quad f'(1) < 0$$

$$\text{et il existe } \rho \in]0,1[\text{ tel que } f < 0 \text{ sur }]0,\rho[\text{ et } f > 0 \text{ sur }]\rho,1[.$$

Le taux de croissance $f(u)$ est donc négatif à faible densité, ce qui correspond à un effet Allee fort [118, 175]. Le paramètre ρ est appelé «seuil de l'effet Allee» en dessous duquel le taux de croissance devient négatif. Les fonctions cubiques $f(u) = u(1-u)(u-\rho)$, avec ρ dans $]0, 1/2[$, sont des nonlinéarités de type bistable. La condition de signe sur l'intégrale de f traduit le fait que l'état 1 est plus stable que l'état 0.

(C) Ignition : f est de type *ignition* si

$$f'(1) < 0 \text{ et il existe } \rho \in]0,1[\text{ tel que } f = 0 \text{ sur }]0,\rho[\text{ et } f > 0 \text{ sur }]\rho,1[.$$

Cette nonlinéarité intervient souvent en combustion. Dans ce cas u est la température de la flamme et ρ est la température d'ignition [27, 29, 152].

Ces trois types de nonlinéarités interviennent dans des contextes variés et ont une influence forte sur le comportement des solutions de (2). En effet, si la nonlinéarité f est monostable (A), toute solution

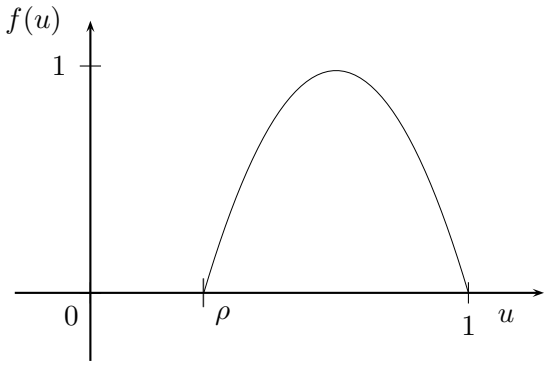

FIGURE 3 – Nonlinéarité de type ignition (C)

bornée du problème de Cauchy associé à l'équation (2), avec une donnée initiale $0 \leq u_0 \leq 1$ telle que $u_0 \neq 0$, convergera localement uniformément vers l'état stationnaire 1 [10, Théorème 3.1]. On dira dans ce cas que la solution survit et se propage dans le milieu. Par contre, lorsque la nonlinéarité f est de type bistable (B) ou ignition (C), nous verrons dans le chapitre 3 que les solutions initialement trop confinées ou trop petites tendent vers l'extinction, c'est-à-dire qu'elles convergent uniformément vers l'état 0, alors que celles initialement assez étendues ou assez grosses «survivront», c'est-à-dire qu'elles convergent localement uniformément vers une quantité strictement positive [9, 58, 195, GHR12].

Revenons sur la nature des équations de réaction-diffusion. Reprenant le cadre de la dynamique des populations, ces équations sont en fait une approximation «locale» dans laquelle on suppose que les individus à l'instant t et à la position x ne se diffusent que vers leurs voisins immédiats.

Cette approche réaction-diffusion devient peu précise lorsque l'on étudie des espèces dont les individus peuvent se déplacer à longue distance. Ces événements de dispersion à longue distance jouent un rôle essentiel dans de nombreux phénomènes comme la pollinisation de certains végétaux ou la propagation d'épidémies. Ils sont souvent dus à des vecteurs extérieurs (humains, animaux, ...) qui favorisent le transport d'individus ou de virus très loin de leur lieu d'origine. Une manière de prendre en compte ces phénomènes de dispersion à longue distance est d'utiliser des équations intégro-différentielles [44, 132] de la forme

$$\frac{\partial u}{\partial t}(t,x) = \int_{\mathbb{R}} J(|x-y|)u(t,y)dy - u(t,x) + f(u(t,x)),\ t>0 \text{ et } x \in \mathbb{R}. \tag{3}$$

où le terme de diffusion $\partial_x^2 u$ est remplacé par un opérateur intégral de la forme $J \star u - u$, avec J une densité de probabilité. Le terme J est appelé *noyau de dispersion* et l'expression $J(|x-y|)$ représente la probabilité qu'un individu provenant du point y arrive en x.

Ces deux types d'équations ont des natures totalement différentes, l'une (2) est locale alors que l'autre (3) est non-locale. Cependant, suivant le type de noyau de dispersion J et le terme de réaction f, le comportement qualitatif des solutions peut rester semblable.

On distingue dans la suite deux types de noyaux de dispersion J : les noyaux *exponentiellement bornés* et les noyaux *non-exponentiellement bornés*. Lorsque le noyau de dispersion J décroît plus rapidement qu'une exponentielle, il est dit exponentiellement borné ou à «queue légère». Les trois exemples classiques de tels noyaux sont les noyaux à support compact $J(x) \propto \mathbb{1}_{[-a,a]}(x)$ avec $a > 0$, les noyaux gaussiens $J(x) \propto e^{-x^2/2\sigma^2}$ et les noyaux exponentiels $J(x) \propto e^{-\lambda|x|}$ avec $\lambda > 0$ (voir figure 4(a)). Ces noyaux exponentiellement bornés sont utilisés pour modéliser des phénomènes de dispersion à courte distance, donc proche de phénomènes de diffusion. Les travaux récents de Carr et

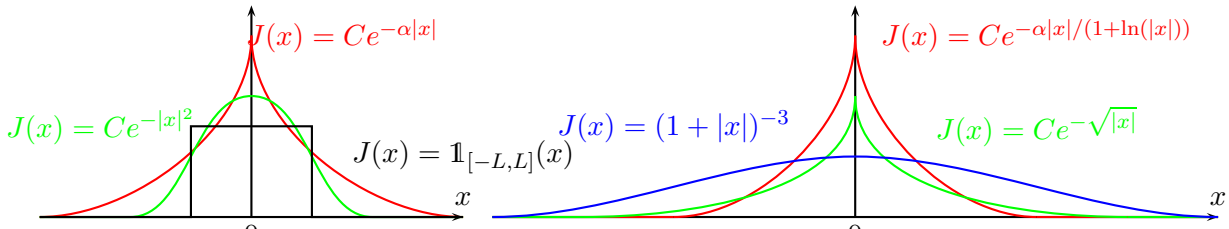

(a) Noyaux exponentiellement bornés (b) Noyaux non exponentiellement bornés

FIGURE 4 – Exemples de noyaux de dispersion J : (a) exponentiellement bornés ; (b) non-exponentiellement bornés

Chmaj [38] et Coville et Dupaigne [47] ont montré que le modèle intégro-différentiel (3) avec un noyau exponentiellement borné se comporte de la même manière que le modèle de réaction-diffusion (2). Plus précisément, ces deux modèles avec des termes de réaction de type monostable (A), bistable (B) ou ignition (C) possèdent des solutions de type *fronts*, en translation uniforme reliant l'état d'équilibre $u \equiv p^+ \equiv 1$ (en $-\infty$) à l'état d'équilibre $u \equiv p_- \equiv 0$ (en $+\infty$) [10, 29, 71, 112, réaction-diffusion] [38, 47, intégro-différentiel]. Elles permettent de décrire l'invasion à vitesse et profil constant d'un espace vierge par une population. Ces solutions sont de la forme $u(t,x) = U(x-ct)$, où c est la *vitesse du front* et U est le *profil du front* connectant les deux états stationnaires p^+ et p_- de l'équation. Le profil U du front vérifie alors l'équation elliptique nonlinéaire suivante :

$$\begin{cases} \mathcal{D}(U)(y) + c\,U'(y) + f(U(y)) = 0, \quad y \in \mathbb{R}, \\ U(-\infty) = 1, \quad U(+\infty) = 0 \quad \text{et} \quad 0 < U < 1 \text{ sur } \mathbb{R}, \end{cases}$$

où l'opérateur de dispersion $\mathcal{D}$ correspond dans le cas d'équations de réaction-diffusion au Laplacien $\partial_x^2 u$ et à l'opérateur intégral $J \star u - u$ dans le cas d'équations intégro-différentielles. Dans tous les cas, le profil U associé à une vitesse c est une fonction décroissante et unique à translation près (cf. figure 5). L'existence de fronts met en évidence un parallèle fort entre les deux types d'équations, réaction-diffusion et équations intégro-différentielles avec noyaux exponentiellement bornés et montre qu'une diffusion locale ou une dispersion à courte distance ont le même effet sur la propagation des solutions.

Cependant, on peut se demander si les fronts progressifs qui apparaissent dans les équations de réaction-diffusion et dans les équations intégro-différentielles sont de même nature. Stokes [172] a été l'un des premiers à distinguer différents types de fronts. Dans le cadre des équations de réaction-diffusion homogènes avec des termes de réaction monostables (A), il a classé les fronts de vitesse minimale en deux catégories : les *fronts tirés* et les *front poussés*. Cette dichotomie porte sur des critères liés à la vitesse des fronts. Un front de vitesse minimale (c^*, U) est tiré si sa vitesse est la même que celle du problème linéarisé autour de l'état stationnaire 0, *i.e.* $c^* = 2\sqrt{f'(0)}$. En terme biologique, un tel front de colonisation est tiré par la population la plus en avant. À l'inverse, un front de vitesse minimale est dit poussé si $c^* > 2\sqrt{f'(0)}$. Dans ce cas, la vitesse de propagation est déterminée par toute la population et pas seulement par la population la plus en avant. Le front est donc poussé par l'intérieur de la population. L'interprétation en dynamique des populations de cette classification montre une différence dans la dynamique interne des fronts. Un des premiers axes d'étude de la thèse a été de comprendre la nature des fronts des équations de réaction-diffusion par l'analyse de leur dynamique interne. Cette nouvelle approche des fronts tirés/poussés, plus intuitive, a aussi des conséquences importantes en génétique des populations, comme nous le verrons dans la suite.

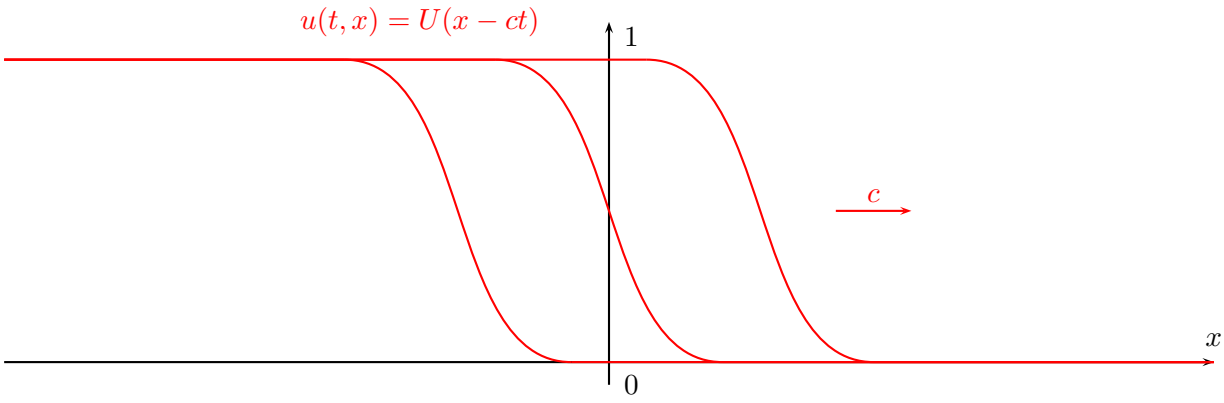

FIGURE 5 – Solution de (1) de type front progressif $u(t,x) = U(x-ct)$ à des temps successifs : le front se déplace de gauche à droite à vitesse c et conserve un profil constant U connectant les états stationnaires 0 et 1.

Si les équations intégro-différentielles avec des noyaux exponentiellement bornés peuvent se rapprocher des équations de réaction-diffusion, une divergence de comportement apparaît lorsque l'on s'intéresse à des noyaux non-exponentiellement bornés, c'est-à-dire des noyaux qui décroissent plus lentement que n'importe quelle exponentielle. Les principaux exemples de tels noyaux dits aussi à «queue lourde» sont les noyaux exponentielle-puissance $J(x) \propto e^{-|x|^\alpha}$ avec $\alpha \in]0,1[$ et les noyaux à décroissance algébrique $J(x) \propto (1+x^n)^{-1}$, avec $n \geq 2$ (voir figure 4(b)). Dans ce cas, on observe une différence qualitative puisque ces équations intégro-différentielles avec noyaux non-exponentiellement bornés ne possèdent pas de fronts progressifs [191]. Cette négation reste cependant peu précise et ne donne aucun renseignement sur la vitesse à laquelle les solutions se propagent ni même sur leurs comportements asymptotiques.

Ainsi, un des axes d'étude de cette thèse a été de comprendre l'influence des noyaux de dispersion non-exponentiellement bornés sur la *vitesse de propagation* et le profil asymptotique des solutions. La vitesse de propagation d'une solution u de l'équation de réaction-dispersion (1), si elle existe, correspond à la plus grande vitesse c^* telle que dans tout repère mobile de vitesse $c < c^*$ la solution converge vers 1 en temps grand,

$$u(t, x+ct) \to 1 \quad \text{localement uniformément lorsque } t \to +\infty, \quad \text{pour tout } c < c^*.$$

Elle correspond aussi à la plus petite vitesse c^* telle que dans tout repère mobile de vitesse $c > c^*$, la solution converge vers 0 en temps grand,

$$u(t, x+ct) \to 0 \quad \text{localement uniformément lorsque } t \to +\infty, \quad \text{pour tout } c > c^*,$$

lorsque la donnée initiale a un support compact.

Dans le cadre des équations de réaction-diffusion homogènes ou des équations intégro-différentielles avec des noyaux exponentiellement bornés, les solutions partant d'une donnée initiale à support compact ont toujours une vitesse de propagation finie et majorée par la plus petite vitesse des fronts progressifs (cf. figure 6). Nous verrons que cette propriété de propagation des solutions à vitesse finie n'est pas conservée par toutes les équations de réaction-dispersion, notamment lorsque le noyau de dispersion est non-exponentiellement borné. Cette propriété peut également être aussi sensible à la donnée initiale. Par exemple, Hamel et Roques [88] ont mis en évidence des phénomènes d'accélérations

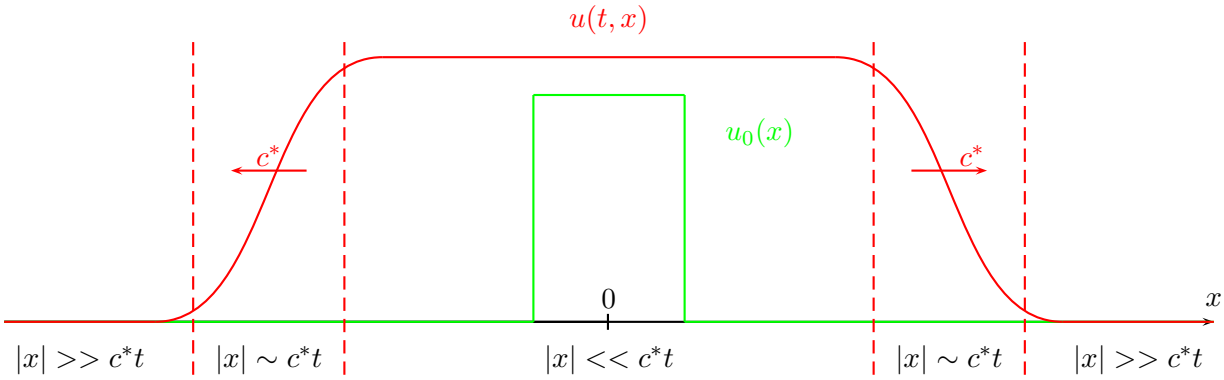

FIGURE 6 – Propagation à vitesse c^* dans les deux directions d'une solution u de (1), partant à $t = 0$ d'une donnée initiale u_0 à support compact.

des solutions d'équations de réaction-diffusion partant de données initiales qui décroissent lentement à l'infini.

D'autres facteurs comme la structuration spatiale de l'environnement peuvent aussi modifier considérablement cette vitesse. En écologie, les ressources sont rarement distribuées de manière uniforme et homogène dans l'espace ce qui crée des zones plus ou moins favorables à la survie de l'espèce considérée. Ces fluctuations du milieu peuvent accélérer ou au contraire ralentir sa propagation. Une manière de prendre en compte les hétérogénéités de l'habitat est de faire dépendre le taux de croissance f non seulement de la densité u mais aussi de la variable d'espace x, $f := f(x, u)$.

En général, l'analyse mathématique de l'effet des hétérogénéités spatiales sur la vitesse d'expansion d'une solution de (1) reste un problème difficile. Dans le cas des équations de réaction-diffusion, quelques cas particuliers ont déjà été traités [cf. 18, 190, pour une revue complète]. Citons par exemple les milieux périodiques [19, 23, 25, 74, 168, 186], pour lesquels la nonlinéarité $f(x, u)$ est périodique en la variable d'espace x. Pour ces environnements et pour des nonlinéarités f de type type KPP, la vitesse de propagation se caractérise grâce aux valeurs propres principales de familles d'opérateurs elliptiques de la forme

$$\mathcal{L}_p : \varphi \mapsto \frac{\partial^2 \varphi}{\partial x^2} - 2p\frac{\partial \varphi}{\partial x} + \Big(p^2 + \frac{\partial f}{\partial u}(x, 0)\Big)\varphi.$$

La généralisation de ces notions de valeurs propres à des opérateurs elliptiques plus complexes et sur des domaines non-bornés, ont permis d'appréhender des problèmes plus réalistes et plus complexes. Ces outils ont notamment permis d'obtenir des estimations sur la vitesse d'expansion dans des milieux hétérogènes généraux [22, 28]. Cependant, ils ne suffisent pas en général à caractériser cette vitesse, notamment lorsque la vitesse d'expansion n'est pas unique mais oscille dans un intervalle de valeurs, comme nous le verrons dans le Chapitre 4.

2 *Résultats*

L'objectif de cette thèse est d'analyser et de comparer les modèles mathématiques de la forme (1) pour différents types de dispersion $\mathcal{D}$, de termes de réaction f et de données initiales, afin de comprendre l'influence de ces composantes sur la propagation des solutions des modèles associés. Dans une première partie, nous nous intéressons aux équations de réaction-diffusion dans des milieux homogènes. L'étude de ces modèles très simples nous a permis de mieux comprendre les mécanismes qui créent la propagation, grâce à une nouvelle caractérisation plus intuitive des fronts progressifs. Ces résultats ont des conséquences importantes en génétique des populations. Ils permettent également de mieux comprendre l'influence de l'effet Allee, correspondant à une diminution de la fertilité à faible densité,

lors d'une colonisation. La seconde partie est dédiée à l'étude des équations de réaction-diffusion en milieu hétérogène. L'objectif est de comprendre comment la fragmentation du milieu modifie la vitesse de propagation des solutions. Nous nous intéressons aussi à un problème inverse afin de mieux cerner les liens entre les sorties du modèle et les paramètres hétérogènes. La troisième et dernière partie sera consacrée à l'analyse des équations intégro-différentielles. L'objectif est de décrire l'influence du mode de dispersion sur la propagation des solutions.

2.1 Équations de réaction-diffusion homogènes : caractérisation des fronts et effet Allee

Dans cette section nous proposons dans un premier temps une nouvelle approche concernant les notions de fronts progressifs tirés et poussés associés à l'équation de réaction-diffusion (2). Ensuite nous présentons les conséquences de ce travail en génétique des populations. Enfin, nous analysons l'effet de la fragmentation de la donnée initiale sur l'évolution de la solution du problème de Cauchy associé à (2).

1.1 Dynamique interne des fronts : une nouvelle approche des fronts tirés et poussés [GGHR12]

Les équations de réaction-diffusion homogènes sont très utilisées dans la modélisation d'espèces en expansion, en grande partie parce qu'elles possèdent des solutions de type front de la forme $u(t,x) = U(x-ct)$, où c est la vitesse du front et U son profil vérifiant l'équation elliptique suivante :

$$\begin{cases} U''(y) + cU'(y) + f(U(y)) = 0, \quad y \in \mathbb{R}, \\ U(-\infty) = 1, \quad U(+\infty) = 0 \ \text{ and } \ 0 < U < 1 \text{ on } \mathbb{R}. \end{cases} \tag{4}$$

Plus précisément, si f est une nonlinéarité monostable de type (A), il existe une vitesse minimale $c^* \geq 2\sqrt{f'(0)} > 0$ telle que l'équation (4) admet des solutions U si et seulement si $c \geq c^*$. La solution de vitesse minimale est appelée *front critique* et celles de vitesse $c > c^*$ *fronts sur-critiques*. Si f est une nonlinéarité bistable (B) ou de type ignition (C), il existe une unique vitesse $c > 0$ telle que l'équation (4) admette une solution.

Depuis les articles de Fisher [72] et Kolmogorov *et al.* [112], la majorité des travaux d'analyse des fronts portent sur leur existence, leur unicité, leur vitesse d'expansion, leur profil ou leur stabilité. En particulier, l'étude de stabilité, menée par Stokes [172] dans le cadre de nonlinéarités monostables (A), a permis de classer les fronts monostables en deux types : les fronts tirés et les fronts poussés. Cette classification repose sur les propriétés de la vitesse c des fronts. Elle est résumée dans les deux définitions suivantes.

Définition 1 (Front tiré [172])**.** *Un front* tiré *est soit un front critique dont la vitesse minimale c^* vérifie $c^* = 2\sqrt{f'(0)}$, soit n'importe quel front sur-critique ($c > c^*$).*

Définition 2 (Front poussé [172])**.** *Un front* poussé *est un front critique dont la vitesse minimale c^* vérifie $c^* > 2\sqrt{f'(0)}$.*

Le terme tiré vient du fait que les fronts critiques tirés ont la même vitesse de propagation que le problème linéarisé autour de l'état stationnaire 0, donc la vitesse du front est déterminée par le taux de croissance des individus les plus à l'avant du front. Le front est donc tiré par ses individus pionniers. À l'inverse, la vitesse d'un front critique poussé est déterminée par toute la population. Le front est poussé de l'intérieur par toute la population.

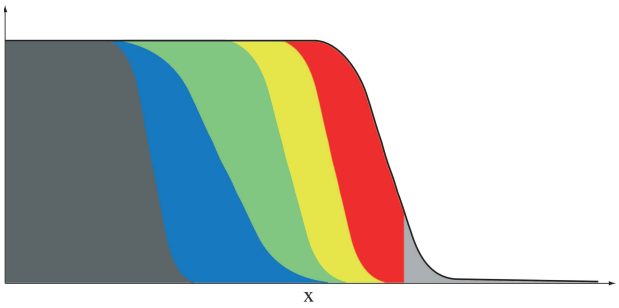

FIGURE 7 – Représentation schématique d'un front u, solution de (4), composé de six fractions. Chaque composante υ^k a une couleur différente et son épaisseur en chaque point x, correspond à sa densité.

Bien que l'interprétation de cette terminologie se base sur la dynamique interne des fronts, l'évolution de la «structure interne» des fronts restait jusqu'alors inconnue. Dans cette thèse nous avons choisi une nouvelle approche totalement différente de celle de Stokes [172] pour comprendre la nature des fronts. Cette approche plus intuitive se base sur l'analyse directe de la dynamique interne des fronts.

Nous nous sommes inspirés des travaux de Hallatschek et Nelson [82, 83] et Vlad *et al.* [181]. L'idée consiste à décomposer le front $u(t,x) = U(x-ct)$ en plusieurs composantes $\upsilon^k(t,x)$ et à étudier le comportement de ces composantes à l'intérieur du front. Plus précisément, on suppose que le front est initialement composé de différents groupes $(\upsilon_0^k(x))_{k\in I}$ vérifiant

$$u_0(x) := u(0,x) = \sum_{k\geq 1} \upsilon_0^k(x), \text{ avec } \upsilon_0^k \geq 0 \text{ pour tout } k \in I.$$

avec $I \subset \mathbb{N}$ (voir figure 7). Ces composantes υ^k ne différent que par leur taille et leur position initiale à l'intérieur du front u. Elles partagent les mêmes caractéristiques d'évolution que le front dans le sens où elles diffusent et croissent de la même manière que le front u. Ainsi leur coefficient de diffusion est égal à 1 et leur taux de croissance par individu $g(u)$ dépend uniquement de la population totale u :

$$g(u(t,x)) := \frac{f(u(t,x))}{u(t,x)} \text{ pour tout } t \geq 0 \text{ et } x \in \mathbb{R}.$$

Par conséquent, ces groupes υ^k vérifient l'équation suivante :

$$\begin{cases} \dfrac{\partial \upsilon^k}{\partial t}(t,x) &= \dfrac{\partial^2 \upsilon^k}{\partial x^2}(t,x) + \upsilon^k(t,x)\, g(u(t,x)),\ t>0,\ x\in\mathbb{R}, \\ \upsilon^k(0,x) &= \upsilon_0^k(x),\ x\in\mathbb{R}. \end{cases} \tag{5}$$

Puisque toutes les composantes υ^k ont les mêmes caractéristiques de croissance et de dispersion, il suffit de regarder l'évolution d'un seul groupe, que l'on notera υ, pour comprendre le comportement de tous les autres. Ce phénomène contraste fortement avec les systèmes compétitifs plus classiques comme le modèle de compétition entre une population résidente et une population invasive, mentionné par Kawasaki et Shigesada [103, Section 7.2]. Dans ce modèle, une des populations prend toujours le dessus sur l'autre, en un certain sens. Ainsi la propagation est dirigée par un seul groupe.

De plus, même si l'équation (2) est homogène en espace et si le système (5) est linéaire, le système (5) est hétérogène en espace et en temps puisque le taux de croissance par individu $g(u(t,x))$ dépend de t et x. En outre, cette hétérogénéité ne remplit aucun critère de périodicité ni de monotonie, ce qui rend le problème totalement hétérogène et donc plus difficile à traiter.

Structure interne des fronts

Suivant la nonlinéarité f et la donnée initiale v_0, la composante v se comporte de deux manières différentes. On s'intéresse tout d'abord à des nonlinéarités f de type monostable (A) et à des fronts tirés (c, U).

Théorème 1 (Cas des fronts tirés)**.** *Un groupe v, initialement localisé à l'intérieur d'un front monostable tiré, au sens où :*

$$\int_0^{+\infty} e^{cx}\, v_0^2(x)\, dx < +\infty, \tag{6}$$

vérifie

$$\limsup_{t\to+\infty} \Big(\max_{x\geq\alpha\sqrt{t}} v(t,x) \Big) \to 0 \quad \textit{lorsque} \quad \alpha \to +\infty. \tag{7}$$

En d'autres termes, les composantes des fronts monostables tirés qui décroissent plus vite que le profil du front U au sens de (6), ne peuvent pas suivre l'avancée du front. En particulier, si on se place dans une fenêtre mobile avançant à la vitesse c du front, la formule (7) implique

$$v(t, x + ct) \to 0 \quad \text{uniformément sur tout compact lorsque} \quad t \to +\infty.$$

Ainsi, seuls les composantes les plus en avant du front contribuent à faire avancer le front. Cette caractérisation est en accord avec la Définition 1 de Stokes [172] et montre que les fronts critiques tirés et les fronts sur-critiques partagent la même dynamique interne.

De manière plus générale, le résultat (7) implique que les composantes ne peuvent se propager vers la droite avec une vitesse strictement positive.

De plus si les composantes sont très confinées, on obtient le résultat suivant :

Proposition 1. *Les composantes v des fronts monostables tirés, initialement confinées au sens où v_0 satisfait* (6) *et :*

$$v_0(x) \to 0 \textit{ lorsque } x \to -\infty, \textit{ ou } v_0 \in L^p(\mathbb{R}) \textit{ pour un certain } p \in [1, +\infty),$$

vérifient

$$v(t, \cdot) \to 0 \quad \textit{uniformément sur } \mathbb{R} \quad \textit{lorsque } t \to +\infty.$$

Ainsi, les composantes très localisées, comme celles de couleur sur la figure 7, tendent à l'extinction en se diffusant autour de leur lieu d'apparition comme on le voit sur la figure 8.

Dans le cas des fronts monostables poussés, bistables ou de type ignition le comportement des composantes est totalement différent.

Théorème 2 (Cas des fronts poussés)**.** *Tout groupe v, dans un front (c, U) monostable poussé, bistable (B) ou de type ignition (C), vérifie*

$$\limsup_{t\to+\infty} \Big(\max_{x\geq\alpha\sqrt{t}} |v(t,x) - p(v_0)U(x-ct)| \Big) \to 0 \quad \textit{lorsque} \quad \alpha \to +\infty,$$

où $p(v_0)$ est la proportion finale du groupe v dans le front U. Elle est donnée par la formule suivante :

$$p(v_0) = \frac{\displaystyle\int_{\mathbb{R}} v_0(x)\, U(x)\, e^{cx}\, dx}{\displaystyle\int_{\mathbb{R}} U^2(x)\, e^{cx}\, dx} \in]0, 1]. \tag{8}$$

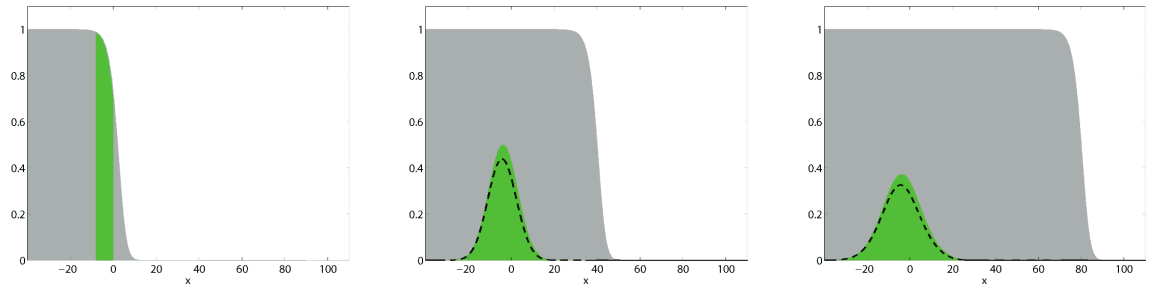

(a) à $t = 0$ (b) à $t = 20$ (c) à $t = 40$

FIGURE 8 – Cas tiré : évolution de la densité d'une fraction $v(t, x)$ (région verte) à l'intérieur de la population totale $u(t, x)$ (région grise) à des temps successifs $t = 0$, $t = 20$ et $t = 40$. La courbe en pointillé représente la solution de l'équation de la chaleur partant de la fraction initiale v_0.

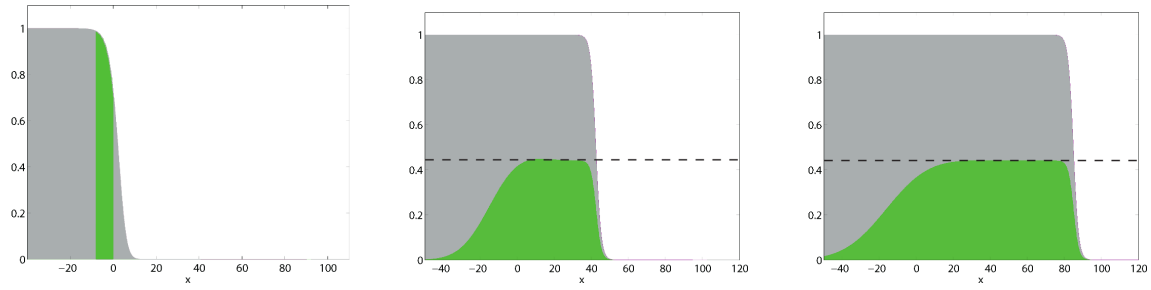

(a) à $t = 0$ (b) à $t = 20$ (c) à $t = 40$

FIGURE 9 – Cas poussé : évolution de la densité d'une fraction $v(t, x)$ (région verte) à l'intérieur de la population totale $u(t, x)$ (région grise) à des temps successifs $t = 0$, $t = 100$ et $t = 200$. La courbe en pointillé représente la proportion finale $p(v_0)$ de la fraction v.

Ces résultats contrastent fortement avec ceux du Théorème 1. En effet, toutes les composantes d'un front monostable poussé, bistable ou de type ignition, suivent l'avancée du front (voir figure 9), dans le sens où

$$v(t, x + ct) \to p(v_0)\, U(x) > 0 \quad \text{uniformément sur tout compact lorsque} \quad t \to +\infty. \tag{9}$$

Ainsi en temps grand, toute composante v, présente initialement dans le front, est représentée dans la proportion $p(v_0)$ à l'avant du front. En d'autres termes le front est poussé de l'intérieur par toutes ses composantes.

Une définition plus générale des fronts poussés et des fronts tirés

Ces résultats permettent de distinguer deux classes de fronts à partir de la dynamique de leurs composantes. Cette classification coïncide avec la terminologie poussé/tiré introduite par Stokes [172] pour des nonlinéarités monostable de type (A). Nos résultats indiquent aussi que les fronts bistables ou de type ignition partagent la même dynamique interne que les fronts monostables poussés. Cette remarque nous a permis de proposer une nouvelle définition de la notion de front poussé et front tiré dans un cadre plus général que celui des équations de réaction-diffusion homogènes. On s'intéresse ici aux solutions de type fronts des équations de réaction-diffusion homogènes ou hétérogènes et des équations intégro-différentielles homogènes. En d'autres termes, on traite des solutions de type fronts de l'équation générale (1), où l'opérateur de dispersion est soit le Laplacien, $\mathcal{D}(u) = \partial_x^2(u)$, soit

l'opérateur intégral $\mathcal{D} = J \star u - u$, et la nonlinéarité f peut dépendre de la variable x. Dans ce cadre général, si u est un front de vitesse $c > 0$, ses composantes v^k vérifient l'équation suivante :

$$\begin{cases} \dfrac{\partial v^k}{\partial t}(t,x) &= \mathcal{D}(v^k)(t,x) + v^k(t,x)\, g(x,u(t,x)),\ t>0,\ x\in\mathbb{R}, \\ v^k(0,x) &= v_0^k(x),\ x\in\mathbb{R}. \end{cases} \tag{10}$$

où $g(x,u) := f(x,u)/u$. Ainsi, on définit les deux notions suivantes :

Définition 3 (Front tiré)**.** *Un front u de vitesse $c \in \mathbb{R}$ est dit* tiré *si pour tout groupe v vérifiant* (10) *et*

$$v_0 \text{ à support compact},\ 0 \le v_0 \le u(0,\cdot) \text{ et } v_0 \not\equiv 0, \tag{11}$$

on a

$$v(t, x+ct) \to 0 \quad \text{uniformément sur tout compact lorsque} \quad t \to +\infty.$$

Définition 4 (Front poussé)**.** *Un front u de vitesse $c \in \mathbb{R}$ est dit* poussé *si pour tout groupe v vérifiant* (10)-(11) *il existe un compact $\mathcal{K}$ tel que*

$$\limsup_{t\to+\infty} \Big(\sup_{x\in\mathcal{K}} v(t, x+ct) \Big) > 0.$$

Dans le Chapitre 1, nous proposons des définitions qui qui peuvent être appliquées aux fronts de transition très généraux introduis par Berestycki et Hamel [21]. En outre, ces nouvelles notions de fronts tirés et poussés basées sur la dynamique interne des fronts plutôt que sur leur vitesse de propagation ont l'avantage de s'adapter à des modèles plus complexes qui ne possèdent pas forcément de solutions de type front. Par exemple, nous pouvons désormais envisager d'étudier la nature poussée ou tirée des solutions :

(i) d'équations intégro-différentielles comportant des événements de dispersion à longue distance dont les solutions sont accélérées [Ga11, 113] ;

(ii) d'équations de réaction-diffusion hétérogènes en espace possédant des fronts pulsatoires ou des fronts de transition [21, 130, 136, 139, 167, 190] ;

(iii) d'équations de réaction-diffusion avec une vitesse forcée, utilisées dans l'article de Berestycki *et al.* [17] pour étudier l'effet du changement climatique sur la dynamique d'espèces biologiques.

1.2 L'effet Allee favorise la diversité génétique à l'intérieur d'un front de colonisation [RGHK12]

L'étude de la dynamique interne des fronts a de nombreuses conséquences, notamment en génétique des populations. Elle montre en particulier la mise en place d'une structure génétique spatiale au cours d'une colonisation. Les travaux présentés dans cette section s'appuient sur nos résultats obtenues dans [GGHR12]. Dans certains cas nous proposons des preuves différentes. En outre nous donnons une interprétation de ces résultats, du point de vue des applications en génétique des populations, destinée à un lectorat plus large.

De nombreuses études écologiques ont montré que l'expansion de l'aire de répartition d'une population entraîne souvent une perte de la diversité génétique le long du front de colonisation [52, 94, 148, 160, 162]. Cette perte de diversité génétique est principalement due à la dérive génétique, c'est-à-dire au fait que seul un échantillon de la population totale colonise de nouveaux habitats [127]

Cependant, dans certains cas, la diversité génétique se maintient au cours de la colonisation. C'est par exemple le cas pour le mélèze *Larix Decidua* dans les Alpes [145]. Ce maintien de la diversité génétique peut s'expliquer grâce à divers phénomènes environnementaux ou endogènes. En effet, des études numériques ont mis en évidence le rôle de la géométrie du milieu envahi [31, 174, 184], l'importance des événements de dispersion à longue distance et de la forme du noyau de dispersion [11, 68, 96], l'effet de la démographie locale [110] ou encore l'impact de l'existence d'une phase juvénile [11] sur le maintien de la diversité.

L'existence d'un effet Allee est un autre facteur déterminant dans la dynamique d'une population en expansion. Cet effet Allee est caractérisé par une diminution du taux de croissance par individu à faible densité [7]. On distingue deux types d'effet Allee : l'effet Allee faible et l'effet Allee fort. Lorsque le taux de croissance par individu n'est pas maximal pour les faibles densités mais reste positif, on parlera d'effet Allee faible. Il est souvent modélisé par des nonlinéarités f monostables (A) dont le graphe ne reste pas sous sa tangente à l'origine, voir figure 1(b), ou des nonlinéarité de type ignition (C), voir figure 3. Lorsque le taux de croissance devient négatif à faible densité, on parlera d'effet Allee fort. On utilise souvent des nonlinéarités bistables (B) pour prendre en compte un effet Allee fort dans les modèles (voir figure 2). L'existence d'un effet Allee a été observé chez de nombreuses populations [53, 114, 179]. Il est connu que sa présence ralentit la vitesse de propagation de la population [13, 118].

Une étude numérique proposée par Hallatschek et Nelson [82] a montré que la présence d'un effet Allee rend possible le phénomène de «surf», c'est-à-dire qu'un gène va pouvoir se propager à la même vitesse que le front de colonisation. Plus précisément, en utilisant une approche «backward», c'est-à-dire en remontant le temps, ils ont étudié la position initiale d'un gène qui a réussi à surfer sur le front et ont noté de grandes différences en fonction de la présence ou non d'un effet Allee. En utilisant le cadre des équations de réaction-diffusion, ils ont pu relier leurs résultats numériques à des formules analytiques. Continuant dans cette voie et réutilisant le cadre de travail mathématique développé dans la section précédente, nous nous sommes intéressés à l'impact de l'effet Allee sur la structure génétique durant un processus de colonisation.

On considère une population de gènes ou d'individus haploïdes dont la densité de population u est modélisée par l'équation de réaction-diffusion unidimensionnelle (2). Depuis les travaux de Skellam [169], cette équation (2) a souvent été utilisée pour étudier une population en expansion. Cependant, peu de travaux théoriques ont analysé l'évolution de la structure interne des solutions du modèle (2) (hormis les travaux présentés dans la section précédente [GGHR12]).

Pour ce type d'équations, si le terme de croissance f vérifie l'une des trois hypothèses monostable KPP (A), bistable (B) ou ignition (C), et si la population initiale u_0 ressemble à un front (c, U) pour des x positifs grands, alors la solution u du problème de Cauchy associé à (2) converge vers ce front de vitesse c et de profil U [9, 33, 69, 71, 116]. Ces solutions de type front décrivent l'invasion à vitesse et profil constant d'un espace vierge. Dans la suite, la population u sera prise à l'équilibre de propagation, c'est-à-dire que u sera une solution de type front de la forme $u(t, x) = U(x - ct)$. On suppose que cette population est composée de plusieurs fractions de gènes neutres. L'étude proposée précédemment sur la structure interne des fronts va nous permettre d'étudier l'évolution spatio-temporelle de ces fractions correspondant à des gènes neutres à l'intérieur de la population u, et de répondre aux questions suivantes :

(i) comment les différentes fractions évoluent à l'intérieur d'un front de colonisation généré par un modèle de type KPP ;

(ii) la présence d'un effet Allee modifie-t-elle les proportions des diverses fractions présentes dans le front ? A-t-on une augmentation ou une perte de diversité à l'intérieur de ces fronts de colonisation ?

(iii) les proportions des différentes fractions évoluent-t-elles rapidement après le passage du front ?

Les dynamiques des fronts, présentées dans les Théorèmes 1, 2 et la Proposition 1, nous renseignent sur la mise en place d'une structure génétique spatiale au cours d'une colonisation. Elles montrent aussi que l'inclusion d'un effet Allee dans les modèles (2) conduit à des différences fondamentales dans la composition des fronts. Dans un souci de clarté, l'effet Allee est modélisé dans notre étude par des nonlinéarités bistables cubiques de la forme :

$$f(u) = u\,(1-u)\,(u-\rho) \quad \text{pour tout} \quad u \in]0,1[, \tag{12}$$

où ρ correspond au seuil de l'effet Allee en dessous duquel le taux de croissance devient négatif [105, 118]. Le taux de croissance par individu $g(u) = f(u)/u$ est négatif à faible densité, ce qui correspond à un effet Allee fort. On oppose ces termes avec effet Allee aux nonlinéarités de type KPP (cf. définition (A)), pour lesquelles le taux de croissance par individu est toujours positif et devient maximal lorsque la densité u est nulle, *i.e.* pas de diminution du taux de croissance *per capita* à faible densité.

Dynamique d'un gène neutre dans la population

On se focalise sur la dynamique d'un gène neutre à l'intérieur de la population totale u. La densité v du gène neutre à l'intérieur du front u vérifie l'équation (5) de la section précédente. D'après les résultats précédents on obtient les deux types de comportements, suivant que la population subit ou non un effet Allee.

Proposition 2 (Cas KPP, sans effet Allee)**.**
(i) ***Dynamique dans le repère mobile de vitesse*** c ***:*** *si la densité initiale* v_0 *converge vers* 0 *plus rapidement que le front* U *lorsque* $x \to +\infty$,[1] *alors*

$$\max_{x\in[A,+\infty)} v(t, x+ct) \to 0 \quad \textit{lorsque } t \to +\infty, \quad \textit{pour tout } A \in \mathbb{R}.$$

(ii) ***Dynamique dans le repère fixe :*** *si la densité initiale* v_0 *est à support compact alors*

$$v(t,x) \to 0 \quad \textit{uniformément sur } \mathbb{R} \quad \textit{lorsque } t \to +\infty.$$

Dans ce cas, aucune fraction, initialement peu représentée à l'avant du front, ne peux se propager à la même vitesse que la population totale.

Notons que les hypothèses concernant le donnée initiale v_0 du (i) de la Proposition 2 sont légèrement différentes de celles du Théorème 1. On demande ici que la fonction $x \mapsto e^{cx/2}v(x)$ soit dans $L^1([0,+\infty[)$ alors que l'on demandait que cette fonction soit dans $L^2([0,+\infty[)$ dans le Théorème 1. Ceci tient au fait que la preuve de la Proposition 2 utilise une méthode spécifique au cas KPP, plus directe que celle du Théorème 1.

Hallatschek et Nelson [82] avaient indiqué que le phénomène de «gene surfing», c'est-à-dire qu'un gène envahit l'avant du front, était impossible avec un terme de croissance logistique, *i.e.* $f(u) =$

1. C'est à dire $\displaystyle\int_0^{+\infty} e^{\frac{cy}{2}}\, v_0(y)dy < \infty$.

$u\,(1-u)$. Pour des fractions initialement à support compact, nos résultats sont cohérent avec leurs conclusions puisque aucune fraction initialement à support compact ne peut surfer. Ces fractions initialement localisées restent à leur place d'origine et se diffusent autour de celle-ci (voir figure 8 et 11(b)). La disparition de ces fractions dans la population totale se fait de manière très lente par rapport à la propagation du front. Le front de colonisation se déplace à vitesse c donc le phénomène de propagation est de l'ordre de t, alors que le phénomène de diffusion se fait lui en $\sqrt{t}$ comme indiqué par la figure 8.

Cependant le phénomène de surf peut se produire pour des données initiales dont le support initial n'est pas compact, même dans le cas d'une croissance logistique. Considérons par exemple la fraction v^r la plus à droite dans le front : à $t=0$, on a $v_0^r =\equiv U\cdot \mathbb{1}_{[\alpha,\infty)}$, où $\mathbb{1}_{[\alpha,\infty)}$ est la fonction indicatrice de l'intervalle $[\alpha,\infty)$, pour un certain $\alpha\in\mathbb{R}$. La fraction correspondant au reste de la population vérifie $v_0^l \equiv U\cdot\mathbb{1}_{(-\infty,\alpha)}$ et satisfait les hypothèses de la première partie de la Proposition 2. Comme $u(t,x)=U(x-c\,t)=v^l(t,x)+v^r(t,x)$, les résultats précédents montrent que $v^r(t,x)$ converge vers $U(x-c\,t)$ dans n'importe quelle demi-droite $[A+c\,t,\infty)$ avançant à vitesse c. Par conséquent, la fraction v^r, initialement la plus en avant du front, réussit à surfer sur le front de colonisation (voir portion en gris clair sur la figure 11(b)).

Proposition 3 (Cas avec effet Allee, voir [GGHR12])**.**
Dynamique dans le repère mobile de vitesse c ***:*** *toute fraction v converge vers une proportion du front u, dans le sens où*

$$\max_{x\in[A,+\infty)} |v(t,x+ct)-p(v_0)U(x)|\to 0 \quad \textit{lorsque } t\to+\infty, \quad \textit{pour tout } A\in\mathbb{R}.$$

La proportion finale $p(v_0)$ de la fraction v est donnée par (8)*.*

Ainsi, toute fraction initialement présente à l'intérieur du front contribue à la colonisation à hauteur de $p(v_0)$ qui dépend de la donnée initiale v_0 (voir figure 9 et 11(c)). La formule (8) donne des informations *a posteriori* sur la position initiale des gènes composant le front en temps grand. En effet, considérons la fraction la plus à gauche définie par $v_0^l\equiv U\cdot\mathbb{1}_{(-\infty,\alpha)}$ pour $\alpha\in\mathbb{R}$. La proportion finale de cette fraction dans le repère mobile de vitesse c est donnée par $p(\alpha):=p[v_0^l]$. Sa dérivée $p'(\alpha)$ correspond à la contribution finale des gènes initialement positionnés en α :

$$p'(\alpha)=U^2(\alpha)\,e^{c\,\alpha}/\left(\int_{-\infty}^{+\infty}U^2(x)\,e^{c\,x}\,dx\right).$$

Pour des nonlinéarités cubiques de la forme (12), la formule explicite du profil U et de la vitesse c nous permettent de montrer que p' atteint son unique maximum à la position :

$$\alpha_{\max}=\sqrt{2}\ln\left(\frac{1-2\,\rho}{1+2\,\rho}\right).$$

Cette valeur correspond à la meilleure position pour être le mieux représenté dans le front en temps grand. On observe que $\alpha_{\max}$ est une fonction décroissante de ρ et que $\alpha_{\max}(1/2)=-\infty$. L'effet Allee avantage donc les fractions qui se situent loin du front de colonisation : plus l'effet Allee est fort, plus les gènes loin du front contribuent significativement à l'avancée du front. Au contraire, lorsque l'effet Allee est faible, avec $\rho=0$ ce qui correspond à une nonlinéarité de type monostable avec une vitesse minimale $c^*>2\sqrt{f'(0)}$, les gènes au centre du front, c'est-à-dire à la position $\alpha=0$, sont ceux qui contribuent le plus significativement à l'avancée du front.

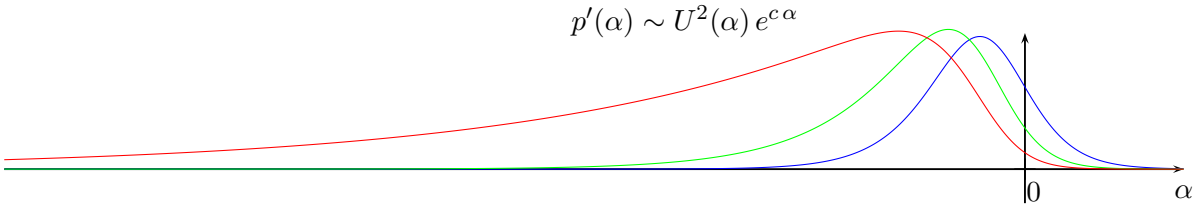

FIGURE 10 – Comportement de $p'(\alpha)$ pour différentes valeur du seuil de l'effet Allee ρ : en bleu $\rho = 0.1$, en vert $\rho = 0.3$ et en rouge $\rho = 0.45$.

Les simulations numériques présentées en figure 11 montrent que l'effet Allee conduit à une structuration horizontale de la diversité, ce qui correspond à une absence de différentiation génétique spatiale. À l'inverse, en l'absence d'effet Allee on obtient une population très structurée en espace.

Nos résultats montrent que l'inclusion d'un effet Allee dans les modèles conduit à des différences fondamentales en terme de structuration génétique et de diversité génétique. L'effet Allee permet un maintien de la diversité génétique au cours de la colonisation (voir figures 11). L'effet Allee ralentit la colonisation mais favorise le maintien de la diversité génétique.

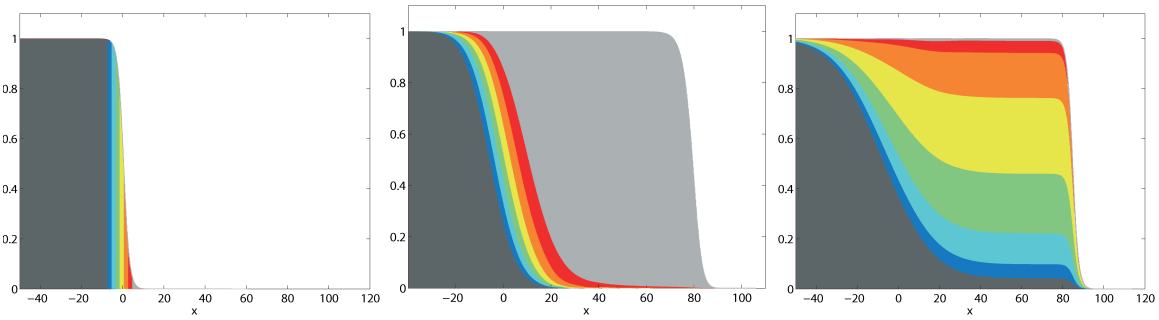

(a) Donnée initiale (b) Colonisation sans effet Allee (c) Colonisation avec effet Allee

FIGURE 11 – Évolution des fractions v^k (bandes de couleur sur (a)) à l'intérieur du front de colonisation : (b) en absence d'effet Allee et (c) en présence d'effet Allee.

1.3 L'impact de l'effet Allee sur le succès d'une invasion biologique [GHR12]

Bien que l'effet Allee semble favorable à la persistance de la diversité génétique d'une population lors de sa phase d'expansion, il peut avoir des conséquences néfastes, voir létales pour la population notamment au début d'une invasion biologique.

En effet, une invasion biologique démarre généralement par l'introduction d'une population réduite d'individus dans un nouveau milieu. C'est la phase d'arrivée. Suit la phase d'installation, durant laquelle la population fondatrice essaie de se reproduire pour créer une colonie. Si cette étape réussit, c'est-à-dire si la colonie prolifère, elle se propage et envahit le nouveau milieu. La phase d'installation est la plus sensible, puisque la quantité d'individus est souvent faible. Son succès est souvent la conséquence de multiples introductions [150, 182]. L'existence d'un effet Allee, qui correspond à une diminution de la fertilité à faible densité, est une des causes de l'échec de l'installation puisqu'il favorise l'extinction de populations de faible densité [56, 117, 193].

Dans la suite, nous analysons l'effet de la distribution spatiale de la population fondatrice, c'est-à-dire la répartition de la population initiale en sous-groupes, sur le succès de l'installation de la

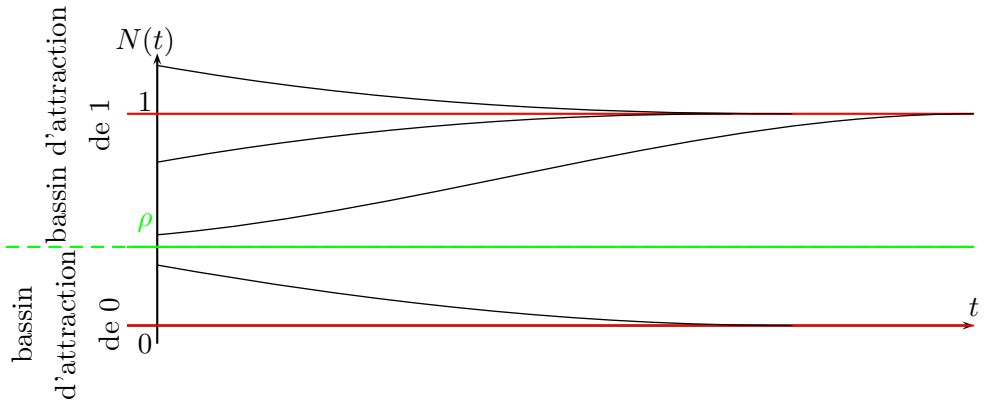

FIGURE 12 – Solutions de l'équation différentielle $N' = f(N) = N(1-N)(N-\rho)$, avec $\rho = 0.3$, partant de différentes données initiales $N_0 \in \{0.2, 0.4, 0.7, 1.2\}$.

population. Cette étude est très différente des précédentes puisqu'ici la population totale u n'est pas en expansion comme dans les sections précédentes. Notre analyse se base sur des modèles d'équations de réaction-diffusion adaptés à l'étude de la persistance et de la propagation d'espèces biologiques [118, 175]. Les premières modèles de réaction-diffusion introduits par Fisher [72] et Kolmogorov, Petrovsky, et Piskunov [112] ne prenaient pas en compte l'existence d'un effet Allee. Dans ces modèles de type Fisher-KPP, la survie de la population ne dépend pas de la donnée initiale, même lorsque le milieu est hétérogène [22, 24, 26]. Par conséquent, la majorité des études sur ces modèles s'intéressent à l'effet de la structure de l'environnement sur la survie et la propagation [24, 45, 103] plutôt qu'à l'effet de la donnée initiale. À l'inverse, dans notre analyse qui prend en compte un effet Allee, nous avons supposé que le milieu était homogène pour isoler l'effet de la structure spatiale de la population initiale. Pour ce type de modèle, d'autres paramètres comme la géométrie du domaine [39] peuvent aussi modifier la propagation.

Dans le cadre des équations de réaction-diffusion, comprendre l'effet de la donnée initiale sur la survie ou l'extinction de la solution revient à étudier les bassins d'attractions des deux états stationnaires $p_- \equiv 0$ et $p^+ \equiv 1$ du problème. Comme dans la section précédente l'effet Allee est modélisé par une nonlinéarité f de type bistable (B) [69, 175].

Dans le cadre des Équations Différentielles Ordinaires autonomes (EDO), l'équation $N' = f(N)$, avec f de type bistable (B), *i.e.* $f(N) \leq 0$, lorsque N est en dessous du seuil ρ, est un cas simple de modèle avec effet Allee. Dans ce cas, si la donnée initiale N_0 est en dessous du seuil ρ, la solution N tend vers 0 en temps grand, alors que si $N_0 > \rho$, N tend vers 1. Il est donc facile dans ce cas de déterminer les bassins d'attraction des solutions stationnaires stables 0 et 1 (voir figure 12).

Dans le cadre des équations de réaction-diffusion, les deux solutions $p_- \equiv 0$ et $p^+ \equiv 1$ sont des états stables de l'équation (2), mais il est difficile de trouver leur bassin d'attraction puisque l'espace des données initiales est beaucoup plus vaste et complexe que dans le cas des EDO. En se restreignant à des familles de données initiales à 1-paramètre, Aronson et Weinberger [10], Fife et McLeod [71], puis Du et Matano [58], Poláčik [146] et Zlatŏs [195] ont réussi à caractériser les ensembles $\omega-$limites de l'équation (2) dans le cas unidimensionnel. Leur paramètre caractérise uniquement la taille initiale de la population puisque son support est supposé connexe. Dans ces études, la répartition spatiale de la donnée initiale n'est pas prise en compte. Or, dans le cadre des invasions biologiques, une même population fondatrice peut être répartie de plusieurs manières différentes sur le domaine d'invasion. Ainsi suivant la répartition et la taille des groupes, l'effet Allee entraîne ou non l'extinction de la population.

Notre étude s'attache à montrer qu'en présence d'un effet Allee, la répartition spatiale initiale de la

population fondatrice joue un rôle important sur le succès de la phase d'installation. On s'est d'abord intéressé au problème unidimensionnel avec des données initiales u_0 dont le support est formé de deux intervalles de taille $L/2$, $L > 0$, distants d'une longueur $\alpha > 0$:

$$u_0(x) = \mathbb{1}_{[-(\alpha/2+L/2),-\alpha/2]}(x) + \mathbb{1}_{[\alpha/2,\alpha/2+L/2]}(x) \quad \text{pour tout } x \in \mathbb{R},$$

où $\mathbb{1}_J$ est la fonction caractéristique de J pour tout ensemble $J \subset \mathbb{R}$, (voir figure 13). La fragmentation du support de u_0 est entièrement définie par α. Les résultats de Du et Matano [58] montrent que pour chaque degré de fragmentation α, il existe une taille critique de la population, notée $L^*(\alpha)$, telle que si $L \geq L^*(\alpha)$, la population survit, alors que si $L < L^*(\alpha)$, la population s'éteint. Nos résultats analytiques et numériques montrent que la taille critique dépend continûment du paramètre de fragmentation α et tend à croître avec α, au moins lorsque α est assez grand (voir figure 14). Ces résultats mettent en évidence l'aspect néfaste de la fragmentation.

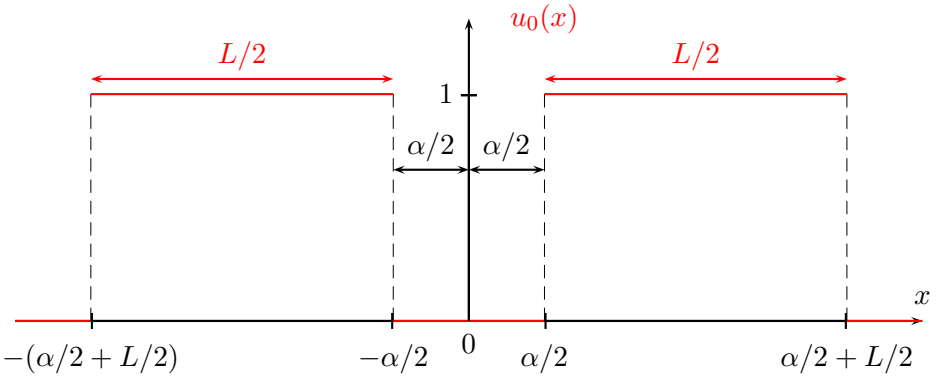

FIGURE 13 – Donnée initiale du problème unidimensionnel caractérisé par un degré de fragmentation α et un indice d'abondance L.

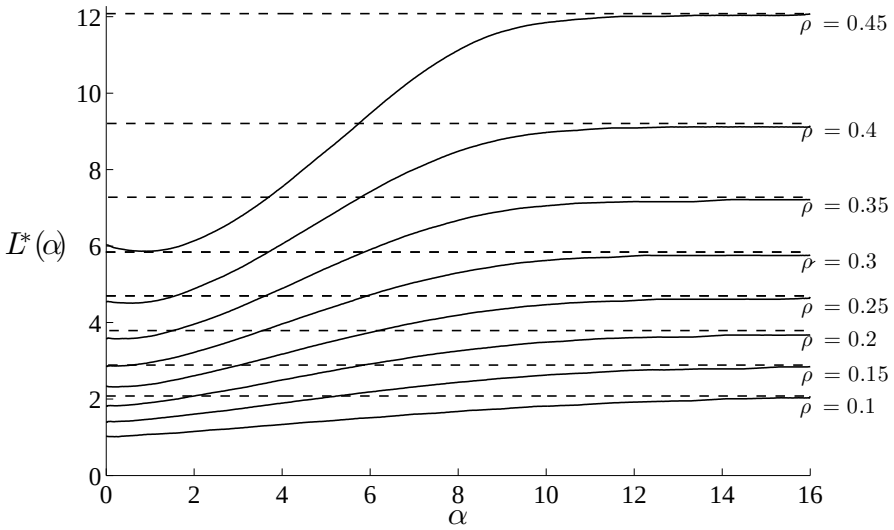

FIGURE 14 – Évolution de la taille critique $L^*(\alpha)$ en fonction de la fragmentation α et du degré de l'effet Allee ρ. Pour chaque valeur de ρ, la ligne pointillée correspond au seuil $2\,L^*(0)$.

Afin d'analyser, dans des conditions plus réalistes, l'effet de la fragmentation du support de la population fondatrice, nous avons construit des données initiales binaires bidimensionnelles du modèle (2) sur $\mathbb{R}^2$. Elles sont caractérisées par deux indices : un indice d'abondance p et un indice de

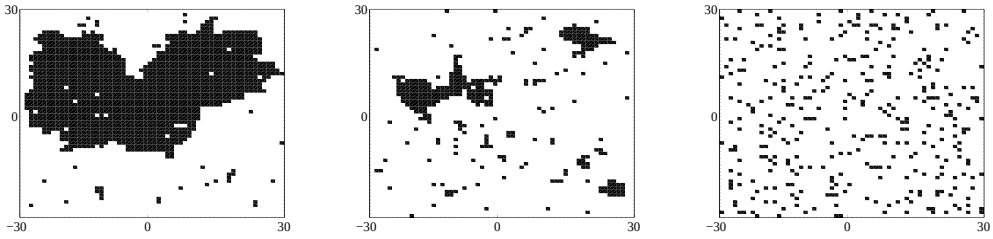

(a) $p = 0.4$, $fr = 0.05$ (b) $p = 0.1$, $fr = 0.4$ (c) $p = 0.1$, $fr = 0.9$

FIGURE 15 – Données initiales bidimensionnelles u_0 pour différentes valeurs de l'abondance p et de la fragmentation fr.

fragmentation fr (cf. figure 15). Ces données initiales sont générées par un algorithme stochastique, comparable au modèle d'Ising. Une des difficultés a été de définir rigoureusement un indice de fragmentation d'une part basé sur les paramètres du modèle stochastique et d'autre part indépendant de l'indice d'abondance p. On définit le taux de fragmentation d'une donnée initiale u_0 et d'abondance $p(u_0)$ par

$$fr(u_0) = 1 - \frac{s(u_0)}{B[p(u_0)]},$$

où $s(u_0)$ correspond au nombre de voisin de chaque case où la fonction u_0 vaut 1 puisque l'espace est discrétisé et $B[p(u_0)]$ est le maximum de s sur l'ensemble des données initiales d'abondance $p(u_0)$. Notre étude qui repose sur cette nouvelle définition rigoureuse du taux de fragmentation (mesuré par l'indice $fr \in [0, 1]$), a permis de décrire complètement les bassins d'attractions des états stationnaires $p_- \equiv 0$ et $p^+ \equiv 1$ grâce aux indices p et fr. Ces bassins apparaissent clairement sur la figure 16 : la région bleue correspond au bassin d'attraction de $p_- \equiv 0$ et la région rouge à celui de $p^+ \equiv 1$. Cette description a conduit à plusieurs constatations non triviales quant à l'effet de la fragmentation du support de la donnée initiale sur le succès de l'étape d'installation lors d'une invasion biologique :

(i) le succès de la phase d'installation dépend presque uniquement des deux indices p et fr et non des autres caractéristiques géométriques du support de la donnée initiale : la zone d'incertitude, en jaune sur la figure 16, est très étroite. En effet, cette zone oscille entre un succès presque sûr et un échec presque sûr ;

(ii) on observe l'existence d'un seuil critique de fragmentation où l'abondance minimale nécessaire au succès de l'installation augmente de façon importante. De part et d'autre de ce seuil, le succès de la phase d'installation dépend peu de l'indice de fragmentation ;

(iii) l'effet de la fragmentation est renforcé lorsque le seuil de l'effet Allee ρ augmente.

Finalement, la fragmentation du support de la population fondatrice u_0 a un effet néfaste sur le succès de la phase d'installation dans un environnement homogène.

2.2 Équations de réaction-diffusion en milieu hétérogène : vitesse de propagation et problèmes inverses

La section précédente a mis en évidence l'effet croisé du terme de croissance et de la structuration spatiale de la donnée initiale sur la propagation et la persistance des solutions du modèle de réaction-diffusion (2), dans le cas d'un milieu homogène.

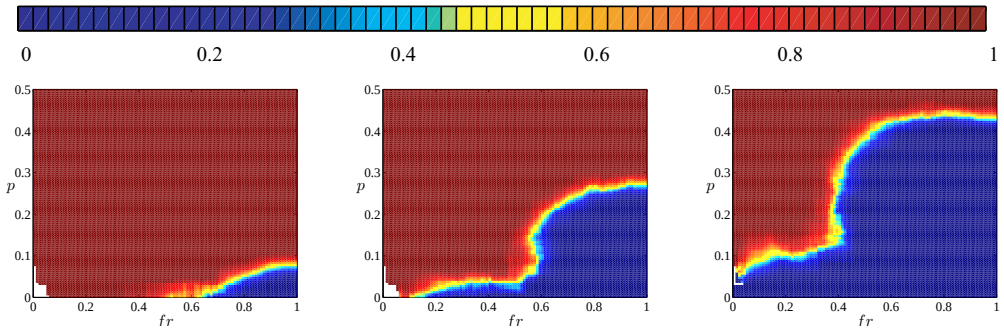

(a) $\rho = 0.1$ (b) $\rho = 0.3$ (c) $\rho = 0.45$

FIGURE 16 – Probabilité de succès de la phase d'installation en fonction de la force de l'effet Allee (caractérisée par $\rho > 0$), de l'indice de fragmentation de la donnée initiale fr et de l'indice d'abondance p de cette population.

En écologie, les ressources environnementales sont rarement distribuées de manière uniforme et homogène. Le paysage comporte souvent des zones plus ou moins favorables à la survie de l'espèce considérée. Ces variations du milieu favorisent ou au contraire ralentissent la propagation de l'espèce. Afin de mieux comprendre l'effet des hétérogénéités spatiales, les modèles ont été adaptés et la non-linéarité $f(u)$ a été remplacée par une fonction dépendant de l'espace $f(x,u)$. Skellam [169], puis Shigesada, Kawasaki, et Teramoto [168] ont été les premiers à étendre le modèle de réaction-diffusion de type KPP, où la nonlinéarité f vérifiait $f(u) = \mu u - \gamma u^2$ avec μ et $\gamma \in \mathbb{R}$, à un milieu hétérogène :

$$\frac{\partial u}{\partial t}(t,x) = \frac{\partial^2 u}{\partial x^2}(t,x) + \mu(x)u(t,x) - \gamma(x)u^2(t,x),\ t > 0 \text{ et } x \in \mathbb{R}.$$

La nonlinéarité hétérogène $f(x,u) := \mu(x)u - \gamma(x)u^2$ possède des coefficients $\mu(x)$ et $\gamma(x)$ qui dépendent de la position x. La fonction μ correspond au taux de croissance intrinsèque de la population et γ représente la compétition intraspécifique. Ainsi, les régions associées aux fortes valeurs de μ correspondent aux régions favorables, alors que celles associées aux valeurs faibles ou négatives de μ correspondent aux régions défavorables. De manière plus générale, les modèles de réaction-diffusion dans un milieu excitable hétérogène s'écrivent de la manière suivante :

$$\frac{\partial u}{\partial t}(t,x) = \frac{\partial^2 u}{\partial x^2}(t,x) + f(x,u(t,x)),\ t > 0 \text{ et } x \in \mathbb{R}, \tag{13}$$

où $f(x,u)$ représente le taux de croissance de la population à la position x.

Dans un premier temps, nous nous intéressons à l'effet des hétérogénéités spatiales du milieu sur la vitesse de propagation des solutions de (13) partant d'une donnée initiale à support compact. Dans un second temps, nous étudions des problèmes inverses liés à la reconstruction de paramètres hétérogènes du modèle (13), par exemple μ et γ, grâce à un minimum d'observations de la solution. Ce sont nos connaissances du comportement des solutions en milieu hétérogène qui vont nous permettre de retrouver le milieu dans lequel évolue notre solution.

2.1 Effet du milieu sur la vitesse de propagation des solutions [GGN12]

Dans un milieu hétérogène apparaissent des zones plus ou moins favorables à la croissance de la solution. Ainsi dans les régions favorables au développement, la solution va pouvoir se propager plus facilement et donc plus rapidement que dans les zones moins favorables voire défavorables. On s'attend

donc à ce que la solution ait une *vitesse minimale de propagation* w_* dans les régions défavorables et une *vitesse maximale de propagation* w^* dans les régions favorables. On définit pour toute solution u du problème de Cauchy associé à (13), partant d'une donnée initiale u_0 à support compact, les deux vitesses de propagation vers la droite suivantes :

$$\begin{aligned} w_* &= \sup\{c>0 \mid \liminf_{t\to+\infty} \inf_{x\in[0,ct]} u(t,x) > 0\}, \\ w^* &= \inf\{c>0 \mid \sup_{x\in[ct,+\infty)} u(t,x) \to 0 \text{ quand } t\to+\infty\}. \end{aligned}$$

Dans le cas d'un milieu homogène, c'est-à-dire lorsque f ne dépend pas de x, Aronson et Weinberger [10] et Fife et McLeod [71] ont montré que si la solution se propage, sa vitesse de propagation est unique et vérifie $w_* = w^* = c^*$, où c^* est la vitesse minimale des fronts pour des nonlinéarités monostable (A), bistable (B) ou de type ignition (C).

Il en va de même lorsque le milieu est périodique en espace. En effet, Freidlin et Gärtner [74] ont montré que $w_* = w^*$ lorsque f est de type KPP et périodique en x. En outre, ils ont caractérisé cette vitesse grâce aux valeurs propres principales périodiques λ_p de la famille d'opérateurs elliptiques linéaires $\mathcal{L}_p$ suivants :

$$\mathcal{L}_p : \varphi \mapsto \frac{\partial^2\varphi}{\partial x^2} - 2p\frac{\partial\varphi}{\partial x} + \Big(p^2 + \frac{\partial f}{\partial u}(x,0)\Big)\varphi.$$

Plus précisément, dans le cas où la fonction f est périodique et vérifie les hypothèses suivantes :

(A') KPP hétérogène : f est de type *KPP hétérogène* si

$$\begin{aligned} &f(x,0) = 0,\ f(x,1) = 0,\ \frac{\partial f}{\partial u}(x,0) > 0, \quad \text{pour tout } x\in\mathbb{R} \\ &\text{et}\ \ 0 < f(x,u) \le \frac{\partial f}{\partial u}(x,0)u \ \ \text{pour tout } (x,u)\in\mathbb{R}\times]0,1[, \end{aligned}$$

la vitesse de propagation est donnée par :

$$w_* = w^* = \min_{p>0} \frac{\lambda_p}{p}. \tag{14}$$

De plus, Berestycki *et al.* [22] et Weinberger [186] ont montré que cette vitesse asymptotique de propagation est égale à la vitesse minimale des fronts pulsatoires, qui est la généralisation de la notion de front aux milieux périodiques. L'existence d'une unique vitesse de propagation, $w^* = w_*$, et la caractérisation (14) sont également valables dans le cas d'hétérogénéités transversales [125], périodiques en temps et en espace ou perturbations à support compact de problèmes homogènes [22].

Dans tous ces cas, l'opérateur $\mathcal{L}_p$ est d'inverse compact et la notion de valeur propre principale est bien définie. Mais lorsque la dépendance de f en x est plus générale, cette notion de valeur propre principale n'est pas toujours bien définie et on doit faire appel aux diverses définitions des valeurs propres généralisées, ce qui complique la caractérisation. De plus, dans des milieux très hétérogènes la propagation n'a pas toujours lieu à vitesse unique, c'est-à-dire que l'on peut avoir $w_* < w^*$. Ce type de comportement a été mis en évidence uniquement dans des milieux périodiques en temps [28] ou pour des données initiales à support non compact [87] mais pas encore pour des milieux hétérogènes en espace avec des données initiales à support compact.

Pour mettre en avant ce phénomène, nous avons étudié un milieu totalement hétérogène qui ressemble à un milieu périodique dont la période augmente de plus en plus lorsque x tend vers $+\infty$. Ce problème s'inspire de travaux récents sur des milieux périodiques lentement oscillants. Pour de

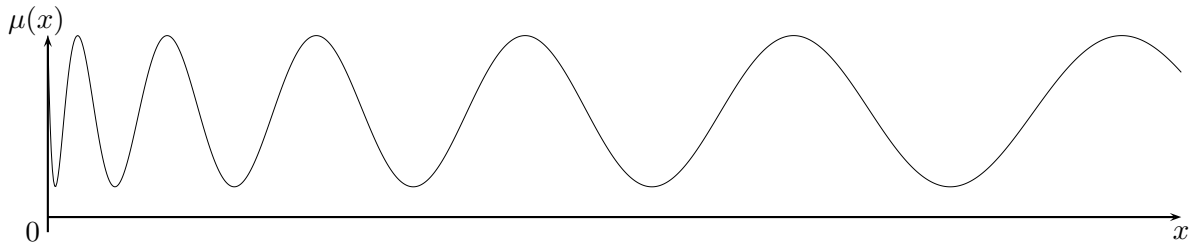

FIGURE 17 – Exemple d'une fonction de croissance intrinsèque $\mu := \mu_0(\phi)$ qui oscille de plus en plus lentement à l'infini : $\mu_0(x) = 0.5\cos(x) + 0.7$ et $\phi(x) = \sqrt{x}$.

tels milieux, Hamel *et al.* [86, 89] ont donné une formule explicite de la vitesse minimale des fronts pulsatoires lorsque la période tend vers l'infini.

Nous définissons notre milieu hétérogène f de plus en plus lentement oscillant de la manière suivante : $f = f(x, u)$ est régulière en x et u, et vérifie l'hypothèse de KPP hétérogène (A'). L'exemple classique d'une telle fonction est $f(x, u) = \mu(x)u(1 - u)$, avec μ une fonction continue, strictement positive et bornée de $\mathbb{R}$. De plus, on suppose que le taux de croissance intrinsèque μ défini par

$$\mu(x) := \frac{\partial f}{\partial u}(x, 0) \text{ pour tout } x \in \mathbb{R},$$

vérifie les hypothèses suivantes : il existe $\mu_0 \in \mathcal{C}^0(\mathbb{R})$ et $\phi \in \mathcal{C}^1(\mathbb{R})$ tels que

$$\begin{cases} \mu(x) = \mu_0(\phi(x)) \text{ pour tout } x \in \mathbb{R}, \\ 0 < \min\limits_{[0,1]} \mu_0 < \max\limits_{[0,1]} \mu_0 \quad \text{et} \quad \mu_0 \text{ est 1-périodique}, \\ \phi'(x) > 0, \ \lim\limits_{x \to +\infty} \phi(x) = +\infty \quad \text{et} \quad \lim\limits_{x \to +\infty} \phi'(x) = 0. \end{cases} \tag{15}$$

L'environnement ainsi créé est totalement hétérogène puisqu'il ne vérifie aucune hypothèse de périodicité ou d'ergodicité. Cependant, il ressemble au milieu périodique, défini par μ_0, dont la période augmente à l'infini grâce à ϕ (voir figure 17).

L'objectif de notre étude est de montrer que suivant la déformation de la période induite par ϕ, la vitesse de propagation va être ou non unique.

Plus précisément, lorsque la période augmente rapidement, *i.e.* ϕ augmente lentement, la fonction μ_0 approche ses valeurs extrémales sur des intervalles de plus en plus grands. Ainsi, la solution u passe un temps de plus en plus long dans chacun de ces intervalles. La vitesse de propagation alterne donc entre les valeurs qu'elle prendrait si le milieu était homogène correspondant aux valeurs extrémales. Dans ce cas la vitesse de propagation n'est pas unique, $w_* < w^*$. Nous montrons rigoureusement dans [GGN12] le résultat suivant :

Théorème 3. *Si ϕ croît sous-logarithmiquement, dans le sens où*

$$\frac{1}{x\phi'(x)} \to C \text{ lorsque } x \to +\infty, \text{ avec } C \in (0, +\infty] \text{ assez grand,} \tag{16}$$

alors

$$w_* < w^*.$$

C'est le premier cas à notre connaissance d'une nonlinéarité $f(x, u)$, uniquement hétérogène en espace, dont les vitesses minimale et maximale de propagation w_* et w^* ne sont pas égales. En outre,

la propriété (16) caractérise la manière dont doit croître la période pour obtenir des vitesses de propagation différentes.

À l'inverse, lorsque la période augmente lentement, *i.e.* ϕ croît rapidement, la vitesse de propagation devient unique $w_* = w^*$. De plus, on obtient une caractérisation de cette vitesse grâce au problème limite de période infinie étudié par Hamel *et al.* [89]. Cette vitesse limite c^*_∞ se caractérise par :

$$c^*_\infty := \min_{p \geq j(M)} \frac{j^{-1}(p)}{p} = \min_{k \geq M} \frac{k}{j(k)},$$

où $M := \max_{x \in \mathbb{R}} \mu_0(x) > 0$ et $j : [M, +\infty) \to [j(M), +\infty)$ est définie par :

$$j(k) := \int_0^1 \sqrt{k - \mu_0(x)} dx.$$

Théorème 4. *Si ϕ croît sur-logarithmiquement, dans le sens où*

$$\frac{\phi''(x)}{\phi'(x)^2} \to 0 \quad \textit{et} \quad \frac{\phi'''(x)}{\phi'(x)^2} \to 0 \quad \textit{lorsque } x \to +\infty \tag{17}$$

alors

$$w_* = w^* = c^*_\infty.$$

Les hypothèses (17) sur la croissance de ϕ impliquent en particulier que $1/(x\phi'(x)) \to 0$ lorsque $x \to +\infty$, ce qui rend ce résultat complémentaire du précédent.

Notre étude a d'abord permis d'exhiber de nouvelles dynamiques entièrement dépendantes de l'hétérogénéité du milieu. La fonction ϕ contrôle la manière dont la période augmente, c'est-à-dire dont la fragmentation du milieu diminue. Ainsi, si la fragmentation du milieu diminue lentement, par exemple :

(i) si ϕ croît logarithmiquement : $\phi(x) = \ln(x)^\alpha$ pour $x > 0$ suffisamment grand, avec $\alpha > 1$,

(ii) si ϕ croît en puissance : $\phi(x) = x^\alpha$ avec $\alpha \in]0, 1[$,

(iii) si ϕ est de la forme : $\phi(x) = x/\ln(x)^\alpha$ avec $\alpha > 0$,

on a toujours $\phi''/\phi'^2(x) \to 0$ et $\phi'''/\phi'^2(x) \to 0$ lorsque $x \to +\infty$. Le Théorème 4 implique $w_* = w^* = c^*_\infty$. À l'inverse, si la fragmentation diminue rapidement, par exemple :

(iv) si ϕ croît en logarithme puissance : $\phi(x) = \ln(x)^\alpha$ pour $x > 0$ suffisamment grand, avec $\alpha \in]0, 1[$,

alors $1/(x\phi'(x)) = \ln(x)^{1-\alpha}/\alpha \to +\infty$ lorsque $x \to +\infty$. Le Théorème 3 implique $w_* < w^*$.

Ce travail nous a permis de développer et d'utiliser des méthodes spécifiques à l'étude des phénomènes de propagation dans des milieux hétérogènes non-périodiques. Nos résultats mettent en évidence un comportement qui n'avait jamais été observé dans les problèmes hétérogènes à savoir la non-unicité de la vitesse de propagation.

2.2 Reconstruction de paramètres hétérogènes pour des équations de réaction-diffusion hétérogènes [CGHR12]

La section précédente a montré que le comportement de la solution u du modèle hétérogène (13) dépend de la forme précise des coefficients de la nonlinéarité f. Plus précisément, les variations du taux de croissance intrinsèque μ défini par (15) modifient la vitesse de propagation des solutions. Ainsi, l'utilisation empirique de ces modèles nécessite une connaissance précise des coefficients qui

le constituent. Malheureusement, en pratique, il est difficile de mesurer directement ces paramètres car ils sont souvent le résultat d'effets croisés de plusieurs facteurs. Par conséquent, ces coefficients sont généralement déterminés grâce à des mesures de la densité $u(t,x)$ [170]. Dans la plupart des cas pratiques, les mesures de la densité u ne peuvent s'effectuer que sur des sous-régions, souvent restreintes, du domaine global [188] que nous notons $]a,b[\subset \mathbb{R}$. De plus, les méthodes d'inférence souvent utilisées pour déterminer ces coefficients hétérogènes sur le domaine tout entier, consistent généralement à comparer les valeurs de la solution u, mesurée sur les sous-régions, à celles de solutions obtenues pour des coefficients hypothétiques [171]. La précision de ces méthodes repose sur le fait que pour chaque valeur de la solution u sur ces sous-régions, il existe un unique jeu de coefficients. Cette hypothèse d'unicité n'est pas vérifiée en général.

Dans la suite, on s'intéresse aux équations de réaction-diffusion hétérogènes de la forme :

$$\frac{\partial u}{\partial t} = D\frac{\partial^2 u}{\partial x^2} + \sum_{k=1}^{N} \mu_k(x)\, u^k + g(x,u), \text{ pour } t>0,\ x\in]a,b[, \tag{18}$$

sur un intervalle borné $]a,b[$ de $\mathbb{R}$. Les $N \geq 1$ fonctions – inconnues – $\mu_k(x)$, $k=1,\dots,N$ sont régulières. On montre des résultats d'unicité du problème inverse constituant à déterminer ces N coefficients hétérogènes $\mu_k(x)$, $k=1,\dots,N$, représentant la partie polynomiale du terme de réaction, à partir de mesure de $u(t,x)$. Plus précisément, on a le résultat suivant

Théorème 5. *Soient $N\in\mathbb{N}^*$, $(\mu_k)_{1\leq k\leq N}$ et $(\tilde{\mu}_k)_{1\leq k\leq N}$ deux familles de coefficients réguliers. Soient $(u_i^0)_{1\leq i\leq N}$ N fonctions positives deux à deux distinctes sur $]a,b[$. Pour chaque $1\leq i\leq N$, on note u_i et $\tilde{u}_i$ les solutions de (18) respectivement pour les (μ_k) et les $(\tilde{\mu}_k)$ et partant des données initiales u_i^0. Supposons que pour $x_0\in]a,b[$ et $\varepsilon>0$, u_i et $\tilde{u}_i$ vérifient :*

$$\begin{cases} u_i(t,x_0) &= \tilde{u}_i(t,x_0), \\ \dfrac{\partial u_i}{\partial x}(t,x_0) &= \dfrac{\partial \tilde{u}_i}{\partial x}(t,x_0), \end{cases} \quad \text{pour tout } t\in(0,\varepsilon) \text{ et tout } i\in\{1,\cdots,N\}.$$

Alors $\mu_k\equiv\tilde{\mu}_k$ sur $[a,b]$ pour tout $k\in\{1,\dots,N\}$, et par conséquent $u_i\equiv\tilde{u}_i$ sur $[0,T[\times[a,b]$ pour tout $i\in\{1,\dots,N\}$, où $T>0$ est le temps de vie maximal des solutions u_i et $\tilde{u}_i$.

Nos résultats donnent une condition suffisante pour déterminer de manière unique les coefficients μ_k à partir d'observations localisées. Cette condition suffisante porte sur une mesure ponctuelle de la solution $u(t,x_0)$ et de sa dérivée spatiale $\partial u/\partial x(t,x_0)$ en un unique point x_0, pendant un petit intervalle de temps $(0,\varepsilon)$ partant de N données initiales différentes u_i^0, $i=1,\dots,N$.

Les différences fondamentales entre nos résultats et les résultats antérieurs sont

(i) la taille de la région d'observation, réduite ici à un seul point ;

(ii) le nombre N de coefficients pouvant être reconstitués, qui est arbitrairement grand ;

(iii) la diversité des nonlinéarités que l'on peut traiter.

En effet, la majorité des résultats sur ce type de problèmes inverses sont basés sur des estimations de type Carleman [35, 109]. Ces méthodes permettent d'obtenir, en plus de l'unicité, des résultats de stabilité. Cependant, elles requièrent en plus d'une mesure ponctuelle durant un petit intervalle de temps, une mesure de la solution $u(\theta,x)$ à un instant $\theta>0$ et pour tous les x du domaine $]a,b[$ [voir 15, 48, 76, 97, 192].

D'autre part, toutes les conditions définies dans le Théorème 5 sont des conditions nécessaires, comme nous le détaillons dans la section 4 du Chapitre 5. En particulier, pour obtenir les conclusions

du Théorème 5, il faut que le nombre de mesures du couple $(u, \partial u/\partial x)(t, x_0)$ soit au moins égal au degré N de la partie polynomiale inconnue.

D'un point de vue pratique, ces mesures peuvent être obtenues par un contrôle de la donnée initiale. Cependant, en l'absence d'inégalités de stabilité assurant que deux jeux de mesures proches proviennent de coefficients proches, la reconstruction des coefficients inconnues μ_k, à partir des mesures ponctuelles, n'est pas automatique. Nos résultats numériques indiquent cependant que dans le cas de $N = 2$ et $N = 3$ coefficients, ces mesures ponctuelles permettent d'obtenir de bonnes approximations numériques de ces coefficients inconnus (voir figure 18).

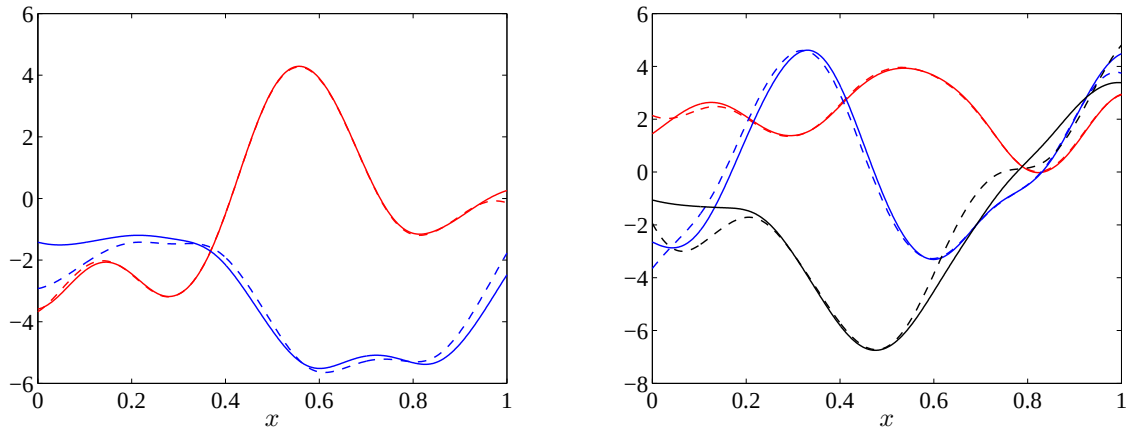

(a) Reconstruction de 2 coefficients

(b) Reconstruction de 3 coefficients

FIGURE 18 – Reconstruction numérique de $N = 2$ et $N = 3$ coefficients de (18) à partir de mesures ponctuelles : Traits pleins : exemples de fonctions μ_1 (rouge), μ_2 (bleu) et μ_3 (noir).
Traits pointillés : les fonctions μ_1^* (rouge), μ_2^* (bleu) et μ_3^* (noir) obtenues en minimisant des fonctionnelles basées sur la norme $L^2(0, \varepsilon)$ de $(u - u^*)$ et $\partial(u - u^*)/\partial x$, où u^* est la solution de (18) calculé avec les μ_k^*.

2.3 Équations intégro-différentielles avec noyaux de dispersion non-exponentiellement bornés : accélération des solutions [Ga11]

Les deux sections précédentes ont montré les effets croisés des interactions entre les individus et du milieu, c'est-à-dire l'influence de la nonlinéarité f, ainsi que des effets de la donnée initiale et de sa structure, sur la propagation de la solution.

Dans cette partie, nous nous intéressons au mode de dispersion. Jusqu'à présent la dispersion a été modélisée par un terme de diffusion $\mathcal{D}(u) = \partial^2 u/\partial x^2$. Cette approche locale suppose que les individus présents à un instant t à la position x ne peuvent diffuser que vers leurs voisins immédiats. Cette dispersion de proche en proche n'est pas adaptée à toutes les situations, notamment lorsque les individus peuvent être déplacés à longue distance. Le célèbre paradoxe de Reid [149], sur la migration rapide d'arbres en Europe, en est une illustration. En étudiant les paléorelevés de la distribution des arbres en Europe (notamment du chêne) depuis la dernière glaciation, Reid a observé une contradiction entre les vitesses de colonisation élevées déduites des relevés et les vitesses plutôt faibles qui peuvent être déduites de simulations. En particulier, il estime que la colonisation de l'Europe par le chêne, qui a commencé après la dernière glaciation, c'est-à-dire il y a 10 000 ans, aurait dû mettre quelques millions d'années pour arriver au stade actuel si on se base sur les taux de dispersion potentiels mesurés par

l'expérience. Les deux explications possibles de cette recolonisation rapide sont l'apparition d'événements rares de dispersion à longue distance durant la recolonisation, qui modifient la migration et augmentent le taux de migration, et l'existence de refuges cryptiques en Europe, qui auraient permis de faire le relais et d'accélérer la recolonisation [157]. Kot *et al.* [113], Clark [43] et Clark *et al.* [44] ont proposé des modèles d'équations intégro-différentielles, avec des noyaux à queue lourde ou non-exponentiellement bornés, de la forme :

$$\frac{\partial u}{\partial t}(t,x) = \int_{\mathbb{R}} J(|x-y|)u(t,y)dy - u(t,x) + f(u(t,x)),\ t>0 \text{ et } x \in \mathbb{R},$$

pour prendre en compte les événements de dispersion à longue distance. Le noyau de dispersion J modélise la manière dont les individus peuvent se déplacer dans l'espace. Plus précisément, le terme $J(|x-y|)dy$ représente la probabilité pour un individu provenant d'un point y d'arriver en un point x par unité de temps. Ainsi la proportion d'individus qui migrent vers la position x durant un pas de temps est donnée par $\int_{\mathbb{R}} J(|x-y|)u(t,y)dy$. La variation temporelle δu d'individus provoquée par la dispersion est donc donnée par :

$$\delta u(t,x) = \int_{\mathbb{R}} J(|x-y|)u(t,y)dy - u(t,x).$$

La nature non-exponentiellement bornée est l'hypothèse fondamentale qui conduit à des comportement qualitativement très différents de ceux attendus pour des équations de réaction-diffusion ou d'équation intégro-différentielles avec noyau de dispersion exponentiellement borné, partant de données initiales à support compact. Ces résultats avaient déjà été mis en évidence dans le cadre des processus de contact [60, 131, 132, 133, 138].

Dans [Ga11], on s'intéresse aux solutions u de (3) partant d'une donnée initiale u_0 à support compact. La nonlinéarité f est régulière et de type monostable (A) et le noyau de dispersion J est une densité de probabilité régulière, symétrique et de premier moment fini :

$$J \in \mathcal{C}^0(\mathbb{R}),\ \ J>0,\ \ J(x)=J(-x),\ \ \int_{\mathbb{R}} J(x)dx = 1 \text{ et } \int_{\mathbb{R}} |x|J(x)dx < \infty,$$

dont la décroissance est lente, au sens où :

$$\text{pour tout } \eta>0, \quad \text{il existe } x_\eta \in \mathbb{R}, \quad \text{tel que } J(x) \geq e^{-\eta x} \text{ dans } [x_\eta, \infty).$$

Ce type de noyau est appelé noyau non-exponentiellement borné. Les exemples les plus classiques de ce type de noyau sont :

(i) les fonctions J à décroissance logarithmique sous linéaire, c'est-à-dire

$$J(x) = Ce^{-\alpha|x|/\ln(|x|)} \text{ pour } |x| \text{ assez grand,} \tag{19}$$

avec $\alpha>0$, $C>0$;

(ii) les fonctions J qui décroissent en exponentielle-puissance, c'est-à-dire

$$J(x) = Ce^{-\beta|x|^\alpha} \text{ pour } |x| \text{ assez grand,} \tag{20}$$

avec $\alpha \in]0,1[$, β, $C>0$;

(iii) les fonctions J à décroissance algébrique, c'est-à-dire

$$J(x) = C|x|^{-\alpha} \text{ pour } |x| \text{ assez grand,} \tag{21}$$

avec $\alpha>2$, $C>0$.

Cette hypothèse de noyau non-exponentiellement borné contraste avec les hypothèses de la plupart des travaux sur les équations intégro-différentielles [8, 47, 54, 173, 185, 186] ou les équations d'intégro-différences [122, 123]. En effet, ces études considèrent généralement des noyaux de dispersion J exponentiellement bornés, dans le sens où :

$$\text{il existe } \eta > 0 \text{ tel que } \int_{\mathbb{R}} J(x)e^{\eta|x|} < \infty.$$

Pour ce type de noyaux, Weinberger [185] a montré que les solutions de (3), avec f monostable (A), partant de données initiales à support compact se propagent asymptotiquement à vitesse finie c^* (voir figure 19(b)). Nous rappelons que cette propriété de propagation à vitesse finie des solutions est aussi partagée par les solutions d'équations de réaction-diffusion en milieu homogène [9, 10, 72, 112]. L'existence d'une unique vitesse de propagation finie reste vraie dans la plupart des équations intégro-différentielles avec un noyau de dispersion exponentiellement borné [8, 54, 173, 185].

À l'inverse, les solutions des équations intégro-différentielles avec noyaux de dispersion non-exponentiellement bornés se comportent totalement différemment. Tout d'abord, ces équations ne possèdent pas de solutions de type front, se propageant à vitesse constante et profil constant [191]. D'autre part, les études numériques et les calculs formels menés par Kot *et al.* [113] sur les équations intégro-différentielles linéaires et par Medlock et Kot [129] sur les équations d'intégro-différences, montrent que la présence de noyaux de dispersion non-exponentiellement bornés entraîne une vitesse asymptotique de propagation infinie et une accélération des solutions.

Notre objectif est d'une part de proposer des résultats théoriques venant corroborer ces études et d'autre part de comprendre le rôle de la queue de distribution du noyau de dispersion dans le phénomène d'accélération. Notre approche s'inspire de celle utilisée par Hamel et Roques [88], grâce à laquelle ils ont montré que les solutions de modèles de réaction-diffusion homogènes, avec des nonlinéarités monostables (A), partant de données initiales non-exponentiellement bornées, accélèrent au cours du temps et ont une vitesse de propagation infinie. Plus précisément, nous nous intéressons à l'évolution au cours du temps des ensembles de niveaux $E_\lambda(t), \lambda \in]0,1[$, de la solution u de (3). Rappelons que par le principe du maximum, si la donnée initiale u_0 est dans $[0,1]$, la solution u reste dans cet ensemble pour tous les temps. Ainsi, pour chaque valeur $\lambda \in]0,1[$, on peut définir pour tout temps t suffisamment grand, l'ensemble de niveau λ, noté $E_\lambda(t)$:

$$E_\lambda(t) := \{x \in \mathbb{R}, \text{ tels que } u(t,x) = \lambda\},$$

l'ensemble des points $x \in \mathbb{R}$ tels que la solution u soit égale à λ à l'instant t. On obtient les résultats suivants :

Théorème 6. *Soit u une solution de (3), avec J un noyau non-exponentiellement borné. Si u part d'une donnée initiale $u_0 : \mathbb{R} \to [0,1]$ ($u_0 \not\equiv 0$), à support compact, alors*
(i) ***Vitesse de propagation infinie :***

$$\textit{pour tout } c \geq 0, \quad \min_{|x| \leq ct} u(t,x) \to 1 \quad \textit{lorsque } t \to \infty.$$

(ii) ***Estimations de l'évolution des*** *E_λ : il existe $\rho \geq f'(0)$, tel que pour tout $\lambda \in]0,1[$ et $\varepsilon \in (0, f'(0))$, il existe $T_{\lambda,\varepsilon} \geq 0$ tel que pour tout $t \geq T_{\lambda,\varepsilon}$:*

$$E_\lambda(t) \subset J^{-1}\left\{\left]0, e^{-(f'(0)-\varepsilon)t}\right]\right\} \tag{22}$$

et

$$E_\lambda(t) \subset J^{-1}\left\{\left[e^{-\rho t}, J(0)\right]\right\}. \tag{23}$$

Le premier résultat implique que la vitesse asymptotique de propagation des lignes de niveau est infinie, dans le sens où :

$$\lim_{t\to+\infty} \frac{\min\left\{E_\lambda(t)\cap[0,+\infty[\right\}}{t} = \lim_{t\to+\infty} \frac{-\max\left\{E_\lambda(t)\cap]-\infty,0]\right\}}{t} = +\infty,$$

pour tout $\lambda \in]0,1[$. Cette accélération des lignes de niveaux est illustrée sur la figure 19(a). On observe que pour un pas de temps fixé entre les différentes courbes, l'écart augmente contrairement au cas d'un noyau de dispersion exponentiellement borné illustré par la figure 19(b). De plus, on observe un aplatissement de la solution. Il indique que les lignes de niveaux s'écartent les unes des autres. En d'autres termes les lignes de niveaux associées à un λ petit vont plus vite que celle associées à un λ proche de 1. Cette déformation de la solution a aussi été observée et démontrée dans les travaux de Hamel et Roques [88].

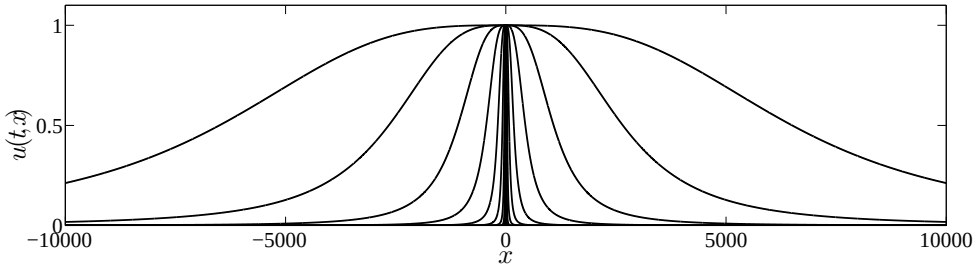

(a) Accélération de la solution

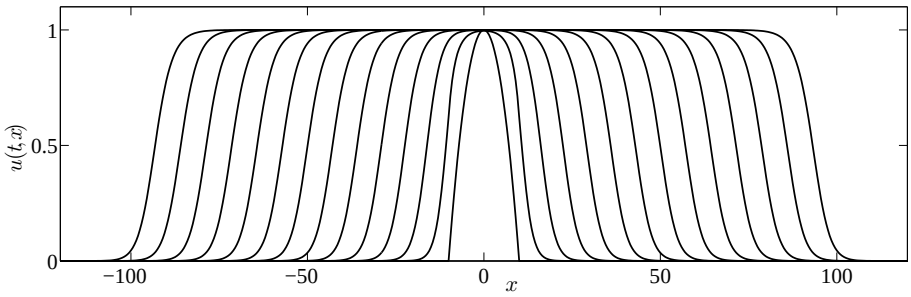

(b) Propagation à vitesse finie constante

FIGURE 19 – La solution $u(t,x)$ du modèle (3) à des temps successifs $t = 0, 3, \ldots, 30$: (a) avec un noyau à queue lourde, (b) avec un noyau à queue légère.

Le second résultat nous donne des estimations de la position des ensembles $E_\lambda(t)$ pour des temps grands. Les inclusions (22) et (23) montrent que tout élément $x_\lambda(t) \in E_\lambda(t)$ vérifie en temps grand les inégalités suivantes :

$$\min\left(J^{-1}\left(e^{-(f'(0)-\varepsilon)t}\right)\cap[0,+\infty)\right) \leq \ |x_\lambda(t)| \ \leq \max\left(J^{-1}\left(e^{-\rho t}\right)\cap[0,+\infty)\right).$$

En particulier, en reprenant les exemples précédents (i)-(iii), on obtient les estimations suivantes :

(i) si J décroît logarithmiquement de manière sous-linéaire, au sens de (19), alors les lignes de niveaux avancent sur-linéairement en temps t et on a pour tout $\lambda \in]0,1[$ et $\varepsilon \in]0, f'(0)[$

$$\frac{f'(0)-\varepsilon}{\alpha}\, t\ln(t) \ \leq \ |x_\lambda(t)| \ \leq \ \frac{\rho}{\alpha} t\ln(t) \ \text{ pour } t \text{ assez grand ;}$$

(ii) si J décroît en exponentielle-puissance, au sens de (20), alors les lignes de niveaux avancent algébriquement en temps t et on a pour tout $\lambda \in]0,1[$ et $\varepsilon \in]0, f'(0)[$

$$\left(\frac{f'(0)-\varepsilon}{\beta}\right)^{1/\alpha} t^{1/\alpha} \leq |x_\lambda(t)| \leq \left(\frac{\rho}{\beta}\right)^{1/\alpha} t^{1/\alpha} \quad \text{pour } t \text{ assez grand ;}$$

Cet exemple est illustré sur la figure 20.

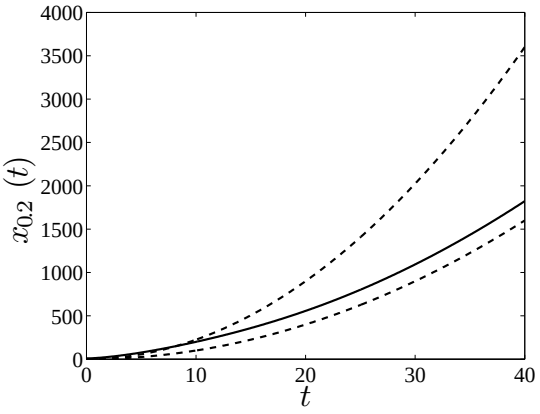

FIGURE 20 – Trait plein : position $x_{0.2}(t)$ de la ligne de niveau $E_{0.2}(t)$ de la solution de (3) avec $f(u) = u(1-u)$, $u_0(x) = \max((1-(x/10)^2), 0)$ et le noyau de dispersion non exponentiellement borné $J(x) = (1/4)e^{-\sqrt{|x|}}$. Cette position $x_{0.2}(t)$ est encadrée par les deux courbes en pointillés $t \mapsto J^{-1}(e^{-f'(0)t}) = (t - \ln(4))^2$ et $J^{-1}(e^{-(f'(0)+1/2)t}) = (3t/2 - \ln(4))^2$ pour des temps t assez grands.

(iii) si J décroît algébriquement, au sens de (21), alors les lignes de niveaux avancent exponentiellement en temps t et on a pour tout $\lambda \in]0,1[$ et $\varepsilon \in]0, f'(0)[$

$$\frac{f'(0)-\varepsilon}{\alpha}\, t \;\leq\; \ln\left(|x_\lambda(t)|\right) \;\leq\; \frac{\rho}{\alpha}\, t \quad \text{pour } t \text{ assez grand .}$$

Nos résultats, obtenus avec des données initiales à support compact et des noyaux de dispersion non exponentiellement bornés, sont comparables à ceux décrits par Hamel et Roques [88]. Leurs données initiales à décroissance non-exponentiellement bornée deviennent à support compact dans nos résultats, donc localisées, alors que leur mode de dispersion local, diffusif, devient non-local et non-exponentiellement borné dans notre étude. Comme nous l'avons souligné précédemment, ces résultats similaires ont des interprétations écologiques totalement différentes. Dans le contexte d'une colonisation post-glaciaire, la décroissance non-exponentiellement bornée de la donnée initiale correspond à l'existence de refuges cryptiques alors qu'un noyau de dispersion non-exponentiellement borné modélise l'apparition de phénomènes de dispersion à longue distance.

D'un point de vue mathématique, bien que les approches soient analogues, la nature non-locale de l'opérateur de dispersion $\mathcal{D}(u) = J \star u - u$ oblige, notamment dans la construction de sur- et sous-solutions, à tenir compte de toute la solution dans les estimations. Par exemple, le fait que le maximum de deux sous-solutions soit une sous-solution, est plus difficilement applicable par rapport au cas d'un opérateur local comme le Laplacien, $\mathcal{D}(u) = \partial^2 u/\partial x^2$. En outre, contrairement au cas de l'équation de la chaleur classique, le noyau de la chaleur $p(t,x)$, associé à l'opérateur non-local $\mathcal{D}(u) = J \star u - u$, vérifiant $\partial_t p = \mathcal{D}(p)$, n'est pas connu explicitement. Chasseigne *et al.* [40] ont donné des estimations de cette solution mais elles ne sont pas assez précises pour être utilisées dans notre étude.

Dans un autre contexte, Cabré et Roquejoffre [36, 37] ont obtenu des estimations plus précise que (22) et (23) pour les lignes de niveaux de solutions d'équations de réaction-diffusion non-locales de la forme, $\partial_t u = Au + f(u)$, avec des nonlinéarités f concaves, *i.e.* vérifiant l'hypothèse KPP, des données initiales à support compact ou de type Heaviside et un opérateur A générateur d'un semi-groupe de Feller. L'exemple classique de tels opérateurs est le Laplacien fractionnaire $A := -(-\Delta)^\alpha$, avec $\alpha \in]0,1[$, défini pour des fonctions u régulières et bornées par

$$(-\Delta)^\alpha u(x) = c_\alpha \int_{\mathbb{R}} \frac{u(x)-u(y)}{|x-y|^{1+2\alpha}} dy, \quad \text{pour tout } x \in \mathbb{R},$$

où c_α est une constante telle que le symbole de $(-\Delta)^\alpha$ soit $|\xi|^{2\alpha}$ et l'intégrale est au sens de la valeur principale de Cauchy. Dans leur cas, l'accélération des solutions vient de la décroissance algébrique du noyau de dispersion $J_\alpha(x) = |x|^{-(1+2\alpha)}$ associé à l'opérateur A. Par exemple, pour $\alpha = 1/2$, $f(u) = u(1-u)$ et des données initiales à support compact, ils obtiennent les encadrements suivants pour toutes les lignes de niveaux $\lambda \in]0,1[$:

$$-C_\lambda e^{t/2} \le x_\lambda^-(t) \le -\frac{1}{C_\lambda} e^{t/2} \quad \text{et} \quad \frac{1}{C_\lambda} e^{t/2} \le x_\lambda^+(t) \le C_\lambda e^{t/2} \quad \text{pour } t \text{ assez grand},$$

avec $C_\lambda > 1$, et $x_\lambda^-(t) = \inf\{x : u(t,x) = \lambda\}$ et $x_\lambda^+(t) = \sup\{x : u(t,x) = \lambda\}$ représentent les éléments de l'ensemble de niveau $E_\lambda(t)$ les plus en avant et les plus en arrière. Ces bornes, plus précises que celles présentées dans nos résultats, sont obtenues grâce à des estimations très fines du noyau de la chaleur associé à l'opérateur A. Elles leur permettent en particulier de construire des sur- et sous-solutions très précises de leur problème. Notons que le noyau J_α de l'opérateur A est singulier en 0 contrairement à nos noyaux de dispersion J réguliers et qu'il est à décroissance algébrique alors que le noyau J peut décroître plus rapidement.

3 Perspectives

3.1 Fronts tirés, fronts poussés et génétique des populations

Dans la première partie, nous avons montré que les notions de fronts tirés et poussés peuvent être définies à partir du comportement interne des solutions. En outre, cette définition coïncide avec celle proposée par Stokes [172] basée sur la vitesse d'expansion des fronts. Notre nouvelle définition, plus intuitive, a l'avantage de s'adapter à des modèles variés et complexes qui ne possèdent pas nécessairement de fronts progressifs. Une perspective de ce travail est de déterminer la nature poussée ou tirée des solutions des problèmes suivants :

(i) les équations intégro-différentielles prenant en compte la dispersion à longue distance et les phénomènes d'accélération [Ga11, 113] ;

(ii) les équations de réaction-diffusion en milieu hétérogène possédant des fronts pulsatoires ou des fronts généralisés [19, 21, 190] ;

(iii) les équations de réaction-diffusion à vitesse forcée, utilisées par Berestycki *et al.* [17] pour étudier l'effet d'un changement climatique sur la dynamique d'espèces biologiques ;

(iv) les équations de réaction-diffusion avec retard en temps, utilisées en écologie pour prendre en compte l'existence d'une phase juvénile [95, 111, 165].

Ces différentes équations modélisent des processus fréquemment étudiés en écologie, mais dont les effets sur la diversité génétique ne sont pas ou peu connus et demandent donc une attention toute particulière.

3.2 Effet de la fragmentation de la donnée initiale en habitat hétérogène

Dans la section 1.3 de la première partie, nous avons montré que la fragmentation du support de la donnée initiale a un effet négatif sur la survie de la solution en habitat homogène et en présence d'un effet Allee. On peut se demander si cet effet néfaste persiste en milieu hétérogène. Prenons par exemple le problème hétérogène suivant :

$$\left\{ \begin{array}{rcl} \dfrac{\partial u}{\partial t}(t,x) & = & \dfrac{\partial^2 u}{\partial x^2}(t,x) + f(u(t,x)) + \nu(x)u(t,x),\ t>0,\ x\in\mathbb{R}^2, \\ u(0,x) & = & u_0(x),\ x\in\mathbb{R}^2. \end{array} \right.$$

où le terme $\nu(x)$ correspond à l'effet de l'environnement sur le taux de croissance de la population. Dans ce cas, l'effet négatif de la fragmentation du support de u_0 peut être compensé par le fait qu'un support fragmenté a plus de chance d'intersecter les zones favorables de l'habitat. On s'attend donc à un effet croisé du degré d'hétérogénéité du milieu et de la fragmentation du support de u_0.

3.3 Vitesse d'expansion en milieu hétérogène

En utilisant nos résultats obtenus dans [GGN12], nous espérons montrer l'existence de fronts de propagation d'une nature plus générale que les fronts étudiés classiquement dans les milieux homogènes ou périodiques. Plus précisément, en s'appuyant sur la définition des fronts généralisés proposée par Berestycki et Hamel [21], une perspective serait de montrer que les solutions de notre problème (13) convergent vers un front généralisé au sens de [21]. Une telle affirmation exhiberait d'une part des fronts de transition qui vont à la vitesse c^*_∞, vitesse du problème périodique de période infinie. D'autre part, elle permettrait de construire des fronts dont la vitesse de propagation n'est pas asymptotiquement constante en temps grand, dans le cas où $w_* < w^*$.

3.4 Dispersion à longue distance

Dans la troisième partie, nous nous sommes principalement intéressés à la propagation des solutions de modèles intégro-différentiels avec noyau de dispersion non-exponentiellement borné. Nous avons montré que ces solutions accélèrent. Une perspective est de décrire le profil avec lequel ces solutions se déplacent. Plus précisément, on peut se demander si ces solutions convergent vers un front accéléré de la forme $u(t,x) = U(x - c(t))$, où $c(t)$ serait une fonction sur-linéaire du temps t. Mes simulations numériques suggèrent que la réponse est négative puisque le profil de la solution s'aplatit au cours du temps (cf. figure 19(a)). Les simulations laissent aussi penser que les solutions ne sont pas des fronts de transition au sens de Berestycki et Hamel [20, 21]. Un résultat similaire a été prouvé par Hamel et Roques [88] pour des solutions de l'équation de réaction-diffusion homogène (2), partant d'une donnée initiale non-exponentiellement bornée. Dans notre cas, une telle preuve semble plus compliquée car l'opérateur de dispersion $\mathcal{D}(u) : u \mapsto J \star u - u$ n'est pas un opérateur différentiel.

Plan de la thèse

Cette thèse se décompose en trois parties. La première est consacrée à l'étude des équations de réaction-diffusion en milieu homogène. Le Chapitre 1 est consacré aux notions de fronts tirés et poussés décrites dans la section 1.1. Les résultats exposés dans ce chapitre ont été publiés dans le *Journal de Mathématiques Pures et Appliquées*. Le Chapitre 2 présente les conséquences bénéfiques de l'effet Allee sur la diversité génétique durant une phase de colonisation. Ces travaux sont publiés dans les *Proceedings of the National Academy of Sciences of the United States of America*. Enfin le dernier chapitre de cette partie, le Chapitre 3, présente les effets de la répartition initiale de la donnée initiale sur le succès de la phase d'installation d'une invasion biologique. Ces résultats ont été publiés dans le *Bulletin of Mathematical Biology*.

Le seconde partie traite des équations de réaction-diffusion en milieu hétérogène. Le premier chapitre de cette partie, le Chapitre 4, développe les résultats obtenus sur la vitesse de propagation des solutions d'équations de réaction-diffusion dans un milieu de plus en plus lentement oscillant. Ces résultats ont été publiés dans le *Journal of Dynamics and Differential Equations*. Le Chapitre 5 décrit des résultats d'unicité des coefficients hétérogènes de problèmes de réaction-diffusion. Ils sont publiés dans les *Communications on Pure and Applied Analysis*.

La troisième et dernière partie est consacrée aux problèmes intégro-différentiels en milieu homogène. Le Chapitre 6 expose les résultats d'accélération des solutions des problèmes intégro-différentiels avec noyaux de dispersion non-exponentiellement bornés. Ce travail a été publié dans *SIAM Journal on Mathematical Analysis*.

Deuxième partie

Les modèles de réaction-diffusion en milieu homogène : effet Allee et structuration spatiale

Chapitre 1

Inside dynamics of pulled and pushed fronts

Ce travail réalisé en collaboration avec Thomas Giletti [a], François Hamel [a,b] et Lionel Roques [c] est publié dans le *Journal de Mathématiques Pures et Appliquées* [GGHR12]

[a] Aix-Marseille Université, LATP UMR 6632, Faculté des Sciences et Techniques
Avenue Escadrille Normandie-Niemen, F-13397 Marseille Cedex 20, France
[b] Institut Universitaire de France
[c] UR 546 Biostatistique et Processus Spatiaux, INRA, F-84000 Avignon, France

Sommaire

1.1 Introduction

In this chapter, we explore the spatial structure of traveling wave solutions of some reaction-diffusion equations. Namely, we consider the following one-dimensional reaction-diffusion model :

$$\partial_t u(t,x) = \partial_x^2 u(t,x) + f(u(t,x)), \quad t>0,\ x\in\mathbb{R}, \tag{1.1}$$

where $u(t,x)\in[0,1]$. This equation arises in various scientific domains of application, namely, population dynamics where the unknown quantity u typically stands for a population density [34, 45, 79, 103, 135], chemistry [32, 70], and combustion [27]. In the context of population dynamics, $f(u)$ corresponds to the population's growth rate. The nonlinear growth term f in (1.1) is assumed to satisfy

$$f\in C^1([0,1]), \quad f(0)=f(1)=0, \quad \int_0^1 f(s)\,ds>0 \tag{1.2}$$

and to be either of the monostable, bistable or ignition type :

(A) Monostable f is *monostable* if it satisfies (1.2), $f'(0)>0$, $f'(1)<0$ and $f>0$ in $(0,1)$.

In this case, the growth rate $f(u)$ is always positive on $(0,1)$. A classical monostable example is $f(u)=u(1-u)(1+au)$, with $a\geq 0$. If $a\leq 1$, the per capita growth rate $f(u)/u$ (defined by $f'(0)$ at $u=0$) is decreasing over the interval $[0,1]$ which means that f is of the KPP (for Kolmogorov-Petrovsky-Piskunov [112]) type. On the other hand, if $a>1$, the maximum of the per capita growth rate is not reached at $u=0$. In population dynamics, this corresponds to a so-called weak Allee effect [175].

(B) Bistable f is *bistable* if it satisfies (1.2), $f'(0)<0$, $f'(1)<0$ and there exists $\rho\in(0,1)$ such that $f<0$ in $(0,\rho)$ and $f>0$ in $(\rho,1)$.

This hypothesis means that the growth rate $f(u)$ is negative at low densities, which corresponds to a strong Allee effect [118, 175]. The parameter ρ corresponds to the so-called "Allee threshold" below which the growth rate becomes negative. For instance, the cubical function $f(u)=u(1-u)(u-\rho)$, where ρ belongs to $(0,1/2)$, is a bistable nonlinearity.

(C) Ignition f is of *ignition* type if it satisfies (1.2), $f'(1)<0$ and there exists $\rho\in(0,1)$ such that $f=0$ in $(0,\rho)$ and $f>0$ in $(\rho,1)$. This reaction term occurs in combustion problems, where u corresponds to a temperature and ρ is the ignition temperature [27, 29, 152].

The equation (1.1) has been extensively used to model spatial propagation of elements in interaction, in parts because it admits traveling wave solutions. These particular solutions keep a constant profile U and move at a constant speed c. Aronson and Weinberger [9, 10] and Kanel [101] have proved that equation (1.1) with monostable, bistable or ignition nonlinearities admits traveling waves solutions of the form $u(t,x)=U(x-ct)$, where $c\in\mathbb{R}$ and the profile U is a $\mathcal{C}^3(\mathbb{R})$ function which satisfies the following nonlinear elliptic equation :

$$\begin{cases} U''(y)+cU'(y)+f(U(y))=0, & y\in\mathbb{R},\\ U(-\infty)=1, \quad U(+\infty)=0 \ \text{ and } \ 0<U<1 \text{ on } \mathbb{R}. \end{cases} \tag{1.3}$$

On the one hand, if f is of the monostable type (A), there exists a minimal speed $c^*\geq 2\sqrt{f'(0)}>0$ such that equation (1.3) admits a solution if and only if $c\geq c^*$. The solution associated to the minimal speed c^* is called the *critical front*, while those associated to speeds $c>c^*$ are called *super-critical fronts.* On the other hand, if f is of the bistable (B) or ignition (C) types there exists a unique speed

$c > 0$ such that equation (1.3) admits a solution. In all cases, if the front (c, U) exists, the profile U is a decreasing function and it is unique up to shift [see e.g. 10, 29, 71]. The asymptotic behavior of $U(y)$ as $|y| \to +\infty$ is also known (see Section 1.2).

The sensitivity of the fronts to noise or a fixed perturbation has also been extensively studied, [see e.g. 33, 61, 71, 116, 163, 164, 177]. In the monostable case, the stability studies lead to a classification of the fronts into two types : "pulled" fronts and "pushed" fronts [161, 172, 178]. A *pulled* front is either a critical front (c^*, U) such that the minimal speed c^* satisfies $c^* = 2\sqrt{f'(0)}$, or any super-critical front. In the critical case the name pulled front comes from the fact that the front moves at the same speed as the solution of the linearized problem around the unstable state 0, which means that it is being pulled along by its leading edge. This denomination is not so immediate for super-critical fronts. A *pushed* front is a critical front (c^*, U) such that the minimal speed c^* satisfies $c^* > 2\sqrt{f'(0)}$. The speed of propagation of a pushed front is determined not by the behavior of the leading edge of the distribution, but by the whole front. This means that the front is pushed from behind by the nonlinear growth rate in the nonlinear front region itself. A substantial analysis which is not restricted to the monostable case and which relies on the variational structure and the exponential decay of the fronts for more general gradient systems has been carried out in [121, 134].

In the present chapter, we use a completely different and new approach, which we believe to be simpler and more intuitive, by analyzing the dynamics of the inside structure of the fronts. The results we obtain on the large-time behavior of the components of the fronts in the moving frame and in the whole real line (the precise statements will be given below) shed a new light on and are in keeping with the pulled/pushed terminology in the monostable case as well as with the fact that the bistable or ignition fronts can be viewed as pushed fronts. Even if more general equations or systems could have been considered, we present the results for the one-dimensional equation (1.1) only, for the sake of simplicity and since this simple one-dimensional situation is sufficient to capture the main interesting properties of the spatial structure of the fronts (however, based on the results of the present chapter and on some recent notions of generalized transition waves, we propose in Section 2.2 some definitions of pulled and pushed transition waves in a more general setting).

Let us now describe more precisely the model used in this chapter. Following the ideas described in [82, 83, 181], we assume that the fronts are made of several components and we study the behavior of these components. Namely, we consider a traveling wave solution

$$u(t, x) = U(x - ct)$$

of (1.1), where the profile U satisfies (1.3) and c is the front speed, and we assume that u is initially composed of different groups $(v_0^i(x))_{i \in I}$ such that, for every $i \in I$,

$$v_0^i \not\equiv 0 \quad \text{and} \quad 0 \leq v_0^i(x) \leq U(x) \text{ for all } x \in \mathbb{R}, \tag{1.4}$$

where I is a subset of $\mathbb{N}$ and

$$u(0, x) = U(x) = \sum_{i \in I} v_0^i(x) \text{ for all } x \in \mathbb{R}.$$

Moreover, all groups v^i are assumed to share the same characteristics in the sense that they diffuse and grow with the same manner inside the front $u(t, x)$, [see 82, 83, 181]. This means that the diffusion coefficient of each group is equal to 1 and that the per capita growth rate of each group depends only

on the entire population and is the same as that of the global front, namely

$$g(u(t,x)) := \frac{f(u(t,x))}{u(t,x)} \text{ for all } t \geq 0 \text{ and } x \in \mathbb{R}.$$

In other words, the groups $(v^i(t,x))_{i\in I}$ satisfy the following equation :

$$\begin{cases} \partial_t v^i(t,x) &= \partial_x^2 v^i(t,x) + g(u(t,x))v^i(t,x), \quad t>0,\ x\in\mathbb{R}, \\ v^i(0,x) &= v_0^i(x), \qquad\qquad\qquad\qquad\quad x\in\mathbb{R}. \end{cases} \tag{1.5}$$

Of course it follows from the uniqueness of the solution that

$$u(t,x) = \sum_{i\in I} v^i(t,x) \text{ for all } t>0 \text{ and } x\in\mathbb{R},$$

which implies that the per capita growth rate $g(u(t,x)) = g\big(\sum_{i\in I} v^i(t,x)\big)$ could be viewed as a coupling term in the system (1.5). The following inequalities also hold from maximum principle

$$0 < v^i(t,x) \leq u(t,x) < 1 \text{ for all } t>0,\ x\in\mathbb{R} \text{ and } i\in I. \tag{1.6}$$

Because the components v^i in (1.5) have identical growth and dispersal characteristics, we only have to focus on the behavior of one arbitrarily chosen component v^i – we call it v in the sequel – to understand the behavior of all the components. This is in sharp contrast with standard competitive systems such as the model of competition between a resident species and an invading species for large open space mentioned in [103, Section 7.2], where usually one of the elements is in some sense stronger than the other one and thus governs the propagation.

Even if the equation (1.1) is homogeneous and the system (1.5) is linear, one of the main difficulties in our study comes from the fact that a space-time heterogeneity is present in the per capita growth rate $g(u(t,x))$ of each element. It turns out that this heterogeneity does not fulfill any periodicity or monotonicity property. Comparable problems have been studied in [30, 84, 85]. In these papers, the authors have considered a reaction term of the form $f(x-ct,v)$, where the function $v \mapsto f(x,v)$ is of the monostable or bistable type for every x and is nonpositive for v large enough uniformly in x. These properties are not fulfilled here by the function $(t,x,v) \mapsto g(u(t,x))\,v$. For instance, if the reaction term f is of type (A), then $g(u(t,x))$ is always positive. Actually, we prove that the behavior of the groups v^i mainly depends on the type of f, as well as on the initial condition.

The next section is devoted to the statement of our main results. We begin by recalling some asymptotic properties of the solution $U(y)$ of (1.3), as $y \to +\infty$. Then, the evolution of the density of a group v solving (1.5) is described in two theorems. Theorem 1 deals with the monostable pulled case and Theorem 2 deals with the monostable pushed case and the bistable and ignition cases. These results show striking differences between the composition of the fronts in the pulled and pushed cases. They lead us to propose new notions of pulled and pushed transition waves in a general setting. The proofs of our results are detailed in Sections 1.3 and 1.4.

1.2 Main Results

Let $u(t,x) = U(x-ct)$ be a traveling wave solution of (1.1) associated to a front (c,U) solving (1.3), where f is either of type (A), (B) or (C). In order to understand the dynamics of a component v solving (1.4)-(1.5), inside the traveling wave solution, it is natural to make the following change of variables :

$$\tilde{u}(t,x) = v(t,x+ct) \text{ for all } t\geq 0 \text{ and } x\in\mathbb{R}.$$

The function $\tilde{u}$ corresponds to the solution v in the moving reference at speed c and it obeys the following equation :

$$\begin{cases} \partial_t \tilde{u}(t,x) &= \partial_x^2 \tilde{u}(t,x) + c\partial_x \tilde{u}(t,x) + g(U(x))\tilde{u}(t,x), & t>0,\ x\in\mathbb{R}, \\ \tilde{u}(0,x) &= v_0(x), & x\in\mathbb{R}. \end{cases} \tag{1.7}$$

Thus, the equation (1.5) which contains a space-time heterogeneous coefficient reduces to a the reaction-diffusion equation with a spatially heterogeneous coefficient $g(U(x))$, which only depends on the profile U of the front. As we will see, the leading edge of U, and therefore its asymptotic behavior as $x \to +\infty$, plays a central role in the dynamics of the solutions of (1.7). Before stating our main results, we recall some useful known facts about the asymptotic behavior of the fronts.

Monostable case (A). On the one hand, a pulled critical front (c^*, U), whose speed c^* satisfies $c^* = 2\sqrt{f'(0)}$, decays to 0 at $+\infty$ as follows [9, 10] :

$$U(y) = (Ay + B)\, e^{-\frac{c^* y}{2}} + O\left(e^{-(\frac{c^*}{2}+\delta)y}\right) \quad \text{as } y \to +\infty, \tag{1.8}$$

where $\delta > 0$, $A \geq 0$, and $B > 0$ if $A = 0$. If f is of the particular KPP type (that is $g(s) = f(s)/s \leq f'(0)$) then $A > 0$. On the other hand, a pushed critical front (c^*, U), whose speed c^* is such that $c^* > 2\sqrt{f'(0)}$, satisfies the following asymptotic property :

$$U(y) = A\, e^{-\lambda_+(c^*)y} + O\left(e^{-(\lambda_+(c^*)+\delta)y}\right) \quad \text{as } y \to +\infty, \tag{1.9}$$

where $\delta > 0$, $A > 0$ and $\lambda_+(c^*) = (c^* + \sqrt{(c^*)^2 - 4f'(0)})/2 > c^*/2$. Thus, the asymptotic behavior of a monostable critical front does depend on its pulled/pushed nature. Lastly, a super-critical front (c, U), where c satisfies $c > c^*$, also decays at an exponential rate slower than $c/2$:

$$U(y) = A\, e^{-\lambda_-(c)y} + O\left(e^{-(\lambda_-(c)+\delta)y}\right) \quad \text{as } y \to +\infty, \tag{1.10}$$

where $\delta > 0$, $A > 0$ and $\lambda_-(c) = (c - \sqrt{c^2 - 4f'(0)})/2 < c/2$.

Bistable case (B). If follows from [9, 10, 71] that the unique front decays to 0 at $+\infty$ as follows :

$$U(y) = A\, e^{-\mu\, y} + O\left(e^{-(\mu+\delta)y}\right) \quad \text{as } y \to +\infty, \tag{1.11}$$

where $\delta > 0$, $A > 0$, and $\mu = (c + \sqrt{c^2 - 4f'(0)})/2 > c > c/2$.

Ignition case (C). The unique front decays to 0 at $+\infty$ as follows :

$$U(y) = A\, e^{-c\, y} \text{ for } y > 0 \text{ large enough}, \tag{1.12}$$

where $A > 0$.

We notice that the asymptotic behaviors as $y \to +\infty$ of the fronts in the monostable pushed critical case and the bistable and ignition cases are quite similar. In all cases, the exponential decay rate is faster than $c/2$, where c is the speed of the front. Let us now state our main results.

2.1 The inside structure of the fronts

We first investigate the case where the nonlinearity f is of the monostable type (A) and (c, U) is a pulled front.

Theorem 1 (Pulled case)**.** *Let f be of the monostable type (A), let (c, U) be a pulled front, that is either $c = c^* = 2\sqrt{f'(0)}$ or $c > c^*$, and let v be the solution of the Cauchy problem* (1.5) *with the initial condition v_0 satisfying* (1.4) *and*

$$\int_0^{+\infty} e^{cx}\, v_0^2(x)\, dx < +\infty. \tag{1.13}$$

Then

$$\limsup_{t\to+\infty} \Big(\max_{x\geq\alpha\sqrt{t}} v(t,x)\Big) \to 0 \text{ as } \alpha \to +\infty.^{\,2} \tag{1.14}$$

In other words, any single component v of the pulled front u, which initially decays faster than the front itself, in the sense of (1.13), cannot follow the propagation of the front. In particular, the formula (1.14) implies that

$$v(t, x + ct) \to 0 \text{ uniformly on compacts as } t \to +\infty. \tag{1.15}$$

The conclusion of Theorem 1 holds if v_0 is of the type $v_0 \equiv U\, \mathbb{1}_{(-\infty,a)}$ or more generally if v_0 satisfies (1.4) and its support is included in $(-\infty, a)$ for some $a \in \mathbb{R}$. This means that the propagation of the traveling wave $u(t, x) = U(x - ct)$ is due to the leading edge of the front. This characterization agrees with the definition of pulled fronts proposed by Stokes [172]. It is noteworthy that pulled critical fronts and super-critical fronts share the same inside structure.

Note that (1.14) also implies that v cannot propagate to the right with a positive speed, in the sense that

$$\max_{x\geq\varepsilon t} v(t,x) \to 0 \text{ as } t \to +\infty$$

for all $\varepsilon > 0$. Actually, under some additional assumptions on v_0, which include the case where v_0 is compactly supported, a stronger uniform convergence result holds :

Proposition 2. *Under the assumptions of Theorem* 1*, and if v_0 satisfies the additional condition*

$$v_0(x) \to 0 \text{ as } x \to -\infty, \text{ or } v_0 \in L^p(\mathbb{R}) \text{ for some } p \in [1, +\infty), \tag{1.16}$$

then

$$v(t, \cdot) \to 0 \text{ uniformly on } \mathbb{R} \text{ as } t \to +\infty. \tag{1.17}$$

In the pushed case, the dynamics of v is completely different, as shown by the following result :

Theorem 2 (Pushed case)**.** *Let f be either of type (A) with the minimal speed c^* satisfying $c^* > 2\sqrt{f'(0)}$, or of type (B) or (C). Let (c, U) be either the critical front with $c = c^* > 2\sqrt{f'(0)}$ in case (A) or the unique front in case (B) or (C). Let v be the solution of the Cauchy problem* (1.5) *with the initial condition v_0 satisfying* (1.4)*. Then*

$$\limsup_{t\to+\infty} \Big(\max_{x\geq\alpha\sqrt{t}} |v(t,x) - p(v_0)U(x - ct)|\Big) \to 0 \text{ as } \alpha \to +\infty, \tag{1.18}$$

where $p(v_0) \in (0, 1]$ is given by

$$p(v_0) = \frac{\displaystyle\int_{\mathbb{R}} v_0(x)\, U(x)\, e^{cx}\, dx}{\displaystyle\int_{\mathbb{R}} U^2(x)\, e^{cx}\, dx}. \tag{1.19}$$

Moreover,

$$\liminf_{t\to+\infty} \Big(\min_{\alpha\sqrt{t}\leq x\leq x_0+ct} v(t,x)\Big) > 0 \text{ for all } \alpha \in \mathbb{R} \text{ and } x_0 \in \mathbb{R}. \tag{1.20}$$

2. Notice that the max in (1.14) is reached from (1.6) and the continuity of $v(t, \cdot)$ for all $t > 0$.

From (1.9), (1.11) and (1.12), $p(v_0)$ is a well defined positive real number. Theorem 2 is in sharp contrast with Theorem 1. Indeed, formula (1.18) in Theorem 2 implies that any small group inside a pushed front is able to follow the traveling wave solution in the sense

$$v(t, x + ct) \to p(v_0)\, U(x) \text{ uniformly on compacts as } t \to +\infty. \tag{1.21}$$

The conclusion (1.21) holds even if v_0 is compactly supported. This formula means that an observer who moves with a speed c will see the component v approach the proportion $p(v_0)$ of the front U. Thus, at large times, the front is made of all its initial components v_0^i defined in (1.4), each one with proportion $p(v_0^i)$. In other words the front is pushed from the inside. Theorem 2 also shows that the inside structure of the pushed monostable critical fronts and of the bistable and ignition fronts share the same dynamics.

The second formula (1.20) in Theorem 2 shows that the left spreading speed of the group v inside the front is at least equal to 0 in the reference frame. More precisely, the group spreads over intervals of the type $(\alpha\sqrt{t}, x_0 + ct)$ for all $\alpha \in \mathbb{R}$ and $x_0 \in \mathbb{R}$. In fact, the next proposition proves that, if the initial condition v_0 is small at $-\infty$, then the solution v spreads to the left with a null speed in the reference frame in the sense that v is asymptotically small in any interval of the type $(-\infty, \alpha\sqrt{t})$ for $-\alpha > 0$ large enough :

Proposition 3. *Under the assumptions of Theorem* 2*, if* v_0 *satisfies the additional assumption* (1.16)*, then*

$$\limsup_{t\to+\infty} \Big(\max_{x\le\alpha\sqrt{t}} v(t, x) \Big) \to 0 \text{ as } \alpha \to -\infty. \tag{1.22}$$

Notice that without the condition (1.16), the conclusion (1.22) may not hold. Take for instance $v_0 \equiv U$, then $v(t, x) = U(x - ct)$ for all $t \ge 0$ and $x \in \mathbb{R}$, and $\sup_{x\le\alpha\sqrt{t}} v(t, x) = 1$ for all $\alpha \in \mathbb{R}$ and $t \ge 0$.

Remark 1. a) One can observe that in the pulled case the function $x \mapsto U(x)e^{cx/2}$ does not belong to $L^2(\mathbb{R})$, from (1.8) and (1.10). Thus, we can set $p(v_0) = 0$ for any compactly supported initial condition v_0 satisfying (1.4). From Theorems 1 and 2, we can say with this convention that for any monostable reaction term f and any compactly supported v_0 fulfilling (1.4), the solution v of (1.5) is such that $v(t, x+ct) \to p(v_0)U(x)$ uniformly on compacts as $t \to +\infty$, where $p(v_0)$ is defined by (1.19) if $x \mapsto U(x)e^{cx/2}$ is in $L^2(\mathbb{R})$ (the pushed case) and $p(v_0) = 0$ otherwise (the pulled case).

b) Let us consider the family of reaction terms $(f_a)_{a\ge0}$ of the monostable type (A), defined by

$$f_a(u) = u(1 - u)(1 + au) \text{ for all } u \in [0, 1] \text{ and } a \ge 0.$$

The minimal speed c_a^* is given by [80]

$$c_a^* = \begin{cases} 2 & \text{if } 0 \le a \le 2, \\ \sqrt{\dfrac{2}{a}} + \sqrt{\dfrac{a}{2}} & \text{if } a > 2. \end{cases}$$

Thus, if $a \in [0, 2]$, the critical front U_a associated with f_a is pulled ($c_a^* = 2 = 2\sqrt{f_a'(0)}$) while if $a > 2$ the critical front is pushed ($c_a^* > 2 = 2\sqrt{f_a'(0)}$). Up to shift, one can normalize U_a so that $U_a(0) = 1/2$ for all $a \ge 0$. A direct computation shows that if $a \ge 2$ then the profile of U_a is then given by

$$U_a(x) = \frac{1}{1 + e^{\kappa_a x}} \text{ for all } x \in \mathbb{R},$$

where $\kappa_a = \sqrt{a/2}$. It is easy to check that, if $a > 2$, then the function $x \mapsto U_a(x)e^{c_a^* x/2}$ is in $L^2(\mathbb{R})$ (a general property shared by all pushed fronts) and $\int_{\mathbb{R}} U_a^2(x)\, e^{c_a^* x}\, dx \geq (\kappa_a - \kappa_a^{-1})^{-1}/4$. Then, consider a fixed compactly supported initial condition v_0 satisfying (1.4) and whose support is included in $[-B, B]$ with $B > 0$. Let $p(v_0, a)$ be defined by (1.19) with $a > 2$, $U = U_a$ and $c = c_a^*$. It follows that

$$0 < p(v_0, a) = \frac{\displaystyle\int_{\mathbb{R}} v_0(x)\, U_a(x)\, e^{c_a^* x}\, dx}{\displaystyle\int_{\mathbb{R}} U_a^2(x)\, e^{c_a^* x}\, dx} \leq 4(\kappa_a - \kappa_a^{-1}) \int_{-B}^{B} U_a^2(x)\, e^{c_a^* x}\, dx \leq \frac{8(\kappa_a - \kappa_a^{-1})\cosh(c_a^* B)}{c_a^*}.$$

Finally, since $\kappa_a \to 1^+$ and $c_a^* \to 2^+$ as $a \to 2^+$, we get that $p(v_0, a) \to 0$ as $a \to 2^+$. Thus, with the convention $p(v_0) = 0$ in the pulled case, this shows the proportion $p(v_0, a)$ is right-continuous at $a = 2$, which corresponds to the transition between pushed fronts and pulled fronts.

2.2 Notions of pulled and pushed transition waves in a more general setting

Our results show that the fronts can be classified in two categories according to the dynamics of their components. This classification agrees with the pulled/pushed terminology introduced by Stokes [172] in the monostable case and shows that the bistable and ignition fronts have same inside structure as the pushed monostable fronts. This classification also allows us to define the notion of pulled and pushed transition waves in a more general framework. Let us consider the following reaction-dispersion equations :

$$\partial_t u(t,x) = \mathcal{D}(u(t,x)) + f(t,x,u(t,x)), \quad t > 0,\ x \in \mathbb{R}, \tag{1.23}$$

where $f(t,x,u)$ is assumed to be of class $\mathcal{C}^{0,\beta}$ (with $\beta > 0$) in (t,x) locally in $u \in [0,+\infty)$, locally Lipschitz-continuous in u uniformly with respect to $(t,x) \in (0,+\infty) \times \mathbb{R}$, $f(\cdot,\cdot,0) = 0$, and $\mathcal{D}$ is a linear operator of dispersion. The classical examples of $\mathcal{D}$ are the homogeneous diffusion operators such as the Laplacian, $\mathcal{D}(u) = D\partial_x^2 u$ with $D > 0$, the heterogeneous diffusion operators of the form $\mathcal{D}(u) = \partial_x(a(t,x)\partial_x u)$ where $a(t,x)$ is of class $\mathcal{C}^{1,\beta}((0,+\infty)\times\mathbb{R})$ and uniformly positive, the fractional Laplacian, and the integro-differential operators $\mathcal{D}(u) = J * u - u$ where $J * u(x) = \int_{\mathbb{R}} J(x-y)u(y)dy$ for all $x \in \mathbb{R}$ and J is a smooth nonnegative kernel of mass 1. Before defining the notion of pulled and pushed waves, we recall from [21] the definition of transition waves, adapted to the Cauchy problem (1.23). Let $p^+ : (0,+\infty)\times\mathbb{R} \to [0,+\infty)$ be a classical solution of (1.23). A *transition wave* connecting $p^- = 0$ and p^+ is a positive solution u of (1.23) such that 1) $u \not\equiv p^\pm$, 2) there exist $n \in \mathbb{N}$ and some disjoint subsets $(\Omega_t^\pm)_{t>0}$ and $(\Gamma_t)_{t>0} = (\{x_t^1, \dots, x_t^n\})_{t>0}$ of $\mathbb{R}$ where $\Gamma_t = \partial\Omega_t^\pm$, $\Omega_t^- \cup \Omega_t^+ \cup \Gamma_t = \mathbb{R}$ and $\sup\{d(x,\Gamma_t) \mid x \in \Omega_t^-\} = \sup\{d(x,\Gamma_t) \mid x \in \Omega_t^+\} = +\infty$ for all $t > 0$, and 3) for all $\varepsilon > 0$ there exists $M > 0$ such that

$$\text{for all } t \in (0,+\infty) \text{ and } x \in \overline{\Omega_t^\pm},\ \Big(d(x,\Gamma_t) \geq M\Big) \Rightarrow \Big(|u(t,x) - p^\pm(t,x)| \leq \varepsilon\Big),$$

where d is the classical distance between subsets of $\mathbb{R}$. The wave u for problem (1.23) is also assumed to have a limit $u(0,\cdot)$ at $t = 0$ (usually, it is defined for all $t \in \mathbb{R}$, and f and p^+ are defined for all $t \in \mathbb{R}$ as well). In the case of Theorems 1 and 2, the travelling front $u(t,x) = U(x - ct)$ is a transition wave connecting 0 and $p^+ = 1$, the interface Γ_t can be reduced to the single point $\Gamma_t = \{x_t\} = \{ct\}$ and the two subsets $\Omega_t^\pm$ can be defined by $\Omega_t^- = (x_t, +\infty)$ and $\Omega_t^+ = (-\infty, x_t)$ for all $t > 0$.

Definition 1 (Pulled transition wave). *We say that a transition wave u connecting 0 and p^+ is* pulled *if for any subgroup v satisfying*

$$\left\{\begin{array}{rcll} \partial_t v(t,x) & = & \mathcal{D}(v(t,x)) + g(t,x,u(t,x))v(t,x), & t>0,\ x\in\mathbb{R}, \\ v(0,x) & = & v_0(x), & x\in\mathbb{R}, \end{array}\right. \tag{1.24}$$

where $g(t,x,s) = f(t,x,s)/s$ and

$$v_0 \text{ is compactly supported, } 0\le v_0\le u(0,\cdot) \text{ and } v_0\not\equiv 0, \tag{1.25}$$

there holds

$$\sup_{d(x,\Gamma_t)\le M} v(t,x)\to 0 \text{ as } t\to+\infty \text{ for all } M\ge 0.$$

Definition 2 (Pushed transition wave). *We say that a transition wave u connecting 0 to p^+ is* pushed *if for any subgroup v satisfying* (1.24)-(1.25) *there exists $M\ge 0$ such that*

$$\limsup_{t\to+\infty}\Big(\sup_{d(x,\Gamma_t)\le M} v(t,x)\Big) > 0.$$

1.3 The description of pulled fronts

We first prove the annihilation of v in the moving frame, that is property (1.15). Then we prove the result (1.14) of Theorem 1 and the result (1.17) described in Proposition 2 under the additional assumption (1.16). The proof of (1.15) draws its inspiration from the front stability analyzes in [163, 164, 178] and especially from the paper of Eckmann and Wayne [61]. It is based on some integral estimates of the ratio $r=\tilde{u}/U$ in a suitable weighted space. The proofs of (1.14) and (1.17) are based on the convergence result (1.15) and on the maximum principle together with the construction of suitable super-solutions.

3.1 Local asymptotic extinction in the moving frame : proof of (1.15)

Let f be of type (A) and let (c,U) denote a pulled front satisfying (1.3), that is c is such that either $c=c^*=2\sqrt{f'(0)}$ or $c>c^*$. Let v be the solution of (1.4)-(1.5) satisfying the condition (1.13) and let us set $\tilde{u}(t,x)=v(t,x+ct)$ for all $t\ge 0$ and $x\in\mathbb{R}$. The function $\tilde{u}$ solves (1.7), while (1.6) implies that

$$0<\tilde{u}(t,x)\le U(x)<1 \text{ for all } t>0 \text{ and } x\in\mathbb{R}. \tag{1.26}$$

Then, let us define the ratio

$$r(t,x)=\frac{\tilde{u}(t,x)}{U(x)} \text{ for all } t\ge 0 \text{ and } x\in\mathbb{R}. \tag{1.27}$$

The function r is at least of class $\mathcal{C}^1$ with respect to t and of class $\mathcal{C}^2$ with respect to x in $(0,+\infty)\times\mathbb{R}$. It satisfies the following Cauchy problem :

$$\left\{\begin{array}{rcll} \partial_t r(t,x)+\mathcal{L}r(t,x) & = & 0, & t>0,\ x\in\mathbb{R}, \\ r(0,x) & = & \dfrac{v_0(x)}{U(x)}, & x\in\mathbb{R}, \end{array}\right. \tag{1.28}$$

where

$$\mathcal{L}=-\partial_x^2-\psi'(x)\partial_x \quad\text{and}\quad \psi(x)=cx+2\ln(U(x)) \text{ for all } x\in\mathbb{R}.$$

Lemma 1. *There exists a constant $k > 0$ such that*

$$|\psi'(x)| + |\psi''(x)| \leq k \quad \textit{for all } x \in \mathbb{R}.$$

Proof. The proof uses standard elementary arguments. We just sketch it for the sake of completeness. If we set $q = U$ and $p = U'$, then $\psi' = c + 2p/q$ and $\psi'' = -2cp/q - 2(p/q)^2 - 2g(q)$. Here we use that $q' = p$ and $p' = -cp - g(q)q$. Clearly $g(q)$ is bounded. Thus we only need to bound p/q. Proposition 4.4 of [10] implies that either $p/q \to -c/2$ at $+\infty$ if $c = c^* = 2\sqrt{f'(0)}$, or $p/q \to -\lambda_-(c)$ at $+\infty$ if $c > c^*$. Moreover, since $p/q \to 0$ at $-\infty$ and p/q is continuous, we conclude that p/q is bounded, which proves Lemma 1. □

Let us now define a weight function σ as follows :

$$\sigma(x) = U^2(x)e^{cx} \text{ for all } x \in \mathbb{R}.$$

Since U satisfies the asymptotic properties (1.8) or (1.10), one has $\liminf_{x\to+\infty} \sigma(x) > 0$. A direct computation shows that

$$\sigma'(x) - \psi'(x)\sigma(x) = 0 \text{ for all } x \in \mathbb{R}. \tag{1.29}$$

In order to lighten the proof, we introduce some norms associated to the weight function σ :

$$\|w\|_2 = \left(\int_{\mathbb{R}} \sigma(x)\, w(x)^2\, dx\right)^{1/2} \text{ and } \|w\|_\infty = \sup_{x\in\mathbb{R}} |\sigma(x)w(x)|,$$

where the supremum is understood as the essential supremum, and we define the standard $L^2(\mathbb{R})$ and $L^\infty(\mathbb{R})$ norms as follows :

$$|w|_2 = \left(\int_{\mathbb{R}} w(x)^2\, dx\right)^{1/2} \text{ and } |w|_\infty = \sup_{x\in\mathbb{R}} |w(x)|.$$

Notice that the hypothesis (1.13) implies that $r(0,\cdot)$ is in the weighted space

$$L^2_\sigma(\mathbb{R}) = \{w \in L^2(\mathbb{R}) \mid \|w\|_2 < \infty\},$$

which is a Hilbert space endowed with the inner product

$$(w, \widetilde{w}) = \int_{\mathbb{R}} w(x)\, \widetilde{w}(x)\, \sigma(x)\, dx \quad \text{for all } w, \widetilde{w} \in L^2_\sigma(\mathbb{R}).$$

Lemma 2. *The solution r of the linear Cauchy problem* (1.28) *satisfies the following properties :*

$$\frac{d}{dt}\left(\frac{1}{2}\|r(t,\cdot)\|_2^2\right) = -\|\partial_x r(t,\cdot)\|_2^2 \quad \textit{for all } t > 0 \tag{1.30}$$

and, for any constant K satisfying $K \geq |\psi''|_\infty + 1$,

$$\frac{d}{dt}\left(\frac{K}{2}\|r(t,\cdot)\|_2^2 + \frac{1}{2}\|\partial_x r(t,\cdot)\|_2^2\right) \leq -\left(\|\partial_x r(t,\cdot)\|_2^2 + \|\partial_x^2 r(t,\cdot)\|_2^2\right) \textit{ for all } \ t > 0.$$

Proof. We first set some properties of the operator $\mathcal{L}$ in the Hilbert space $L^2_\sigma(\mathbb{R})$. We define its domain $D(\mathcal{L})$ as

$$D(\mathcal{L}) = H^2_\sigma(\mathbb{R}) = \{w \in L^2_\sigma(\mathbb{R}) \mid w',\, w'' \in L^2_\sigma(\mathbb{R})\},$$

where w' and w'' are the first- and second-order derivatives of w in the sense of distributions. The domain $D(\mathcal{L})$ is dense in $L^2_\sigma(\mathbb{R})$ and since $\mathcal{C}^\infty_c(\mathbb{R})$ is also dense in $H^2_\sigma(\mathbb{R})$ (with the obvious norm in $H^2_\sigma(\mathbb{R})$), it follows that

$$(\mathcal{L}w, w) = -\int_{\mathbb{R}} w''w\sigma - \int_{\mathbb{R}} \psi' w' w\sigma = \int_{\mathbb{R}} w'(w\sigma)' - \int_{\mathbb{R}} \psi' w' w\sigma = \int_{\mathbb{R}} (w')^2\sigma + \int_{\mathbb{R}} w'w(\sigma' - \psi'\sigma) = \|w'\|_2^2 \geq 0$$

for all $w \in D(\mathcal{L})$, that is $\mathcal{L}$ is monotone. Furthermore, $\mathcal{L}$ is maximal in the sense that

$$\forall\, f \in L^2_\sigma(\mathbb{R}),\ \exists\, w \in D(\mathcal{L}),\ w + \mathcal{L}w = f.$$

This equation can be solved by approximation (namely, one can first solve the equation $w_n + \mathcal{L}w_n = f$ in $H^2(-n,n) \cap H^1_0(-n,n)$, then show that the sequence $(\|w_n\|_{H^2_\sigma(-n,n)})_{n\in\mathbb{N}}$ is bounded and thus pass to the limit as $n \to +\infty$ to get a solution w). Moreover, the operator $\mathcal{L}$ is symmetric since

$$(\mathcal{L}w, \widetilde{w}) = \int_{\mathbb{R}} w'(\widetilde{w}\sigma)' - \int_{\mathbb{R}} \psi' w' \widetilde{w}\sigma = \int_{\mathbb{R}} w'\widetilde{w}'\sigma = (w, \mathcal{L}\widetilde{w})$$

for all w, $\widetilde{w} \in D(\mathcal{L})$. Since $\mathcal{L}$ is maximal, monotone and symmetric, it is thus self-adjoint. Then, since v_0 is in $L^2_\sigma(\mathbb{R})$, Hille-Yosida Theorem implies that the solution r of the linear Cauchy problem (1.28) is such that

$$r \in \mathcal{C}^k\big((0,+\infty), H^l_\sigma(\mathbb{R})\big) \cap \mathcal{C}\big([0,+\infty), L^2_\sigma(\mathbb{R})\big) \text{ for all } k, l \in \mathbb{N}, \tag{1.31}$$

where $H^l_\sigma(\mathbb{R})$ is the set of functions in $L^2_\sigma(\mathbb{R})$ whose derivatives up to the $l-$th order are in $L^2_\sigma(\mathbb{R})$.

We can now define two additional functions W and Z. First we set,

$$W(t) = \frac{1}{2}\int_{\mathbb{R}} \sigma(x) r^2(t,x)dx = \frac{1}{2}\|r(t,\cdot)\|_2^2 \ \text{ for all } t \geq 0.$$

Let K be a positive constant satisfying $K \geq |\psi''|_\infty + 1$. We define the function Z as follows :

$$Z(t) = KW(t) + \frac{1}{2}\int_{\mathbb{R}} \sigma(x)\,(\partial_x r)^2(t,x)\,dx = \frac{K}{2}\|r(t,\cdot)\|_2^2 + \frac{1}{2}\|\partial_x r(t,\cdot)\|_2^2 \ \text{ for all } t > 0.$$

The functions W and Z are of the class $\mathcal{C}^\infty$ on $(0,+\infty)$ and W is continuous on $[0,+\infty)$. Since r satisfies (1.28) and (1.31) and σ obeys (1.29), we get that

$$W'(t) = \frac{d}{dt}\Big(\frac{1}{2}\|r(t,\cdot)\|_2^2\Big) = \frac{1}{2}\frac{d}{dt}\int_{\mathbb{R}} \sigma(x)\, r^2(t,x)\,dx = -\big(\mathcal{L}r(t,\cdot), r(t,\cdot)\big) = -\|\partial_x r(t,\cdot)\|_2^2$$

for all $t > 0$. On the other hand, since r satisfies (1.31), there holds

$$Z'(t) = KW'(t) + \frac{1}{2}\frac{d}{dt}\int_{\mathbb{R}} \sigma(x)\,(\partial_x r)^2(t,x)\,dx = KW'(t) + \int_{\mathbb{R}} \partial_x(\sigma\partial_x r)(t,x)\,\mathcal{L}r(t,x)\,dx \tag{1.32}$$

for all $t > 0$. One can also observe that, for all $t > 0$,

$$\begin{aligned} -\int_{\mathbb{R}} \partial_x(\sigma\partial_x r)(t,x)\,\partial_x^2 r(t,x)\,dx &= -\int_{\mathbb{R}} \sigma(x)\,(\partial_x^2 r)^2(t,x)\,dx - \frac{1}{2}\int_{\mathbb{R}} \sigma'(x)\,\partial_x((\partial_x r)^2)(t,x)\,dx \\ &= -\int_{\mathbb{R}} \sigma(x)\,(\partial_x^2 r)^2(t,x)\,dx + \frac{1}{2}\int_{\mathbb{R}} \sigma''(x)\,(\partial_x r)^2(t,x)\,dx \end{aligned}$$

and

$$\begin{aligned} -\int_{\mathbb{R}} \partial_x(\sigma\partial_x r)(t,x)\,\psi'(x)\,\partial_x r(t,x)\,dx & \\ = -\frac{1}{2}\int_{\mathbb{R}} \sigma(x)\,\psi'(x)\,\partial_x((\partial_x r)^2)(t,x)\,dx - \int_{\mathbb{R}} \sigma'(x)\,\psi'(x)\,(\partial_x r)^2(t,x)\,dx & \\ = \frac{1}{2}\int_{\mathbb{R}} (\sigma\psi')'(x)\,(\partial_x r)^2(t,x)\,dx - \int_{\mathbb{R}} \sigma'(x)\,\psi'(x)\,(\partial_x r)^2(t,x)\,dx. & \end{aligned}$$

Notice that all above integrals exist and all integrations by parts are valid from the density of $\mathcal{C}^\infty_c(\mathbb{R})$ in $H^2_\sigma(\mathbb{R})$ and from Lemma 1 and (1.29) (in particular, σ'/σ and σ''/σ are bounded). Moreover, it follows from (1.29) that

$$\frac{1}{2}(\sigma\psi')'(x) - \sigma'(x)\psi'(x) + \frac{1}{2}\sigma''(x) = \sigma(x)\psi''(x) \le \sigma(x)|\psi''|_\infty$$

for all $x \in \mathbb{R}$. Thus, the last integral in (1.32) is bounded from above by

$$\int_{\mathbb{R}} \partial_x(\sigma\partial_x r)(t,x)\,\mathcal{L}r(t,x)\,dx \le -\int_{\mathbb{R}} \sigma(x)\,(\partial^2_x r)^2(t,x)\,dx + |\psi''|_\infty \int_{\mathbb{R}} \sigma(x)\,(\partial_x r)^2(t,x)\,dx.$$

Then, for all $t > 0$,

$$\begin{aligned} Z'(t) &\le -\int_{\mathbb{R}} \sigma(x)\,(\partial^2_x r)^2(t,x)\,dx - (K - |\psi''|_\infty)\int_{\mathbb{R}} \sigma(x)\,(\partial_x r)^2(t,x)\,dx, \\ &\le -\int_{\mathbb{R}} \sigma(x)\,(\partial^2_x r)^2(t,x)\,dx - \int_{\mathbb{R}} \sigma(x)\,(\partial_x r)^2(t,x)\,dx, \end{aligned}$$

from the choice of K. The proof of Lemma 2 is thereby complete. □

Proof of property (1.15). We are now ready to state some convergence results for the function v. Note first that $W(t) \ge 0$ and $W'(t) \le 0$ for all $t > 0$. Thus $W(t)$ converges to $W_\infty \ge 0$ as $t \to +\infty$. Similarly, $Z(t)$ converges to $Z_\infty \ge 0$ as $t \to +\infty$, which implies that $\|\partial_x r(t,\cdot)\|_2$ also converges as $t \to +\infty$. From (1.30) and the convergence of $\|r(t,\cdot)\|_2$ and $\|\partial_x r(t,\cdot)\|_2$ to finite limits, it also follows that

$$\|\partial_x r(t,\cdot)\|_2 \to 0 \ \text{ as } t \to +\infty.$$

On the other hand, for all $t > 0$, there holds

$$\|r^2(t,\cdot)\|_\infty \le \frac{1}{2}\int_{\mathbb{R}} |\partial_x(\sigma r^2)(t,x)|\,dx \le \int_{\mathbb{R}} \sigma(x)\,|r(t,x)|\,|\partial_x r(t,x)|\,dx + \frac{1}{2}\int_{\mathbb{R}} |\sigma'(x)|\,r^2(t,x)\,dx. \quad (1.33)$$

Using Cauchy-Schwarz inequality, we can see that the first term goes to 0 as $t \to +\infty$ since $\|\partial_x r(t,\cdot)\|_2$ goes to 0 and $\|r(t,\cdot)\|_2$ is bounded. If σ' were nonnegative on $\mathbb{R}$, we could drop the modulus in the second term and then, integrating by parts, we would get as above that $\|r^2(t,\cdot)\|_\infty \le 2\|r(t,\cdot)\|_2\|\partial_x r(t,\cdot)\|_2$ for all $t > 0$.

However, the function σ' may not be nonnegative on $\mathbb{R}$. Let us now prove that $\|r^2(t,\cdot)\|_\infty$ still goes to 0 as $t \to +\infty$ in the general case. First, since ψ' is bounded from Lemma 1 and $\sigma(x) \sim e^{cx}$ as $x \to -\infty$, there holds $\sigma'(x) = \psi'(x)\sigma(x) \to 0$ as $x \to -\infty$. Moreover, if $c = c^* = 2\sqrt{f'(0)}$, it follows from the asymptotic property (1.8) that

$$\sigma(x) = (Ax+B)^2 + o(1) \text{ as } x \to +\infty \ \text{ if } U(x) = (Ax+B)e^{-c^*x/2} + O\left(e^{-(c^*/2+\delta)x}\right) \text{ as } x \to +\infty$$

with $\delta > 0$, $A > 0$ and $B \in \mathbb{R}$, or

$$\sigma(x) \to B^2 > 0 \text{ as } x \to +\infty \ \text{ if } U(x) = Be^{-c^*x/2} + O\left(e^{-(c^*/2+\delta)x}\right) \text{ as } x \to +\infty,$$

where $\delta > 0$ and $B > 0$. On the other hand, if $c > c^*$, it follows from (1.10), (1.29) and the proof of Lemma 1 that

$$\sigma'(x) \to +\infty \ \text{ as } \ x \to +\infty.$$

Finally, in all cases it is possible to construct a constant $S > 0$ and a function $\rho \in \mathcal{C}^1(\mathbb{R})$ such that $\rho' \ge 0$ on $\mathbb{R}$ and

$$S\sigma(x) \le \rho(x) \le \sigma(x) \text{ for all } x \in \mathbb{R}.$$

The norms associated to ρ are equivalent to those defined by σ. Then, denoting

$$\|w\|_{\rho,2} = \left(\int_{\mathbb{R}} \rho(x)w^2(x)dx\right)^{1/2} \quad \text{and} \quad \|w\|_{\rho,\infty} = \sup_{x\in\mathbb{R}} |\rho(x)w(x)|,$$

and applying equation (1.33) to these norms, one infers that

$$S\|r^2(t,\cdot)\|_\infty \le \|r^2(t,\cdot)\|_{\rho,\infty} \le 2\|r(t,\cdot)\|_{\rho,2}\|\partial_x r(t,\cdot)\|_{\rho,2} \le 2\|r(t,\cdot)\|_2\|\partial_x r(t,\cdot)\|_2$$

for all $t > 0$. Since $\|r(t,\cdot)\|_2$ is bounded and $\|\partial_x r(t,\cdot)\|_2 \to 0$ as $t \to +\infty$, it follows that

$$\lim_{t\to+\infty} \Big(\sup_{x\in\mathbb{R}} \big(\sigma(x)r^2(t,x)\big)\Big) = 0. \tag{1.34}$$

Moreover, (1.27) implies that

$$0 \le \tilde{u}(t,x) = \big(U^2(x)r^2(t,x)\big)^{1/2} = \big(\sigma(x)r^2(t,x)\big)^{1/2} e^{-cx/2}$$

for all $t > 0$ and $x \in \mathbb{R}$. Then, for any compact set $\mathcal{K}$, one has

$$\max_{x\in\mathcal{K}} v(t,x+ct) = \max_{x\in\mathcal{K}} \tilde{u}(t,x) \le \Big(\max_{x\in\mathcal{K}} e^{-cx/2}\Big) \times \Big(\sup_{x\in\mathbb{R}} \big(\sigma(x)r^2(t,x)\big)^{1/2}\Big).$$

Finally, equation (1.34) implies that $\tilde{u}$ converge to 0 uniformly on compacts as $t \to +\infty$, which yields (1.15). One can also say that

$$\lim_{t\to+\infty} \Big(\max_{x\ge A} v(t,x+ct)\Big) = \lim_{t\to+\infty} \Big(\max_{x\ge A+ct} v(t,x)\Big) = 0. \tag{1.35}$$

for all $A \in \mathbb{R}$, where we recall that the maxima in (1.35) are reached from (1.6) and the continuity of $v(t,\cdot)$ for all $t > 0$. □

3.2 Extinction in $(\alpha\sqrt{t},+\infty)$ and in $\mathbb{R}$: proofs of Theorem 1 and Proposition 2

Before completing the proof of Theorem 1 and Proposition 2, let us first state two auxiliary lemmas. They provide some uniform estimates of v in intervals of the type $(\alpha\sqrt{t}, A+ct)$ or the whole real line $\mathbb{R}$ when bounds for $v(t,\cdot)$ are known at the positions $A+ct$, in the intervals $(A+ct,+\infty)$ and/or at $-\infty$. These two lemmas will be used in all cases (A), (B) and (C).

Lemma 3. *Let f be of type (A), (B) or (C), let (c,U) be a front satisfying (1.3) and let v solve (1.5) with v_0 satisfying (1.4). Let $\mu \in [0,1]$ and $A_0 \in \mathbb{R}$ be such that $\limsup_{t\to+\infty} v(t,A+ct) \le \mu$ (resp. $\liminf_{t\to+\infty} v(t,A+ct) \ge \mu$) for all $A < A_0$. Then, for all $\varepsilon > 0$, there exist $\alpha_0 > 0$ and $A < A_0$ such that*

$$\limsup_{t\to+\infty} \Big(\max_{\alpha\sqrt{t}\le x\le A+ct} v(t,x)\Big) \le \mu+\varepsilon \quad \text{for all } \alpha \ge \alpha_0, \tag{1.36}$$

resp.

$$\liminf_{t\to+\infty} \Big(\min_{\alpha\sqrt{t}\le x\le A+ct} v(t,x)\Big) \ge \mu-\varepsilon \quad \text{for all } \alpha \ge \alpha_0.$$

Lemma 4. *Let f be of type (A), (B) or (C), let (c,U) be a front satisfying (1.3) and let v solve (1.5) with v_0 satisfying (1.4). Let λ and $\mu \in [0,1]$ be such that either $\limsup_{x\to-\infty} v_0(x) \le \lambda$ or $\max(v_0-\lambda,0) \in L^p(\mathbb{R})$ for some $p \in [1,+\infty)$, and $\limsup_{t\to+\infty} \big(\max_{x\ge A+ct} v(t,x)\big) \le \mu$ for all $A \in \mathbb{R}$. Then*

$$\limsup_{t\to+\infty} \Big(\sup_{x\in\mathbb{R}} v(t,x)\Big) \le \max(\lambda,\mu). \tag{1.37}$$

The proofs of Lemmas 3 and 4 are postponed at the end of this section.

End of the proof of Theorem 1. Let v be the solution of (1.5) with v_0 satisfying (1.4) and (1.13). To get (1.14), pick any $\varepsilon > 0$ and observe that property (1.15) and Lemma 3 with $\mu = 0$ (and an arbitrary A_0) yield the existence of $\alpha_0 > 0$ and $A \in \mathbb{R}$ such that

$$\limsup_{t\to+\infty} \Big(\max_{\alpha\sqrt{t}\le x\le A+ct} v(t,x) \Big) \le \varepsilon \text{ for all } \alpha \ge \alpha_0.$$

Property (1.14) follows then from (1.35). This proves Theorem 1. □

End of the proof of Proposition 2. We make the additional assumption (1.16). Notice that the assumptions of Lemma 4 are fulfilled with $\lambda = \mu = 0$, from (1.16) and (1.35). It follows that the inequality (1.37) holds with $\lambda = \mu = 0$, which implies that $v(t,x) \to 0$ uniformly on $\mathbb{R}$ as $t \to +\infty$. The proof of Proposition 2 is thereby complete. □

The proofs of Lemmas 3 and 4 are based on the construction of explicit sub- or super-solutions of (1.5) in suitable domains in the (t,x) coordinates, and on the fact that the coefficient $g(u(t,x)) = g(U(x-ct))$ in (1.5) is exponentially small when $x - ct \to -\infty$.

Proof of Lemma 3. Let us first consider the case of the upper bounds. Let $\mu \in [0,1]$ and $A_0 \in \mathbb{R}$ be as in the statement and pick any $\varepsilon \in (0,1)$. Let j_ε be the positive function defined on $(-\infty, 0)$ by

$$j_\varepsilon(y) = \varepsilon \left(1 - \frac{1}{1-y} \right) \quad \text{for all } y < 0. \tag{1.38}$$

The functions j_ε' and j_ε'' are negative on $(-\infty,0)$ and $-j_\varepsilon''(y) - cj_\varepsilon'(y) \sim \varepsilon c/y^2$ as $y \to -\infty$. We recall the asymptotic behavior of U at $-\infty$:

$$U(y) = 1 - Be^{\nu y} + O\left(e^{(\nu+\delta)y}\right) \quad \text{as } y \to -\infty, \tag{1.39}$$

where $\delta > 0$, $B > 0$ and $\nu = (-c + \sqrt{c^2 - 4f'(1)})/2 > 0$. This property (1.39) and the negativity of $f'(1)$ yield the existence of a real number $A < \min(A_0, 0)$ such that

$$0 \le g(U(y)) \le \frac{-j_\varepsilon''(y) - cj_\varepsilon'(y)}{2+\varepsilon} \quad \text{for all } y \in (-\infty, A]. \tag{1.40}$$

From the assumptions made in Lemma 3, there is $t_0 > 0$ such that

$$v(t, A+ct) \le \mu + \varepsilon \text{ for all } t \ge t_0.$$

Now, let us define the function $\overline{v}$ by

$$\overline{v}(t,x) = h(t - t_0, x - A - ct_0) + j_\varepsilon(x - ct) \text{ for all } t \ge t_0 \text{ and } x \in [A + ct_0, A + ct],$$

where h solves the heat equation

$$\begin{cases} \partial_t h(t,x) &= \partial_x^2 h(t,x), & t > 0,\ x \in \mathbb{R}, \\ h(0,x) &= 2\mathbb{1}_{(-\infty,0)}(x) + (\mu+\varepsilon)\mathbb{1}_{(0,+\infty)}(x), & x \in \mathbb{R}. \end{cases}$$

Let us check that $\overline{v}$ is a supersolution of (1.5) in the domain $t \ge t_0$ and $x \in [A + ct_0, A + ct]$. Firstly, observe that

$$\mu + \varepsilon \le \overline{v}(t,x) \le 2 + \varepsilon \tag{1.41}$$

for all $t \geq t_0$ and $x \in [A+ct_0, A+ct]$ since $\mu+\varepsilon < 2$ and $0 < j_\varepsilon < \varepsilon$ on $(-\infty, 0)$. It follows from (1.26) that

$$v(t, A+ct_0) < 1 \leq \frac{2+\mu+\varepsilon}{2} = h(t-t_0, 0) \leq \overline{v}(t, A+ct_0) \text{ for all } t > t_0.$$

On the other hand,

$$v(t, A+ct) \leq \mu+\varepsilon \leq h(t-t_0, c(t-t_0)) \leq \overline{v}(t, A+ct) \text{ for all } t \geq t_0.$$

Lastly, from (1.40) and (1.41), the function $\overline{v}$ satisfies, for all $t > t_0$ and $x \in (A+ct_0, A+ct)$,

$$\begin{aligned} \partial_t \overline{v}(t,x) - \partial_x^2 \overline{v}(t,x) - g(U(x-ct))\overline{v}(t,x) & \\ = \; & -j_\varepsilon''(x-ct) - cj_\varepsilon'(x-ct) - g(U(x-ct))\overline{v}(t,x) \\ \geq \; & -g(U(x-ct))(2+\varepsilon) - j_\varepsilon''(x-ct) - cj_\varepsilon'(x-ct) \\ \geq \; & 0. \end{aligned} \tag{1.42}$$

The maximum principle applied to (1.5) implies that

$$v(t,x) \leq \overline{v}(t,x) \text{ for all } t \geq t_0 \text{ and } x \in [A+ct_0, A+ct].$$

Fix $\alpha_0 > 0$ so that

$$\frac{2-\mu-\varepsilon}{\sqrt{\pi}} \int_{-\infty}^{-\alpha_0/2} e^{-z^2} dz \leq \varepsilon.$$

Let $\alpha \geq \alpha_0$ and $t_1 > t_0$ be such that $A+ct_0 < \alpha\sqrt{t} < A+ct$ for all $t \geq t_1$. Since $h(t,\cdot)$ is decreasing for all $t > 0$, there holds, for all $t \geq t_1$,

$$\begin{aligned} \max_{\alpha\sqrt{t} \leq x \leq A+ct} v(t,x) \; & \leq \; \max_{\alpha\sqrt{t} \leq x \leq A+ct} \overline{v}(t,x) \\ & = \; \max_{\alpha\sqrt{t} \leq x \leq A+ct} \big(h(t-t_0, x-A-ct_0) + j_\varepsilon(x-ct) \big) \\ & \leq \; h(t-t_0, \alpha\sqrt{t}-A-ct_0) + \varepsilon \\ & \leq \; \mu + 2\varepsilon + \frac{2-\mu-\varepsilon}{\sqrt{\pi}} \int_{-\infty}^{(-\alpha\sqrt{t}+A+ct_0)/\sqrt{4(t-t_0)}} e^{-y^2} dy. \end{aligned}$$

Hence, for all $\alpha \geq \alpha_0$,

$$\limsup_{t \to +\infty} \Big(\max_{\alpha\sqrt{t} \leq x \leq A+ct} v(t,x) \Big) \leq \mu + 2\varepsilon + \frac{2-\mu-\varepsilon}{\sqrt{\pi}} \int_{-\infty}^{-\alpha/2} e^{-y^2} dy \leq \mu + 3\varepsilon.$$

Since $\varepsilon > 0$ is arbitrarily small, the conclusion (1.36) follows.

As far as the lower bounds are concerned, with the same type of arguments as above and since $g(U(y))$ is nonnegative near $-\infty$, one can show that for any $\varepsilon \in (0,1)$, there exist $A < A_0$ and $t_0 > 0$ such that

$$v(t,x) \geq h(t-t_0, x-A-ct_0) \text{ for all } t \geq t_0 \text{ and } x \in [A+ct_0, A+ct],$$

where h solves the heat equation in $\mathbb{R}$ with initial condition $h(0,\cdot) = -\mathbb{1}_{(-\infty,0)} + (\mu-\varepsilon)\mathbb{1}_{(0,+\infty)}$. It follows that

$$\liminf_{t \to +\infty} \Big(\min_{\alpha\sqrt{t} \leq x \leq A+ct} v(t,x) \Big) \geq \mu - 2\varepsilon \text{ for } \alpha > 0 \text{ large enough.}$$

The proof of Lemma 3 is thereby complete. □

Proof of Lemma 4. Let $\lambda \in [0,1]$ and $\mu \in [0,1]$ be given as in the statement and pick any $\varepsilon > 0$. Let j_ε be the function defined as in (1.38) and let $A < 0$ be such that

$$0 \leq g(U(y)) \leq \frac{-j_\varepsilon''(y) - cj_\varepsilon'(y)}{\max(\max(\lambda,\mu)+\varepsilon,1)+\varepsilon} \text{ for all } y \in (-\infty, A]. \tag{1.43}$$

The assumptions made in Lemma 4 yield the existence of $t_0 > 0$ such that

$$v(t,x) \leq \mu + \varepsilon \text{ for all } t \geq t_0 \text{ and } x \in [A+ct, +\infty). \tag{1.44}$$

If v_0 satisfies $\limsup_{x\to-\infty} v_0(x) \leq \lambda$, then the comparison with the heat equation and the equality $g(1) = 0$ imply that $\limsup_{x\to-\infty} v(t,x) \leq \lambda$ for all $t > 0$. On the other hand, if w solves (1.5) with an initial condition w_0 in $L^p(\mathbb{R})$ for some $p \in [1, +\infty)$, then heat kernel estimates and the boundedness of $g(U(x-ct))$ imply that $w(t,\cdot)$ is also in $L^p(\mathbb{R})$ for all $t > 0$, while $w(t,\cdot)$ is uniformly continuous on $\mathbb{R}$ from standard parabolic estimates. Finally, $w(t,x) \to 0$ as $x \to -\infty$ for all $t > 0$. Now, if $\max(v_0 - \lambda, 0) \in L^p(\mathbb{R})$ for some $p \in [1, +\infty)$, then by writing $v_0 \leq \lambda + \max(v_0 - \lambda, 0)$, the previous arguments and the linearity of (1.5) imply that $\limsup_{x\to-\infty} v(t,x) \leq \lambda$ for all $t > 0$. In any case, at time $t = t_0$, there exists $B \leq A$ such that

$$v(t_0,x) \leq \lambda + \varepsilon \text{ for all } x \in (-\infty, B + ct_0]. \tag{1.45}$$

Now, let us define the function $\overline{v}$ by

$$\overline{v}(t,x) = h(t-t_0,x) + j_\varepsilon(x-ct) \text{ for all } t \geq t_0 \text{ and } x \in (-\infty, A+ct],$$

where h solves the heat equation

$$\left\{ \begin{array}{rcll} \partial_t h(t,x) & = & \partial_x^2 h(t,x), & t > 0,\ x \in \mathbb{R}, \\ h(0,x) & = & \max(\max(\lambda,\mu)+\varepsilon, v(t_0,x)), & x \in \mathbb{R}. \end{array} \right. \tag{1.46}$$

Let us check that $\overline{v}$ is a supersolution of (1.5) in the domain $t \geq t_0$ and $x \leq A + ct$. Firstly, observe that

$$\max(\lambda,\mu) + \varepsilon \leq \overline{v}(t,x) \leq \max(\max(\lambda,\mu)+\varepsilon, 1) + \varepsilon \tag{1.47}$$

for all $t \geq t_0$ and $x \leq A + ct$, from (1.26), (1.38) and the maximum principle applied to the heat equation (1.46). Then, from equation (1.44), we get that

$$v(t, A+ct) \leq \mu + \varepsilon \leq \overline{v}(t, A+ct) \text{ for all } t \geq t_0.$$

Moreover, by definition of $\overline{v}(t_0,\cdot)$, there holds

$$v(t_0,x) \leq \max(\max(\lambda,\mu)+\varepsilon, v(t_0,x)) \leq \overline{v}(t_0,x) \text{ for all } x \in (-\infty, A+ct_0].$$

Finally, from (1.43) and (1.47), $\overline{v}$ satisfies the following inequality, for all $t > t_0$ and $x \in (-\infty, A+ct)$,

$$\begin{aligned} &\partial_t \overline{v}(t,x) - \partial_x^2 \overline{v}(t,x) - g(U(x-ct))\overline{v}(t,x) \\ &\quad = -j_\varepsilon''(x-ct) - cj_\varepsilon'(x-ct) - g(U(x-ct))\overline{v}(t,x) \\ &\quad \geq -g(U(x-ct))\big(\max(\max(\lambda,\mu)+\varepsilon,1)+\varepsilon\big) - j_\varepsilon''(x-ct) - cj_\varepsilon'(x-ct) \\ &\quad \geq 0. \end{aligned}$$

The maximum principle applied to (1.5) implies that

$$v(t,x) \le \overline{v}(t,x) \text{ for all } t \ge t_0 \text{ and } x \in (-\infty, A+ct]. \tag{1.48}$$

Next, we claim that

$$\overline{v}(t,x) - j_\varepsilon(x-ct) \to \max(\lambda,\mu) + \varepsilon \text{ uniformly on } (-\infty, A+ct] \text{ as } t \to +\infty.$$

Indeed, since $v(t_0,\cdot)$ satisfies (1.44) and (1.45), the initial condition $h(0,\cdot)$ of h is the sum of the constant $\max(\lambda,\mu)+\varepsilon$ and a nonnegative compactly supported continuous function. By linearity and standard properties of the heat equation on $\mathbb{R}$, it follows that $h(t,\cdot) \to \max(\lambda,\mu)+\varepsilon$ uniformly on $\mathbb{R}$ as $t \to +\infty$. Hence, $\overline{v}(t,x) - j_\varepsilon(x-ct) \to \max(\lambda,\mu)+\varepsilon$ uniformly on $(-\infty, A+ct]$ as $t \to +\infty$. From (1.48), we get that

$$\limsup_{t\to+\infty} \Big(\sup_{x\in(-\infty,A+ct]} v(t,x) \Big) \le \max(\lambda,\mu) + \varepsilon + \sup_{y\in(-\infty,A]} j_\varepsilon(y) = \max(\lambda,\mu) + 2\varepsilon.$$

Then, from equation (1.44) we get that

$$\limsup_{t\to+\infty} \Big(\sup_{x\in\mathbb{R}} v(t,x) \Big) \le \max(\lambda,\mu) + 2\varepsilon.$$

Since $\varepsilon > 0$ is arbitrary, the conclusion (1.37) follows and the proof of Lemma 4 is complete. □

Remark 2. If the initial condition v_0 of (1.5) is such that $v_0(x) \to \lambda \in [0,1]$ as $x \to -\infty$, then, as already noticed, $v(t,x) \to \lambda$ as $x \to -\infty$ for all $t > 0$, since $g(1) = 0$. In particular, $\sup_{\mathbb{R}} v(t,\cdot) \ge \lambda$ for all $t > 0$. Therefore, if v_0 satisfies (1.4), (1.13) and $\lim_{x\to-\infty} v_0(x) = \lambda \in [0,1]$, then the proof of Lemma 4 shows that $\sup_{\mathbb{R}} v(t,\cdot) \to \lambda$ as $t \to +\infty$.

1.4 The description of pushed fronts

This section is devoted to the proofs of Theorem 2 and Proposition 3. We begin by proving formula (1.21). The proof of this formula draws its inspiration from the front stability analysis [163, 164] and especially from the lecture notes of Gallay [77]. It is based on some properties of the self-adjoint Schrödinger operator $\mathcal{L}$ defined by

$$\mathcal{L} = -\partial_x^2 + \left(\frac{c^2}{4} - g(U(x)) \right) \tag{1.49}$$

with domain $H^2(\mathbb{R})$, where $g(s) = f(s)/s$, f satisfies the hypotheses of Theorem 2, and (c,U) is either the pushed critical front in case (A) when $c = c^* > 2\sqrt{f'(0)}$, or the unique front satisfying (1.3) in case (B) or (C). The properties of the semigroup generated by $-\mathcal{L}$ play an essential role in the large time behavior of the solution $\tilde{u}$ of the Cauchy problem (1.7). Indeed, the function v^* defined by

$$u^*(t,x) = e^{cx/2}\, \tilde{u}(t,x) \text{ for all } t \ge 0 \text{ and } x \in \mathbb{R} \tag{1.50}$$

satisfies the Cauchy problem

$$\begin{cases} \partial_t u^*(t,x) + \mathcal{L} u^*(t,x) &= 0, & t > 0,\ x \in \mathbb{R}, \\ u^*(0,x) &= v_0(x)\, e^{cx/2}, & x \in \mathbb{R}. \end{cases} \tag{1.51}$$

The main spectral properties of $\mathcal{L}$ are stated in Section 4.1. Then, Section 4.2 is devoted to the proof of formula (1.21). The proofs of Theorem 2 and Proposition 3 are given in Section 4.3.

4.1 Preliminary lemmas

Let $X_{c/2}$ be the weighted space defined by

$$X_{c/2} = \left\{ w \in L^2_{loc}(\mathbb{R}) \,|\, \int_{\mathbb{R}} w^2(x)\, e^{cx}\, dx < \infty \right\}. \tag{1.52}$$

Lemma 5. *If the front U solving (1.3) with $c > 0$ belongs to $X_{c/2}$, then the operator $\mathcal{L}$ defined by (1.49) satisfies the following properties :*

i) The essential spectrum $\sigma_e(\mathcal{L})$ of $\mathcal{L}$ is equal to $[c^2/4 - \max(f'(0), 0), +\infty)$.

ii) The point spectrum of $\mathcal{L}$ is included in $[0, c^2/4 - \max(f'(0), 0))$. Moreover, $\lambda = 0$ is the smallest eigenvalue of $\mathcal{L}$ and the function $x \mapsto \phi(x) = U(x)\, e^{cx/2}$ spans the kernel of $\mathcal{L}$.

iii) The following spectral decomposition of $L^2(\mathbb{R})$ holds :

$$L^2(\mathbb{R}) = \mathrm{Im}(P) \oplus \ker(P), \tag{1.53}$$

where the operator $P : L^2(\mathbb{R}) \to L^2(\mathbb{R})$ is the spectral projection onto the kernel of $\mathcal{L}$, that is $P(w) = \left(\int_{\mathbb{R}} \varphi w \right) \varphi$ for all $w \in L^2(\mathbb{R})$ with $\varphi = \phi / \|\phi\|_{L^2(\mathbb{R})}$.

Proof. It uses standard results and it is just sketched here for the sake of completeness.

i) The coefficients of the operator $\mathcal{L}$ are not constant but converge exponentially to two limits as $x \to \pm\infty$. It follows that $\mathcal{L}$ is a relatively compact perturbation of the operator $\mathcal{L}_0$ defined by $\mathcal{L}_0 = -\partial_x^2 + (c^2/4 - g_\infty(x))$, where

$$g_\infty(x) = \begin{cases} g(0) = f'(0) & \text{if } x < 0, \\ g(1) = 0 & \text{if } x > 0. \end{cases}$$

Then, Theorem A.2 in [93] implies that the essential spectrum $\sigma_e(\mathcal{L})$ of the operator $\mathcal{L}$ is equal to the spectrum $\sigma(\mathcal{L}_0)$ of the operator $\mathcal{L}_0$. Since $\mathcal{L}_0$ is self-adjoint in $L^2(\mathbb{R})$, we get

$$\sigma_e(\mathcal{L}) = \sigma(\mathcal{L}_0) = [c^2/4 - \max(f'(0), 0), +\infty).$$

ii) The operator $\mathcal{L}$ is a self-adjoint operator in $L^2(\mathbb{R})$, so the eigenvalues of $\mathcal{L}$ are in $\mathbb{R}$. Moreover, since (c, U) satisfies equation (1.3) and U belongs to $X_{c/2}$, one has necessarily that $c^2 > 4f'(0)$ (whatever the sign of $f'(0)$ be) and the function $x \mapsto \phi(x) = U(x)e^{cx/2}$ is in $L^2(\mathbb{R})$ (and then in $H^2(\mathbb{R})$ by adapting the arguments used the proof of Lemma 1). Furthermore, ϕ is an eigenvector of $\mathcal{L}$ associated to the eigenvalue $\lambda = 0$, that is $\mathcal{L}\phi = 0$, and the eigenvalue is simple, from elementary arguments based on the exponential behavior at $\pm\infty$. On the other hand, since ϕ is positive, Sturm-Liouville theory implies that $\lambda = 0$ is the lowest value of the spectrum of $\mathcal{L}$. Together with *i)*, we finally get that the point spectrum of $\mathcal{L}$ is a discrete subset of the interval $[0, c^2/4 - \max(f'(0), 0))$.

iii) The function $\varphi = \phi / \|\phi\|_{L^2(\mathbb{R})}$ is a normalized eigenvector of $\mathcal{L}$ associated to the eigenvalue 0. Since $\mathcal{L}$ is self-adjoint, the operator $P : L^2(\mathbb{R}) \to L^2(\mathbb{R})$ defined as in Lemma 5 is the spectral projection onto the kernel of $\mathcal{L}$. Then, the spectral decomposition (1.53) holds, where $\mathrm{Im}(P) = \{\beta\varphi,\ \beta \in \mathbb{R}\}$ and $\ker(P) = \{w \in L^2(\mathbb{R}) \,|\, \int_{\mathbb{R}} \varphi w = 0\}$. □

Let us come back to the Cauchy problem $\partial_t w + \mathcal{L}w = 0$. From Lemma 5, the semigroup $\left(e^{-t\mathcal{L}}\right)_{t \geq 0}$ generated by $-\mathcal{L}$ satisfies the following properties :

Lemma 6. *If the front U solving (1.3) with $c > 0$ belongs to $X_{c/2}$, then there exist two constants $C > 0$ and $\eta > 0$ such that*

$$|e^{-t\mathcal{L}} w|_\infty \leq C e^{-\eta t} |w|_\infty \text{ for all } t \geq 0 \text{ and } w \in \ker(P) \cap L^\infty(\mathbb{R}). \tag{1.54}$$

Proof. From Lemma 5, the decomposition (1.53) is stable by $\mathcal{L}$. Moreover, the restriction of $\mathcal{L}$ to the space $\ker(P)$ is a sectorial operator whose spectrum is included in $\{z \in \mathbb{C} \,|\, \Re e(z) > \eta\}$ for some small $\eta > 0$. The conclusion (1.54) follows from [93, 142]. □

4.2 Proof of formula (1.21)

Let f satisfy the assumptions of Theorem 2 and let (c, U) be either the pushed critical front when $c = c^* > 2\sqrt{f'(0)}$ in case (A) or the unique front satisfying (1.3) in cases (B) and (C). Let v be the solution of the Cauchy problem (1.4)-(1.5) and let $\tilde{u}$ be defined by $\tilde{u}(t,x) = v(t, x+ct)$. First of all, $\tilde{u}$ solves (1.7) and from the maximum principle the comparison (1.26) still holds. Moreover, since U satisfies (1.9), (1.11) or (1.12), U and $\tilde{u}(t,\cdot)$ – for all $t \geq 0$ – belong to the weighted space $X_{c/2}$ defined by (1.52). Next, let u^* be defined by (1.50). Since $\tilde{u}(t,\cdot)$ is in $X_{c/2}$ for all $t \geq 0$, the function $u^*(t,\cdot)$ belongs to $L^2(\mathbb{R})$, for all $t \geq 0$. Furthermore, φ and $u^*(0,\cdot)$ belong to $L^\infty(\mathbb{R})$ from (1.9), (1.11) and (1.12). From (1.51) and Lemma 5, the initial condition $u^*(0,\cdot)$ can be split in $L^2(\mathbb{R})$ as follows :

$$u^*(0,\cdot) = P(u^*(0,\cdot)) + w,$$

where

$$\left\{ \begin{array}{l} P(u^*(0,\cdot)) = \left(\displaystyle\int_{\mathbb{R}} \varphi(s)\, u^*(0,s)\, ds \right) \varphi \quad \text{and} \quad \varphi(x) = \dfrac{e^{cx/2} U(x)}{\left(\displaystyle\int_{\mathbb{R}} U^2(s)\, e^{cs}\, ds \right)^{1/2}} \text{ for all } x \in \mathbb{R}, \\ \\ w = u^*(0,\cdot) - P(u^*(0,\cdot)) \in \ker(P) \cap L^\infty(\mathbb{R}). \end{array} \right.$$

Since $\mathcal{L}\varphi = 0$, it follows that

$$u^*(t,\cdot) = P(u^*(0,\cdot)) + e^{-t\mathcal{L}} w \text{ for all } t \geq 0. \tag{1.55}$$

Lemma 6 yields the existence of $C > 0$ and $\eta > 0$ such that

$$|u^*(t,\cdot) - P(u^*(0,\cdot))|_\infty = |e^{-t\mathcal{L}} w|_\infty \leq C e^{-\eta t} |w|_\infty \text{ for all } t \geq 0. \tag{1.56}$$

Equation (1.55) and the definition (1.50) of u^* imply then that, for all $t > 0$ and $x \in \mathbb{R}$,

$$\begin{array}{rcl} \tilde{u}(t,x) & = & e^{-cx/2} \big(P(u^*(0,\cdot))(x) + (e^{-t\mathcal{L}} w)(x) \big) \\ & = & e^{-cx/2} \varphi(x) \left(\displaystyle\int_{\mathbb{R}} \varphi(s)\, u^*(0,s)\, ds \right) + e^{-cx/2} (e^{-t\mathcal{L}} w)(x) \\ & = & p(v_0) U(x) + e^{-cx/2} (e^{-t\mathcal{L}} w)(x), \end{array}$$

where $p(v_0) \in (0,1]$ is given in (1.19). It follows from (1.56) that $v(t, x+ct) - p(v_0)U(x) \to 0$ uniformly on compacts as $t \to +\infty$ and even uniformly in any interval of the type $[A, +\infty)$ with $A \in \mathbb{R}$. This proves (1.21). □

Under an additional assumption on v_0, the following lemma holds :

Lemma 7. *Under the assumptions of Theorem 2, if v_0 satisfies the additional assumption*

$$\limsup_{x \to -\infty} v_0(x) \leq p(v_0), \;\; \textit{or} \;\; \max\left(v_0 - p(v_0), 0\right) \in L^p(\mathbb{R}) \textit{ for some } p \in [1, +\infty), \tag{1.57}$$

then

$$\sup_{\mathbb{R}} v(t,\cdot) \to p(v_0) \textit{ as } t \to +\infty. \tag{1.58}$$

Proof. The proof of (1.58) is a consequence of (1.21) and Lemma 4. More precisely, let ε be any positive real number in $(0,1)$ and let A be any real number. From the previous paragraph there is $t_0 > 0$ such that

$$v(t,x) \leq p(v_0)U(x-ct) + \varepsilon \leq p(v_0) + \varepsilon \text{ for all } t \geq t_0 \text{ and } x \geq A + ct.$$

Lemma 4 applied with $\lambda = \mu = p(v_0)$ implies that

$$\limsup_{t\to+\infty} \Big(\sup_{x\in\mathbb{R}} v(t,x) \Big) \leq p(v_0).$$

On the other hand, since $\liminf_{t\to+\infty} (\sup_{\mathbb{R}} v(t,\cdot)) \geq p(v_0)$ from (1.21) and $U(-\infty) = 1$, we get that $\sup_{\mathbb{R}} v(t,\cdot) \to p(v_0)$ as $t \to +\infty$. □

Remark 3. As in Remark 2, the above proof implies that if v_0 satisfies (1.4) and $v_0(x) \to \lambda \in [0,1]$ as $x \to -\infty$, then $\sup_{\mathbb{R}} v(t,\cdot) \to \max(\lambda, p(v_0))$ as $t \to +\infty$.

4.3 Spreading properties inside the pushed fronts : proofs of Theorem 2 and Proposition 3

The previous section 4.2 shows that, in the pushed case, the right spreading speed of v in the reference frame is equal to c, in the sense that

$$c = \inf\{\gamma > 0 \mid v(t, \cdot + \gamma t) \to 0 \text{ uniformly in } (0,+\infty) \text{ as } t \to +\infty\}.$$

In this section, we prove that in the pushed case the left spreading speed of v is actually at least equal to 0. More precisely, we prove that the solution v moves to the left in the reference frame, at least at a sublinear rate proportional to $\sqrt{t}$, in the sense that $\liminf_{t\to+\infty} v(t, \alpha\sqrt{t}) > 0$ for all $\alpha \leq 0$ (and, in fact, for all $\alpha \in \mathbb{R}$). This corresponds to formula (1.20) in Theorem 2. We also obtain some estimates, which are more precise than (1.21), on the asymptotic profile of the solution v in sets of the type $(\alpha\sqrt{t}, +\infty)$ with $\alpha > 0$ large enough. Lastly, we prove Proposition 3, which shows that the solution v cannot spread to the left with a positive speed if v_0 is small near $-\infty$, in the sense of (1.16). The proofs of the pointwise estimates stated in Theorem 2 are based on formula (1.21) and on the construction of explicit sub- and super-solutions of (1.5) in the reference frame.

3.1 Description of the right spreading speed and the asymptotic profile of solutions : proof of Theorem 2

Let f fulfill the assumptions of Theorem 2 and let (c,U) be either the pushed critical front in the monostable case (A) with speed $c = c^* > 2\sqrt{f'(0)}$, or the unique front in the bistable (B) and ignition (C) cases. First, as in the first inequality of (1.40), since $g(U(y)) \to 0^+$ as $y \to -\infty$, there is $A \in \mathbb{R}$ such that

$$g(U(y)) \geq 0 \text{ for all } y \in (-\infty, A]. \tag{1.59}$$

Let v be the solution of problem (1.5) with initial condition v_0 satisfying (1.4). Theorem 2 implies that $v(t, A+ct) \to p(v_0)U(A) > 0$ as $t \to +\infty$. Choose any real number ν such that $0 < \nu < p(v_0)U(A)$ and let $t_0 > 0$ be such that

$$v(t, A+ct) \geq \nu \text{ for all } t \geq t_0.$$

Now, let us construct a subsolution $\underline{v}$ of the problem (1.5) in the domain $t \geq t_0$ and $x \leq A + ct$. Let $\underline{v}$ be defined by

$$\underline{v}(t,x) = h(t - t_0, x - A - ct_0) \text{ for all } t \geq t_0 \text{ and } x \leq A + ct,$$

where h is the solution of the heat equation $\partial_t h = \partial_x^2 h$ with initial condition $h(0,\cdot) = \nu \mathbb{1}_{(0,+\infty)}$ in $\mathbb{R}$. On the one hand, there holds

$$\underline{v}(t, A+ct) \le \sup_{\mathbb{R}} h(t-t_0,\cdot) \le \nu \le v(t, A+ct) \text{ for all } t \ge t_0$$

and

$$\underline{v}(t_0, x) = \nu \mathbb{1}_{(0,+\infty)}(x - A - ct_0) = 0 \le v(t_0, x) \text{ for all } x \in (-\infty, A+ct_0),$$

while, on the other hand, it follows from (1.59) that

$$\partial_t \underline{v}(t,x) - \partial_x^2 \underline{v}(t,x) - g(U(x-ct))\underline{v}(t,x) \le 0$$

for all $t > t_0$ and $x \in (-\infty, A+ct)$. Then the maximum principle applied to (1.5) implies that

$$v(t,x) \ge \underline{v}(t,x) \text{ for all } t \ge t_0 \text{ and } x \le A+ct.$$

Lastly, let α be any fixed real number. There exists $t_1 > t_0$ such that, for all $t \ge t_1$, one has $\alpha\sqrt{t} < ct + A$ and

$$v(t,x) \ge \underline{v}(t,x) = h(t-t_0, x-A-ct_0) \text{ for all } x \in [\alpha\sqrt{t}, ct+A].$$

Since $h(t,\cdot)$ is increasing in $\mathbb{R}$ for all $t > 0$, we get, that for all $t \ge t_1$ and $x \in [\alpha\sqrt{t}, ct+A]$,

$$v(t,x) \ge h(t-t_0, \alpha\sqrt{t} - A - ct_0) = \frac{\nu}{\sqrt{\pi}} \int_{(-\alpha\sqrt{t}+A+ct_0)/\sqrt{4(t-t_0)}}^{+\infty} e^{-y^2}\, dy.$$

Therefore,

$$\liminf_{t\to+\infty} \Big(\min_{\alpha\sqrt{t} \le x \le ct+A} v(t,x) \Big) \ge \frac{\nu}{\sqrt{\pi}} \int_{-\alpha/2}^{+\infty} e^{-y^2} dy > 0,$$

which together with (1.21) yields (1.20).

Let us now turn to the proof of property (1.18). Let ε be any positive real number less than $2p(v_0)$. From (1.21) and $U \le U(-\infty) = 1$, Lemma 3 applied with $\mu = p(v_0)$ (upper bound) and with $\mu = p(v_0) - \varepsilon/2$ (lower bound) yields the existence of $\alpha_0 > 0$, $A \in \mathbb{R}$ and $t_1 > 0$ such that $\alpha\sqrt{t} < A + ct$ for all $t \ge t_1$ and

$$p(v_0) - \varepsilon \le v(t,x) \le p(v_0) + \varepsilon \ \text{ for all } t \ge t_1,\ x \in [\alpha\sqrt{t}, A+ct] \text{ and } \alpha \ge \alpha_0.$$

Even if it means decreasing A, one can assume without loss of generality that $p(v_0)(1 - U(A)) \le \varepsilon$. This implies that, for all $t \ge t_1$ and $\alpha \ge \alpha_0$,

$$\max_{\alpha\sqrt{t} \le x \le A+ct} |v(t,x) - p(v_0)U(x-ct)| \le \max_{\alpha\sqrt{t} \le x \le A+ct} |v(t,x) - p(v_0)| + p(v_0)(1-U(A)) \le 2\varepsilon.$$

From property (1.21) (and the fact that $v(t, x+ct) - p(v_0)U(x) \to 0$ as $t \to +\infty$ uniformly in $[A, +\infty)$, as observed at the end of the proof of (1.21)), we also know that there exists $t_2 \ge t_1$ such that for all $t \ge t_2$,

$$\max_{x \ge A+ct} |v(t,x) - p(v_0)U(x-ct)| \le \varepsilon.$$

Remember that, in the above formula, the supremum is a maximum, from (1.26) and the continuity of U and $v(t,\cdot)$ for all $t > 0$. We conclude that

$$\limsup_{t\to+\infty} \Big(\max_{x \ge \alpha\sqrt{t}} |v(t,x) - p(v_0)U(x-ct)| \Big) \le 2\varepsilon \ \text{ for all } \alpha \ge \alpha_0.$$

Since $\varepsilon > 0$ is arbitrarily small, this completes the proof of Theorem 2. □

3.2 Description of the left spreading speed : proof of Proposition 3

In addition to (1.4), we assume that v_0 satisfies (1.16). As already observed in the proof of Lemma 4, this implies that $v(t,x) \to 0$ as $x \to -\infty$ for all $t > 0$. Let ε be any real number in $(0,1)$ and let j_ε be the function defined on $(-\infty, 0)$ by (1.38). Let $A < 0$ be such that (1.40) holds. Since $v(1,x) \to 0$ as $x \to -\infty$, one can assume without loss of generality that $v(1,x) \leq \varepsilon$ for all $x \leq A$.

As in the proof of Lemmas 3 and 4, let us now construct a super-solution $\overline{v}$ of (1.5) in the domain $t \geq 1$ and $x \leq A$. More precisely, let us set

$$\overline{v}(t,x) = h(t-1, x-A) + j_\varepsilon(x-ct) \text{ for all } t \geq 1 \text{ and } x \leq A,$$

where h solves the heat equation

$$\left\{ \begin{array}{rcll} \partial_t h(t,x) & = & \partial_x^2 h(t,x), & t > 0,\ x \in \mathbb{R}, \\ h(0,x) & = & \varepsilon\, \mathbb{1}_{(-\infty,0)}(x) + 2\, \mathbb{1}_{(0,+\infty)}(x), & x \in \mathbb{R}. \end{array} \right.$$

There holds $v(1,x) \leq \varepsilon \leq \overline{v}(1,x)$ for all $x < A$, while $v(t,A) \leq 1 \leq (2+\varepsilon)/2 = h(t-1,0) \leq \overline{v}(t,A)$ for all $t > 1$ from (1.26) and (1.38). Furthermore,

$$\partial_t \overline{v}(t,x) - \partial_x^2 \overline{v}(t,x) - g(U(x-ct))\overline{v}(t,x) \geq 0 \text{ for all } t > 1 \text{ and } x < A,$$

as in (1.42). It follows from the maximum principle applied to (1.5) that

$$v(t,x) \leq \overline{v}(t,x) \text{ for all } t \geq 1 \text{ and } x \leq A.$$

For any fixed $\alpha < 0$, and $t > 0$ large enough so that $\alpha\sqrt{t} < A$, the maximum of $v(t,\cdot)$ on $(-\infty, \alpha\sqrt{t}]$ is reached since $v \geq 0$ and $v(t,-\infty) = 0$, and there holds

$$\max_{x \leq \alpha\sqrt{t}} v(t,x) \leq \sup_{x \leq \alpha\sqrt{t}} \big(h(t-1,x-A) + j_\varepsilon(x-ct)\big) \leq h(t-1, \alpha\sqrt{t} - A) + \varepsilon$$

since $h(t,\cdot)$ is increasing in $\mathbb{R}$ for all $t > 0$. Thus, for any fixed $\alpha < 0$,

$$\max_{x \leq \alpha\sqrt{t}} v(t,x) \leq 2\varepsilon + \frac{2-\varepsilon}{\sqrt{\pi}} \int_{-(A+\alpha\sqrt{t})/\sqrt{4(t-1)}}^{+\infty} e^{-y^2}\, dy$$

for t large enough, whence

$$\limsup_{t \to +\infty} \Big(\max_{x \leq \alpha\sqrt{t}} v(t,x) \Big) \leq 3\varepsilon \ \text{ for all } \alpha \leq \alpha_0 < 0$$

with $|\alpha_0|$ large enough. Since ε can be arbitrarily small, the proof of Proposition 3 is thereby complete. □

Remark 4. The proof of the lower bound of v given in Subsection 3.1 implies immediately that, under the assumptions of Theorem 2, $\liminf_{t \to +\infty} v(t,x) \geq p(v_0)/2$ locally uniformly in $x \in \mathbb{R}$. Furthermore, for any $\varepsilon > 0$, an adaptation of the above proof given in the present subsection implies that, under the assumptions of Proposition 3, there are $A < 0$ negative enough, $t_0 > 0$ positive enough and $B < \min(A + ct_0, 0)$ negative enough such that $v(t,x) \leq h(t-t_0, x) + j_\varepsilon(x-ct)$ for all $t > t_0$ and $x \leq ct + A$, where h solves the heat equation $\partial_t h = \partial_x^2 h$ with initial condition $h(0,\cdot) = \varepsilon \mathbb{1}_{(-\infty,B)} + \mathbb{1}_{(B,ct_0+A)} + (p(v_0)+\varepsilon)\mathbb{1}_{(ct_0+A,+\infty)}$. Therefore, since $\varepsilon > 0$ can be arbitrarily small, it follows that, under the assumptions of Proposition 3, $\limsup_{t \to +\infty} v(t,x) \leq p(v_0)/2$ locally uniformly in $x \in \mathbb{R}$, and finally $v(t,x) \to p(v_0)/2$ as $t \to +\infty$ locally uniformly in $x \in \mathbb{R}$.

Chapitre 2

Allee effect promotes diversity in traveling waves of colonization

Ce travail réalisé en collaboration avec Lionel Roques [a], François Hamel [b,c] et Etienne Klein [a]
est publié en ligne dans les *Proceedings of the National Academy of Sciences of the United States of America* [RGHK12]

[a] UR 546 Biostatistique et Processus Spatiaux, INRA, F-84000 Avignon, France
[b] Aix-Marseille Université, LATP UMR 6632, Faculté des Sciences et Techniques
Avenue Escadrille Normandie-Niemen, F-13397 Marseille Cedex 20, France
[c] Institut Universitaire de France

Sommaire

2.1 Introduction

Rapid increases in the number of biological invasions by alien organisms [50] and the movement of species in response to their climatic niches shifting as a result of climate change have caused a growing number of empirical and observational studies to address the phenomenon of range expansion. Numerous mathematical approaches and simulations have been developed to analyze the processes of these expansions [103, 175]. Most results focus on the rate of range expansion [92], and the genetic consequences of range expansion have received little attention from mathematicians and modelers [65]. However, range expansions are known to have an important effect on genetic diversity [52, 94] and generally lead to a loss of genetic diversity along the expansion axis due to successive founder effects [162]. Simulation studies have already investigated the role of the geometry of the invaded territory [31, 174, 184], the importance of long distance dispersal and the shape of the dispersal kernel [11, 68, 96], the effects of local demography [110] or existence of a juvenile stage [11]. Further research is needed to obtain mathematical results supporting these empirical and simulation studies, as such results could determine the causes of diversity loss and the factors capable of increasing or reducing it.

In a simulation study using a stepping-stone model with a lattice structure, Edmonds *et al.* [62] analyzed the fate of a neutral mutation present in the leading edge of an expanding population. Although in most cases the mutation remains at a low frequency in its original position, in some cases the mutation increases in frequency and propagates among the leading edge. This phenomenon is described as “surfing" [110]. Surfing is caused by the strong genetic drift taking place on the edge of the population wave [65, 66] because the local growth rate of the low density individuals on the edge of the expanding wave is typically higher than the growth rate for the bulk of the population [110]. The existence of surfing events has a significant impact on the subsequent genetic patterns of the population after expansion [81] and their occurrence can be influenced by the existence of long distance dispersal events [68], local demography [110] or selection [174].

The existence of an Allee effect is another critical factor affecting the dynamics of the leading edge of a population expansion. The Allee effect is characterized by a decrease in the per capita growth rate at low densities, and this can be due to increased damage from bioagressors, increased mortality due to interspecific competition or reduced fitness due to suboptimal mating opportunities [16]. This dynamic has been observed in many populations [53, 114, 179]. The Allee effect is known to affect the rate of spread of a population [13, 118] and is expected to modify genetic drift on the edge of that population. Using simulation models with stochastic demography, Hallatschek and Nelson [82] provided a numerical analysis of the surfing phenomenon in the presence of an Allee effect. More precisely, using a backward-time approach, they analyzed the initial position of successful surfers in the wave. Significant differences in the probability distributions of the successful surfers were found between populations that experience an Allee effect and populations that do not. Using the framework of reaction-diffusion equations, they were able to connect their numerical findings to analytical formulas. Among other things, they concluded that surfing is not possible in deterministic reaction-diffusion, KPP type models [72, 112], i.e., without an Allee effect. The goal of our study is to investigate how the Allee effect determines genetic diversity in a colonization front and to do so in a context broader than that considered in the surfing phenomenon.

Following the framework provided by Hallatschek and Nelson [82] and Vlad *et al.* [181], we focus

on one-dimensional reaction-diffusion equations of the form :

$$\partial_t u = \partial_{xx} u + f(u),\ t > 0,\ x \in (-\infty, +\infty), \tag{2.1}$$

where $u = u(t, x)$ is the density of the population (of genes or haploid individuals) at time t and space position x. It evolves in time under the joint effects of local dispersal accounted for by the diffusion term and local reproduction described by the growth function f. Since Skellam's work [169], these models have commonly been used to explore population range expansions. However, little is known regarding the evolution of the inside structure of these models' solutions, that is, the dynamics of the components through which the structure of a population is determined.

Under some assumptions on the function f and the initial population u_0, the solutions of (2.1) converge to traveling wave solutions [9, 71, 112]. These solutions describe the invasion of the unoccupied region with a constant speed c and a constant density profile U and the population density can be written as $u(t, x) = U(x - c\,t)$. In this study, we focus on such traveling wave solutions, and our aim is to study the evolution of their inside structure depending on the growth term f.

Assuming that a population is initially composed of several neutral fractions, we provide a mathematical analysis of the spatio-temporal evolution of these fractions, i.e., of the proportion of each fraction at each position in the colonization front. Our mathematical analysis of the models investigates the following questions : (i) how do the proportions of the different fractions evolve in a traveling wave generated by a classical KPP model ; (ii) does the presence of an Allee effect modify the proportions of the different fractions in a traveling wave, i.e., does it enhance or reduce diversity in the colonization front ; and (iii) do the proportions of the different fractions at a particular location evolve rapidly after the traveling wave has passed, i.e., is the diversity determined by the front durable.

2.2 The model, main hypotheses and classical results

We assume that the population is composed of genes or haploid individuals. Its total density u satisfies the equation (2.1). This population is made of several *neutral* fractions v^k ; see Fig. 2.1. In particular, at time $t = 0$:

$$u_0(x) := u(0, x) = \sum_{k \geq 1} v_0^k(x),\ \text{with } v_0^k \geq 0 \text{ for all } k \geq 1.$$

We assume that the genes (or the individuals) in each fraction only differ by their position and their allele (or their label), while their dispersal and growth capabilities are the same as the total population u, in the sense that the density of each fraction verifies an equation of the form :

$$\left\{ \begin{array}{rcl} \partial_t v^k & = & \partial_{xx} v^k + v^k\, g(u),\ t > 0,\ x \in \mathbb{R}, \\ v^k(0, x) & = & v_0^k(x),\ x \in \mathbb{R}. \end{array} \right. \tag{2.2}$$

with $g(u) = f(u)/u$. Thus, the per capita growth rate $g(u)$ of each fraction v^k is equal to the per capita growth rate of the total population. Also note that each fraction v^k is positive everywhere at positive times, and that, as expected, the sum of the fraction densities verifies (2.1). Given the uniqueness of the solution to the initial value problem associated with (2.1), this sum is equal to $u(t, x)$.

Note that for diploid populations, the system (2.2), which governs the dynamics of the allelic densities, can also be derived from a weighted sum of the equations governing the genotype densities, such as those given in [9].

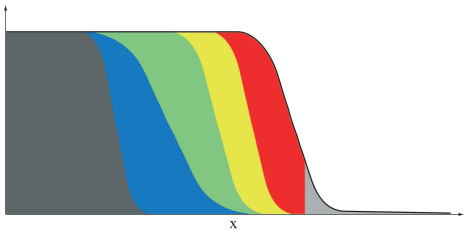

FIGURE 2.1 – A schematic representation of a traveling wave solution $u(t,x)$ of (2.1) made of six fractions. Each fraction is depicted with a different color and with a thickness which corresponds, at each position x, to the density v^k of the fraction.

2.1 Growth functions

We assume that f is continuous, continuously differentiable and vanishes at 0 and 1, with $f'(1) < 0$. Under the above assumptions, 0 and 1 are stationary states of the main equation (2.1). When $u = 0$, the species is not present, and when $u = 1$, the environment is fully colonized.

The first type of growth functions that we consider are of KPP type.

Definition 1. *A growth function is said to be of KPP type if, in addition to the above assumptions, it satisfies*

$$0 < f(u) \leq f'(0)\, u, \ \textit{for all } u \in (0,1). \tag{2.3}$$

Under this assumption, the per capita growth rate $g(u) = f(u)/u$ always remains smaller than its value at $u = 0$, i.e., $f'(0)$. This means that higher densities result in lower individual reproductive success, i.e., that the individuals compete with each other and that there is no cooperation between them. A typical example of function f satisfying the KPP assumption is the logistic function defined by $f(u) = u\,(1-u)$, which was used in [82] and [181].

The second type of growth function that we consider is a cubical polynomial that does not verify the KPP assumption.

Definition 2. *A growth function is said to be of the Allee type if it satisfies, for some* $\rho \in (0, 1/2)$,

$$f(u) = u\,(1-u)\,(u-\rho) \ \textit{for all } u \in (0,1). \tag{2.4}$$

In this case, the per capita growth rate $g(u) = f(u)/u$ is negative for low values of the density u, which corresponds to a strong Allee effect. The parameter ρ corresponds to the so-called "Allee threshold", below which the growth rate becomes negative [9, 105, 118]. Other functions f could have been considered that may not be cubical polynomials and have an $f'(0)$ value that is still negative. We chose to address only functions of the type (2.4) for the sake of simplicity, as the profile of the unique global front is known and the subsequent calculations are explicit.

2.2 Traveling wave solutions

The traveling wave solutions verify $u(t,x) = U(x - c\,t)$, for the speeds $c > 0$ precised below. Substituting this expression into (2.1), it follows that the profiles U of the traveling waves satisfy the following ordinary differential equation :

$$U'' + c\,U' + f(U) = 0 \text{ in } \mathbb{R} \text{ and } \ U(-\infty) = 1 \text{ and } U(+\infty) = 0.$$

Such traveling waves propagate from left to right and describe the invasion of an environment where the species is not present with a constant speed c and a constant density profile U.

The existence of such solutions has been proved in [72, 112] for KPP growth functions and in [9, 71] for growth functions of the Allee type. These studies show that, starting from a step-function ($u_0(x) = 1$ for $x \leq 0$ and $u_0(x) = 0$ for $x > 0$), the solution of the equation (2.1) converges to a traveling wave. In the KPP case, this traveling wave propagates at the speed $c = 2\sqrt{f'(0)}$ [112].

Under the Allee assumption, the profile U (up to shifts in x) and the speed c of the traveling wave are known :

$$U(x) = \frac{1}{1 + e^{x/\sqrt{2}}} \text{ and } c = \frac{1 - 2\rho}{\sqrt{2}}. \tag{2.5}$$

In the KPP case, the traveling wave with minimal speed $c = 2\sqrt{f'(0)}$ propagates at the same speed as the solution of the linear equation :

$$\partial_t u = \partial_{xx} u + f'(0)\, u. \tag{2.6}$$

This corresponds to a *pulled wave* [172], where the wave is pulled by the leading edge of the population distribution. Under the KPP assumption, other waves propagating at speeds $c > 2\sqrt{f'(0)}$ are known to exist, and Stokes [172] defines them as being pulled. When the Allee effect is present, there is a unique traveling wave, given by (2.5). Its speed $c = (1 - 2\rho)/\sqrt{2}$ is strictly positive, whereas the solution of the linear equation (2.6) converges uniformly to 0. The corresponding wave is called a *pushed wave* [172, 161].

The results shown in the next sections provide a new and intuitive explanation of these notions of pushed and pulled waves.

2.3 Results : how the fractions propagate

We consider an arbitrarily chosen fraction v^k that satisfies (2.2) –we call it v in the sequel– and we study the evolution of the density $v(t, x)$. From our assumptions, the total population $u(t, x)$ verifies that $u(t, x) = U(x - c\,t)$. Thus, the density of the fraction satisfies :

$$\partial_t v = \partial_{xx} v + v\, g(U(x - c\,t)),\ t > 0,\ x \in \mathbb{R}. \tag{2.7}$$

Moreover, when $t = 0$, $u_0(x) = U(x)$ and $v_0(x) = v(0, x)$ corresponds to a fraction of the quantity $U(x)$, thus $0 \leq v_0(x) \leq U(x)$ for all $x \in \mathbb{R}$. From the stability properties of the traveling waves, considering the initial condition $u_0(x) = U(x)$ is equivalent to defining the fractions inside a population which has already reached its stationary profile. Biologically, this means that we consider the spatio-temporal evolution of the diversity distributed at a given time in an ongoing wave of colonization.

Using the properties of the growth function f and the subsequent properties of the profile U and of the speed c, we can describe the evolution of v in a moving interval with speed c, as well as behind the waves.

3.1 Evolution of the density v of the fraction in a moving frame

In this section, we study the evolution of the density v of the fraction in an interval moving at the same speed c as the total population. Two situations may occur herein. Either the fraction is able to follow the total population and spreads with the same speed c, or the fraction is not able to follow the total population.

Our first result is concerned with the KPP case and is valid under general assumptions on the initial density v_0 of the fraction. These assumptions include the particular case of compactly supported initial fractions (i.e., $v_0(x) = 0$ outside a bounded set) and are verified by all the fractions depicted in Fig. 2.1, with the exception of the rightmost (light grey) one.

Result 1a (KPP case, see proof in Appendix A) : *If the initial density v_0 of the fraction converges to 0 faster than U as $x \to +\infty$,*[3] *then, for any $A \in \mathbb{R}$, the density $v(t,x)$ of the fraction converges (as $t \to \infty$) to 0 uniformly in the moving half-line $[A + c\,t, \infty)$.*

This result shows that under the KPP assumption any fraction v whose initial density $v_0(x)$ is 0 for large x cannot expand with the total population.

It was stated in [82] that gene surfing was not possible for the logistic growth function $f(u) = u\,(1-u)$. If by gene surfing we mean that the wave tends to be made of a single fraction, then our result also shows that surfing is not possible for fractions with compactly supported initial densities. However, the surfing of fractions that are not initially compactly supported can occur, even with logistic growth functions. Consider the rightmost fraction v^r (the light grey fraction in Fig. 2.1) : at $t = 0$, $v_0^r = U \cdot \mathbb{1}_{[\alpha,\infty)}$, where $\mathbb{1}_{[\alpha,\infty)}$ denotes the indicator function of the interval $[\alpha, \infty)$, for some $\alpha \in \mathbb{R}$. The fraction corresponding to the remaining part of the population verifies $v_0^l = U \cdot \mathbb{1}_{(-\infty,\alpha)}$ as well as the assumption of Result 1a. Because $u(t,x) = U(x - c\,t) = v^l(t,x) + v^r(t,x)$, this result shows that $v^r(t,x)$ converges to $U(x - c\,t)$ in any moving half-line $[A + c\,t, \infty)$. This means that the fraction v^r manages to "surf" on the wave.

Result 2a (Allee case, see proof in Appendix B) : *For any $A \in \mathbb{R}$, the density v of the fraction converges (as $t \to \infty$) to a proportion $p[v_0]$ of the total population $u(t,x)$ in the moving half-line $[A + c\,t, \infty)$, that is $v(t,x) - p[v_0]u(t,x) = v(t,x) - p[v_0]U(x - c\,t) \to 0$ as $t \to \infty$, uniformly in $[A + c\,t, \infty)$. The proportion $p[v_0]$ can be computed explicitly :*

$$p[v_0] = \frac{\displaystyle\int_{-\infty}^{+\infty} v_0(x)\,U(x)\,e^{c\,x}\,dx}{\displaystyle\int_{-\infty}^{+\infty} U^2(x)\,e^{c\,x}\,dx} \in [0,1]. \tag{2.8}$$

This result shows that any fraction v with a non-zero initial density v_0 follows the total population. Moreover, in the interval moving with speed c, the profile $v(t, c\,t + \cdot)$ of the fraction tends to resemble the profile U of the total population, with a scaling factor $p[v_0]$ dependent on the initial density v_0. Note that the integral terms in the expression of p are well-defined, and this can be easily checked using the formulas (2.5). This would not be true under the KPP assumption [9].

The formula (2.8) provides precise information regarding the origin of the individuals that compose the wave at large times. Let us again consider the "leftmost" fraction defined by $v_0^l = U \cdot \mathbb{1}_{(-\infty,\alpha)}$ for $\alpha \in \mathbb{R}$. The asymptotic proportion of this fraction in any moving half-line with speed c is $p(\alpha) := p[v_0^l]$. Differentiating $p(\alpha)$ with respect to α, we obtain a quantity $p'(\alpha)$ that can be interpreted as the relative

3. This means that $\displaystyle\int_0^{+\infty} e^{\frac{c\,y}{2}}\,v_0(y)dy < \infty$.

contribution to the wave of the individuals with an initial position α :

$$p'(\alpha) = U^2(\alpha)\, e^{c\,\alpha} / \left(\int_{-\infty}^{+\infty} U^2(x)\, e^{c\,x}\, dx \right).$$

Using a similar formula, and replacing U with the solution of a stochastic simulation model incorporating an Allee effect, Hallatschek and Nelson [82] obtained a good fit of the probability of gene surfing in their model.

Here, the density profile U is known explicitly. Using formula (2.5), we observe that $p'(\pm\infty) = 0$ and that p' reaches a unique maximum at

$$\alpha_{\max} = \sqrt{2} \ln \left(\frac{1 - 2\,\rho}{1 + 2\,\rho} \right). \tag{2.9}$$

Interestingly, $\alpha_{\max}$ is a decreasing function of ρ, with $\alpha_{\max}(0) = 0$, corresponding to the position of the inflexion point of the profile U, and $\alpha_{\max}(1/2) = -\infty$. This formula emphasizes the advantageous role of the Allee effect for the fractions situated deep in the core of the population ; the stronger the Allee effect, the more these individuals will contribute to the wave.

3.2 Evolution of the density v of the fraction behind the wave

The aim of the previous section was to analyze the behavior of an arbitrarily chosen fraction in a moving interval $[A+c\,t, \infty)$, with speed c equal to the spreading speed of the total population. Here, we analyze the evolution of the density of the fraction in the remaining part of the space : $(-\infty, A + c\,t)$. We assume that the initial density $v_0(x)$ of the fraction converges to 0 as $x \to -\infty$.

Result 1b (KPP case, see proof in Appendix C) : *If the initial density v_0 of the fraction converges to 0 faster than U as $x \to +\infty$, [1] then for any $A \in \mathbb{R}$, the density of the fraction converges (as $t \to \infty$) to 0 uniformly in the moving half-line $(-\infty, A + c\,t)$.*

This result, together with Result 1a, implies that the density $v(t,x)$ of the fraction converges to 0 uniformly in $\mathbb{R}$ as $t \to \infty$. Thus, under the KPP assumption, any compactly supported fraction will vanish in the sense that, at large times, its density becomes negligible at any point of the space, as a result of dilution.

Result 2b (Allee case, see proof in Appendix D) : *For any speed $c' \in (0, c)$ and any $A \in \mathbb{R}$, the density $v(t,x)$ of the fraction converges (as $t \to \infty$) to the proportion $p[v_0]\, u(t,x)$ in a set of the form $(c'\,t, A + c\,t)$. Besides, for any $\varepsilon > 0$ and $B > 0$, $p[v_0]/2 - \varepsilon < v(t,x) < p[v_0] + \varepsilon$ in the set $[-B, A + c\,t)$ for $t > 0$ and $-A > 0$ large enough.*

Result 2a shows that, in any moving half-line $[A + c\,t, \infty)$, the density v of the fraction tends to resemble a proportion $p[v_0]$ of the total population u when the Allee effect is present. Result 2b shows that this is actually true in $(c'\,t, +\infty)$, for any $c' > 0$. This result also indicates that the fraction v propagates to the right with the same speed as the total population, but also propagates in the opposite direction, given that B can be chosen arbitrarily large. Moreover, this result implies that the fraction centroid moves to the right at a speed lesser or equal to $c/2$.

2.4 Numerical computations

Our analytical results were derived for a front-like initial condition $u_0(x) = U(x)$, corresponding to an already established traveling wave. We investigate numerically whether these results remain qualitatively true when u_0 is a compactly supported step function (Fig. 2.2 a) which has not yet reached a traveling wave profile. We assume that the population is made of $N = 9$ fractions υ^k which verify, at $t = 0$, $\upsilon_0^1 = \mathbb{1}_{(-40,-21]}$, $\upsilon_0^k = \mathbb{1}_{(x_{k-1},x_k]}$ for $k = 2, \ldots, N$ for the sequence $x_1 < x_2 < \ldots < x_N = 0$ of evenly spaced points. We numerically solved equation (2.2) with KPP and Allee growth terms. In both cases, we observed that the solution $u(t, x)$ rapidly converges to a traveling wave profile (dashed curves in Fig. 2.2).

4.1 KPP case

The figure 2.2 b shows the evolution of the spatial structure of the solution $u(t, x)$ of (2.1) with a KPP growth term. As predicted by Results 1a and 1b, only the rightmost fraction follows the propagation to the right of the total population. The mass of the rightmost fraction, which was initially small, increases linearly with time. This could be interpreted as a form of surfing. We can observe that this fraction slowly diffuses into the bulk of the population, but with a null speed (i.e., sublinearly).

We observe that the spatial structure of the population has a “vertical pattern", meaning that the population is highly spatially structured. Fig. 2.2 b shows that the evolution of this pattern is slow compared to the rate at which the population propagates. Actually, since the growth term $\upsilon^k\, g(u)$ in (2.2) is always positive, the density of the fractions $2, \ldots, N-1$ cannot decrease to 0 faster than the solution of the heat equation $\partial_t \upsilon = \partial_{xx} \upsilon$, i.e., cannot decrease faster than the order $1/\sqrt{t}$.

4.2 Allee case

With the Allee growth function (2.4), the numerical results of Fig. 2.2 c and Fig. 2.2 d show that the theoretical predictions of Results 2a and 2b remain qualitatively true when u_0 is compactly supported. In particular, the stronger the Allee effect is, the more the fractions situated deep in the core of the population contribute to the wave.

The rightmost fraction remains the most represented in the colonization front. However, contrary to the KPP case, all the other fractions are conserved in the colonization front, leading to a spatial structure of the population with a “horizontal pattern".

2.5 Discussion

Using a mathematical model commonly recognized in the literature as a robust descriptor of a population colonizing an empty space [92, 103, 175], we showed that the presence of an Allee effect drastically modifies genetic diversity in the colonization front. When an Allee effect is present, all of the fractions of a population are conserved in the colonization front, even if their proportions differ according to their initial distribution. In the absence of an Allee effect, only the furthest forward fraction in the initial population eventually remains in the colonization front, indicating a strong erosion of diversity due to the demographic advantage of isolated individuals ahead of the colonization front. Under this classical KPP model, any fraction except that located at the head of the front

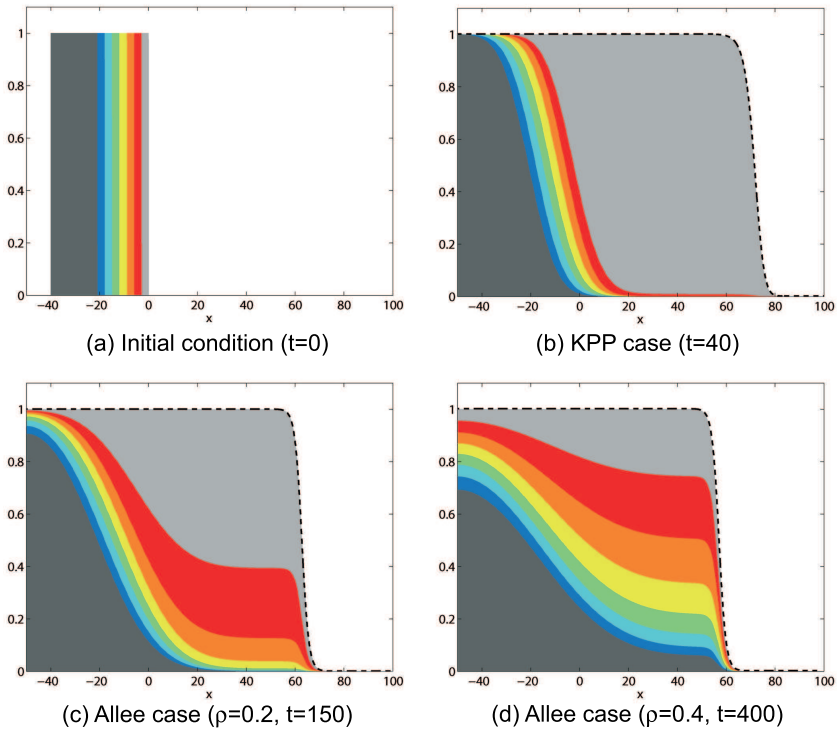

FIGURE 2.2 – Evolution of the spatial structure of the solution $u(t,x)$ of (2.1). (a) : initial distribution of the fractions ; (b) : spatial structure of the colonization wave $u(t,x)$ with the KPP growth term $f(u) = u\,(1-u)$; (c) and (d) : spatial structure of the colonization wave $u(t,x)$ with the growth term $f(u) = u\,(1-u)\,(u-\rho)$. In each case, the dashed black curve corresponds to the profile U of the stable traveling wave solution of (2.1).

vanishes progressively ; this shows that the “enhanced transport" of neutral fractions described by Vlad *et al.* [181] for similar equations is only a transient phenomenon.

These results diversify the commonly held perspective that the Allee effect possesses net adverse consequences. This perspective is inherited from demographic studies of range expansion, which demonstrate that an Allee effect reduces the speed of colonization [118, 119] and can even stop it in heterogeneous environments [13]. Reducing the growth rate of the individuals ahead of the colonization front simultaneously reduces the speed of colonization and enables a diversity of genes coming from the core of the population to remain on the front, as demonstrated by Result 2a and formula (2.9). Other mechanisms that reduce the growth rate of the individuals ahead of the front should also result in greater conservation of the genetic diversity of a population. For instance, Pluess [145] demonstrated how a retreating glacier limited the spread of a population of European larch, thereby functioning as an extreme Allee effect where all of the seeds falling on the icecap die. Given our results, this should lead to high genetic diversity in the colonization front, which was actually observed [145]. The Allee effect could be a partial or alternative explanation to the argument of long-distance mixing of genes advanced in [145]. Our results are also consistent with the findings in [12] which showed that the existence of a juvenile phase (i.e., a non-reproductive life-stage) in the life-cycle of an organism can lead to higher levels of genetic diversity. Although the juvenile phase does not generate an Allee effect in the strictest sense, it slows down the colonization process in a similar way, thus enabling an accumulation of genetic diversity in the colonization front.

The Allee effect also affects the spatial distribution of diversity. As Fig. 2.2 c and Fig. 2.2 d illustrate, this effect leads to a “horizontal pattern" of genetic diversity (i.e., an absence of genetic differentiation in space), and Result 2b shows that, after the population has reached its maximum capacity, this pattern diffuses in the opposite direction within the core of the population. Conversely, we observed a “vertical pattern" of genetic diversity in the absence of an Allee effect (i.e., a strongly structured spatial distribution of population fractions ; see Fig. 2.2 b). This genetic structure eventually attenuates due to diffusion in the saturated population and each fraction becomes negligible. However, in both cases the diffusion in the saturated population occurs at a much lower rate than the rate of colonization (sublinear diffusion vs. linear propagation). These two time-scales are consistent with the results obtained in [11] with a stepping-stone model.

Genetic drift is not taken into account in our forward-time approach, and this is an important difference between this study and [82]. In [82], the dominant role of genetic drift eventually leads to the fixation of a single gene in the colonization front, leading to a total loss of diversity. However consistent results are obtained from their backward-time approach. In the absence of stochastic genetic drift, the deterministic evolution of the allelic densities does not depend on the distribution of the alleles within and among diploid individuals [91]. Our results can therefore be applied to the dynamics of genetic diversity in haploid as well as diploid populations.

Our forward-time approach also underlines the ambiguity in the definition of the surfing phenomenon. Surfing can be associated with either (i) a rare gene becoming drastically dominant in the front or, (ii) with a gene initially present on the front being propagated alongside others present in the front. These two definitions lead to contradictory results, as with definition (i), gene surfing is only possible without an Allee effect and for the furthest forward fraction of the front, and definition (ii) dictates that gene surfing is promoted by the Allee effect. In the presence of an Allee effect, the centroid of any fraction of the front is propagated at speed $c/2$, which is consistent with the fact that any fraction spreads between its initial location and the leading point of the front [62, 65].

From a mathematical standpoint, our study contributes a new perspective to the extensively studied topic of reaction-diffusion equations. One of the main features of these equations is their exhibition of traveling wave solutions that keep a constant profile. Earlier approaches were concerned with the dynamics of the total waves, making our study the first, to our knowledge, to mathematically analyze the dynamics of the inside structure of these waves. Our results show that these dynamics are strongly dependent on the type of growth function f, and seem to be determined by the pulled-pushed nature of the waves. Conversely, our observations show that the notions of pulled and pushed solutions can be defined based on the inside structure of the solutions rather than on their speed of propagation. This new conceptualization of pushed and pulled solutions, whose mathematical definitions will be given in a future work, has the advantage of being intuitive and adaptable to more complex models that do not necessarily admit traveling wave solutions. For instance, we should now be able to determine the pushed-pulled nature of the solutions of (i) integro-differential equations including long distance dispersal events and resulting in accelerating waves [Ga11, 113], (ii) reaction-diffusion equations with spatially heterogeneous coefficients that lead to pulsating or generalized transition waves [21, 190], (iii) reaction-diffusion equations with forced speed, which have been used in [17] to study the effects of a shifting climate on the dynamics of a biological species. These processes are known in ecology to be determinants of the colonization patterns of many organisms [52, 103] and their effects on genetic diversity require further investigation [65].

2.6 Appendices

6.1 Appendix A : Proof of Result 1a

The main idea of the proof is to compare the equation verified by v with a homogeneous linear equation, and to compute explicitly the solution of the linear equation.

Recall that v satisfies (2.7). From the KPP assumption, we know that $g(U(x-ct)) \leq f'(0)$. Thus, a comparison argument implies that v is smaller than the solution w of the equation : $\partial_t w = \partial_{xx} w + w\, f'(0)$, with the same initial condition $w(0,x) = v_0(x)$. This function w can be computed explicitly. Fix $A \in \mathbb{R}$ and consider an element $x_0 + ct$ in the moving half-line $[A + ct, \infty)$. Since $c = 2\sqrt{f'(0)}$, we have :

$$w(t, x_0 + ct) = \frac{e^{\frac{-x_0\, c}{2}}}{\sqrt{4\pi t}} \int_{-\infty}^{\infty} e^{\frac{cy}{2}}\, v_0(y)\, e^{-\frac{(x_0-y)^2}{4t}}\, dy.$$

Finally, since $x_0 \geq A$ and $\displaystyle\int_{-\infty}^{+\infty} e^{\frac{cy}{2}}\, v_0(y) dy < \infty$, we get :

$$w(t, x_0 + ct) \leq \frac{e^{\frac{-A\, c}{2}}}{\sqrt{4\pi t}} \int_{-\infty}^{\infty} e^{\frac{cy}{2}}\, v_0(y)\, dy \;\to\; 0 \text{ as } t \to \infty,$$

and the above convergence is uniform in $x_0 \in [A, +\infty)$. Since $0 \leq v(t,x) \leq w(t,x)$, this implies the assertion in Result 1a.

6.2 Appendix B : Proof of Result 2a

In the moving frame with speed c, the fraction density can be written $\tilde{u}(t,x) = v(t, x+ct)$. In order to remove the advection terms which appear in the equation verified by $\tilde{u}$, we set $v^*(t,x) = \tilde{u}(t,x)\, e^{cx/2}$. Then, we can check that the function v^* is a solution of a linear equation without advection term :

$$\partial_t v^* = \partial_{xx} v^* + v^* \left[g(U(x)) - \frac{c^2}{4} \right], \tag{2.10}$$

with the initial condition $v^*(0,x) = v_0(x)\, e^{c\,x/2}$. In the remaining part of the proof, we show that v^* can be written as the sum of a stationary function and of a function which converges to 0 exponentially fast as $t \to \infty$.

Note that $\varphi(x) = e^{c\,x/2}\, U(x)$ is a positive eigenfunction of the operator which appears in the right hand side of (2.10), and that the associated eigenvalue is 0. The Sturm-Liouville theory implies that 0 is the largest eigenvalue of this operator, the remaining part of the spectrum being located at the left of some negative constant $-\mu$. Thus, we can write :

$$v^*(t,x) = p\,\varphi(x) + z(t,x), \tag{2.11}$$

where $p \in \mathbb{R}$ and z is "orthogonal" to φ in the sense that $\displaystyle\int_{-\infty}^{\infty} z(t,x)\varphi(x)\,dx = 0$, for each $t \geq 0$. Moreover, $|z(t,x)| \leq K\, e^{-\mu\, t}$, for some constant $K > 0$. Multiplying the expression (2.11) at $t = 0$ by φ and integrating, we get the expression (2.8) for p.

Finally, we have $|v^*(t,x) - p\,\varphi(x)| \leq K\, e^{-\mu\, t}$ and therefore $\tilde{u}(t,x) - p\,U(x)| \leq K\, e^{-\mu\, t - c\,x/2}$. This shows that $\tilde{u}(t,x)$ converges to $p\,U(x)$ uniformly in any moving half-line $[A - c'\,t, +\infty)$ with $c' \in [0, 2\,\mu/c)$. In particular, taking $c' = 0$ and using $v(t,x) = \tilde{u}(t, x - c\,t)$ we obtain that, for any $A \in \mathbb{R}$, the fraction density converges to a proportion p of the total population $u(t,x) = U(x - c\,t)$, uniformly in the moving half-line $[A + c\,t, +\infty)$.

6.3 Appendix C : Proof of Result 1b

Take any $\varepsilon > 0$. From Result 1a, we already know that for any $A < 0$ there exists a time $t_A > 0$ such that $0 < v(t, A + c\,t) < \varepsilon/2$ for all $t \geq t_A$. Again, we place ourselves in the moving frame with speed c : $\tilde{u}(t,x) = v(t, x + c\,t)$ satisfies $0 < \tilde{u}(t,A) < \varepsilon/2$ and verifies the equation :

$$\partial_t \tilde{u} = \partial_{xx}\tilde{u} + c\,\partial_x \tilde{u} + g(U(x))\tilde{u},\ t > 0,\ x \in \mathbb{R}. \tag{2.12}$$

By constructing a super-solution to (2.12) close to the solution of the heat equation, we are going to show that $\tilde{u} \to 0$ in $(-\infty, A]$ as $t \to \infty$.

The assumption $v_0(x) \to 0$ as $x \to -\infty$ implies that, for any $t > 0$, $\tilde{u}(t,x) \to 0$ as $x \to -\infty$. In particular, there exists a point $x_A < A$ such that $\tilde{u}(t_A, x) \leq \varepsilon/2$ for all $x \leq x_A$. Thus, in the interval $(-\infty, A]$, and for times larger than t_A, $\tilde{u}$ is smaller than the solution $\overline{u}$ of :

$$\begin{cases} \partial_t \overline{u} = \partial_{xx}\overline{u} + c\,\partial_x \overline{u} + f(U(x)),\ t \geq t_A,\ x < A, \\ \overline{u}(t,A) = \varepsilon/2,\ t \geq t_A, \\ \overline{u}(t_A, x) = \begin{cases} 1 & \text{if } x \in (x_A, A), \\ \varepsilon/2 & \text{if } x \leq x_A. \end{cases} \end{cases} \tag{2.13}$$

Consider the auxiliary problem

$$\begin{cases} \partial_t \overline{u}^1 = \partial_{xx}\overline{u}^1 + c\,\partial_x \overline{u}^1,\ t \geq t_A,\ x \in \mathbb{R}, \\ \overline{u}^1(t_A, x) = \begin{cases} 1 & \text{if } x \in (x_A, A), \\ \varepsilon/2 & \text{if } x \leq x_A \text{ or } x \geq A. \end{cases} \end{cases} \tag{2.14}$$

Then, $\overline{u}^1$ is simply the solution of the heat equation with an advection term and can be computed explicitly. In particular, we have $\max_{x\in\mathbb{R}} \overline{u}^1(t,x) \leq \varepsilon/2 + C/\sqrt{t}$ for some constant $C > 0$. Setting $j(x) = -\varepsilon\, x/(1 - x)$ for $x < 0$, we observe that $-j'' - c\,j'$ is positive and decreases like $c\,\varepsilon/x^2$ as $x \to -\infty$. Under the KPP assumption, it is known [10] that the profile $U(x)$ of the traveling wave converges exponentially to 1 as $x \to -\infty$. Using $f(1) = 0$ and $f'(1) < 0$, this implies that

$f(U(x))$ converges exponentially to 0 as $x \to -\infty$. Thus, if A is chosen negative enough, $f(U(x)) \leq -j''(x) - c\,j'(x)$ in $(-\infty, A]$. The parabolic maximum principle then shows that $\overline{u}^1(t,x) + j(x) \geq \overline{u}(t,x)$ in $(-\infty, A]$, for all $t \geq t_A$. We finally get :

$$\varepsilon + C/\sqrt{t} \geq \overline{u}^1(t,x) + j(x) \geq \overline{u}(t,x) \geq \tilde{u}(t,x), \tag{2.15}$$

for all $t \geq t_A$, $x \in (-\infty, A]$. Thus, $v(t,x) \leq \varepsilon + C/\sqrt{t}$ in $(-\infty, A + c\,t]$ for all $t \geq t_A$.

6.4 Appendix D : Proof of Result 2b

From Result 2a, we know that for any $A \in \mathbb{R}$ there exists a time t_A such that $|v(t, A+c\,t) - p\,U(A)| < \varepsilon/4$ for all $t \geq t_A$. Thus, if A is negative enough, since $U(-\infty) = 1$, we have $|v(t, A + c\,t) - p| < \varepsilon/3$ for $t \geq t_A$. Using the same arguments as in the proof of Result 1b, we can show that $v(t,x)$ is smaller than $p + \varepsilon$ in the half-line $(-\infty, A + c\,t]$ for t large enough.

In order to construct a lower bound for v, we construct an appropriate sub-solution. First, one can choose $A < 0$ such that $f(U(x)) \geq 0$ for all $x \leq A$. Then, setting

$$\left\{ \begin{array}{l} \partial_t \underline{u} = \partial_{xx} \underline{u} + c\,\partial_x \underline{u},\ t \geq t_A,\ x \in \mathbb{R}, \\ \underline{u}(t_A, x) = \left\{ \begin{array}{ll} 0 & \text{if } x \leq A, \\ p - \varepsilon/2 & \text{if } x \geq A, \end{array} \right. \end{array} \right. \tag{2.16}$$

a comparison argument implies that $\tilde{u}(t,x) = v(t, x+c\,t)$ is larger than $\underline{u}(t,x)$ for all $t \geq t_A$ and $x \leq A$. Again, the equation (2.16) simply corresponds to the heat equation with an advection term and its solution can be computed explicitly. For any $t > t_A$, the function $\underline{u}(t,\cdot)$ is increasing and therefore $\underline{u}(t + t_A, x) \geq \underline{u}(t + t_A, c'(t + t_A) - c\,t - B)$ for all $t > 0$, $B \geq 0$ and $x \geq c'(t + t_A) - c\,t - B$, which gives :

$$\underline{u}(t + t_A, x) \geq \frac{p - \varepsilon/2}{\sqrt{\pi}} \int_{\frac{A - B - c'(t + t_A)}{2\sqrt{t}}}^{\infty} e^{-z^2}\, dz.$$

As a consequence, if $0 < c' < c$, $v(t,x)$ is larger than $p - \varepsilon$ in $(c'\,t, A + c\,t)$ for t large enough. We also observe (with $c' = 0$) that $v(t,x)$ is larger than $p/2 - \varepsilon$ in $[-B, A + c\,t)$ for t large enough.

Acknowledgments

The authors are supported by the French “Agence Nationale de la Recherche" within the projects ColonSGS, PREFERED and URTICLIM. We thank Bruno Fady, Claire Lavigne, Samuel Soubeyrand and an anonymous reviewer for their insightful comments.

Chapitre 3

Success rate of a biological invasion in terms of the spatial distribution of the founding population

Ce travail réalisé en collaboration avec Lionel Roques [a], et François Hamel [b,c]
est publié dans le *Bulletin of Mathematical Biology* [GHR12]

[a] UR 546 Biostatistique et Processus Spatiaux, INRA, F-84000 Avignon, France
[b] Aix-Marseille Université, LATP, Faculté des Sciences et Techniques
Avenue Escadrille Normandie-Niemen, F-13397 Marseille Cedex 20, France
[c] Institut Universitaire de France

Sommaire

3.1 Introduction

Over the last decades, the number of biological invasions by alien organisms has increased exponentially [50], in large part because of human activities such as trade and travel. These biological invasions are characterized by a rapid expansion of the invasive organism's range. They are usually associated with biodiversity losses [98, 99, 107] and often cause significant harm to ecosystem functioning [150, 180], socio-economic values [106] and human health [151, 180] in the invaded regions.

The typical sequential stages of a successful invasion process begin with the introduction of a small founding population (that is, arrival), followed by the establishment and spread stages [55, 182]. During the establishment stage, the individuals in the founding population reproduce and increase in number to form a colony that is self-perpetuating. The spread corresponds to the expansion of the species range into its new habitat.

Successful establishment often requires multiple introductions [150, 182]. The success of the establishment phase indeed depends on the size of the founding population as well as on several endogenous and exogenous factors. Understanding the intertwined roles of these factors is of critical importance to slow down the rate at which biological invasions occur. In this chapter, we investigate the interactions between founding population characteristics (namely, size and spatial distribution) and the profile of the growth function associated with the population.

Environmental factors such as resource availability, spatial heterogeneity [24, 45, 67, 156, 159] and climate conditions [158, 182] can play an important role in the persistence of the newly introduced population. Additionally, because of the typically small size of the founding population, it is widely accepted that the Allee effect plays a critical role in the success of establishment [56, 117, 193]. The Allee effect can be seen in many species [7, 53, 114, 179] ; it indicates that the per capita growth rate of individuals decreases at low densities. This effect may result from several processes that can co-occur [16], such as diminished chances of finding mates at low densities [128], demographic stochasticity [115] or fitness decreases due to consanguinity.

In the present work, we analyze the effect of the spatial distribution of the founding population – that is, the repartition of the initial population into subgroups – on the success rate of an invasion. The relationships between successful establishment, the size of the founding population and the Allee effect have already been investigated in empirical (references above) and theoretical studies [10, 58, 118, 135, 175, 195]. The influence of the corrugation of the edge of the founding population on the invasion speed has also been studied by Lewis and Kareiva [118]. However, the effect of the spatial distribution of the founding population has received less attention. Considering a closely related problem based on a stochastic reaction-diffusion equation with successive random immigration events, Drury *et al.* [57] have shown the important role of the spatial distribution of the immigration events on the invasion risks. This suggests that the spatial distribution of the founding population, and in particular its rate of fragmentation, also plays an important role.

Because they draw on well-developed mathematical theory, reaction-diffusion models have been the main analytical framework to study the persistence and spread of biological organisms since the early work of Skellam [169]. One of the most frequent reaction-diffusion models is the Fisher-Kolmogorov-Petrovsky-Piskunov (FKPP) [72, 112] equation, which was first intended to describe the propagation of advantageous genes inside a population. However, this equation does not take the Allee effect into account. Thus, in FKPP models, the persistence of the population does not depend at all on the characteristics of the initial population, even in heterogeneous environments [22, 24, 26].

As a consequence, most studies that use FKPP-like models focus on the effects of environmental characteristics on persistence and spread [24, 45, 103] rather than on the effect of the initial condition. In contrast, we assume in this work that the underlying environment is homogeneous to isolate the effects of the characteristics of the initial population.

In the differential equations framework, the spatially homogeneous equation $N' = f(N)$, with $f(N) \leq 0$ for N below some threshold ρ, is a very simple example of a model involving an Allee effect. In this case, the dependence on the initial condition is obvious. In reaction-diffusion models, the Allee effect is typically modeled through bistable nonlinear terms [69, 175]. The dependence of the behavior of such models on initial conditions was first investigated by Aronson and Weinberger [10] and Fife and McLeod [71], and then by Zlatŏs [195] and Du and Matano [58] for one-dimensional models. In particular, for one-parameter families of initial conditions $u_0(L)$ that are strictly monotone with respect to the parameter L, it is shown in [58] that there is a unique critical threshold $L = L^*$ between extinction and propagation (see Section 3.3 for more details).

In this chapter, the effect of the spatial structure of the founding population u_0 (i.e., the initial condition in the model) is investigated for one-dimensional (1D) and two-dimensional (2D) models presented in Section 2.1. In both 1D and 2D cases, the initial conditions that we consider are binary functions which can only take the values 0 (absence of the species) and 1 (presence of the species). Because of their simple nature, these initial conditions are completely determined by their support, i.e., the regions where the species is present at $t = 0$. This allows us to focus on the effect of the geometrical properties of the support, namely its size and its fragmentation rate, on the outcome of the invasion. In the 1D case, to derive analytical computations, we consider a simple class of initial conditions which include the initial conditions which have been considered by Zlatŏs [195]. Their support is made of two intervals of the same length $L/2$, separated by a distance α, as described in Section 2.1. This distance is understood as a measure of the rate of fragmentation of u_0. In the 2D case, we consider more general, stochastically generated initial conditions, and we give a new rigorous definition of the rate of fragmentation in Section 2.2. Results are provided in Section 3.3. In the 1D case, the effects of fragmentation on the success of establishment and spread are investigated through analytical and numerical computations. In the 2D case, we carry out a statistical analysis of the probability of successful establishment, depending on the size of the support and the fragmentation rate of the initial condition.

3.2 Materials and methods

2.1 The reaction-diffusion model

Throughout this chapter, we assume that the population density $u(t, x)$ is driven by the following reaction-diffusion equation :

$$\begin{cases} u_t = D\,\Delta\, u + f(u), & \text{for } t > 0 \text{ and } x \in \mathbb{R}^n, \\ u(0, x) = u_0(x), & \text{for } x \in \mathbb{R}^n, \end{cases} \tag{3.1}$$

with $n = 1$ or $n = 2$ and $D > 0$.

The non-linear growth term $f(u)$ in (3.1) is assumed to satisfy :

$$f \in C^1(\mathbb{R}),\ f' \text{ is Lipschitz-continuous, } f(0) = f(1) = 0 \text{ and } \int_0^1 f(s)ds > 0. \tag{3.2}$$

In addition, we assume that the function f takes a strong Allee effect into account :

$$\text{There exists } \rho \in (0,1) \text{ such that } f < 0 \text{ in } (0,\rho) \text{ and } f > 0 \text{ in } (\rho,1). \tag{3.3}$$

This hypothesis means that the growth rate $f(u)$ is negative at low densities, which corresponds to a strong Allee effect. The parameter ρ corresponds to the so-called "Allee threshold", below which the growth rate becomes negative. It therefore measures the strength of the Allee effect. Under these assumptions, the solution to (3.1) may have several behaviors, depending on f and the initial density at $t = 0$. To provide a biological interpretation of these possible behaviors, we make the following definitions :

Definition 3 (Founding population)**.** *The founding population corresponds to the initial population at $t = 0 : u_0(x) = u(0,x) \in [0,1]$ for $x \in \mathbb{R}^n$, which is assumed to be compactly supported.*

Definition 4 (Successful establishment)**.** *We say that the establishment is successful if $u(t,x)$ converges to a positive stationary state as $t \to \infty$.*

Definition 5 (Successful invasion)**.** *We say that the invasion is successful if $u(t,x)$ converges to the stationary state 1 as $t \to \infty$.*

Definition 6 (Establishment failure)**.** *We say that the establishment phase has failed if $u(t,x)$ converges to the stationary state 0 uniformly in x as $t \to \infty$.*

Remark 5. *Note that successful establishment without successful invasion is possible but rare (see Section 3.1). In the 1D case, when the invasion is successful in the sense of Def. 5, then*

$$\begin{cases} \min\limits_{|x|\le ct} u(t,x) \to 1 \text{ as } t \to \infty & \text{for each } 0 \le c < c_0, \\ \max\limits_{|x|\ge c't} u(t,x) \to 0 \text{ as } t \to \infty & \text{for each } c' > c_0. \end{cases}$$

Note that $c_0 > 0$ is the unique speed of the traveling front $\phi(x - c_0 t)$ connecting 0 to 1 at $+\infty$ and $-\infty$ respectively [10].

For real populations, successful establishment without invasion can occur [several examples are given in 50, 51]. This corresponds to steady state populations with finite range. The existence of such steady states can be a consequence of environmental heterogeneity [e.g. the location of the species bioclimatic envelop, see Section 3.2 in 86]. In such heterogeneous environments, even when the population can adapt to its local conditions, gene flow can cause maladaptation of the peripheral groups and lead to finite range populations [108].

2.2 Initial conditions

Depending on the founding population u_0, establishment failure or establishment success can occur. To study this dependence, we consider particular types of initial binary conditions, namely $u_0 = 1$ or 0 almost everywhere. Note that support may vary in size and shape ; we focus in particular on the fragmentation of this support.

2.1 One-dimensional case

To derive analytical computations in the case $n = 1$, we consider a simple case of fragmentation.

$$u_0(x) = \chi_{[-(\alpha/2+L/2),-\alpha/2]}(x) + \chi_{[\alpha/2,\alpha/2+L/2]}(x) \text{ for } x \in \mathbb{R}. \tag{3.4}$$

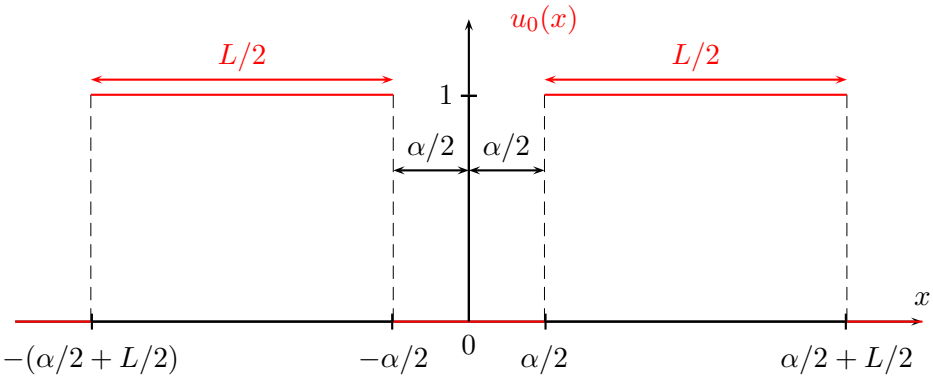

FIGURE 3.1 – An initial condition u_0 as defined by (3.4).

Note that for any set $J \subset \mathbb{R}$, χ_J is the characteristic function of J, that is, $\chi_J(x) = 1$ if $x \in J$ and $\chi_J(x) = 0$ otherwise.

This corresponds to an initial population density, whose support is split into two equal parts of length $L/2 > 0$ separated by a distance α (see Fig. 3.1). Problem (3.1) with "aggregated" initial conditions (i.e., with $u_0 = \chi_{[-L/2,L/2]}$, that is, $\alpha = 0$) has been investigated by several authors [102, 195].

Remark 6. *The problem* (3.1)*, with* $n = 1$ *and initial condition* (3.4)*, is equivalent to the Neumann problem.*

$$\begin{cases} u_t = D\,u_{xx} + f(u) \text{ for } t > 0 \text{ and } x \geq 0, \\ u_x(t,0) = 0 \text{ for } t > 0, \\ u(0,x) = \chi_{(\alpha/2,\alpha/2+L/2]}(x) \text{ for } x \geq 0. \end{cases} \tag{3.5}$$

Indeed, if u *solves* (3.1), (3.4)*, then* $u(t,-x)$ *also solves* (3.1), (3.4)*. By uniqueness, we obtain that* $u(t,x) = u(t,-x)$ *for all* $t > 0$ *and* $x \in \mathbb{R}$*. Thus,* u *also satisfies* (3.5)*. Conversely, by uniqueness of the solution of* (3.5) *and by extending it by symmetry on* $(-\infty, 0]$*, we obtain equivalence between* (3.1), (3.4) *and* (3.5)*.*

2.2 The two-dimensional case, the notion of abundance and the measure of fragmentation

The effect of the spatial distribution of the founding population can also be assessed in the two-dimensional case $n = 2$ through the numerical investigation of the behavior of the model solution (3.1) over a large number of stochastically generated initial conditions.

As in the 1D case, we assume the initial conditions u_0 to be binary functions, where

$$\text{at each point } (x,y) \text{ in } \mathbb{R}^2,\ u_0(x,y) \text{ either takes the value 0 or 1.} \tag{3.6}$$

We furthermore assume that the support of u_0 is included in a closed square C :

$$\text{for all } (x,y) \in \mathbb{R}^2,\ u(x,y) = 0 \text{ if } (x,y) \notin C. \tag{3.7}$$

To build samples of functions u_0 with various spatial distributions, we used a model developed by Roques and Stoica [159] and inspired by statistical physics. In this model, the square C is divided into n_C closed equi-measurable subsquares C_i, with interiors being pairwise disjoint. The obtained functions u_0 satisfy :

$$\text{for all } i = 1, \ldots, n_C,\ u_0 \text{ is constant over the interior of } C_i. \tag{3.8}$$

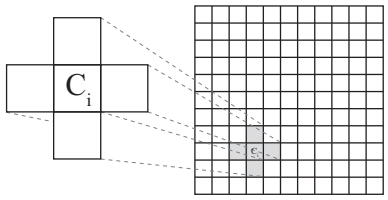

FIGURE 3.2 – The four-neighborhood system : an element C_i of C and its four neighbors.

As key properties, this stochastic model allows exact control over the population abundance level

$$p(u_0) = \frac{1}{|C|} \int_C u_0(x, y)\, dxdy,$$

and leads to configurations with different levels of fragmentation. The notion of fragmentation is defined as follows.

The lattice made of cells C_i is equipped with a four-neighborhood system $V(C_i)$ (Fig. 3.2). For each function u_0, constant on the subsquares C_i, we define

$$s(u_0) = \frac{1}{2} \sum_{C_i \subset C} \sum_{C_j \in V(C_i)} \mathbb{1}\{u_0(C_j) = u_0(C_i) = 1\},$$

the number of pairs of neighbors (C_i, C_j) such that u_0 takes the value 1 on C_i and C_j. Then $\mathbb{1}\{\cdot\}$ denotes the indicator function, namely, $\mathbb{1}\{P\} = 1$ if property P is satisfied and 0, otherwise. As already observed in the literature [153, 154, 159], the value $s(u_0)$ is directly linked to fragmentation. Assuming abundance $p(u_0)$ is fixed, the higher $s(u_0)$ is, the more aggregated the region $\{u_0 = 1\}$ is.

We define pattern fragmentation by comparing the value of $s(u_0)$ with the maximum possible value of the index s among functions with a given abundance p. This maximum value $B[p]$ can be computed explicitly as an immediate consequence of the results of Harary and Harborth [90] on polyominoes.

Lemma 8 (Harary and Harborth [90])**.** *Choose $p \in [0, 1]$ such that $p \times n_C \in \mathbb{N}$ and*

$$U_0 := \{u_0 \text{ satisfying (3.6)-(3.8), and } p(u_0) = p\}.$$

We have

$$B[p] := \max_{u_0 \in U_0} s(u_0) = 2n_+ - \lceil 2\sqrt{n_+} \rceil,$$

where $n_+ = p \times n_C$ and $\lceil 2\sqrt{n_+} \rceil$ is the smallest integer that is greater than or equal to $2\sqrt{n_+}$.

Then, we set

$$fr(u_0) = 1 - \frac{s(u_0)}{B[p(u_0)]}. \tag{3.9}$$

The index fr belongs to $[0, 1]$. Whatever the abundance p is, the most aggregated configurations (in the sense $s(u_0) = B[p]$) verify $fr(u_0) = 0$, whereas the most fragmented configurations (in the sense $s(u_0) = 0$) verify $fr(u_0) = 1$. In the sequel, $fr(u_0)$ is referred to as *the fragmentation rate* of u_0. Samples of functions u_0 obtained with the model from [159] with various values of $fr(u_0)$ and $p(u_0)$ are shown in Fig. 3.3.

Remark 7. *There exist several ways of generating binary patterns. The most common are neutral models, originally introduced by Gardner* et al. *[78]. They can include parameters that regulate fragmentation [104]. The model that we use here is also a neutral model in the sense that it is a stochastic*

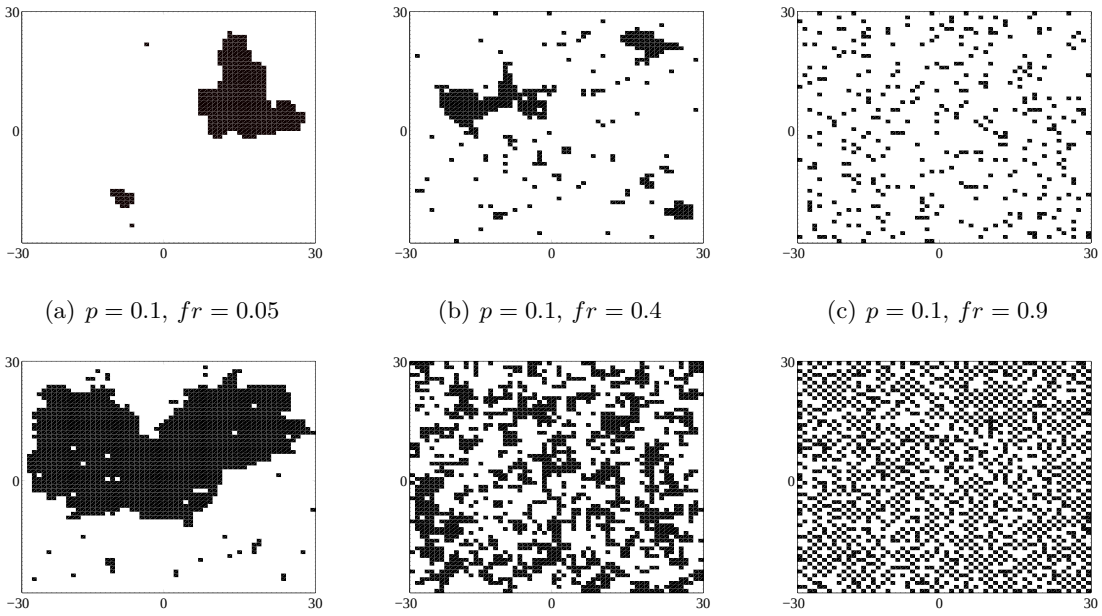

(a) $p = 0.1$, $fr = 0.05$ (b) $p = 0.1$, $fr = 0.4$ (c) $p = 0.1$, $fr = 0.9$

(d) $p = 0.4$, $fr = 0.05$ (e) $p = 0.4$, $fr = 0.4$ (f) $p = 0.4$, $fr = 0.9$

FIGURE 3.3 – Initial conditions u_0 in the two-dimensional case : examples of patterns with different abundance and fragmentation rates. Note that $C = [-30, 30] \times [-30, 30]$ and $n_C = 3600$.

model of pattern generation. The abundance p and the number of pairs s are controlled during the process of pattern generation ; this allows for good sampling over the parameter space $(fr, p) \in [0, 1] \times [0, 1]$ *(see Fig. 3.5).*

3.3 Results

In this section, we present analytical and numerical results on the effect of the spatial distribution of the founding population u_0 on the outcome of the invasion modeled by equation (3.4).

3.1 Analytical result in the one-dimensional case

We first mention some results in [58] that prove the existence of a threshold value for the size of the support of u_0 such that establishment fails (i.e., $u(t, x) \to 0$ as $t \to \infty$) if and only if the size of the support is below this threshold, and invasion is successful (i.e., $u(t, x) \to 1$ as $t \to \infty$) if and only if the size of the support is above this threshold. The symmetry of the problem (3.1), (3.4) together with the uniqueness of its solution imply that the solution is symmetrical with respect to $\{x = 0\}$ for all $t \geq 0$.

Theorem 3 (case $\alpha = 0$: Zlatǒs [195], case $\alpha \geq 0$: Du and Matano [58])**.** *Let* $\alpha \geq 0$. *Assume that f satisfies (3.2-3.3). Then, there exists* $L^*(\alpha) > 0$ *such that :*

i *For any* $L < L^*(\alpha)$, *the solution to* (3.1), (3.4) *converges to* 0 *as* $t \to \infty$, *uniformly in* $\mathbb{R}$.

ii *For any* $L > L^*(\alpha)$, *the solution to* (3.1), (3.4) *converges to* 1 *as* $t \to \infty$, *uniformly on compacts.*

iii *If* $L = L^*(\alpha)$, *the solution to* (3.1), (3.4) *converges to a positive stationary solution* $\tilde{u}$ *uniformly in* $\mathbb{R}$ *as* $t \to +\infty$, *where* $\tilde{u}$ *verifies* $-D\tilde{u}'' = f(\tilde{u})$, $\tilde{u}(0) = \rho_1 := \sup \left\{ \rho' \in (0, 1) \text{ such that } \int_0^{\rho'} f(s)ds \leq 0 \right\}$

and $\tilde{u}'(0) = 0$. *Moreover,* $\tilde{u}$ *is symmetrically decreasing, i.e.,* $\tilde{u}(x) = \tilde{u}(-x)$ *and* $\tilde{u}'(x) < 0$ *for all* $x > 0$.

The next result analyzes the effect of fragmentation by studying the dependence of the threshold value $L^*(\alpha)$ with respect to the size (α) of the gap between the two components of the support of u_0.

Theorem 4. *Let* $\alpha \geq 0$ *and* $L^*(\alpha)$ *be defined by Theorem 3. Then the function* $\alpha \mapsto L^*(\alpha)$ *is continuous on* $[0, +\infty)$. *Furthermore,* $L^*(\alpha) < 2\,L^*(0)$ *for all* $\alpha \geq 0$ *and*

$$L^*(\alpha) \to 2L^*(0) \text{ as } \alpha \to \infty. \tag{3.10}$$

This result highlights the global detrimental effect of fragmentation on the success of establishment and invasion. Indeed, when the gap α between the two components of the support of u_0 is large, the minimal viable size $L^*(\alpha)$ of support of the founding population tends to become twice as large as if the individuals were gathered in a single group. However, the strict sign in the inequality $L^*(\alpha) < 2\,L^*(0)$ shows that, whatever the distance α separating the two groups, there is at least some cooperation between them. Moreover, the result of Theorem 4 implies that the amplitude of variation of the threshold $L^*(\alpha)$ is at least equal to $L^*(0)$. Thus, the spatial structure of the support of the founding population u_0 plays an important role on invasion success. The proof of Theorem 4 is presented in Appendix 5.1.

In the next section, we use numerical computations to study whether there is an increasing relationship between $L^*(\alpha)$ and the distance α.

3.2 Numerical results

We carried out numerical computations in one- and two-dimensional space. We refer to Appendix 5.2 for some details on the numerical method that was used for solving equation (3.1). In these numerical computations, the function f in (3.1) was assumed to be of the following cubical form :

$$f(s) = rs\left(1 - \frac{s}{K}\right)\left(\frac{s-\rho}{K}\right),$$

with $\rho \in (0, K/2)$. Such a growth function is a typical example of a reaction term involving an Allee effect [105, 118, 158]. Without loss of generality, with the substitutions $v(t,x) = u(t,x)/K$ and $w(t,x) = v(t/r, x\sqrt{D/r})$ into equation (3.1), we can assume that $K = r = D = 1$ and $\rho \in (0, 1/2)$. Thus,

$$f(s) = s(1-s)(s-\rho). \tag{3.11}$$

Since $\rho \in (0, 1/2)$, the quantity $\int_0^1 f(s)ds$ is positive. The function f defined by (3.11) therefore fulfils the assumptions (3.2-3.3).

2.1 The one-dimensional case

The aim of this section is (i) to study the relationship between the minimum viable population size $L^*(\alpha)$ and the distance α and (ii) to study the effect of the Allee threshold ρ on the above relationship. The value of $L^*(\alpha)$, as defined in Theorem 3, has been computed for $\alpha \in [0, 16]$ and several values of the parameter ρ.

The results of these computations are depicted in Fig. 3.4. As expected from Theorem 4, $L^*(\alpha) \to 2\,L^*(0)$ for large values of α : for each value of ρ, $L^*(\alpha)$ is very close to $2\,L^*(0)$ when $\alpha = 16$.

This justifies the choice of the study interval $\alpha \in [0, 16]$. Moreover, Fig. 3.4 shows an increasing trend between the threshold $L^*(\alpha)$ and α, at least when α is not too small. This increasing relationship means that the more fragmented the founding population is, the larger it needs to be for the invasion to be successful. Additionally, the dependence between $L^*(\alpha)$ and α is nonlinear ; the curves corresponding to $L^*(\alpha)$ have a steeper slope for intermediate values of α.

However, we observe that for small values of α, $L^*(\alpha)$ slightly decreases with α. This phenomenon can be clearly seen on Fig. 3.4 for $\rho \geq 0.4$; the numerical simulations indicate that it is also true for smaller values of ρ. In particular, $L^*(\alpha)$ can reach values smaller than $L^*(0)$. Roughly speaking, this means that when α is very small, the gap between $-\alpha/2$ and $\alpha/2$ is filled by diffusion at a time (of the order α^2) which is much smaller than the time it takes for the interfaces at the positions $-(\alpha/2+L/2)$ and $(\alpha/2 + L/2)$ to move.

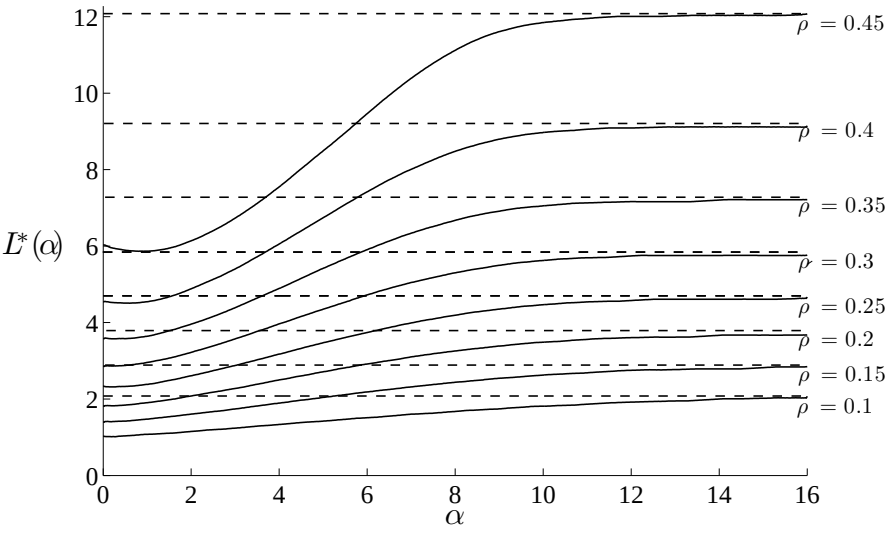

FIGURE 3.4 – Value of the critical threshold $L^*(\alpha)$ in terms of the distance α and the Allee threshold ρ. For each value of ρ, the dotted line corresponds to the associated value of $2\,L^*(0)$.

Regarding the effect of ρ, we observe that $L^*(\alpha)$ tends to increase with ρ. This is an obvious consequence of the parabolic maximum principle ; for any $\alpha \geq 0$, $L > 0$ and $\rho \in (0, 1/2)$, let us denote the solution to (3.1), (3.4) by $u_\rho^{L,\alpha}(t, x)$, where f is defined by (3.11). We thus have the following lemma :

Lemma 9. *Let $0 < \rho_1 \leq \rho_2 < 1/2$. For all $\alpha \geq 0$ and $L > 0$,*

$$u_{\rho_1}^{L,\alpha}(t, x) \geq u_{\rho_2}^{L,\alpha}(t, x) \text{ for all } t \geq 0,\ x \in \mathbb{R}.$$

The proof of this lemma is given in Appendix 5.1. According to the definition of $L^*(\alpha)$, $L^*(\alpha)$ is an increasing function of ρ. In particular, $L^*(0)$ is an increasing function of ρ. Thus, the result of Theorem 4 together with the monotonic trend between α and $L^*(\alpha)$ imply that the amplitude of the variation of the critical size $L^*(\alpha)$ (that is, the quantity $\sup_\alpha L^*(\alpha) - \inf_\alpha L^*(\alpha)$) tends to increase as ρ increases. In other words, the effect of fragmentation tends to increase with the strength of the Allee effect.

2.2 The two-dimensional case

The aim of this section is to study the effect of spatial fragmentation of the founding population's support in more realistic scenarios than those studied in the 1D case.

The model (3.1), with the function f defined by (3.11), was solved using stochastically generated initial conditions u_0 that satisfy the conditions (3.6)-(3.8), as described in Section 2.2. Those conditions u_0 are characterized by two indices, namely, an abundance index $p(u_0) \in [0,1]$ and a fragmentation rate $fr(u_0) \in [0,1]$. For our computations, we assumed that the support of the initial conditions was included in the set $C = [-30,30] \times [-30,30]$, which was divided into $n_C = 60 \times 60$ subsquares C_i, on which the functions u_0 are constant.

Using the stochastic model described in Section 2.2, we derived $1.5 \cdot 10^4$ functions $u_{0,k}$, $k = 1 \dots 1.5 \cdot 10^4$, with various abundance indices and fragmentation rates. Then, (3.1) was solved with each u_0 as initial condition. The computations were carried out with several values of the Allee threshold, including $\rho = 0.1,\ 0.3$ and 0.45. Some details on the numerical method which was used to solve this equation are given in Appendix 5.2.

The results of these computations are presented in Fig. 3.5. Each point in the figure is attached to a certain behavior of the model, namely, successful establishment or establishment failure. It appears that for each value of ρ, there are two distinct regions in the parameter space (fr, p), one corresponding to successful establishment and the other one to establishment failure. These regions are separated by a narrow interface in which the two behaviors are possible. In this narrow interface, and in the surrounding regions of the parameter space, the proportion of successful establishment cannot be directly inferred from Fig. 3.5. This proportion corresponds to the probability of successful establishment.

Remark 8. *In the region of the parameter space (fr, p) where $p > 0.5$, establishment was always successful. Thus, this region is not represented in Fig. 3.5.*

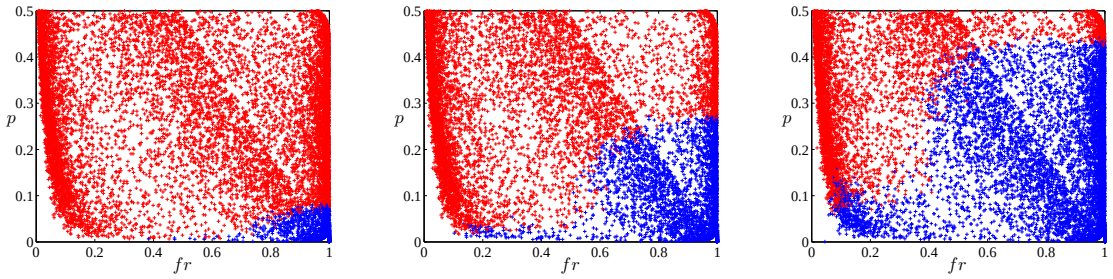

(a) $\rho = 0.1$ (b) $\rho = 0.3$ (c) $\rho = 0.45$

FIGURE 3.5 – Establishment success for the initial conditions $u_{0,k}$, $k = 1 \dots 1.5 \cdot 10^4$, in terms of the fragmentation rate $fr(u_{0,k})$ and abundance $p(u_{0,k})$, for three values of the Allee threshold ρ. Red crosses correspond to successful establishment and blue crosses correspond to establishment failure.

To study the probability of successful establishment in terms of the values of fr and p, we defined a function Y such that $Y(u_{0,k}) = 1$ if the initial condition $u_{0,k}$ leads to successful establishment and $Y(u_{0,k}) = 0$, otherwise. We then applied a smoothing regression to the data $(fr(u_{0,k}), p(u_{0,k}), Y(u_{0,k}))$. More precisely, the data were fitted with an algorithm to replace each point with the average of the closest points surrounding it (i.e., in a rectangular neighborhood of size 0.1×0.05). That is, Y was

fitted by the estimator $\hat{Y}$, which is defined over $[0,1] \times [0,1]$:

$$\hat{Y}(fr,p) = \frac{\sum\limits_{\substack{\|(fr(u_{0,k}),p(u_{0,k}))-(fr,p)\|<\varepsilon \\ k=1...1.5\cdot 10^4}} Y(fr(u_{0,k}),p(u_{0,k}))}{\sum\limits_{\substack{\|(fr(u_{0,k}),p(u_{0,k}))-(fr,p)\|<\varepsilon \\ k=1...1.5\cdot 10^4}} 1}. \tag{3.12}$$

Thus, to each point (fr,p) in $[0,1]\times[0,1]$ is attached a value of $\hat{Y}(fr,p)$ which measures the probability of successful establishment. This function $\hat{Y}(fr,p)$ is depicted in Fig. 3.6, for $\rho = 0.1,\ 0.3$, and 0.45.

An analysis of Fig. 3.6 reveals that for each fixed value of p, the probability of successful establishment decreases with the fragmentation rate fr. Moreover, the interface in which the probability $\hat{Y}(fr,p)$ is neither close to 0 nor to 1 is narrow in the parameter space (that is, the region where $\hat{Y}(fr,p) \in (0.1, 0.9)$ occupies approximately 1/40, 1/16, 1/12 of the parameter space $[0,1] \times [0,1]$ for $\rho = 0.1$, 0.3 and 0.45, respectively). Thus, the behavior of the solution of (3.1) with an initial condition u_0 satisfying (3.6)-(3.8) is almost completely determined by fr and p.

For each $fr \in [0,1]$, let us define $P_{1/2}(fr)$ as the minimum abundance such that establishment is successful with probability 1/2. The yellow curves in Fig. 3.6 correspond to a probability 1/2 of successful establishment). We observe that for each value of the Allee threshold ρ, $P_{1/2}(1)$ is much larger than $P_{1/2}(0)$. Thus, the minimum required abundance for the establishment to be successful is much larger for fragmented founding populations as compared to aggregated ones. Furthermore, the relationship $fr \mapsto P_{1/2}(fr)$ is comparable to the dependence $\alpha \mapsto L^*(\alpha)$, which was observed in the 1D case (Section 2.1). This dependence is highly nonlinear. On the one hand, for aggregated initial conditions (i.e., with small values of $fr(u_0)$) as well as very fragmented initial conditions (i.e., with values of $fr(u_0)$ close to 1), this dependence is almost flat. On the other hand, for intermediate values of the fragmentation rate, we observe a sudden increase in $P_{1/2}(fr)$, especially when $\rho = 0.3$ and $\rho = 0.45$. For $\rho = 0.3$, we have $P_{1/2}(0.6) - P_{1/2}(0.52) = 0.15$, and for $\rho = 0.45$, we have $P_{1/2}(0.5) - P_{1/2}(0.36) = 0.23$. Note that the probability of successful establishment decreases with ρ, especially for a fragmented initial condition. This property is the counterpart in the two-dimensional case of the monotonicity of $L^*(\alpha)$ with respect to ρ mentioned in Section 2.1 (see Lemma 9).

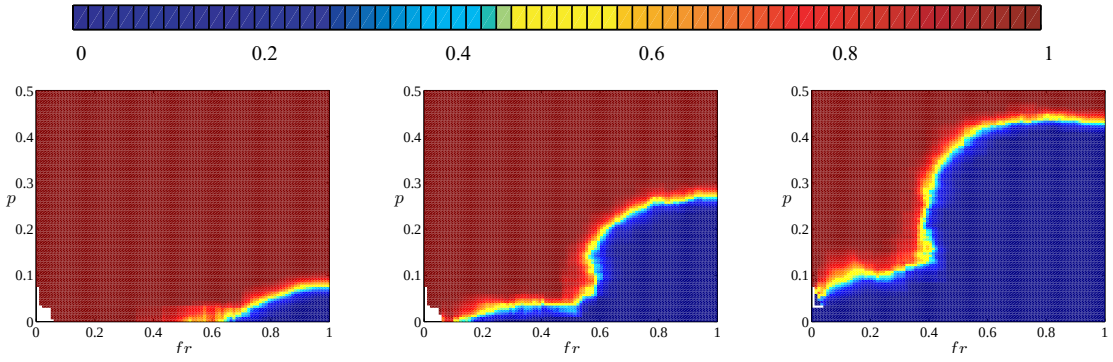

(a) $\rho = 0.1$ (b) $\rho = 0.3$ (c) $\rho = 0.45$

FIGURE 3.6 – Probability of successful establishment measured through $\hat{Y}$, in terms of the fragmentation rate fr and the abundance p of the founding population.

Remark 9.

- *We note in Fig. 3.6 that the minimum abundance $P_1(fr)$ such that establishment probability $\hat{Y}(fr, P_1(fr))$ is equal to 1 converges to a value close to ρ in the three cases considered here as $fr \to 1$. This is the case for $\rho = 0.1 : P_1(1) = 0.11$, for $\rho = 0.3 : P_1(1) = 0.31$ and for $\rho = 0.45 : P_1(1) = 0.47$. An explanation of this fact is as follows. Let $\tilde{u}$ be the solution of the following problem.*

$$\begin{cases} \tilde{u}_t = \Delta\tilde{u} + f(\tilde{u}) \text{ for } t > 0,\ x \in C, \\ \tilde{u} \text{ satisfies Neumann conditions on the boundary of } C \text{ for } t > 0, \\ u(0,x) = u_0(x) \text{ for } x \in C, \end{cases} \tag{3.13}$$

with f satisfying (3.2) and (3.3) and u_0 satisfying (3.6), (3.8) and $fr(u_0) = 1$. We conjecture that as the number n_C of subsquares C_i converges to $+\infty$, the behavior of $\tilde{u}$ (i.e., convergence to 0 or to 1 as $t \to \infty$) becomes similar to the behavior of a homogenized problem in which u_0 is replaced with the constant initial condition $\overline{u_0} = \dfrac{1}{|C|}\displaystyle\int_C u_0(s)ds = p(u_0)$, which in turn is equivalent to the ordinary differential equation $N' = f(N)$ with initial condition $N(0) = p(u_0)$. Thus, in this asymptotic regime, we would obtain $\tilde{u}(t,x) \to 1$ in C if and only if $p(u_0) > \rho$. The comparison principle implies that if the problems (3.1) and (3.13) are solved with the same initial condition u_0, we have $u \leq \tilde{u}$ for $t > 0$ and $x \in C$. As a consequence, we finally obtain the inequality $P_1(1) \geq \rho$, for adequately large n_C.

- *Using a formula by [118] we can compute the minimum abundance for successful establishment when the initial condition is ball-shaped :*

$$p_B = \frac{\pi}{2|C|}\frac{1}{(1/2-\rho)^2}.$$

For $\rho = 0.1$, we get $p_B = 3\,10^{-3}$, for $\rho = 0.3$, we have $p_B = 0.01$ and for $\rho = 0.45$, we obtain $p_B = 0.17$. We can observe in Fig. 3.6 that these values of p_B are not too far from the values of the minimum abundances $P_1(fr)$ for small values of fr. This is not surprising when fr is close to 0 since the initial condition consists in a single aggregated group [90].

3.4 Discussion

We have analyzed the role of the spatial distribution of the initial condition in reaction-diffusion models of biological invasions. These models incorporate reaction terms that take the Allee effect into account.

In many simplified models, the Allee effect is not taken into account. The initial conditions therefore do not play an important role. This is probably why a number of recent studies have focused on the effect of environmental heterogeneities rather than on the role of initial conditions. However, the Allee effect is known to occur in many invasive species. In such cases, the precise shape of the initial (or founding) population is of crucial importance when predicting successful invasion, as emphasized in our study.

Our first result is an analytical result. In the 1D case, we considered schematic examples of founding populations that were made of two identical groups separated by a distance α.

We have shown that the minimum size $L^*(\alpha)$ of the support of the founding population for successful establishment and invasion is a continuous function of the distance α. Moreover, when this distance becomes large, $L^*(\alpha)$ becomes twice as large as if the individuals were assembled in a single

group. This result shows that the spatial structure of the founding population indeed has an effect on the success of an invasion. Moreover, it is a first indication of the adverse effect of fragmentation. This adverse effect is confirmed by our numerical simulations. As illustrated in Fig. 3.4, the minimum viable size $L^*(\alpha)$ tends to increase with the distance α that separates the two subgroups, at least for not too small values of α. The amplitude of variation of the minimum viable size with respect to α (that is, the quantity $\sup_\alpha L^*(\alpha) - \inf_\alpha L^*(\alpha)$) also tends to increase with the strength of the Allee effect as measured by the Allee threshold ρ. It should nevertheless be noted that for small values of α, the minimum viable size decreases slightly with α. Thus, the breaking apart of the founding population into two subgroups may have a beneficial effect on the success of the invasion when these subgroups are very close to each other. From a mathematical standpoint, the proof of the non-monotonicity of the function $\alpha \mapsto L^*(\alpha)$ is a challenging open problem.

In the 2D case, we considered much more realistic examples of founding populations. Using a stochastic model of pattern generation, we constructed a large number of initial conditions with various abundances (measured by the index $p \in [0,1]$) and fragmentation rates. Using a new, rigorous definition of the fragmentation rate (measured by the index $fr \in [0,1]$; see eq. (3.9)), we were able to describe the outcome of an invasion in terms of two attributes of the founding population u_0, namely, $p(u_0)$ and $fr(u_0)$. Interestingly, the outcome of the invasion is indeed almost completely determined by the values of $p(u_0)$ and $fr(u_0)$; for each value of the Allee threshold ρ, we obtained two distinct regions in the parameter space (fr, p). One region corresponds to successful establishment, and the other one corresponds to establishment failure. The interface between these regions corresponds to a narrow region in the parameter space (Figs. 3.5 and 3.6). In our computations, we also observed that the set of initial conditions leading to successful establishment without successful invasion was very small (see also Remark 5 and Theorem 3 in the 1D case).

The results of Section 2.2 also show that the minimum abundance p required for successful establishment tends to increase with the fragmentation rate fr. As in the 1D case, the effect of fragmentation is enhanced as the Allee threshold ρ is increased. In addition, the relationship between the minimum abundance and the fragmentation rate is highly nonlinear and steep, threshold-like. Indeed, there is threshold value, say fr^*, where the minimum abundance for successful establishment dramatically increases. On both sides of this threshold, establishment success is almost independent on fr. On the one hand, if the rate of fragmentation is higher than fr^*, then the behavior of the model is close to the behavior of a homogenized problem (see first point in Remark 9). On the other hand, if the rate of fragmentation is lower than fr^*, the model almost behaves as if the initial condition was replaced by a single ball-shaped group (see second point in Remark 9). The existence of such a threshold fr^* implies that small changes in the fragmentation rate can therefore drastically modify the outcome of an invasion if fr is close to fr^*.

Finally, we have shown that the fragmentation of the support of a founding population u_0 tends to have a negative effect on invasion success in a homogeneous environment. We might wonder what would happen in heterogeneous environments. That is, instead of (3.1), consider the following model

$$\begin{cases} u_t = D\,\Delta\, u + f(u) + \nu(x)u, \text{ for } t > 0 \text{ and } x \in \mathbb{R}^n, \\ u(0,x) = u_0(x), \text{ for } x \in \mathbb{R}^n. \end{cases}$$

Note that $\nu(x)$ corresponds to the effect of the environment on the species local growth rate ; this model has been investigated for $n = 1$ in [86]. In this case, the negative effect of the fragmentation of u_0 may be compensated by the fact that fragmented supports may have more chances to intersect

with favorable regions. Thus, we could expect nontrivial intertwined effects between the level of environmental heterogeneity and the fragmentation of the initial condition. Other reaction-diffusion based models enable evolution and adaption [108, 143]. In a recent study, [100] have shown that, for species which can adaptively respond to overcome Allee effects, even small invading populations can survive. In such cases, fragmentation may also have a different effect.

3.5 Appendices

5.1 Appendix A : Proofs of Theorem 4 and Lemma 9

Proof of Theorem 4. For all $\alpha \geq 0$ and $L > 0$, we denote the solution of (3.1) with the initial condition (3.4) by $u^{L,\alpha}(t,x)$.

1. We first show that $L^*(\alpha) \leq 2\,L^*(0)$ for all $\alpha \geq 0$ and that $L^*(\alpha) \to 2L^*(0)$ as $\alpha \to \infty$.

Fix $\alpha \geq 0$. Let $\varepsilon \in (0, 2\,L^*(0))$, and set $L^\varepsilon = L^*(0) - \varepsilon/2$. Let $v(t,x) = u^{L^\varepsilon,0}(t, x - L^\varepsilon/2 - \alpha/2)$ for all $t \geq 0$ and $x \in \mathbb{R}$. From Theorem 3(i), $u^{L^\varepsilon,0}(t,x) \to 0$ uniformly in $\mathbb{R}$ as $t \to \infty$. Thus, we obtain the existence of some $t^* > 0$ such that

$$0 \leq v(t,x) = u^{L^\varepsilon,0}(t, x - L^\varepsilon/2 - \alpha/2) < \rho/4 \text{ for all } t \geq t^* \text{ and } x \in \mathbb{R}. \tag{3.14}$$

Now, let $w := u^{2\,L^\varepsilon,\alpha} - v$. Then $w(0,\cdot) = \chi_{[-(\alpha/2+L^\varepsilon),-\alpha/2]}$. Since $0 \leq u(0,\cdot), v(0,\cdot), w(0,\cdot) \leq 1$ and $f(0) = f(1) = 0$, it follows from the parabolic maximum principle (Ch. 2 in Friedman [75] and Ch. 3 in Protter and Weinberger [147]) that $u, v, w \in [0,1]$. Moreover, w satisfies :

$$w_t = D\,w_{xx} + f(u^{2\,L^\varepsilon,\alpha}) - f(v) \leq D\,w_{xx} + K\,w, \tag{3.15}$$

with $K = \|f'\|_{L^\infty(0,1)}$.

Let ϕ be the solution to the linear equation $\phi_t = D\,\phi_{xx} + K\,\phi$ with the initial condition $\phi(0,x) = w(0,x)$. Then $\phi(t^*,0) \to 0$ as $\alpha \to \infty$. Thus, for adequately large α, $\phi(t^*,0) < \rho/4$. Since $x \mapsto \phi(t^*,x)$ is decreasing in $[0,\infty)$, we obtain :

$$\phi(t^*,x) < \rho/4 \text{ for all } x \geq 0 \text{ and } \alpha \text{ large enough.} \tag{3.16}$$

Moreover, the maximum principle implies that $w \leq \phi$ in $[0,\infty) \times \mathbb{R}$. Then $u^{2\,L^\varepsilon,\alpha} = v + w \leq \phi + v$ in $[0,\infty) \times \mathbb{R}$, and finally, using (3.14) and (3.16), we obtain

$$u^{2\,L^\varepsilon,\alpha}(t^*,x) < \rho/2 \text{ for all } x \geq 0 \text{ and } \alpha > 0 \text{ large enough.}$$

Therefore, the evenness of $u^{2\,L^\varepsilon,\alpha}$ implies that $u^{2\,L^\varepsilon,\alpha}(t^*,x) < \rho/2$ for all $x \in \mathbb{R}$ and $\alpha > 0$ large enough. Comparing with the solution of the ODE $N' = f(N)$ with $N(t^*) = \rho/2$, for α large enough, we obtain that $u^{2\,L^\varepsilon,\alpha}(t,x) \to 0$ uniformly in $x \in \mathbb{R}$ as $t \to \infty$. According to the definition of $L^*(\alpha)$, this implies that $L^*(\alpha) > 2\,L^\varepsilon$, i.e.,

$$2\,L^*(0) - \varepsilon < L^*(\alpha) \text{ for } \alpha > 0 \text{ large enough.}$$

Since $\varepsilon > 0$ can be arbitrarily small, we conclude that

$$\liminf_{\alpha \to +\infty} L^*(\alpha) \geq 2\,L^*(0). \tag{3.17}$$

Let us now check that for all $\alpha \geq 0$, $L^*(\alpha) < 2\,L^*(0)$. Let $\alpha \geq 0$ be fixed. For all $L > 0$, we have $u^{L,\alpha}(0,\cdot) \geq u^{L/2,0}(0,\cdot - \alpha/2 - L/4)$. Thus, the parabolic maximum principle leads to

$$u^{L,\alpha}(t,\cdot) \geq u^{L/2,0}(t,\cdot - \alpha/2 - L/4) \text{ for all } t \geq 0. \tag{3.18}$$

Take $L = 2\,L^*(0)$. Theorem 3 (iii) shows that $u^{L^*(0),0}(t,\cdot - \alpha/2 - L^*(0)/2)$ converges uniformly in $\mathbb{R}$ as $t \to +\infty$ to the stationary solution $\tilde{u}(\cdot - \alpha/2 - L^*(0)/2)$ of (3.1), where $\tilde{u}$ verifies $\tilde{u}(0) = \rho_1 > \rho > 0$, $\tilde{u}'(0) = 0$ and $\tilde{u}$ is symmetrically decreasing. Thus, using (3.18), we get

$$u^{2\,L^*(0),\alpha} \not\to 0 \text{ as } t \to +\infty.$$

Theorem 3 (i) thus implies that $L^*(\alpha) \leq 2\,L^*(0)$. Assume that $L^*(\alpha) = 2\,L^*(0)$. Then, from Theorem 3 (iii), we know that $u^{2\,L^*(0),\alpha}$ converges to $\tilde{u}$, uniformly in $\mathbb{R}$ as $t \to +\infty$. Using inequality (3.18), we obtain

$$\tilde{u}(x) \geq \tilde{u}(x - \alpha/2 - L^*(0)/2) \text{ for all } x \in \mathbb{R}.$$

In particular, we get $\tilde{u}(\alpha/2 + L^*(0)/2) \geq \tilde{u}(0)$ which is impossible since $\tilde{u}$ is symmetrically decreasing. Thus, we finally obtain

$$L^*(\alpha) < 2\,L^*(0), \tag{3.19}$$

and together with (3.17), this shows that $L^*(\alpha) \to 2L^*(0)$ as $\alpha \to +\infty$.

2. We prove that the function $\alpha \mapsto L^*(\alpha)$ is continuous on $[0,\infty)$. For any $0 \leq \alpha \leq \beta$, we have $u^{L^*(\alpha)-(\beta-\alpha),\beta}(0,\cdot) \leq u^{L^*(\alpha),\alpha}(0,\cdot)$ if $L^*(\alpha) - (\beta - \alpha) > 0$. Therefore, the parabolic maximum principle together with Theorem 1 imply that

$$L^*(\beta) \geq L^*(\alpha) - (\beta - \alpha), \quad \text{for all } 0 \leq \alpha \leq \beta, \tag{3.20}$$

whenever $L^*(\alpha) - (\beta - \alpha)$ is positive or not. In other words, the function $\alpha \mapsto L^*(\alpha) + \alpha$ is non-decreasing, which implies that the function $\alpha \mapsto L^*(\alpha)$ is right lower and left upper semicontinuous. In order to complete the proof of Theorem 4, one is left to prove that the function $\alpha \mapsto L^*(\alpha)$ is right upper and left lower semicontinuous.

Step (i). We first show that the function $\alpha \mapsto L^*(\alpha)$ is right upper semicontinuous on $[0,+\infty)$. Let $\alpha \geq 0$, and set $\overline{L^+} = \limsup_{\beta \to \alpha^+} L^*(\beta)$. We deduce from (3.19) and (3.20) that $\overline{L^+} \in [L^*(\alpha), 2\,L^*(0)]$. Assume now that $\overline{L^+} > L^*(\alpha)$ and set

$$\tilde{L} = \frac{\overline{L^+} + L^*(\alpha)}{2}.$$

From the definition of $\overline{L^+}$ we know that there exists a decreasing sequence $(\alpha_n)_{n\geq 0}$ such that $\alpha_n \in (\alpha, \alpha + \tilde{L})$ for all $n \geq 0$, $\alpha_n \to \alpha$ and $L^*(\alpha_n) \to \overline{L^+}$ as $n \to \infty$. Since $\overline{L^+} > \tilde{L}$, there exists $N \geq 0$ such that for all $n \geq N$, $L^*(\alpha_n) > \tilde{L}$. Then, from Theorem 3 Part (i), for all $n \geq N$, we have

$$u^{\tilde{L},\alpha_n}(t,\cdot) \to 0 \text{ uniformly in } \mathbb{R} \text{ as } t \to \infty, \tag{3.21}$$

which in turn implies that

$$u^{\tilde{L}-(\alpha_n-\alpha),\alpha_n}(t,\cdot) \to 0 \text{ uniformly in } \mathbb{R} \text{ as } t \to \infty \tag{3.22}$$

since $0 < \tilde{L} - (\alpha_n - \alpha) < \tilde{L}$. Then, define the family $(\phi_\lambda)_{\lambda \geq 0}$ as follows

$$\phi_\lambda(\cdot) = \begin{cases} u^{\lambda, \tilde{L}+\alpha-\lambda}(0, \cdot), & \text{for } \lambda \in [0, \tilde{L}), \\ u^{\lambda,\alpha}(0, \cdot), & \text{for } \lambda \geq \tilde{L}. \end{cases}$$

This is a monotone increasing family in the sense of Theorem 1.3 in [58]. Since $\tilde{L} > L^*(\alpha)$, it follows from Theorem 3 Part (ii) that the solution $u^{\tilde{L},\alpha}$ of (3.1) with initial condition $\phi_{\tilde{L}}$ verifies $u^{\tilde{L},\alpha} \to 1$ uniformly on compacts as $t \to \infty$. Besides, we know from (3.22) that the solution $u^{\tilde{L}-(\alpha_N-\alpha),\alpha_N}$ of (3.1) with initial condition $\phi_{\tilde{L}-(\alpha_N-\alpha)}$ converges to 0 uniformly in $\mathbb{R}$ as $t \to \infty$. Since $\tilde{L}-(\alpha_N-\alpha) < \tilde{L}$, it follows then from Theorem 1.3 in [58] that there exists $\tilde{\lambda} \in (\tilde{L}-(\alpha_N-\alpha), \tilde{L})$ such that for all $\lambda > \tilde{\lambda}$, the solution of (3.1) with initial condition ϕ_λ converges to 1 uniformly on compacts as $t \to \infty$. Thus, for any $N_1 > N$ such that $\tilde{L} - (\alpha_{N_1} - \alpha) > \tilde{\lambda}$, the solution of (3.1) with initial condition $\phi_{\tilde{L}-(\alpha_{N_1}-\alpha)}$ converges to 1 uniformly on compacts as $t \to \infty$. This means that $u^{\tilde{L}-(\alpha_{N_1}-\alpha),\alpha_{N_1}} \to 1$ uniformly on compacts as $t \to \infty$ and contradicts (3.22). Thus, we have shown that $\overline{L^+} = L^*(\alpha)$. This means that the function $\alpha \mapsto L^*(\alpha)$ is right upper semicontinuous on $[0, +\infty)$. As it is already known to be right lower semicontinuous, it is then right-continuous.

Step (ii). We show that the function $\alpha \mapsto L^*(\alpha)$ is left lower semicontinuous in $(0, +\infty)$. Let $\alpha > 0$, and set $\underline{L^-} = \liminf_{\beta \to \alpha^-} L^*(\beta)$. The inequality (3.20) implies that $\underline{L^-} \in [0, L^*(\alpha)]$. Assume by contradiction that $\underline{L^-} < L^*(\alpha)$ and set

$$\hat{L} = \frac{\underline{L^-} + L^*(\alpha)}{2}.$$

Let $(\alpha_n)_{n \geq 0}$ be a positive and increasing sequence such that $\alpha_n \to \alpha$ and $L^*(\alpha_n) \to \underline{L^-}$ as $n \to \infty$. Since $\underline{L^-} < \hat{L}$, there exists $N \geq 0$ such that for all $n \geq N$, $L^*(\alpha_n) < \hat{L}$ and therefore, from Theorem 3 Part (ii), $u^{\hat{L},\alpha_n}(t, \cdot) \to 1$ uniformly on compacts as $t \to \infty$. As a consequence, we also have, for all $n \geq N$,

$$u^{\hat{L}+\alpha-\alpha_n,\alpha_n}(t, \cdot) \to 1 \text{ uniformly on compacts as } t \to \infty, \tag{3.23}$$

since $0 < \hat{L} < \hat{L} + \alpha - \alpha_n$. Let us define the family $(\psi_\lambda)_{\lambda \geq 0}$ by

$$\psi_\lambda(\cdot) = \begin{cases} u^{\lambda, \hat{L}+\alpha-\lambda}(0, \cdot), & \text{for } \lambda \in [0, \hat{L} + \alpha), \\ u^{\lambda,0}(0, \cdot), & \text{for } \lambda \geq \hat{L} + \alpha. \end{cases}$$

The family $(\psi_\lambda)_{\lambda \geq 0}$ is monotone increasing. Furthermore, since $\hat{L} < L^*(\alpha)$, the solution $u^{\hat{L},\alpha}$ of (3.1) with initial condition $\psi_{\hat{L}}$ converges to 0 uniformly in $\mathbb{R}$ as $t \to \infty$. Conversely, we know (see eq. (3.23)) that the solution $u^{\hat{L}+\alpha-\alpha_N,\alpha_N}$ of (3.1) with initial condition $\psi_{\hat{L}+\alpha-\alpha_N}$ converges to 1 uniformly on compacts as $t \to \infty$. Thus, using again the result of Theorem 1.3 in [58], we obtain the existence of $\hat{\lambda} \in (\hat{L}, \hat{L} + \alpha - \alpha_N)$ such that, for all $\lambda < \hat{\lambda}$, the solution of (3.1) with initial condition ψ_λ converges to 0 as $t \to \infty$. Let $N_1 \geq N$ be such that $\hat{L} + \alpha - \alpha_{N_1} < \hat{\lambda}$. The above result implies that the solution of (3.1) with initial condition $\psi_{\hat{L}+\alpha-\alpha_{N_1}}$ converges to 0 as $t \to \infty$. This contradicts (3.23). Thus, we have proved that $\underline{L^-} = L^*(\alpha)$. This means that the function $\alpha \mapsto L^*(\alpha)$ is left lower semicontinuous on $(0, +\infty)$. As it is already known to be left upper semicontinuous, it is then left-continuous.

Finally, we have shown that the function $\alpha \mapsto L^*(\alpha)$ is continuous on $[0, +\infty)$ and the proof of Theorem 4 is thereby complete. □

Proof of Lemma 9. For any $\alpha \geq 0$, $L > 0$ and $\rho \in (0, 1/2)$, we denote the solution of (3.1), (3.4) by $u_\rho^{L,\alpha}(t,x)$, where f is defined by (3.11). Since $f(0) = f(1) = 0$ and $u_\rho^{L,\alpha}(0,x) \in [0,1]$, it follows from the parabolic maximum principle that $u_\rho^{L,\alpha}(t,x) \in [0,1]$ for all $t \geq 0$ and $x \in \mathbb{R}$.

Let $0 < \rho_1 \leq \rho_2 < 1/2$. Then, for all $s \in [0,1]$, $s(1-s)(s-\rho_1) \geq s(1-s)(s-\rho_2)$. Since $u_{\rho_2}^{L,\alpha}(t,x) \in [0,1]$ for all $t \geq 0$ and $x \in \mathbb{R}$, $u_{\rho_2}^{L,\alpha}$ is a subsolution of the equation satisfied by $u_{\rho_1}^{L,\alpha}$. It follows from the parabolic maximum principle that $u_{\rho_1}^{L,\alpha} \geq u_{\rho_2}^{L,\alpha}$. □

5.2 Appendix B : Numerical solution of (3.1)

The equation (with $n = 1$ and $n = 2$) was solved using Comsol Multiphysics® time-dependent solver, using second order finite element method (FEM). This solver uses a so-called lines approach method incorporating variable-order variable-stepsize backward differentiation formulas. Nonlinearity are treated using a Newton's method.

In the 1D case, for the numerical computation of $L^*(\alpha)$, we used a so-called "large" time ($t = 50$). The solution of (3.1) was estimated by solving the problem on the bounded interval $\Omega = (-100, 100)$ with Dirichlet boundary conditions. In the 2D case, we estimated the solution of (3.1) by solving the problem on a bounded domain $\Omega = (-100, 100) \times (-100, 100)$ with Dirichlet boundary conditions.

In both 1D and 2D cases, the outcome of the invasion was measured at $t = 50$: the establishment stage was considered to be successful if and only if $\min_{x \in \Omega} u(50, x) > \rho$, where ρ is the Allee threshold defined in (3.3). Note that this definition can lead to overestimate the success rate of the establishment stage if the time required for the population density to be uniformly below ρ is larger than 50. However, in most cases except when ρ was very close to $1/2$, we observed that the outcome of the establishment stage was already clear at $t = 50$.

Acknowledgements

The authors are supported by the French "Agence Nationale de la Recherche" within the projects ColonSGS, PREFERED and URTICLIM. The third author is also indebted to the Alexander von Humboldt Foundation for its support.

Troisième partie

Les modèles de réaction-diffusion en milieu hétérogène

Chapitre 4

Maximal and minimal spreading speeds for reaction diffusion equations in nonperiodic slowly varying media

Ce travail réalisé en collaboration avec Thomas Giletti [a] et Grégoire Nadin [b]
est à paraître dans le *Journal of Dynamics and Differential Equation*s [GGN12]

[a] Aix-Marseille Université, LATP UMR 6632, Faculté des Sciences et Techniques
Avenue Escadrille Normandie-Niemen, F-13397 Marseille Cedex 20, France
[b] CNRS, UMR 7598, Laboratoire Jacques-Louis Lions, F-75005 Paris, France

Sommaire

This work was partially supported by the French ANR project *Prefered*.

4.1 Introduction

1.1 Hypotheses

We consider the following reaction-diffusion equation in $(0,+\infty)\times\mathbb{R}$:

$$\partial_t u = \partial_{xx} u + f(x,u). \tag{4.1}$$

We assume that $f = f(x,u)$ is locally Lipschitz-continuous in u and of class $\mathcal{C}^1$ in the neighborhood of $u = 0$ uniformly with respect to x, so that we can define

$$\mu(x) := f'_u(x,0).$$

Moreover, f is of the KPP type, that is

$$f(x,0) = 0,\ \ f(x,1) \le 0,\ \ \mu(x) > 0 \ \text{ and } f(x,u) \le \mu(x)u \ \text{ for all } (x,u) \in \mathbb{R}\times(0,1).$$

A typical f which satisfies these hypotheses is $f(x,u) = \mu(x)u(1-u)$, where μ is a continuous, positive and bounded function.

The very specific hypothesis we make on f in this chapter is the following : there exist $\mu_0 \in \mathcal{C}^0(\mathbb{R})$ and $\phi \in \mathcal{C}^1(\mathbb{R})$ such that

$$\begin{cases} \mu(x) = \mu_0(\phi(x)) \text{ for all } x \in \mathbb{R}, \\ 0 < \min\limits_{[0,1]} \mu_0 < \max\limits_{[0,1]} \mu_0 \ \text{ and } \ \mu_0 \text{ is 1-periodic}, \\ \phi'(x) > 0,\ \lim\limits_{x\to+\infty} \phi(x) = +\infty \ \text{ and } \lim\limits_{x\to+\infty} \phi'(x) = 0. \end{cases} \tag{4.2}$$

That is, our reaction-diffusion equation is strictly heterogeneous (it is not even almost periodic or ergodic), which means that it can provide useful information on both efficiency of recently developed tools and properties of the general heterogeneous problem. But it also satisfies some periodicity properties with a growing period near $+\infty$. We aim to look at the influence of the varying period $L(x) := x/\phi(x)$ on the propagation of the solutions.

Note that we do not assume here that there exists a positive stationary solution of (4.1). We require several assumptions that involve the linearization of f near $u = 0$ but our only assumption which is related to the behavior of $f = f(x,u)$ with respect to $u > 0$ is that $f(x,1) \le 0$, that is, 1 is a supersolution of (4.1) (it is clear that, up to some change of variables, 1 could be replaced by any positive constant in this inequality). It is possible to prove that there exists a minimal and stable positive stationary solution of (4.1) by using this hypothesis and the fact that μ_0 is positive [20], but we will not discuss this problem since this is not the main topic of this chapter.

1.2 Definitions of the spreading speeds and earlier works

For any compactly supported initial condition u_0 with $0 \le u_0 \le 1$ and $u_0 \not\equiv 0$, we define the *minimal and maximal spreading speeds* as :

$$\begin{aligned} w_* &= \sup\{c > 0 \mid \liminf \inf_{x\in[0,ct]} u(t,x) > 0 \text{ as } t \to +\infty\}, \\ w^* &= \inf\{c > 0 \mid \sup_{x\in[ct,+\infty)} u(t,x) \to 0 \text{ as } t \to +\infty\}. \end{aligned}$$

Note that it is clear, from the strong maximum principle, that for any $t > 0$ and $x \in \mathbb{R}$, one has $0 < u(t,x) < 1$. One can also easily derive from the homogeneous case [10] that

$$2\sqrt{\min \mu_0} \leq w_* \leq w^* \leq 2\sqrt{\max \mu_0}.$$

The reader could also remark that we just require $\liminf_{t\to+\infty} u(t, x + ct) > 0$ in the definition of w_*. This is because we did not assume the existence of a positive stationary solution. Hence, we just require u to "take off" from the unstable steady state 0.

The aim of this chapter is to determine if some of these inequalities are indeed equalities.

The first result on spreading speeds is due to Aronson and Weinberger [10]. They proved that $w^* = w_* = 2\sqrt{f'(0)}$ in the case where f does not depend on x. More generally, even if f does not satisfy $f(u) \leq f'(0)u$ for all $u \in [0,1]$, then $w^* = w_*$ is the minimal speed of existence of traveling fronts [10]. However, because of the numerous applications in various fields of natural sciences, the role of heterogeneity has become an important topic in the mathematical analysis.

When f is periodic in x, Freidlin and Gartner [74] and Freidlin [73] proved that $w_* = w^*$ using probabilistic techniques. In this case, the spreading speed is characterized using periodic principal eigenvalues. Namely, assume that f is 1-periodic in x, set $\mu_0(x) := f'_u(x,0)$ and define for all $p \in \mathbb{R}$ the elliptic operator

$$\mathcal{L}_p\varphi := \varphi'' - 2p\varphi' + (p^2 + \mu_0(x))\varphi. \tag{4.3}$$

It is known from the Krein-Rutman theory that this operator admits a unique periodic principal eigenvalue $\lambda_p(\mu_0)$, defined by the existence of a positive 1-periodic function $\varphi_p \in \mathcal{C}^2(\mathbb{R})$ so that $\mathcal{L}_p\varphi_p = \lambda_p(\mu_0)\varphi_p$. The characterization of the spreading speed [74] reads

$$w_* = w^* = \min_{p>0} \frac{\lambda_p(\mu_0)}{p}. \tag{4.4}$$

Such a formula is very useful to investigate the dependence between the spreading speed and the growth rate μ_0. Several alternative proofs of this characterization, based on different techniques, have been given in [22, 186]. The spreading speed $w_* = w^*$ has also been identified later as the minimal speed of existence of pulsating traveling fronts, which is the appropriate generalization of the notion of traveling fronts to periodic media [19]. Let us mention, without getting into details, that the equality $w_* = w^*$ and the characterization (4.4) have been extended when the heterogeneity is transverse [125], space-time periodic or compactly supported [22], or random stationary ergodic [74, 140]. In this last case one has to use Lyapounov exponents instead of principal eigenvalues.

In all these cases (except in the random one), the operator $\mathcal{L}_p$ is compact and thus principal eigenvalues are well-defined. When the dependence of f with respect to x is more general, then classical principal eigenvalues are not always defined, which makes the computation of the spreading speeds much more difficult. Moreover, in general heterogeneous media, it may happen that $w_* < w^*$. No example of such phenomenon has been given in space heterogeneous media, but there exist examples in time heterogeneous media [28] or when the initial datum is not compactly supported [87].

Spreading properties in general heterogeneous media have recently been investigated by Berestycki, Hamel and the third author in [22]. These authors clarified the links between the different notions of spreading speeds and gave some estimates on the spreading speeds. More recently, Berestycki and the third author gave sharper bounds using the notion of generalized principal eigenvalues [28]. These estimates are optimal when the nonlinearity is periodic, almost periodic or random stationary ergodic.

In these cases, one gets $w_* = w^*$ and this spreading speed can be characterized through a formula which is similar to (4.4), involving generalized principal eigenvalues instead of periodic principal eigenvalues.

4.2 Statement of the results

Before enouncing our results, let us first roughly describe the situation. As $\phi'(x) \to 0$ as $x \to +\infty$, the function ϕ is sublinear at infinity and thus $\mu(x) = \mu_0(\phi(x))$ stays near its extremal values $\max \mu_0$ or $\min \mu_0$ on larger and larger intervals. If these intervals are sufficiently large, that is, if ϕ increases sufficiently slowly, the solution u of (4.1) should propagate alternately at speeds close to $2\sqrt{\max \mu_0}$ and $2\sqrt{\min \mu_0}$. Hence, we expect in such a case that $w^* = 2\sqrt{\max \mu_0}$ and $w_* = 2\sqrt{\min \mu_0}$.

On the other hand, if one writes $\phi(x) = x/L(x)$, then the reaction-term locally looks like an $L(x)$-periodic function. Since $L(x) \to +\infty$, as clearly follows from the fact that $\phi'(x) \to 0$ as $x \to +\infty$, one might expect to find a link between the spreading speeds and the limit of the spreading speed w_L associated with the L-periodic growth rate $\mu_L(x) := \mu_0(x/L)$ when $L \to +\infty$. This limit has recently been computed by Hamel, Roques and the third author [89]. As μ_L is periodic, w_L is characterized by (4.4) and one can compute the limit of w_L by computing the limit of $\lambda_p(\mu_L)$ for all p. This is how the authors of [89] proved that

$$\lim_{L \to +\infty} w_L = \min_{k \geq M} \frac{k}{j(k)}, \tag{4.5}$$

where $M := \max_{x \in \mathbb{R}} \mu_0(x) > 0$ and $j : [M, +\infty) \to [j(M), +\infty)$ is defined for all $k \geq M$ by

$$j(k) := \int_0^1 \sqrt{k - \mu_0(x)} dx. \tag{4.6}$$

If ϕ increases rapidly, that is, the period $L(x)$ increases slowly, then we expect to recover this type of behavior. More precisely, we expect that $w^* = w_* = \min_{k \geq M} k/j(k)$.

We are now in position to state our results.

2.1 Slowly increasing ϕ

We first consider the case when ϕ converges very slowly to $+\infty$ as $x \to +\infty$. As expected, we prove in this case that $w_* < w^*$.

Theorem . *(i) Assume that* $\dfrac{1}{x\phi'(x)} \to +\infty$ *as* $x \to +\infty$. *Then*

$$w_* = 2\sqrt{\min \mu_0} < w^* = 2\sqrt{\max \mu_0}.$$

(ii) Assume that $\dfrac{1}{x\phi'(x)} \to C$ *as* $x \to +\infty$. *If* C *is large enough (depending on* μ_0*), then*

$$w_* < w^*.$$

This is the first example, as far as we know, of a space heterogeneous nonlinearity $f(x, u)$ for which the spreading speeds w_* and w^* associated with compactly supported initial data are not equal.

In order to prove this Theorem, we will first consider the particular case when μ_0 is discontinuous and only takes two values (see Proposition 4 below). In this case, we are able to construct sub- and super-solutions on each interval where μ is constant, and to conclude under some hypotheses on the length of those intervals. Then, in the general continuous case, our hypotheses on $(x\phi'(x))^{-1}$ allow us to bound μ from below and above by some two values functions, and our results then follow from the preliminary case.

Remark . *Note that such a two values case is not continuous, so that our Theorem holds under more general hypotheses. In fact, one would only need that μ_0 is continuous on two points such that μ_0 attains its maximum and minimum there, so that, from the asymptotics of $\phi(x)$, the function $\mu(x) = \mu_0(\phi(x))$ will be close to its maximum and minimum on very large intervals as $x \to +\infty$.*

2.2 Rapidly increasing ϕ

We remind the reader that $M := \max_{x\in\mathbb{R}} \mu_0(x) > 0$ and $j : [M, +\infty) \to [j(M), +\infty)$ is defined by (4.6). We expect to characterize the spreading speeds w_* and w^* using these quantities, as in [89].

Note that $j(M) > 0$ since $\min \mu_0 < M$. The function j is clearly a bijection and thus one can define

$$w_\infty := \min_{\lambda\geq j(M)} \frac{j^{-1}(\lambda)}{\lambda} = \min_{k\geq M} \frac{k}{j(k)}. \tag{4.7}$$

We need in this section an additional mild hypothesis on f :

$$\exists\, C > 0, \gamma > 0 \text{ such that } \quad f(x,u) \geq f'_u(x,0)u - Cu^{1+\gamma} \quad \text{for all } (x,u) \in \mathbb{R}\times(0,+\infty). \tag{4.8}$$

Theorem . *Under the additional assumptions* (4.8)*, $\phi \in \mathcal{C}^3(\mathbb{R})$ and*

$$\phi''(x)/\phi'(x)^2 \to 0, \quad \textit{and } \phi'''(x)/\phi'(x)^2 \to 0, \ \textit{as } x \to +\infty, \tag{4.9}$$

one has

$$w_* = w^* = w_\infty.$$

Note that (4.9) implies $(x\phi'(x))^{-1} \to 0$ as $x \to +\infty$. Hence, this result is somehow complementary to Theorem . However, this is not optimal as this does not cover all cases. An interesting and open question would be to refine those results to get more precise necessary and sufficient conditions for the equality $w_* = w^*$ to be satisfied. This could provide some insight on the general heterogeneous case, where the establishment of such criteria is an important issue.

This result will mainly be derived from Theorem 2.1 of [28]. We first construct some appropriate test-functions using the asymptotic problem associated with $\mu_L(x) = \mu_0(x/L)$ as $L \to +\infty$. This will enable us to compute the generalized principal eigenvalues and the computation of the spreading speeds will follow from Theorem 2.1 in [28].

2.3 Examples

We end the statement of our results with some examples which illustrate the different possible behaviors.

Example 1 : $\phi(x) = \beta(\ln x)^\alpha$, with $\alpha, \beta > 0$. This function clearly satisfies the hypotheses in (4.2).

- If $\alpha \in (0,1)$, one has $1/(x\phi'(x)) = (\ln x)^{1-\alpha}/(\beta\alpha) \to +\infty$ as $x \to +\infty$. Hence, the assumptions of case 1 in Theorem are satisfied and one has $w_* = 2\sqrt{\min \mu_0}$ and $w^* = 2\sqrt{\max \mu_0}$.
- If $\alpha = 1$, then $x\phi'(x) = \beta$ for all x and thus we are in the framework of case 2 in Theorem , which means that we can conclude that $w_* < w^*$ provided that β is small enough.
- Lastly, if $\alpha > 1$, then straightforward computations give

$$\phi''(x)/\phi'(x)^2 \sim -\frac{1}{\beta\alpha}(\ln x)^{1-\alpha} \to 0 \text{ as } x \to +\infty,$$

$$\phi'''(x)/\phi'(x)^2 \sim \frac{2}{\beta\alpha x}(\ln x)^{1-\alpha} \to 0 \text{ as } x \to +\infty.$$

Hence, the assumptions of Theorem are satisfied and there exists a unique spreading speed : $w_* = w^* = w_\infty$.

Example 2 : $\phi(x) = x^\alpha, \alpha \in (0,1)$**.** This function clearly satisfies the hypotheses in (4.2) since $\alpha < 1$. One has $\phi''(x)/\phi'(x)^2 = \frac{\alpha-1}{\alpha x^\alpha} \to 0$ and $\phi'''(x)/\phi'(x)^2 = \frac{(\alpha-1)(\alpha-2)}{\alpha x^{1+\alpha}} \to 0$ as $x \to +\infty$. Thus, the assumptions of Theorem are satisfied and $w_* = w^* = w_\infty$.

Example 3 : $\phi(x) = x/(\ln x)^\alpha, \alpha > 0$**.** This function satisfies (4.2) and one has

$$\phi'(x) = \frac{1}{(\ln x)^\alpha} - \frac{\alpha}{(\ln x)^{\alpha+1}},$$

$$\phi''(x) = \frac{-\alpha}{x(\ln x)^{1+\alpha}} + \frac{\alpha(\alpha+1)}{x(\ln x)^{\alpha+2}},$$

$$\phi'''(x) = \frac{\alpha}{x^2(\ln x)^{1+\alpha}} - \frac{\alpha(\alpha+1)(\alpha+2)}{x^2(\ln x)^{\alpha+3}}.$$

It follows that $\phi''(x)/\phi'(x)^2 \to 0$ and $\phi'''(x)/\phi'(x)^2 \to 0$ as $x \to +\infty$ since the terms in x will decrease faster than the terms in $\ln x$. Thus, the assumptions of Theorem are satisfied and $w_* = w^* = w_\infty$.

Organization of the chapter : Theorem will be proved in Section 4.4. As a first step to prove this Theorem, we will investigate in Section 4.3 the case where μ_0 is not continuous anymore but only takes two values μ_+ and μ_-. Lastly, Section 4.5 is dedicated to the proof of Theorem .

Acknowledgements : The authors would like to thank François Hamel and Lionel Roques for having drawn their attention to the problems investigated in this chapter. The article associated with this chapter was completed while the third author was visiting the Department of mathematical sciences of Bath whose hospitality is gratefully acknowledged.

4.3 The two values case

We assume first that μ is discontinuous and only takes two distinct values μ_-, $\mu_+ \in (0, +\infty)$. Moreover, we assume that there exist two increasing sequences $(x_n)_n$ and $(y_n)_n$ such that $x_{n+1} \geq y_n \geq x_n$ for all n, $\lim_{n\to+\infty} x_n = +\infty$ and

$$\mu(x) = \begin{cases} \mu_+ \text{ if } x \in (x_n, y_n), \\ \mu_- \text{ if } x \in (y_n, x_{n+1}). \end{cases} \tag{4.10}$$

Proposition 4. *We have :*

(i) If $y_n/x_n \to +\infty$*, then* $w^* = 2\sqrt{\mu_+}$.

(ii) If $x_{n+1}/y_n \to +\infty$*, then* $w_* = 2\sqrt{\mu_-}$.

(iii) If $y_n/x_n \to K > 1$*, then* $w^* \geq 2\sqrt{\mu_+}\dfrac{K}{(K-1)+\sqrt{\mu_+/\mu_-}}$.

(iv) If $x_{n+1}/y_n \to K > 1$*, then* $w_* \leq 2\sqrt{\mu_-}\dfrac{K+\sqrt{\mu_+/\mu_-}}{K+\sqrt{\mu_-/\mu_+}}$.

It is clear in part 3 (resp. 4) of Proposition 4 that the lower bound on w^* (resp. upper bound on w_*) goes to $2\sqrt{\mu_+}$ (resp. $2\sqrt{\mu_-}$) as $K \to +\infty$. Hence, for K large enough, we get the wanted result $w_* < w^*$.

3.1 Maximal speed : proof of parts 1 and 3 of Proposition 4

1. We first look for a subsolution of equation (4.1) going at some speed c close to $2\sqrt{\mu_-}$. Let ϕ_R be a solution of the principal eigenvalue problem :

$$\begin{cases} \partial_{xx}\phi_R = \lambda_R \phi_R & \text{in } B_R, \\ \phi_R = 0 & \text{on } \partial B_R, \\ \phi_R > 0 & \text{in } B_R. \end{cases} \tag{4.11}$$

We normalize ϕ_R by $\|\phi_R\|_\infty = 1$. We know that $\lambda_R \to 0$ as $R \to +\infty$. Let $c < 2\sqrt{\mu_-}$ and R large enough so that $-\lambda_R < \mu_- - c^2/4$. Then $v(x) = e^{\frac{-cx}{2}}\phi_R(x)$ satisfies :

$$\partial_{xx} v + c\partial_x v + \mu_- v = \Big(\mu_- - \frac{c^2}{4} + \lambda_R\Big) v > 0 \text{ in } B_R.$$

By extending ϕ_R by 0 outside B_R, by regularity of f and since $f'_u(x,0) \geq \mu_-$ for any $x \in \mathbb{R}$, for some small κ, we also have in $(0,+\infty)\times\mathbb{R}$:

$$\partial_{xx}\kappa v + c\partial_x \kappa v + f(x+ct, \kappa v) \geq 0.$$

Hence, $w(t,x) := \kappa v(x-ct)$ is a subsolution of (4.1). Without loss of generality, we can assume that $u(1,x) \geq w(1,x)$, thus for any $t \geq 1$, $u(t,x) \geq w(t,x)$. That is, for any speed $c < 2\sqrt{\mu_-}$, we have bounded u from below by a subsolution of (4.1) with speed c. In particular,

$$\text{let } t_n := \frac{x_n + R}{c}, \text{ then } u(t_n, x) \geq w(t_n, x) \text{ for all } x \in \mathbb{R},$$

which is positive on a ball of radius R around $x_n + R$.

2. Take an arbitrary $c' < 2\sqrt{\mu_+}$ and let $\phi_{R'}$ a solution of the principal eigenvalue problem (4.11) with R' such that $-\lambda_{R'} < \mu_+ - c'^2/4$. As above, there exists $\tilde{v}(x) = \kappa' e^{\frac{-c'x}{2}}\phi_{R'}(x)$ compactly supported such that

$$\partial_{xx}\tilde{v} + c'\partial_x \tilde{v} + f(x + x_n + R + c't, \tilde{v}) \geq 0, \tag{4.12}$$

as long as $\tilde{v} = 0$ where $f'_u(x + x_n + R + c't, 0) \neq \mu_+$, that is

$$(-R' + x_n + R + c't, R' + x_n + R + c't) \subset (x_n, y_n),$$

which is true for $R > R'$ and

$$0 \leq t \leq \frac{y_n - x_n - R - R'}{c'}.$$

As R could be chosen arbitrarily large, we can assume that the condition $R > R'$ is indeed satisfied. Moreover, as $\liminf_{n\to+\infty} y_n/x_n > 1$ and $\lim_{n\to+\infty} x_n = +\infty$, we can assume that n is large enough so that $y_n - x_n > 2R$ and thus the second condition is also satisfied. Hence, $\tilde{w}(t_n + t, x) := \tilde{v}(x - x_n - R - c't)$ is a subsolution of (4.1) for $t \in (0, \frac{y_n - x_n - R - R'}{c'})$ and $x \in \mathbb{R}$. We can take κ' small enough so that

$$\kappa \min_{y \in B(0,R')} \phi_R(y) > \kappa' e^{\frac{|c-c'|}{2}R'}. \tag{4.13}$$

For all $x \in B(ct_n, R')$, one has :

$$\begin{aligned} w(t_n, x) = \kappa e^{\frac{-c(x-ct_n)}{2}}\phi_R(x - ct_n) &\geq \kappa\Big(\min_{y\in B(0,R')} \phi_R(y)\Big)\, e^{\frac{-(c-c')}{2}(x-ct_n)} e^{\frac{-c'}{2}(x-ct_n)} \\ &\geq \kappa\Big(\min_{y\in B(0,R')} \phi_R(y)\Big)\, e^{\frac{-|c-c'|}{2}R'} e^{\frac{-c'}{2}(x-ct_n)} \\ &\geq \kappa' e^{\frac{-c'}{2}(x-ct_n)} \\ &\geq \kappa' e^{\frac{-c'(x-ct_n)}{2}}\phi_{R'}(x - ct_n) = \tilde{w}(t_n, x), \end{aligned} \tag{4.14}$$

since $ct_n = x_n + R$ by definition. Moreover, $u(t_n, x) \geq w(t_n, x)$ for all $x \in \mathbb{R}$. The parabolic maximum principle thus gives

$$u(t_n + t, x) \geq \tilde{w}(t_n + t, x) \text{ for all } t \in \left(0, \frac{y_n - x_n - R - R'}{c'}\right) \text{ and } x \in \mathbb{R}.$$

3. We can now conclude. Indeed, for n large enough one has :

$$u\left(t_n + \frac{y_n - x_n - R - R'}{c'}, y_n - R'\right) \geq \tilde{w}\left(t_n + \frac{y_n - x_n - R - R'}{c'}, y_n - R'\right) = \tilde{v}(0).$$

Since the construction of $\tilde{v}$ did not depend on n, the above inequality holds independently of n, which implies that :

$$\inf_n u\left(t_n + \frac{y_n - x_n - R - R'}{c'}, y_n - R'\right) > 0.$$

If $y_n/x_n \to +\infty$, we have

$$\frac{y_n - R'}{t_n + \frac{y_n - x_n - R - R'}{c'}} = \frac{y_n - R'}{\frac{x_n}{c} + \frac{y_n - x_n - R - R'}{c'}} \to c' \text{ as } n \to +\infty.$$

It follows that $w^* \geq c'$ for any $c' < 2\sqrt{\mu_+}$. The proof of part 1 of Proposition 4 is completed.

If $y_n/x_n \to K$, we have

$$\frac{y_n - R'}{t_n + \frac{y_n - x_n - R - R'}{c'}} \to \frac{K}{\frac{1}{c} + \frac{K-1}{c'}} \text{ as } n \to +\infty.$$

As this is true for any $c' < 2\sqrt{\mu_+}$ and $c < 2\sqrt{\mu_-}$, this concludes the proof of part 3 of Proposition 4. □

3.2 Minimal speed : proof of parts 2 and 4 of Proposition 4

Let $\lambda_+ = \sqrt{\mu_+}$ be the solution of $\lambda_+^2 - 2\sqrt{\mu_+}\lambda_+ = -\mu_+$. One can then easily check, from the KPP hypothesis, that the function

$$v(t, x) := \min\left(1, \kappa e^{-\lambda_+(x - 2\sqrt{\mu_+}t)}\right)$$

is a supersolution of equation (4.1) going at the speed $2\sqrt{\mu_+}$, for any $\kappa > 0$. Since u_0 is compactly supported, we can choose κ such that $v(0, \cdot) \geq u_0$ in $\mathbb{R}$. Thus, for any $t \geq 0$ and $x \in \mathbb{R}$, $u(t, x) \leq v(t, x)$. In particular, the inequality holds for $t = t_n$ the smallest time such that $v(t, y_n) = 1$. Note that $t_n = y_n/(2\sqrt{\mu_+}) + C$ where C is a constant independent of n. Then for all $x \in \mathbb{R}$,

$$u(t_n, y_n + x) \leq v(t_n, y_n + x) = \min\left(1, e^{-\lambda_+ x}\right).$$

We now look for a supersolution moving with speed $2\sqrt{\mu_-}$ locally in time around t_n. Let us define

$$w(t_n + t, y_n + x) := \min\left(v(t_n + t, y_n + x), e^{-\lambda_-(x - 2\sqrt{\mu_-}t)}\right)$$

where $\lambda_- = \sqrt{\mu_-}$. Note that $\lambda_- < \lambda_+$, thus $u(t_n, y_n + x) \leq v(t_n, y_n + x) = w(t_n, y_n + x)$.

We now check that w is indeed a supersolution of equation (4.1). We already know that v is a supersolution and it can easily be seen as above from the KPP hypothesis that $(t, x) \mapsto e^{-\lambda_-(x - 2\sqrt{\mu_-}t)}$ is a supersolution only where $f_u'(\cdot, 0) = \mu_-$. Thus, we want the inequality $v(t_n + t, y_n + x) \leq e^{-\lambda_-(x - 2\sqrt{\mu_-}t)}$

to be satisfied if $y_n + x \notin (y_n, x_{n+1})$. Recall that $v(t_n + t, y_n + x) = \min\left(1, e^{-\lambda_+(x-2\sqrt{\mu_+}t)}\right)$ for all $t > 0$ and $x \in \mathbb{R}$. Thus, the inequality is satisfied if $t \geq 0$ and $x \leq 0$ or if

$$x \geq 2\frac{\lambda_+\sqrt{\mu_+} - \lambda_-\sqrt{\mu_-}}{\lambda_+ - \lambda_-}t = 2(\lambda_+ + \lambda_-)t.$$

It follows that $w(t_n + t, y_n + x)$ is indeed a supersolution of equation (4.1) in $\mathbb{R}$ as long as

$$0 \leq 2(\lambda_+ + \lambda_-)t \leq x_{n+1} - y_n, \tag{4.15}$$

and that $u(t_n + t, y_n + x) \leq w(t_n + t, y_n + x)$ for any t verifying the above inequality.

To conclude, let now $2\sqrt{\mu_+} > c > 2\sqrt{\mu_-}$, and t'_n the largest t satisfying (4.15), i.e.

$$t'_n = \frac{x_{n+1} - y_n}{2(\lambda_+ + \lambda_-)}.$$

The sequence $(t'_n)_n$ tends to $+\infty$ as $n \to +\infty$ since $\liminf_{n\to+\infty} x_{n+1}/y_n > 1$ and $\lim_{n\to+\infty} y_n = +\infty$. Moreover, one has

$$u(t_n + t'_n, y_n + ct'_n) \leq w(t_n + t'_n, y_n + ct'_n) \to 0 \text{ as } n \to +\infty$$

since $c > 2\sqrt{\mu_-}$.

If $x_{n+1}/y_n \to +\infty$ as $n \to +\infty$, as $t_n = y_n/(2\sqrt{\mu_+}) + C$, one gets $t'_n/t_n \to +\infty$ as $n \to +\infty$. Hence,

$$\frac{y_n + ct'_n}{t_n + t'_n} \to c \text{ as } n \to +\infty.$$

It follows that $w_* \leq c$ for any $c > 2\sqrt{\mu_-}$. This proves part 2 of Proposition 4.

If $x_{n+1}/y_n \to K$ as $n \to +\infty$, we compute

$$\frac{y_n + ct'_n}{t_n + t'_n} \to \frac{1 + \frac{c}{2(\lambda_+ + \lambda_-)}(K-1)}{\frac{1}{2\sqrt{\mu_+}} + \frac{K-1}{2(\lambda_+ + \lambda_-)}} \text{ as } n \to +\infty.$$

Hence, w_* is smaller than the right hand-side. As $c \in (2\sqrt{\mu_-}, 2\sqrt{\mu_+})$ is arbitrary, $\lambda_- = \sqrt{\mu_-}$ and $\lambda_+ = \sqrt{\mu_+}$, we eventually get

$$w_* \leq 2\sqrt{\mu_-}\frac{K + \sqrt{\mu_+/\mu_-}}{K + \sqrt{\mu_-/\mu_+}},$$

which concludes the proof of part 4 of Proposition 4. □

4.4 The continuous case

4.1 Proof of part 1 of Theorem

We assume that μ_0 is a continuous and 1-periodic function. Let now ε be a small positive constant and define $\mu_- < \mu_+$ by :

$$\begin{cases} \mu_+ &:= \max \mu_0 - \varepsilon, \\ \mu_- &:= \min \mu_0. \end{cases}$$

We want to bound μ from below by a function taking only the values μ_- and μ_+, in order to apply Theorem 4. Note first that there exist $x_{-1} \in (0,1)$ and $\delta \in (0,1)$ such that $\mu_0(x) > \mu_+$ for any $x \in (x_{-1}, x_{-1} + \delta)$. We now let the two sequences $(x_n)_{n\in\mathbb{N}}$ and $(y_n)_{n\in\mathbb{N}}$ defined for any n by :

$$\begin{cases} \phi(x_n) &= x_{-1} + n, \\ \phi(y_n) &= x_{-1} + n + \delta. \end{cases}$$

Note that since ϕ is strictly increasing and $\phi(+\infty) = +\infty$, then those sequences indeed exist, tend to $+\infty$ as $n \to +\infty$, and satisfy for any n, $x_n < y_n < x_{n+1}$. It also immediately follows from their definition that for all $x \in \mathbb{R}$,

$$\mu(x) \geq \tilde{\mu}(x) \text{ where } \tilde{\mu}(x) := \begin{cases} \mu_+ \text{ if } x \in (x_n, y_n), \\ \mu_- \text{ if } x \in (y_n, x_{n+1}). \end{cases}$$

We now have to estimate the ratio y_n/x_n in order to apply Proposition 4. Note that :

$$\delta = \phi(y_n) - \phi(x_n) = \int_{x_n}^{y_n} \phi'(x)dx. \tag{4.16}$$

Moreover, under the hypothesis $x\phi'(x) \to 0$ as $x \to +\infty$, and since $(x_n)_n$, $(y_n)_n$ tend to $+\infty$ as $n \to +\infty$:

$$\int_{x_n}^{y_n} \phi'(x)dx = \int_{x_n}^{y_n} \left(x\phi'(x) \times \frac{1}{x} \right) dx = o\left(\ln\left(\frac{y_n}{x_n} \right) \right) \text{ as } n \to +\infty. \tag{4.17}$$

From (4.16) and (4.17), we have that $\frac{y_n}{x_n} \to +\infty$. To conclude, we use the parabolic maximum principle and part 1 of Proposition 4 applied to problem (4.1) with a reaction term $\tilde{f} \leq f$ such that

$$\tilde{f}'_u(x, 0) = \tilde{\mu}(x) \text{ for all } x \in \mathbb{R}.$$

It immediately follows that $w^* \geq 2\sqrt{\max \mu_0 - \varepsilon}$. Since this inequality holds for any $\varepsilon > 0$, we get $w^* = 2\sqrt{\max \mu_0}$.

We omit the details of the proof of $w_* = 2\sqrt{\min \mu_0}$ since it follows from the same method. Indeed, one only have to choose y'_{-1} and δ' in $(0, 1)$ such that $\mu_0(x) < \min \mu_0 + \varepsilon$ for any $x \in (y'_{-1}, y'_{-1} + \delta')$ and let two sequences such that

$$\begin{cases} \phi(y'_n) &= y'_{-1} + n, \\ \phi(x'_{n+1}) &= y'_{-1} + n + \delta'. \end{cases}$$

One can then easily conclude as above using part 2 of Proposition 4. □

4.2 Proof of part 2 of Theorem

As before, we bound μ_0 from below by a two values function, that is, for all $x \in \mathbb{R}$,

$$\mu(x) \geq \tilde{\mu}(x) \text{ where } \tilde{\mu}(x) := \begin{cases} \mu_+ = \max \mu_0 - \varepsilon \text{ if } x \in (x_n, y_n), \\ \mu_- = \min \mu_0 \text{ if } x \in (y_n, x_{n+1}), \end{cases}$$

where ε a small positive constant and the two sequences $(x_n)_n$ and $(y_n)_n$ satisfy for any n :

$$\begin{cases} x_n < y_n < x_{n+1}, \\ \phi(x_n) = x_{-1} + n, \\ \phi(y_n) = x_{-1} + n + \delta(\varepsilon) \text{ for some } \delta(\varepsilon) > 0, \\ x_n \to +\infty \text{ and } y_n \to +\infty. \end{cases}$$

Here, under the assumption that $x\phi'(x) \to 1/C$, we get

$$\begin{aligned} \delta(\varepsilon) = \phi(y_n) - \phi(x_n) &= \int_{x_n}^{y_n} \phi'(x)dx \\ &= \int_{x_n}^{y_n} \left(x\phi'(x) \times \frac{1}{x} \right) dx \\ &= \frac{1}{C} \ln\left(\frac{y_n}{x_n} \right) + o\left(\ln\left(\frac{y_n}{x_n} \right) \right) \text{ as } n \to +\infty. \end{aligned}$$

Hence,

$$\frac{y_n}{x_n} \to e^{\delta(\varepsilon)C} \text{ as } n \to +\infty.$$

We can now apply the parabolic maximum principle and part 3 of Proposition 4 to get

$$w^* \geq 2\sqrt{\max \mu_0 - \varepsilon}\, \frac{e^{\delta(\varepsilon)C}}{(e^{\delta(\varepsilon)C} - 1) + \sqrt{(\max \mu_0 - \varepsilon)/\min \mu_0}}. \tag{4.18}$$

Notice that the dependence of δ on ε prevents us from passing to the limit as $\varepsilon \to 0$ as we did to prove part 1 of Theorem . However, for any fixed $\varepsilon > 0$, one can easily check that the right-hand side in the inequation (4.18) converges as $C \to +\infty$ to $2\sqrt{\max \mu_0 - \varepsilon}$.

One can proceed similarly to get an upper bound on w_*, that is :

$$w_* \leq 2\sqrt{\min \mu_0 + \varepsilon}\, \frac{e^{\delta'(\varepsilon)C} + \sqrt{\max \mu_0/(\min \mu_0 + \varepsilon)}}{e^{\delta'(\varepsilon)C} + \sqrt{(\min \mu_0 + \varepsilon)/\max \mu_0}}, \tag{4.19}$$

where ε can be chosen arbitrary small and $\delta'(\varepsilon)$ is such that $\mu_0(x) \leq \min \mu_0 + \varepsilon$ on some interval of length $\delta'(\varepsilon)$. It is clear that the right-hand side of (4.19) converges to $2\sqrt{\min \mu_0 + \varepsilon}$ as $C \to +\infty$.

Therefore, by choosing $\varepsilon < (\max \mu_0 - \min \mu_0)/2$, one easily gets from (4.18) and (4.19) that for C large enough, $w_* < w^*$. This concludes the proof of part 2 of Theorem . Moreover, note that the choice of C to get this strict inequality depends only on the function μ_0, by the intermediate of the functions $\delta(\varepsilon)$ and $\delta'(\varepsilon)$. □

4.5 The unique spreading speed case

We begin with some preliminary work that will be needed to estimate the spreading speeds. The proof of Theorem is then separated into two parts : the first part (Section 5.2) is devoted to the proof that $w^* \leq w_\infty$, while in the second part (Section 5.3) we prove that $w_* \geq w_\infty$.

5.1 Construction of the approximated eigenfunctions

For all $p \in \mathbb{R}$, we define

$$H(p) := \begin{cases} j^{-1}(|p|) & \text{if} \quad |p| \geq j(M), \\ M & \text{if} \quad |p| < j(M). \end{cases} \tag{4.20}$$

The fundamental property of this function is given by the following result.

Proposition 5. *(Propositions* 3.1 *and* 3.2 *in [89]) For all $p \in \mathbb{R}$, $H(p)$ is the unique real number such that there exists a continuous* 1*-periodic viscosity solution v of*

$$(v'(y) - p)^2 + \mu_0(y) = H(p) \text{ over } \mathbb{R}. \tag{4.21}$$

Next, we will need, as a first step of our proof, the function v given by Proposition 5 to be piecewise $\mathcal{C}^2$. This is true under some non-degeneracy hypothesis on μ_0. We will check below in the second part of the proof of Theorem that it is always possible to assume that this hypothesis is satisfied by approximation.

Lemma 10. *Assume that $\mu_0 \in \mathcal{C}^2(\mathbb{R})$ and that*

$$\text{if } \mu_0(x_0) = \max_{\mathbb{R}} \mu_0, \text{ then } \mu_0''(x_0) < 0. \tag{4.22}$$

Then for all $p \in \mathbb{R}$, equation (4.21) admits a 1*-periodic solution $v_p \in W^{2,\infty}(\mathbb{R})$ which is piecewise $\mathcal{C}^2(\mathbb{R})$.*

Proof. The proof relies on the explicit formulation of v_p. Assume first that $p > j(M) = j(\|\mu_0\|_\infty)$. Then it is easy to check (see [89]) that

$$v_p(x) := px - \int_0^x \sqrt{H(p) - \mu_0(y)}dy \tag{4.23}$$

satisfies (4.21). Then, the definition of j implies that v_p is 1-periodic and, as $\mu_0 \in \mathcal{C}^1(\mathbb{R})$ and $H(p) > \mu_0(y)$ for all $y \in \mathbb{R}$, the function v_p is $\mathcal{C}^2(\mathbb{R})$. The case $p < -j(M)$ is treated similarly.

Next, if $|p| \leq j(M)$, let F define for all $Y \in [0,1]$ by :

$$F(Y) := p + \int_Y^1 \sqrt{M - \mu_0(y)}dy - \int_0^Y \sqrt{M - \mu_0(y)}dy.$$

Then F is continuous and, as $|p| \leq j(M)$,

$$F(0) = p + \int_0^1 \sqrt{M - \mu_0(y)}dy = p + j(M) \geq 0.$$

Similarly, $F(1) = p - j(M) \leq 0$. Thus, there exists $X \in [0,1]$ so that $F(X) = 0$. We now define :

$$v_p(x) = \begin{cases} px - \displaystyle\int_0^x \sqrt{M - \mu_0(y)}dy & \text{for all} \quad x \in [0, X], \\ px - \displaystyle\int_0^X \sqrt{M - \mu_0(y)}dy + \int_X^x \sqrt{M - \mu_0(y)}dy & \text{for all} \quad x \in [X, 1]. \end{cases} \tag{4.24}$$

From the definition of X, the function v_p is 1-periodic. It is continuous and derivable at any point $x \in [0,1)\backslash\{X\}$ with

$$v_p'(x) = \begin{cases} p - \sqrt{M - \mu_0(x)} & \text{for all} \quad x \in [0, X), \\ p + \sqrt{M - \mu_0(x)} & \text{for all} \quad x \in (X, 1). \end{cases}$$

Hence, it satisfies (4.21) in the sense of viscosity solutions. Lastly, for all $x \in (0, X)$ so that $\mu_0(x) \neq M$, one has

$$v_p''(x) = \frac{\mu_0'(x)}{2\sqrt{M - \mu_0(x)}}.$$

If $\mu_0(x_M) = M$, then (4.22) implies that $\mu_0(x) < M$ for all $x \neq x_M$ close to x_M and a Taylor expansion gives

$$\lim_{x \to x_M, x \neq x_M} v_p''(x) = \sqrt{-\mu_0''(x_M)/2}.$$

Hence, v_p'' can be extended to a continuous function over $(0, X)$. Similarly, it can be extended over $(X, 1)$. It follows that v_p'' is bounded over $[0,1]$ and that it is piecewise $\mathcal{C}^2(\mathbb{R})$. □

For any $p \in \mathbb{R}$, define the elliptic operator :

$$L_p\varphi := \varphi'' - 2p\varphi' + (p^2 + \mu_0(\phi(x)))\varphi.$$

Lemma 11. *For all $p \in \mathbb{R}$, let*

$$\varphi_p(x) := \exp\Big(\frac{v_p(\phi(x))}{\phi'(x)}\Big). \tag{4.25}$$

If (4.22) holds and $\mu_0 \in \mathcal{C}^2(\mathbb{R})$, then φ_p is piecewise $\mathcal{C}^2(\mathbb{R})$ and one has

$$\frac{L_p\varphi_p(x) - H(p)\varphi_p(x)}{\varphi_p(x)} \to 0 \text{ as } x \to +\infty. \tag{4.26}$$

Proof. The function φ_p is piecewise $\mathcal{C}^2(\mathbb{R})$ since v_p is piecewise $\mathcal{C}^2(\mathbb{R})$. For all x so that v_p is $\mathcal{C}^2$ in x, we can compute

$$\begin{aligned}
\varphi_p'(x) &= \left(v_p'(\phi(x)) - \frac{\phi''(x)}{(\phi'(x))^2}v_p(\phi(x))\right)\varphi_p(x),\\
\varphi_p''(x) &= \left(\phi'(x)v_p''(\phi(x)) - \frac{\phi''(x)}{\phi'(x)}v_p'(\phi(x)) + \left(2\frac{(\phi''(x))^2}{(\phi'(x))^3} - \frac{\phi'''(x)}{(\phi'(x))^2}\right)v_p(\phi(x))\right)\varphi_p(x)\\
&\quad + \left(v_p'(\phi(x)) - \frac{\phi''(x)}{(\phi'(x))^2}v_p(\phi(x))\right)^2\varphi_p(x).
\end{aligned}$$

This gives

$$\begin{aligned}
\frac{L_p\varphi_p(x) - H(p)\varphi_p(x)}{\varphi_p(x)} &= \phi'(x)v_p''(\phi(x)) - \frac{\phi''(x)}{\phi'(x)}v_p'(\phi(x)) + \left(2\frac{(\phi''(x))^2}{(\phi'(x))^3} - \frac{\phi'''(x)}{(\phi'(x))^2}\right)v_p(\phi(x))\\
&\quad -2\frac{\phi''(x)}{(\phi'(x))^2}v_p(\phi(x))v_p'(\phi(x)) + \left(\frac{\phi''(x)}{(\phi'(x))^2}v_p(\phi(x))\right)^2 + v_p'(\phi(x))^2\\
&\quad -2p\left(v_p'(\phi(x)) - \frac{\phi''(x)}{(\phi'(x))^2}v_p(\phi(x))\right) + p^2 + \mu_0(\phi(x)) - H(p),\\
&= \phi'(x)v_p''(\phi(x)) - \frac{\phi''(x)}{\phi'(x)}v_p'(\phi(x)) + \left(2\frac{(\phi''(x))^2}{(\phi'(x))^3} - \frac{\phi'''(x)}{(\phi'(x))^2}\right)v_p(\phi(x))\\
&\quad -2\frac{\phi''(x)}{(\phi'(x))^2}v_p(\phi(x))v_p'(\phi(x)) + \left(\frac{\phi''(x)}{(\phi'(x))^2}v_p(\phi(x))\right)^2\\
&\quad +2p\frac{\phi''(x)}{(\phi'(x))^2}v_p(\phi(x)).
\end{aligned}$$

As v_p is periodic and $W^{2,\infty}$, v_p'' is bounded. It follows from (4.9) that

$$\frac{L_p\varphi_p(x) - H(p)\varphi_p(x)}{\varphi_p(x)} \to 0 \text{ as } x \to +\infty.$$

□

Lemma 12. *Define φ_p as in Lemma 11. Then*

$$\frac{\ln\varphi_p(x)}{x} \to 0 \text{ as } x \to +\infty. \tag{4.27}$$

Proof. One has

$$\frac{\ln\varphi_p(x)}{x} = \frac{v_p(\phi(x))}{\phi'(x)x} \text{ for all } x \in \mathbb{R}. \tag{4.28}$$

The function $x \mapsto v_p(\phi(x))$ is clearly bounded since v_p is periodic. Hence, (4.9) gives the conclusion. □

5.2 Upper bound for the spreading speed

Proof of part 1 of Theorem . We first assume that $\mu_0 \in \mathcal{C}^2(\mathbb{R})$. Let us now show that $w^* \le w_\infty$. Let $c > w_\infty$ and $c_1 \in (w_\infty, c)$. We know that there exists $p \ge j(M) > 0$ such that

$$w_\infty = \min_{p' \ge j(M)} H(p')/p' = H(p)/p.$$

Let $k \ge M$ so that $p = j(k) > 0$, and φ_p defined as in Lemma 11. We know from Lemma 11 that there exists $X > 0$ such that :

$$|L_p\varphi_p(x) - k\varphi_p(x)| \le (c_1 - w_\infty)j(k)\varphi_p(x) \text{ for all } x > X. \tag{4.29}$$

Let $\overline{u}$ be defined for all $(t,x) \in [0,+\infty) \times \mathbb{R}$ by :

$$\overline{u}(t,x) := \min\{1, \varphi_p(x) e^{-j(k)(x-h-c_1 t)}\},$$

where $h \in \mathbb{R}$ is large enough so that $u_0(x) \leq \overline{u}(0,x)$ for all $x \in \mathbb{R}$ (this is always possible since u_0 is compactly supported). Moreover, $\overline{u}(t,x) < 1$ if and only if $\varphi_p(x) < e^{j(k)(x-h-c_1 t)}$, which is equivalent to $x - v_p(\phi(x))/(j(k)\phi'(x)) > h + c_1 t \geq h$. Lemma 12 yields that the left hand-side of this inequality goes to $+\infty$ as $x \to +\infty$. Hence, we can always take h large enough so that $\overline{u}(t,x) < 1$ implies $x > X$. It follows that for all $(t,x) \in [0,+\infty) \times \mathbb{R}$ such that $\overline{u}(t,x) < 1$, one has

$$\begin{aligned}
\partial_t \overline{u} - \partial_{xx} \overline{u} - f(x,\overline{u}) &\geq \partial_t \overline{u} - \partial_{xx} \overline{u} - \mu(x)\overline{u} \\
&\geq j(k) c_1 \overline{u} - L_{j(k)}(\varphi_p)(x) e^{-j(k)(x-h-c_1 t)} \\
&\geq j(k) c_1 \overline{u} - k\overline{u} - (c_1 - w_\infty) j(k) \overline{u} \\
&\geq \big(j(k) w_\infty - k\big)\overline{u} = 0.
\end{aligned}$$

It follows from the parabolic maximum principle that $\overline{u}(t,x) \geq u(t,x)$ for all $(t,x) \in [0,+\infty) \times \mathbb{R}$. Hence, for all given $x \in \mathbb{R}$,

$$u(t,x) \leq \varphi_p(x) e^{-j(k)(x-h-c_1 t)} \text{ for all } t > 0.$$

Let $\varepsilon > 0$ so that $\varepsilon < j(k)(c - c_1)/c$. Lemma 12 yields that there exists $R > 0$ so that for all $x > R, \ln(\varphi_p(x)) \leq \varepsilon x$. Let $T = R/c$ and take $t \geq T$ and $x \geq ct$. One has

$$\begin{aligned}
\ln\Big(\varphi_p(x) e^{-j(k)(x-h-c_1 t)}\Big) &= \ln(\varphi_p(x)) - j(k)(x - h - c_1 t) \\
&\leq (\varepsilon - j(k))x + j(k)(h + c_1 t) \\
&\leq \big(\varepsilon c + j(k)(c_1 - c)\big)t + j(k)h \\
&\to -\infty \text{ as } t \to +\infty
\end{aligned}$$

since $\varepsilon c < j(k)(c - c_1)$. Hence,

$$\lim_{t \to +\infty} \max_{x \geq ct} \Big(\varphi_p(x) e^{-j(k)(x-h-c_1 t)}\Big) = 0 \text{ as } t \to +\infty,$$

which ends the proof in the case $\mu_0 \in \mathcal{C}^2(\mathbb{R})$.

Lastly, if $\mu_0 \in \mathcal{C}^0(\mathbb{R})$ is an arbitrary 1-periodic function, then one easily concludes by smoothing μ_0 from above. Indeed, one can find a sequence $(\mu_0^n)_n \in \mathcal{C}^2(\mathbb{R})^{\mathbb{N}}$ converging uniformly to μ_0, and such that for all $n \in \mathbb{N}$ and $x \in \mathbb{R}$, $\mu_0(x) \leq \mu_0^n(x)$.

It follows from the maximum principle that

$$\lim_{t \to +\infty} \max_{x \geq ct} u(t,x) = 0 \text{ for all } w > \min_{k \geq M} k/j^n(k),$$

where $j^n(k) = \displaystyle\int_0^1 \sqrt{k - \mu_0^n(x)}dx \geq j(k) > 0$. Letting $n \to +\infty$, one gets

$$\lim_{t \to +\infty} \max_{x \geq ct} u(t,x) = 0 \text{ for all } w > w_\infty,$$

which concludes the proof. □

5.3 Lower bound on the spreading speed

Proof of part 2 of Theorem . First, assume that $\mu_0 \in \mathcal{C}^2(\mathbb{R})$ satisfies (4.22). Let φ_p as in Lemma 11. For all $\delta > 0$, take R large enough so that $L_p\varphi_p \geq (H(p) - \delta)\varphi_p$ at any point of $(R, +\infty)$ where φ_p is piecewise $\mathcal{C}^2$. It is easy to derive from the proof of Lemma 11 that φ_p'/φ_p is bounded and uniformly continuous. Take $C > 0$ so that $|\varphi_p'(x)| \leq C\varphi_p(x)$ for all $x \in \mathbb{R}$.

We need more regularity in order to apply the results of [28]. Consider a compactly supported nonnegative mollifier $\chi \in \mathcal{C}^\infty(\mathbb{R})$ so that $\int_{\mathbb{R}} \chi = 1$ and define the convoled function $\psi_p := \exp\big(\chi \star \ln \varphi_p\big) \in \mathcal{C}^2(\mathbb{R})$. One has $\psi_p'/\psi_p = \chi \star \Big(\varphi_p'/\varphi_p\Big)$. Hence, $|\psi_p'(x)| \leq C\psi_p(x)$ for all $x \in \mathbb{R}$ and, as φ_p'/φ_p and $\big(\varphi_p'/\varphi_p\big)^2$ are uniformly continuous, up to some rescaling of χ, we can assume that

$$\Big\| |\chi \star \Big(\frac{\varphi_p'}{\varphi_p}\Big)|^2 - |\frac{\varphi_p'}{\varphi_p}|^2 \Big\|_\infty \leq \delta, \ \Big\| \chi \star \Big(|\frac{\varphi_p'}{\varphi_p}|^2\Big) - |\frac{\varphi_p'}{\varphi_p}|^2 \Big\|_\infty \leq \delta \text{ and } \|\chi \star \mu - \mu\|_\infty \leq \delta.$$

We now compute

$$\frac{\psi_p''}{\psi_p} = \Big|\frac{\psi_p'}{\psi_p}\Big|^2 + \chi \star \Big(\frac{\varphi_p''}{\varphi_p} - \Big|\frac{\varphi_p'}{\varphi_p}\Big|^2\Big) = \Big|\chi \star \Big(\frac{\varphi_p'}{\varphi_p}\Big)\Big|^2 - \chi \star \Big(\Big|\frac{\varphi_p'}{\varphi_p}\Big|^2\Big) + \chi \star \Big(\frac{\varphi_p''}{\varphi_p}\Big) \geq -2\delta + \chi \star \Big(\frac{\varphi_p''}{\varphi_p}\Big).$$

It follows that

$$\begin{aligned} \frac{L_p\psi_p}{\psi_p} = \frac{\psi_p'' - 2p\psi_p' + \mu(x)\psi_p}{\psi_p} &\geq -2\delta + \chi \star \Big(\frac{\varphi_p''}{\varphi_p} - 2p\frac{\varphi_p'}{\varphi_p}\Big) + \mu(x) \\ &\geq -2\delta + \chi \star \Big(H(p) - \mu - \delta\Big) + \mu(x) \\ &\geq -3\delta + H(p) + \mu(x) - \chi \star \mu(x) \\ &\geq -4\delta + H(p) \end{aligned}$$

in $(R, +\infty)$. On the other hand, Lemma 12 yields $\psi_p \in \mathcal{A}_R$, where $\mathcal{A}_R$ is the set of admissible test-functions (in the sense of [28]) over (R, ∞) :

$$\begin{aligned} \mathcal{A}_R := \{ \quad & \psi \in \mathcal{C}^0([R,\infty)) \cap \mathcal{C}^2((R,\infty)), \\ & \psi'/\psi \in L^\infty((R,\infty)), \ \psi > 0 \text{ in } [R,\infty), \ \lim_{x\to+\infty} \tfrac{1}{x} \ln \psi(x) = 0 \quad \}. \end{aligned} \tag{4.30}$$

Thus, one has $\underline{\lambda_1}(L_p, (R, +\infty)) \geq H(p) - 4\delta$, where the principal eigenvalue $\underline{\lambda_1}$ is defined by

$$\underline{\lambda_1}(L_p, (R,\infty)) := \inf\{\lambda \mid \exists \phi \in \mathcal{A}_R \text{ such that } L_p\phi \geq \lambda\phi \text{ in } (R,\infty)\}, \tag{4.31}$$

Hence, $\lim_{R\to+\infty} \underline{\lambda_1}(L_p, (R, +\infty)) \geq H(p)$ for all $p > 0$.

In order to use Theorem 2.1 of [28], we need the nonlinearity to have two steady states and to be positive between these two steady states. It is not the case here but we will bound f from below by such a nonlinearity. As $\min_{\mathbb{R}} \mu_0 > 0$ and f is of class $\mathcal{C}^1$ in the neighborhood of $u = 0$, we know that there exists $\theta \in (0, 1)$ so that

$$f(x, u) > 0 \text{ for all } x \in \mathbb{R} \ \text{ and } \ u \in (0, \theta).$$

Let $\zeta = \zeta(u)$ a smooth function so that

$$0 < \zeta(u) \leq 1 \text{ for all } u \in (0,\theta), \ \ \zeta(u) = 0 \text{ for all } u \geq \theta \ \text{ and } \ \zeta(u) = 1 \text{ for all } u \in (0, \frac{\theta}{2}).$$

Define $\underline{f}(x, u) := \zeta(u)f(x, u)$ for all $(x, u) \in \mathbb{R} \times [0, 1]$. Then

$$\underline{f} \leq f \text{ in } \mathbb{R} \times [0,1] \ \text{ and } \ \underline{f}_u'(x, 0) = f_u'(x, 0) = \mu_0(\phi(x)) \text{ for all } x \in \mathbb{R}.$$

Let $\underline{u}$ the solution of (4.1) with nonlinearity $\underline{f}$ instead of f and initial datum u_0. The parabolic maximum principle yields $u \geq \underline{u}$.

Since the function $\underline{f}$ satisfies the hypotheses of Theorem 2.1 in [28], we conclude that

$$\lim_{t\to+\infty} \min_{x\in[0,wt]} \underline{u}(t,x) = 1 \text{ for all } w \in \Big(0, \min_{p>0} \frac{H(p)}{p}\Big).$$

It follows that

$$w_* \geq \min_{p>0} \frac{H(p)}{p} = \min_{k\geq M} \frac{k}{j(k)}.$$

Next, assume that $\mu_0 \in \mathcal{C}^2(\mathbb{R})$ does not satisfy (4.22). Let $\overline{y} \in \mathbb{R}$ so that $\mu_0(\overline{y}) = \max_{y\in\mathbb{R}} \mu_0(y)$. Take a 1-periodic function $\chi \in \mathcal{C}^2(\mathbb{R})$ so that $\chi(0) = 0$, $\chi(y) > 0$ for all $y \neq 0$ and $\chi''(0) > 0$. Define for all $n \in \mathbb{N}$ and $x \in \mathbb{R}$:

$$\mu_0^n(y) := \mu_0(y) - \frac{1}{n}\chi(y - \overline{y}).$$

This 1-periodic function satisfies (4.22) for all n and one has $0 < \mu_0^n \leq \mu_0$ for n large enough. It follows from the maximum principle that

$$\liminf_{t\to+\infty} \min_{0\leq x\leq wt} u(t,x) > 0 \text{ for all } w \in \Big(0, \min_{k\geq M} \frac{k}{j^n(k)}\Big),$$

where $j^n(k) = \displaystyle\int_0^1 \sqrt{k - \mu_0^n(x)}dx \geq j(k) > 0$ for all $k \geq M$. Letting $n \to +\infty$, one has $\mu_0^n(y) \to \mu_0(y)$ uniformly in $y \in \mathbb{R}$ and thus

$$\liminf_{t\to+\infty} \min_{0\leq x\leq wt} u(t,x) > 0 \text{ for all } w \in (0, w_\infty),$$

which concludes the proof in this case.

Lastly, if $\mu_0 \in \mathcal{C}^0(\mathbb{R})$ is an arbitrary 1-periodic function, then one easily concludes by smoothing μ_0 as in the previous step. □

Chapitre 5

Uniqueness from pointwise observations in a multi-parameter inverse problem

Ce travail réalisé en collaboration avec Michel Cristofol [a], François Hamel [a,b] et Lionel Roques [c] est publié dans les *Communications on Pure and Applied Analysis* [CGHR12]

[a] Aix-Marseille Université, LATP, Faculté des Sciences et Techniques
Avenue Escadrille Normandie-Niemen, F-13397 Marseille Cedex 20, France
[b] Institut Universitaire de France
[c] UR 546 Biostatistique et Processus Spatiaux, INRA, F-84000 Avignon, France

Sommaire

5.1 Introduction

Reaction-diffusion equations arise as models in many fields of mathematical biology [135]. From morphogenesis [176] to population genetics [72, 112] and spatial ecology [103, 169, 175], these partial differential equations benefit from a well-developed mathematical theory.

In the context of spatial ecology, single-species reaction-diffusion models generally deal with polynomial reaction terms. In a one-dimensional case, and if the environment is supposed to be homogeneous they take the form :

$$\frac{\partial u}{\partial t} - D\frac{\partial^2 u}{\partial x^2} = P(u), \tag{5.1}$$

where $u = u(t, x)$ is the population density at time t and space position x and $D > 0$ is the diffusion coefficient. The function P, which stands for the growth of the population, is a polynomial of order $N \geq 1$. The Fisher-Kolmogorov, Petrovsky, Piskunov (F-KPP) equation is the archetype of such models. In this model, we have $P(u) = \mu\, u - \gamma u^2$. The constant parameters μ and γ respectively correspond to the intrinsic growth rate and intraspecific competition coefficients. In this model, the lower the population density u, the higher the per capita growth rate $P(u)/u$. More complex models can involve polynomial nonlinearities of higher order. Examples are those taking account of an Allee effect. This effect occurs when the per capita growth rate $P(u)/u$ reaches its maximum at a strictly positive population density and is known in many species [7, 53, 179]. A typical example of reaction term involving an Allee effect is [105, 118, 158] :

$$P(u) = ru\,(1-u)\,(u-\rho)\,,$$

with $r > 0$ and $\rho \in (0, 1)$. The parameter ρ corresponds in that case to the "Allee threshold" below which the growth rate becomes negative.

In the previous examples, the reaction terms were assumed to be independent of the space variable. However, real world is far from begin homogeneous. In order to take the heterogeneities into account, models have been adapted and constant coefficients have been replaced by space or time dependant functions. In his pioneering work, Skellam [169] (and later, Shigesada, Kawasaki and Teramoto [168]) mentioned the following extension of the F-KPP model to heterogeneous environments :

$$\frac{\partial u}{\partial t} - D\frac{\partial^2 u}{\partial x^2} = \mu(x)\, u - \gamma(x) u^2. \tag{5.2}$$

Here, the values of $\mu(x)$ and $\gamma(x)$ depend on the position x. For instance, regions of the space associated with high values of $\mu(x)$ correspond to favorable regions, whereas those associated with low or negative values of $\mu(x)$ correspond to unfavorable regions. As emphasized by recent works, the precise spatial arrangement of these regions plays a crucial role in this model, since it controls persistence and spreading of the population [24, 45, 64, 153, 156, 159, 103]. Models involving an Allee effect can be extended as well to heterogeneous environments, as in [86, 158], where the effects of spatial heterogeneities are discussed for models of the type :

$$\frac{\partial u}{\partial t} = D\frac{\partial^2 u}{\partial x^2} + r(x)\, u\,[(1-u)(u-\rho(x)) + \nu(x)]\,. \tag{5.3}$$

We also refer to [126] for an analysis of propagation phenomena related to a reaction-diffusion model with an Allee effect in infinite cylinders having undulating boundaries.

In this chapter, we focus on reaction-diffusion models with more general heterogeneous nonlinearities :

$$\frac{\partial u}{\partial t} = D\frac{\partial^2 u}{\partial x^2} + \sum_{k=1}^{N} \mu_k(x)\, u^k + g(x,u), \text{ for } t > 0,\ x \in (a,b), \tag{5.4}$$

for some interval (a,b) in $\mathbb{R}$.

Since the behavior of such models depends on the precise form of the coefficients, their empirical use requires an accurate knowledge of the coefficients. Unfortunately, in applications, the coefficients cannot be directly measured since they generally result from intertwined effects of several factors. Thus, the coefficients are generally measured through the density $u(t,x)$ [170]. From a theoretical viewpoint, if $u(t,x)$ is measured at any time $t \geq 0$ and at all points x in the considered domain, all the coefficients in the model can generally be determined. However, in most cases, $u(t,x)$ can only be measured in some – possibly small – subregions of the domain (a,b) [188]. For reaction-diffusion models as well as for many other types of models, the determination of the coefficients in the whole domain (a,b) bears on inference methods which consist in comparing the solution of the model with hypothetical values of coefficients $\tilde{\mu}_k$, with the measurements on the subregions [171]. The underlying assumption behind this inference process is that there is a one-to-one and onto relationship between the value of the solutions of the model over the subregions and the space of coefficients. This assumption is of course not true in general.

In this chapter, we obtain uniqueness results for the coefficients $\mu_k(x)$, $k = 1,\dots,N$, based on localized measurements of the solution $u(t,x)$ of (5.4). The major differences with previous works dealing with comparable uniqueness results are (1) the size of the region, namely a singleton, where $u(t,x)$ has to be known in order to prove uniqueness, (2) the number of parameters we are able to determine, and (3) the general type of nonlinearity we deal with.

Uniqueness of the parameters, given some values of the solution, corresponds to an inverse coefficient problem, which is generally dealt with – for such reaction-diffusion equations – using the method of Carleman estimates [35, 109]. This method provides Lipschitz stability, in addition to the uniqueness of the coefficients. However, this method requires, among other measurements, the knowledge of the density $u(\theta,x)$ at some time θ and for all x in the domain (a,b) (see [15, 48, 76, 97, 192]). The uniqueness of the couple $(u,\mu(x))$ satisfying the equation (5.2) given such measurements has been investigated in a previous work [49], in any space dimension. Uniqueness and stability results can also be derived from boundary measurements. In particular, there is a huge literature on the determination of nonlinear spatially homogeneous terms $f(u)$ in reaction-diffusion equations from such boundary measurements [42, 59, 63, 120, 137, 144].

In a recent work, Roques and Cristofol [155] have proved the uniqueness of the coefficient $\mu(x)$ in (5.2) when $\gamma(x)$ is known under the assumption that the density $u(t,x_0)$ and its spatial derivative $\frac{\partial u}{\partial x}(t,x_0)$ are known at a point x_0 in (a,b) for all $t \in (0,\varepsilon)$ and that the initial density $u(0,x)$ is known over (a,b). This result shows that the coefficient $\mu(x)$ is uniquely determined in the whole domain (a,b) by the value of the solution $u(t,x)$ and of its spatial derivative at a single point x_0. The present work extends this result to the case of several coefficients $\mu_k(x)$, $k = 1,\dots,N$: given any point x_0 in (a,b) we establish a uniqueness result for the $N-$uple $(\mu_1(x),\dots,\mu_N(x))$ given measurements of the N solutions $u(t,x)$ of (5.4) and of their first spatial derivatives in $(0,\varepsilon)\times\{x_0\}$, starting with N nonintersecting initial conditions.

5.2 Hypotheses and main result

Let (a,b) be a bounded interval in $\mathbb{R}$. We consider, for some $T>0$, the problem :

$$\left\{\begin{array}{l} \dfrac{\partial u}{\partial t} - D\dfrac{\partial^2 u}{\partial x^2} = \displaystyle\sum_{k=1}^{N} \mu_k(x)u^k + g(x,u), \quad t\in(0,T), \quad x\in(a,b), \\ \alpha_1 u(t,a) - \beta_1 \dfrac{\partial u}{\partial x}(t,a) = 0, \quad t>0, \\ \alpha_2 u(t,b) + \beta_2 \dfrac{\partial u}{\partial x}(t,b) = 0, \quad t>0, \\ u(0,x) = u^0(x), \quad x\in(a,b), \end{array}\right. \tag{$\mathcal{P}^{u^0}_{(\mu_k)}$}$$

for some $N\in\mathbb{N}^*$, and for – unknown – functions μ_k which belong to the following space $\mathcal{M}$:

$$\mathcal{M} := \{\psi\in C^{0,\eta}([a,b]) \text{ s. t. } \psi \text{ is piecewise analytic on } (a,b)\}, \tag{5.5}$$

for some $\eta\in(0,1]$. The space $C^{0,\eta}$ corresponds to Hölder continuous functions with exponent η (see e.g. [75]). A function $\psi\in C^{0,\eta}([a,b])$ is called piecewise analytic if their exist $n>0$ and an increasing sequence $(\kappa_j)_{1\le j\le n}$ such that $\kappa_1=a$, $\kappa_n=b$, and

$$\text{for all } x\in(a,b),\ \psi(x) = \sum_{j=1}^{n-1} \chi_{[\kappa_j,\kappa_{j+1})}(x)\varphi_j(x),$$

for some analytic functions φ_j, defined on the intervals $[\kappa_j,\kappa_{j+1}]$, and where $\chi_{[\kappa_j,\kappa_{j+1})}$ are the characteristic functions of the intervals $[\kappa_j,\kappa_{j+1})$ for $j=1,\dots,n-1$. In particular, if $\psi\in\mathcal{M}$, then, for each $x\in[a,b)$ (resp. $x\in(a,b]$), there exists $r=r_x>0$ such that ψ is analytic on $[x,x+r]$ (resp. $[x-r,x]$).

The assumptions on the function g are :

$$\left\{\begin{array}{l} g(\cdot,u)\in C^{0,\eta}([a,b]) \text{ for all } u\in\mathbb{R},\ g(x,\cdot)\in C^1(\mathbb{R}) \text{ for all } x\in[a,b], \\ g(\cdot,0)=0 \text{ in } [a,b]. \end{array}\right. \tag{5.6}$$

We also assume that the diffusion coefficient D is positive and that the boundary coefficients satisfy :

$$\alpha_1^2+\beta_1^2>0 \text{ and } \alpha_2^2+\beta_2^2>0. \tag{5.7}$$

We furthermore make the following hypotheses on the initial condition :

$$u^0>0 \text{ in } (a,b) \text{ and } u^0\in C^{2,\eta}([a,b]), \tag{5.8}$$

that is u^0 is a C^2 function such that $(u^0)''$ is Hölder continuous. In addition to that, we assume the following compatibility conditions :

$$\begin{array}{l} \alpha_1 u^0(a) - \beta_1 (u^0)'(a) = 0 \ \text{ and } \ -D\,(u^0)''(a) = g(a,0) \ \text{ if } \beta_1=0, \\ \alpha_2 u^0(b) + \beta_2 (u^0)'(b) = 0 \ \text{ and } \ -D\,(u^0)''(b) = g(b,0) \ \text{ if } \beta_2=0. \end{array} \tag{5.9}$$

Under the assumptions (5.5)-(5.9), for each sequence $(\mu_k)_{1\le k\le N}\in\mathcal{M}^N$, there exists a time $T^{u^0}_{(\mu_k)}\in(0,+\infty]$ such that the problem $(\mathcal{P}^{u^0}_{(\mu_k)})$ has a unique solution $u\in C^{2,\eta}_{1,\eta/2}([0,T^{u^0}_{(\mu_k)})\times[a,b])$ (i.e. the derivatives up to order two in x and order one in t are Hölder continuous). Existence, uniqueness and regularity of the solution u are classical (see e.g. [141]).

Our main result is a uniqueness result for the sequence of coefficients $(\mu_k)_{1\leq k\leq N}$ associated with observations of the solution and of its spatial derivative at a single point x_0 in $[a,b]$. Consider N ordered initial conditions u_i^0 and, for each sequence $(\mu_k)_{1\leq k\leq N}$, let u_i be the solution of $(\mathcal{P}^{u_i^0}_{(\mu_k)})$. Our result shows that for any finite subset $\mathcal{Q}\subset\mathcal{M}^N$ and any $\varepsilon\in(0,\min\limits_{(\mu_k)\in\mathcal{Q},1\leq i\leq N} T^{u_i^0}_{(\mu_k)})$, the function

$$G:\begin{array}{ccc}\mathcal{Q} & \to & C^1((0,\varepsilon))^{2\,N}\\ (\mu_k)_{1\leq k\leq N} & \mapsto & (u_i(\cdot,x_0),\partial u_i/\partial x(\cdot,x_0))_{1\leq i\leq N}\end{array},$$

is one-to-one. In other words, we have the following theorem :

Theorem 5. *Let $N\in\mathbb{N}^*$, $(\mu_k)_{1\leq k\leq N}$ and $(\tilde\mu_k)_{1\leq k\leq N}$ be two families of coefficients in $\mathcal{M}$. Let $(u_i^0)_{1\leq i\leq N}$ be N positive functions fulfilling (5.8) and (5.9) and such that $u_i^0(x)\neq u_j^0(x)$ for all $x\in(a,b)$ and all $i\neq j$. Let u_i and $\tilde u_i$ be the solutions of $(\mathcal{P}^{u_i^0}_{(\mu_k)})$ and $(\mathcal{P}^{u_i^0}_{(\tilde\mu_k)})$, respectively, on $[0,T)\times[a,b]$, with $T=\min_{1\leq i\leq N}\{T^{u_i^0}_{(\mu_k)},T^{u_i^0}_{(\tilde\mu_k)}\}$. We assume that u_i and $\tilde u_i$ satisfy at some $x_0\in(a,b)$, and for some $\varepsilon\in(0,T]$:*

$$\left\{\begin{array}{rcl} u_i(t,x_0) & = & \tilde u_i(t,x_0),\\ \dfrac{\partial u_i}{\partial x}(t,x_0) & = & \dfrac{\partial\tilde u_i}{\partial x}(t,x_0),\end{array}\right.\quad \textit{for all } t\in(0,\varepsilon) \textit{ and all } i\in\{1,\cdots,N\}. \tag{5.10}$$

Then $\mu_k\equiv\tilde\mu_k$ on $[a,b]$ for all $k\in\{1,\cdots,N\}$, and consequently $u_i\equiv\tilde u_i$ in $[0,T)\times[a,b]$ for all i.

Remark 10. *The conclusion of Theorem 5 is still valid when $x_0=a$ and $\beta_1\neq 0$ (resp. $x_0=b$ and $\beta_2\neq 0$) if the initial conditions u_i^0 are assumed to be positive in $[a,b)$ (resp. $(a,b]$).*

The main result in [155] was a particular case of Theorem 5. A similar conclusion was indeed proved in the case $N=1$ and for $g(x,u)=-\gamma\,u^2$. In such case, the determination of one coefficient $\mu_1(x)$ only requires the knowledge of the initial condition u^0 and of $(u(t,x_0),\partial u/\partial x(t,x_0))$ for $t\in(0,\varepsilon)$. When $N\geq 2$, the above theorem requires more than the knowledge of the initial condition for the determination of the coefficients : we need a control on the initial condition, which enables to obtain N measurements of the solution of $(\mathcal{P}^{u^0}_{(\mu_k)})$, starting from N different initial conditions. A natural question is whether the result of Theorem 5 remains true when the number of measurements is smaller than N. In Section 5.4, we prove that the answer is negative in general.

5.3 Proof of Theorem 5

For the sake of clarity, we begin with proving Theorem 5 in the particular case $N=2$ (the proof in the case $N=1$ would be similar to that of [155], which was concerned with $g(x,u)=-\gamma\,u^2$). We then deal with the general case of problems $(\mathcal{P}^{u_i^0}_{(\mu_k)})$ and $(\mathcal{P}^{u_i^0}_{(\tilde\mu_k)})$ with $N\geq 1$.

3.1 Proof of Theorem 5, case $N=2$.

Let (μ_1,μ_2) and $(\tilde\mu_1,\tilde\mu_2)$ be two pairs of coefficients in $\mathcal{M}$. Let $u_1^0(x),u_2^0(x)$ be two functions verifying (5.8) and (5.9) and such that $u_1^0(x)\neq u_2^0(x)$ in (a,b). Let u_1 and $\tilde u_1$ be respectively the solutions of $(\mathcal{P}^{u_1^0}_{\mu_1,\mu_2})$ and $(\mathcal{P}^{u_1^0}_{\tilde\mu_1,\tilde\mu_2})$ and u_2 and $\tilde u_2$ be the solutions of $(\mathcal{P}^{u_2^0}_{\mu_1,\mu_2})$ and $(\mathcal{P}^{u_2^0}_{\tilde\mu_1,\tilde\mu_2})$.

We set, for $i=1,2$,

$$U_i:=u_i-\tilde u_i,\ m_1:=\mu_1-\tilde\mu_1 \text{ and } m_2:=\mu_2-\tilde\mu_2.$$

The functions U_i satisfy :

$$\frac{\partial U_i}{\partial t} - D\frac{\partial^2 U_i}{\partial x^2} = b_i(t,x)U_i + h(x,u_i(t,x)), \tag{5.11}$$

for $t \in [0,T)$ and $x \in [a,b]$, where

$$\begin{aligned} b_i(t,x) &= \tilde{\mu}_1(x) + \tilde{\mu}_2(x)\left(u_i(t,x) + \tilde{u}_i(t,x)\right) + c_i(t,x), \\ c_i(t,x) &= \begin{cases} \dfrac{g(x,u_i(t,x)) - g(x,\tilde{u}_i(t,x))}{u_i(t,x) - \tilde{u}_i(t,x)} \text{ if } u_i(t,x) \neq \tilde{u}_i(t,x), \\ \dfrac{\partial g}{\partial u}(x,u_i(t,x)) \text{ if } u_i(t,x) = \tilde{u}_i(t,x), \end{cases} \\ h(x,s) &= s\left(m_1(x) + m_2(x)s\right), \end{aligned} \tag{5.12}$$

and the boundary and initial conditions :

$$\begin{cases} \alpha_1 U_i(t,a) - \beta_1 \dfrac{\partial U_i}{\partial x}(t,a) = 0, \ t > 0, \\ \alpha_2 U_i(t,b) + \beta_2 \dfrac{\partial U_i}{\partial x}(t,b) = 0, \ t > 0, \\ U_i(0,x) = 0, \ x \in (a,b). \end{cases} \tag{5.13}$$

Let us set :

$$\mathcal{A}_+ = \Big\{ x \geq x_0 \text{ s.t. } m_1(y) \equiv m_2(y) \equiv 0 \text{ for all } y \in [x_0,x] \Big\},$$

and

$$x_1 := \begin{cases} \sup(\mathcal{A}_+) & \text{if } \mathcal{A}_+ \text{ is not empty,} \\ x_0 & \text{if } \mathcal{A}_+ \text{ is empty.} \end{cases}$$

If $x_1 = b$, then $m_1(x) \equiv m_2(x) \equiv 0$ on $[x_0,b]$. Let us assume on the contrary that $x_1 < b$.

Step 1 : We show that there exist $\theta > 0$, $x_2 \in (x_1,b)$ and $j \in \{1,2\}$ such that the function $(t,x) \mapsto h(x,u_j(t,x))$ has a constant strict sign on $[0,\theta] \times (x_1,x_2]$, i.e. $h(x,u_j(t,x)) > 0$ or $h(x,u_j(t,x)) < 0$ in $[0,\theta] \times (x_1,x_2]$.

To do so, let us define, for all $x \in [x_1,b)$:

$$z(x) = \begin{cases} -\dfrac{m_1(x)}{m_2(x)} & \text{if } m_2(x) \neq 0, \\ \lim\limits_{y \to x^+} -\dfrac{m_1(y)}{m_2(y)} & \text{if } m_1(x) = m_2(x) = 0 \\ & \text{and } m_2(y) \neq 0 \text{ in a right neighborhood of } x, \\ +\infty & \text{otherwise.} \end{cases} \tag{5.14}$$

Whenever $m_2(x) \neq 0$, $z(x)$ is a root of the polynomial $h(x,\cdot)$. Notice also that the limit $\lim_{y \to x^+} -\frac{m_1(y)}{m_2(y)}$ in the second case of the definition of $z(x)$ is well defined since m_1 and m_2 are analytic on $[x,y]$ for $y - x > 0$ small enough.

Since, $u_1^0(x_1) \neq u_2^0(x_1)$, we have $|u_j^0(x_1) - z(x_1)| > 0$ for some $j \in \{1,2\}$. Moreover, there exists $\delta > 0$ such that $x_1 + \delta < b$ and

$$|u_j^0(x) - z(x)| \geq r > 0 \text{ on } [x_1, x_1 + \delta], \text{ for some } r > 0. \tag{5.15}$$

Indeed, if $z(x_1) = \pm\infty$, we clearly have (5.15). If $z(x_1) \neq \pm\infty$, from (5.14), z is continuous in a right neighborhood of x_1. As the function u_j^0 is also continuous in this neighborhood, we get (5.15).

Moreover, $u_j(t,x) \in C^{2,\eta}_{1,\eta/2}([0,T)\times[a,b])$. This implies that u_j is continuous at $(t,x)=(0,x_1)$. As a consequence, there exists $\theta>0$ small enough so that $|u_j(t,x)-u_j^0(x_1)| \le r/4$ in $[0,\theta]\times[x_1,x_1+\theta]$, whence

$$|u_j(t,x)-u_j^0(x)| \le \frac{r}{2} \text{ in } (t,x)\in[0,\theta]\times[x_1,x_1+\theta]. \tag{5.16}$$

Finally, setting $\delta'=\min\{\theta,\delta\}$, we have, from (5.15) and (5.16) :

$$|u_j(t,x)-z(x)| \ge \Big|\,|u_j(t,x)-u_j^0(x)|-|u_j^0(x)-z(x)|\,\Big| \ge \frac{r}{2}>0 \tag{5.17}$$

for all $(t,x)\in[0,\theta]\times[x_1,x_1+\delta']$.

Now, the definition of x_1 and the piecewise analyticity of m_1 and m_2 imply that there exists $\delta''\in(0,\delta')$ such that :

$$\begin{array}{c}\text{for all } x\in(x_1,x_1+\delta''],\\ \text{the polynomial function } h(x,\cdot) \text{ verifies } h(x,\cdot)\not\equiv 0 \text{ in } \mathbb{R}.\end{array} \tag{5.18}$$

Indeed, assume on the contrary that there is a decreasing sequence $y_n\to x_1$ such that $h(y_n,\cdot)\equiv 0$ in $\mathbb{R}$. Since the functions $h(y_n,\cdot)$ are polynomial, we get $m_1(y_n)=m_2(y_n)=0$ for all $n\in\mathbb{N}$. Besides, as m_1 and m_2 belong to $\mathcal{M}$, for n large enough, m_1 and m_2 are analytic on $[x_1,y_n]$, which implies that $m_1\equiv m_2\equiv 0$ on $[x_1,x_n]$ for n large enough. This contradicts the definition of x_1 and we get (5.18).

From the expression (5.12) of h and using (5.18), we observe that for each $x\in(x_1,x_1+\delta'']$, either $s=0$ is the unique solution of $h(x,s)=0$ or $m_2(x)\neq 0$ and the equation $h(x,s)=0$ admits exactly two solutions $s=0$ and $s=z(x)$. Let us set $x_2=x_1+\delta''\in(x_1,b)$. By continuity of u_j in $[0,T)\times[a,b]$, and since $[x_1,x_2]\subset(a,b)$ and $u_j^0>0$ in (a,b), we have $u_j(t,x)>0$ in $[0,\theta]\times(x_1,x_2]$ for θ small enough. Thus, using (5.17) we finally get :

$$h(x,u_j(t,x))\neq 0 \text{ in } [0,\theta]\times(x_1,x_2].$$

This concludes the proof of step 1.

Step 2 : We prove that $x_1=b$.

From Step 1, let us assume in the sequel – without loss of generality – that $(t,x)\mapsto h(x,u_j(t,x))$ is positive on $[0,\theta]\times(x_1,x_2]$ (the case $h(x,u_j(t,x))<0$ could be treated similarly). Then, from the definition of x_1, we deduce that $h(x,u_j(t,x))$ is nonnegative for all $(t,x)\in[0,\theta]\times[x_0,x_2]$.

Since $h(x_2,u_j(0,x_2))>0$ and $U_j(0,\cdot)\equiv 0$, it follows from (5.11) that

$$\frac{\partial U_j}{\partial t}(0,x_2)=h(x_2,u_j(0,x_2))>0.$$

Thus, for $\varepsilon'\in(0,\theta)$ small enough, $U_j(t,x_2)>0$ for $t\in(0,\varepsilon')$. As a consequence, and from the assumption of Theorem 5, U_j satisfies :

$$\begin{cases} \dfrac{\partial U_j}{\partial t}-D\dfrac{\partial^2 U_j}{\partial x^2}-b_j(t,x)U_j\ge 0,\ t\in(0,\varepsilon'),\ x\in[x_0,x_2],\\ U_j(t,x_0)=0 \text{ and } U_j(t,x_2)>0,\ t\in(0,\varepsilon'),\\ U_j(0,x)=0,\ x\in(x_0,x_2). \end{cases}$$

Moreover, the weak and strong parabolic maximum principles give that $U_j(t,x)>0$ in $(0,\varepsilon')\times(x_0,x_2)$. Since $U_j(t,x_0)=0$, the Hopf's lemma also implies that

$$\frac{\partial U_j}{\partial x}(t,x_0)>0 \text{ for all } t\in(0,\varepsilon').$$

This contradicts the assumption (5.10) of Theorem 5. Finally, we necessarily have $x_1 = b$ and therefore $m_1 \equiv m_2 \equiv 0$ on $[x_0, b]$.

Step 3 : We prove that $m_1 \equiv m_2 \equiv 0$ *on* $[a, b]$.

Setting :

$$\mathcal{A}_- = \Big\{ x \leq x_0 \text{ s.t. } m_1(y) = m_2(y) = 0 \text{ for all } y \in [x, x_0] \Big\},$$

and

$$y_1 := \begin{cases} \inf(\mathcal{A}_-) & \text{if } \mathcal{A}_- \text{ is not empty,} \\ x_0 & \text{if } \mathcal{A}_- \text{ is empty,} \end{cases}$$

we can prove, by applying the same arguments as above, that $y_1 = a$ and consequently $m_1 \equiv m_2 \equiv 0$ on $[a, x_0]$.

Finally, $m_1 \equiv m_2 \equiv 0$ on $[a, b]$ which concludes the proof of Theorem 5 in the case $N = 2$. □

Remark 11. *Apart from the radially symmetric case, the extension of the above arguments to higher dimensions is not straightforward. Indeed, let us replace the interval* (a, b) *by a bounded domain* Ω *of* $\mathbb{R}^d$*, with* $d \geq 2$*, and consider the simplest case* $N = 1$ *and* $u_1^0 > 0$ *in* $\overline{\Omega}$*. Assume that* $u_1 = \tilde{u}_1$ *in a set* $(0, \varepsilon) \times \omega$ *where* $\varepsilon > 0$ *and* $\omega \subset \Omega$ *is a subset of* Ω*. Then, one can check that* $m_1 = \mu_1 - \tilde{\mu}_1 \equiv 0$ *in* ω*. We may define* $\mathcal{A}_+$ *as the largest closed subset of* Ω*, containing* ω*, and such that* $m_1 \equiv 0$ *on* $\mathcal{A}_+$*. Define* $\theta > 0$ *such that* $u_1 > 0$ *in* $[0, \theta] \times \Omega$*. Then, if* $\mathcal{A}_+ \neq \Omega$*, there exists a set* $\mathcal{A}_1 \supset \mathcal{A}_+$*, such that* $\mathcal{A}_1 \neq \mathcal{A}_+$ *and* m_1 *has a constant strict sign in* $\mathcal{A}_1 \setminus \mathcal{A}_+$*. Thus, instead of the result of Step 1 above, we know that* $(t, x) \mapsto h(x, u_1(t, x)) = u_1(t, x)\, m_1(x)$ *has a constant strict sign on* $[0, \theta] \times \{\mathcal{A}_1 \setminus \mathcal{A}_+\}$*. We may try to use an argument similar to that of Step 2, with* $\mathcal{A}_2 = \mathcal{A}_1 \setminus \omega$ *instead of* $[x_0, x_2]$*. However,* $U_1(t, x) = u_1 - \tilde{u}_1$ *does not necessarily have a constant sign on the boundary of* $\mathcal{A}_2$*, even for small times* $t > 0$*. As a consequence, the above argument cannot be applied as such.*

3.2 Proof of Theorem 5, general case $N \geq 1$.

We set for all $i, k \in \{1, \cdots, N\}$,

$$U_i := u_i - \tilde{u}_i, \;\; m_k := \mu_k - \tilde{\mu}_k.$$

The functions U_i satisfy :

$$\frac{\partial U_i}{\partial t} - D \frac{\partial^2 U_i}{\partial x^2} = b_i(t, x) U_i + h(x, u_i(t, x)), \tag{5.19}$$

for $t \in [0, T)$ and $x \in [a, b]$, where

$$b_i(t, x) = \begin{cases} \dfrac{(\tilde{f} + g)(x, u_i(t, x)) - (\tilde{f} + g)(x, \tilde{u}_i(t, x))}{u_i(t, x) - \tilde{u}_i(t, x)} \text{ if } u_i(t, x) \neq \tilde{u}_i(t, x), \\ \dfrac{\partial (\tilde{f} + g)}{\partial u}(x, u_i(t, x)) \text{ if } u_i(t, x) = \tilde{u}_i(t, x), \end{cases}$$

$$h(x, s) = \sum_{k=1}^{N} m_k(x) s^k,$$

and

$$\tilde{f}(x, u) = \sum_{k=1}^{N} \tilde{\mu}_k(x) u^k.$$

Moreover, the functions U_i satisfy the following boundary and initial conditions :

$$\begin{cases} \alpha_1 U_i(t,a) - \beta_1 \dfrac{\partial U_i}{\partial x}(t,a) = 0, \ t>0, \\ \alpha_2 U_i(t,b) + \beta_2 \dfrac{\partial U_i}{\partial x}(t,b) = 0, \ t>0, \\ U_i(0,x) = 0, \ x \in (a,b). \end{cases} \tag{5.20}$$

Let us set

$$\mathcal{A}_+ = \Big\{ x \geq x_0 \text{ s.t. } m_k \equiv 0 \text{ on } [x_0,x] \text{ for all } k \in \{1,\cdots,N\} \Big\},$$

and

$$x_1 := \begin{cases} \sup(\mathcal{A}_+) & \text{if } \mathcal{A}_+ \text{ is not empty,} \\ x_0 & \text{if } \mathcal{A}_+ \text{ is empty.} \end{cases}$$

If $x_1 = b$, then for all k, $m_k(x) \equiv 0$ on $[x_0,b]$. Let us assume by contradiction that $x_1 < b$. As in the case $N=2$, we prove, as a first step, that there exist $\theta \in (0,T)$, $x_2 \in (x_1,b)$ and $j \in \{1,\dots,N\}$ such that the function $(t,x) \mapsto h(x,u_j(t,x))$ has a constant strict sign on $[0,\theta]\times(x_1,x_2]$, i.e. $h(x,u_j(t,x)) > 0$ or $h(x,u_j(t,x)) < 0$ in $[0,\theta]\times(x_1,x_2]$.

To do so, observe that, from the definitions of x_1 and $\mathcal{M}$, there exists $\delta > 0$ such that $x_1+\delta < b$ and all functions m_k are analytic on $[x_1,x_1+\delta]$ and not all identically zero. Therefore, the integer

$$\rho = \max\Big\{ \rho' \in \mathbb{N}, \ m_k(x) = O\Big((x-x_1)^{\rho'}\Big) \text{ as } x \to x_1^+ \text{ for all } k \in \{1,\dots,N\} \Big\}$$

is well-defined. Furthermore, the function h can then be written as

$$h(x,s) = (x-x_1)^\rho \times H(x,s) \text{ for all } (x,s) \in [x_1,x_1+\delta]\times\mathbb{R},$$

where

$$H(x,s) = M_1(x)\, s + \cdots + M_N(x)\, s^N$$

and the functions $M_1,\dots,M_N$ are analytic on $[x_1,x_1+\delta]$ and not all zero at the point x_1 (namely, there exists $i \in \{1,\dots,N\}$ such that $M_i(x_1) \neq 0$). In other words, the polynomial $H(x_1,\cdot)$ is not identically zero. Since its degree is not larger than N and since $H(x_1,0) = 0$ and the real numbers $u_1^0(x_1),\dots,u_N^0(x_1)$ are all positive and pairwise different, there exists $j \in \{1,\dots,N\}$ such that

$$H(x_1,u_j^0(x_1)) \neq 0.$$

By continuity of H in $[x_1,x_1+\delta]\times\mathbb{R}$ and of u_j on $[0,T)\times[a,b]$, it follows that there exist $\theta \in (0,T)$ and $x_2 \in (x_1,b)$ such that

$$H(x,u_j(t,x)) \neq 0 \text{ for all } (t,x) \in [0,\theta]\times[x_1,x_2].$$

Consequently,

$$h(x,u_j(t,x)) \neq 0 \text{ for all } (t,x) \in [0,\theta]\times(x_1,x_2].$$

The remaining part of the proof of Theorem 5 in the general case $N \geq 1$ is then similar to Steps 2 and 3 of the proof in the particular case $N=2$. Namely, we eventually get a contradiction with the assumption that $\frac{\partial U_j}{\partial x}(t,x_0) = 0$ for all $t \in (0,\varepsilon)$, yielding $x_1 = b$ and $m_k = 0$ on $[x_0,b]$ for all $k \in \{1,\dots,N\}$. Similarly, $m_k = 0$ on $[a,x_0]$ for all $k \in \{1,\dots,N\}$. □

5.4 Non-uniqueness results

This section deals with non-uniqueness results for the coefficients (μ_k) in $(\mathcal{P}^{u^0}_{(\mu_k)})$ under assumptions weaker than those of Theorem 5. These results emphasize the optimality of the assumptions of Theorem 5.

1–Number of measurements smaller than number of unknown coefficients.

We give a counter-example to the uniqueness result of Theorem 5 in the case where the number of measurements is smaller than the number of unknown coefficients N.

Assume that the coefficients $\mu_1, \dots, \mu_N$ are constant, not all zero, and such that the polynomial

$$f(x,u) = f(u) = \sum_{k=1}^{N} \mu_k \, u^k$$

admits exactly $N-1$ positive and distinct roots $z_1, \dots, z_{N-1}$. Assume furthermore that $\alpha_1 = \alpha_2 = 0$ (Neumann boundary conditions) and that $g \equiv 0$. Then for each $i = 1, \dots, N-1$, z_i is a (stationary) solution of $(\mathcal{P}^{z_i}_{(\mu_k)})$. Consider a similar problem with the coefficients $\tilde{\mu}_k = \tau \, \mu_k$ for $\tau \neq 1$ and $k = 1, \dots, N$. Then, again, for each $i = 1, \dots, N-1$, z_i is a solution of $(\mathcal{P}^{z_i}_{(\tilde{\mu}_k)})$. In particular, assumption (5.10) is fulfilled at any point $x_0 \in [a,b]$ for $k \in \{1, \dots, N-1\}$. However $(\mu_1(x), \dots, \mu_N(x)) \neq (\tilde{\mu}_1(x), \dots, \tilde{\mu}_N(x))$.

This shows that the determination of N coefficients $(\mu_k)_{1 \leq k \leq N}$ requires in general N observations of the solution of $(\mathcal{P}^{u^0}_{(\mu_k)})$, starting from N different initial conditions.

2–Lack of measurement of the spatial derivatives.

We show that if hypothesis (5.10) in Theorem 5 is replaced with the weaker assumption :

$$u_i(t,x_0) = \tilde{u}_i(t,x_0), \text{ for all } t \in (0,\varepsilon) \text{ and all } i \in \{1, \cdots, N\}, \tag{5.21}$$

then the conclusion of the theorem is false in general.

Let $(\mu_k)_{1 \leq k \leq N} \in \mathcal{M}^N$ and assume that $\alpha_1 = \alpha_2 = 0$ (Neumann boundary conditions). Let $(u_i^0)_{1 \leq i \leq N}$ satisfy the assumptions of Theorem 5 and assume furthermore that the functions u_i^0 and $g(\cdot, u)$ are symmetric with respect to $x = (a+b)/2$, i.e.

$$\begin{cases} (u_i^0)_{1 \leq i \leq N}(x) = (u_i^0)_{1 \leq i \leq N}(b - (x-a)) \\ g(x,\cdot) = g(b-(x-a),\cdot) \end{cases} \quad \text{for all } x \in [a,b].$$

Let $\tilde{\mu}_k := \mu_k(b-(x-a))$ for all $x \in [a,b]$ and $k \in \{1, \cdots, N\}$.

Then, we claim that the solutions u_i and $\tilde{u}_i$ of $(\mathcal{P}^{u_i^0}_{(\mu_k)})$ and $(\mathcal{P}^{u_i^0}_{(\tilde{\mu}_k)})$ satisfy (5.21) at $x_0 = \frac{a+b}{2}$ and for ε small enough. Indeed, we observe that, for each $i \in \{1, \cdots, N\}$, $\tilde{u}_i(t, b-(x-a))$ is a solution of $(\mathcal{P}^{u_i^0}_{(\mu_k)})$. By uniqueness, we have

$$u_i(t,x) = \tilde{u}_i(t, b-(x-a)), \text{ for all } t \in (0,T), \text{ all } x \in [a,b] \text{ and all } i \in \{1, \cdots, N\}.$$

In particular, $u_i(t, \frac{a+b}{2}) = \tilde{u}_i(t, \frac{a+b}{2})$ for $t \in (0,T)$ and $i \in \{1, \cdots, N\}$.

This shows that the assumption (5.21) alone is not sufficient to determine the coefficients $(\mu_k)_{1 \leq k \leq N}$.

The above result is an adaptation of Proposition 2.3 in [155] to the general case $N \geq 1$.

3–Time-dependent coefficients.

We show here that the result of Theorem 5 is not true in general when the coefficients (μ_k) are allowed to depend on the variable t.

We place ourselves in the simple case $N = 1$ and $g \equiv 0$, and we assume that $\alpha_1 = \alpha_2 = 0$ (Neumann boundary conditions). We assume that $(a, b) = (0, \pi)$, and we set $u(t, x) = 1 + t\,\cos^2(x)$ and $\tilde{u}(t, x) = 1 + t\,\sin^2(2x)$.

Let us set

$$\mu_1(t,x) = \frac{1}{u}\left(\frac{\partial u}{\partial t} - D\,\frac{\partial^2 u}{\partial x^2}\right)(t,x) \text{ and } \tilde{\mu}_1(t,x) = \frac{1}{\tilde{u}}\left(\frac{\partial \tilde{u}}{\partial t} - D\,\frac{\partial^2 \tilde{u}}{\partial x^2}\right)(t,x)),$$

i.e.,

$$\mu_1(t,x) = \frac{(4Dt+1)\cos^2(x) - 2Dt}{1 + t\,\cos^2(x)} \text{ and } \tilde{\mu}_1(t,x) = \frac{(16Dt+1)\sin^2(2x) - 8Dt}{1 + t\,\sin^2(2x)}.$$

Then, for each $t \in [0, +\infty)$, $\mu_1(t, \cdot)$ and $\tilde{\mu}_1(t, \cdot)$ belong to $\mathcal{M}$. The functions u and $\tilde{u}$ are solutions of $(\mathcal{P}^1_{(\mu_1)})$ and $(\mathcal{P}^1_{(\tilde{\mu}_1)})$, respectively, and they satisfy the assumption (5.10) of Theorem 5 at $x_0 = \pi/2$. However, the conclusion of Theorem 5 does not hold since $\mu_1 \not\equiv \tilde{\mu}_1$.

4–Unknown initial data.

We show here that the result of Theorem 5 is not true in general if the functions u_i and $\tilde{u}_i$ are solutions of $(\mathcal{P}^{u_i^0}_{(\mu_k)})$ and $(\mathcal{P}^{\tilde{u}_i^0}_{(\tilde{\mu}_k)})$, with $u_i^0 \not\equiv \tilde{u}_i^0$. This means that the coefficients (μ_k) cannot be determined, given only the measurements $(u_i(t, x_0), \partial u_i/\partial x(t, x_0))_{1 \le i \le N}$ for $t \in (0, \varepsilon)$, if the initial conditions u_i^0 are unknown.

We build an explicit counter-example in the simple case $N = 1$ and $g \equiv 0$, with $\alpha_1 = \alpha_2 = 0$. Assume that $(a, b) = (0, \pi)$, and let us set $u(t, x) = (1 + \cos^2(x))\, e^{\rho\, t}$ for some $\rho > 0$, and $\tilde{u}(t, x) = (1 + \sin^2(2x))\, e^{\rho\, t}$. We furthermore set

$$\mu_1(x) = \frac{1}{u}\left(\frac{\partial u}{\partial t} - D\,\frac{\partial^2 u}{\partial x^2}\right) \text{ and } \tilde{\mu}_1(x) = \frac{1}{\tilde{u}}\left(\frac{\partial \tilde{u}}{\partial t} - D\,\frac{\partial^2 \tilde{u}}{\partial x^2}\right),$$

i.e.,

$$\mu_1(x) = \frac{(4D+\rho)\cos^2(x) + \rho - 2\,D}{1 + \cos^2(x)} \text{ and } \tilde{\mu}_1(x) = \frac{(16D+\rho)\sin^2(2x) + \rho - 8\,D}{1 + \sin^2(2x)},$$

thus μ_1 and $\tilde{\mu}_1$ belong to $\mathcal{M}$. Besides, u and $\tilde{u}$ are solutions of $(\mathcal{P}^{1+\cos^2(x)}_{\mu_1})$ and $(\mathcal{P}^{1+\sin^2(2x)}_{\tilde{\mu}_1})$ respectively, and they satisfy the assumption (5.10) of Theorem 5 at $x_0 = \pi/2$. However, we obviously have $\mu_1 \not\equiv \tilde{\mu}_1$.

5.5 Numerical determination of several coefficients

In the particular case $N = 1$, it was shown in [155] that the measurements (5.10) of Theorem 5 are sufficient to obtain a good numerical approximation of a coefficient $\mu_1(x)$. In this section, we check whether the measurements (5.10) of Theorem 5 also allow for an accurate reconstruction of N coefficients $(\mu_k)_{1 \le k \le N}$ in the cases $N = 2$ and $N = 3$.

Given the initial data u_i^0 and the measurements $u_i(t, x_0)$ and $\frac{\partial u_i}{\partial x}(t, x_0)$, for $t \in (0, \varepsilon)$ and $i \in \{1, \cdots, N\}$, we can look for the sequence $(\mu_k)_{1 \le k \le N}$ as a minimizer of some functional $G_{(\mu_k)}$. Indeed, for any sequence $(\tilde{\mu}_k)_{1 \le k \le N}$ in $\mathcal{M}^N$, the distance between the measurements of the solutions u_i of $(\mathcal{P}^{u_i^0}_{(\mu_k)})$ and $\tilde{u}_i$ of $(\mathcal{P}^{u_i^0}_{(\tilde{\mu}_k)})$, $i \in \{1, \cdots, N\}$ can be evaluated through the function :

$$G_{(\mu_k)}[(\tilde{\mu}_k)] = \sum_{i=1}^{N} \|u_i(\cdot, x_0) - \tilde{u}_i(\cdot, x_0)\|_{L^2(0,\varepsilon)} + \|\frac{\partial u_i}{\partial x}(\cdot, x_0) - \frac{\partial \tilde{u}_i}{\partial x}(\cdot, x_0)\|_{L^2(0,\varepsilon)}.$$

Then, $G_{(\mu_k)}[(\mu_k)] = 0$ and from Theorem 5 this is the unique global minimum of $G_{(\mu_k)}$ in $\mathcal{M}^N$.

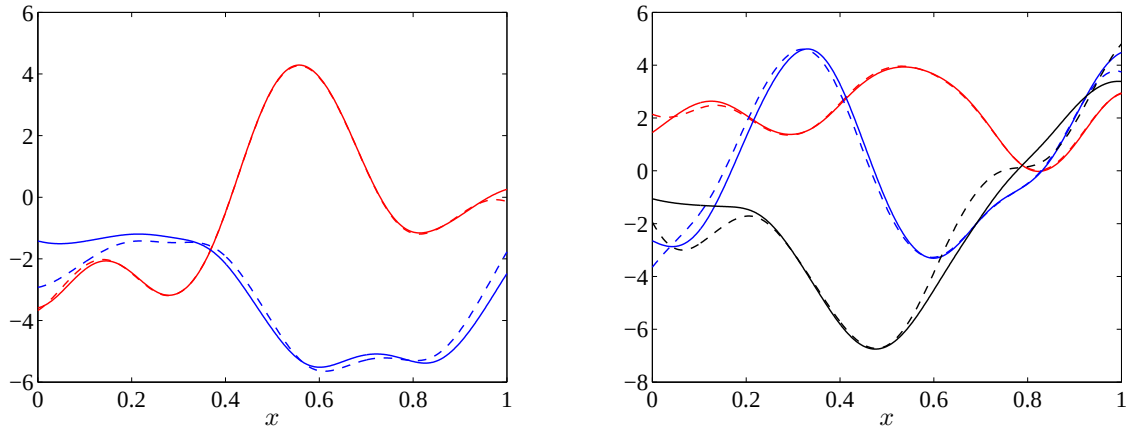

(a) Determination of 2 coefficients

(b) Determination of 3 coefficients

FIGURE 5.1 – (a) Plain lines : examples of functions μ_1 (red line) and μ_2 (blue line) in E. Dashed lines : the functions μ_1^* (in red) and μ_2^* (in blue) obtained by minimizing $G_{(\mu_1,\mu_2)}$. In this case $\|\mu_1 - \mu_1^*\|_{L^2(0,1)} + \|\mu_2 - \mu_2^*\|_{L^2(0,1)} = 0.15$, and $G_{(\mu_1,\mu_2)}[(\mu_1^*, \mu_2^*)] = 9 \cdot 10^{-6}$. (b) Plain lines : functions μ_1 (red line), μ_2 (blue line) and μ_3 (black line) in E. Dashed lines : the functions μ_1^* (in red), μ_2^* (in blue), μ_3^* (in black) obtained by minimizing $G_{(\mu_1,\mu_2,\mu_2)}$. Here, $\|\mu_1 - \mu_1^*\|_{L^2(0,1)} + \|\mu_2 - \mu_2^*\|_{L^2(0,1)} + \|\mu_3 - \mu_3^*\|_{L^2(0,1)} = 0.38$ and $G_{(\mu_1,\mu_2,\mu_3)}[(\mu_1^*, \mu_2^*, \mu_3^*)] = 3 \cdot 10^{-5}$.

In our numerical computations, we fixed $(a, b) = (0, 1)$, $D = 0.1$, $\alpha_1 = \alpha_2 = 0$ and $\beta_1 = \beta_2 = 1$ (Neumann boundary conditions), $x_0 = 2/3$ and $\varepsilon = 0.3$. Besides, we assumed the coefficients μ_k to belong to a finite-dimensional subspace $E \subset \mathcal{M}$:

$$E := \Big\{ \rho \in C^{0,\eta}([0,1]) \,|\, \exists\ (h_j)_{0\le j\le n} \in \mathbb{R}^{n+1}, \\ \rho(x) = \textstyle\sum_{j=0}^{n} h_j \cdot J\left((n-2)\,(x - c_j)\right) \text{ on } [0,1] \Big\},$$

with $c_j = \frac{j-1}{n-2}$ and $J(x) = \dfrac{(x-2)^4(x+2)^4}{2^8}$ if $x \in (-2, 2)$, and $J(x) = 0$ otherwise. In our computations, the integer n was set to 10.

Case $N = 2$: 25 couples of functions (μ_1, μ_2) have been randomly sampled in E^2 : for $k = 1$ and $k = 2$, the components h_j^k, in the expression

$$\mu_k(x) = \sum_{j=0}^{n} h_j^k \cdot J\left((n-2)\,(x - c_j)\right),$$

were randomly drawn from a uniform distribution in $(-5, 5)$.

Starting from the initial data $u_1^0 \equiv 0.1$, and $u_2^0 \equiv 0.2$, the corresponding values of $u_1(t, x_0)$, $\frac{\partial u_1}{\partial x}(t, x_0)$, $u_2(t, x_0)$, $\frac{\partial u_2}{\partial x}(t, x_0)$ were recorded [4], which enabled us to compute $G_{(\mu_1,\mu_2)}[(\tilde{\mu}_1, \tilde{\mu}_2)]$ for any couple $(\tilde{\mu}_1, \tilde{\mu}_2)$ in E^2. The minimizations [5] of the functions $G_{(\mu_1,\mu_2)}$ lead to 25 couples (μ_1^*, μ_2^*), each one corresponding to a computed minimizer of the function $G_{(\mu_1,\mu_2)}$.

4. Numerical computation of u and $\tilde{u}$ were carried out with Comsol Multiphysics® time-dependent solver. We used a second order finite element method (FEM) with 960 elements. This solver uses a method of lines approach incorporating variable order and variable stepsize backward differentiation formulas.

5. The minimizations of the functions $G_{(\mu_k)}$ were performed using MATLAB's® *fminunc* solver. This optimization algorithm uses a Quasi-Newton method with a mixed quadratic and cubic line search procedure. The stopping criterion was based on the number of evaluations of the function $G_{(\mu_1,\mu_2)}$ which was set at $4 \cdot 10^3$.

The average value of the quantity $\|\mu_1 - \mu_1^*\|_{L^2(0,1)} + \|\mu_2 - \mu_2^*\|_{L^2(0,1)}$, over the 25 samples of couples (μ_1, μ_2) is 0.25. The corresponding average value of $G_{(\mu_1,\mu_2)}(\mu_1^*, \mu_2^*)$ is $1.5 \cdot 10^{-5}$. Fig. 5.1 (a) depicts an example of a couple (μ_1, μ_2) in E, together with the couple (μ_1^*, μ_2^*) which was obtained by minimizing $G_{(\mu_1,\mu_2)}$.

Case $N = 3$: in this case, the minimization of the function $G_{(\mu_1,\mu_2,\mu_3)}$ is more time-consuming. We therefore focused on a unique example of a triple (μ_1, μ_2, μ_3) in E^3. The initial data were chosen as follows : $u_1^0 \equiv 0.1$, $u_2^0 \equiv 0.2$, and $u_3^0 \equiv 0.3$. Fig. 5.1 (b) depicts the triple (μ_1, μ_2, μ_3) in E, together with the triple $(\mu_1^*, \mu_2^*, \mu_3^*)$ obtained by minimizing $G_{(\mu_1,\mu_2,\mu_3)}$.

5.6 Discussion

We have obtained a uniqueness result in the inverse problem of determining several non-constant coefficients of reaction-diffusion equations. With a reaction term containing an unknown polynomial part of the form $\sum_{k=1}^{N} \mu_k(x)\, u^k$, our result provides a sufficient condition for the uniqueness of the determination of this nonlinear polynomial part.

This sufficient condition, which is detailed in Theorem 5, involves pointwise measurements of the solution $u(t, x_0)$ and of its spatial derivative $\partial u/\partial x(t, x_0)$ at a single point x_0, during a time interval $(0, \varepsilon)$, and starting with N nonintersecting initial conditions.

The results of Section 5.4 show that most conditions of Theorem 5 are in fact necessary. In particular, the first counter-example of Section 5.4 shows that, for the result of Theorem 5 to hold in general, the number of measurements of the couple $(u, \partial u/\partial x)(t, x_0)$ needs to be at least equal to the degree (N) of the unknown polynomial term.

From a practical point of view, such measurements can be obtained if one has a control on the initial condition. Nevertheless, since our result does not provide a stability inequality, the possibility to do a numerical reconstruction of the unknown coefficients μ_k, on the basis of pointwise measurements, was uncertain. In Section 5.5, we have shown in the cases $N = 2$ and $N = 3$ – which include the classical models (5.2) and (5.3) – that such measurements can indeed lead to good numerical approximations of the unknown coefficients, at least if they are assumed to belong to a known finite-dimensional space.

Acknowledgments

The authors are supported by the French “Agence Nationale de la Recherche" within the projects ColonSGS (third and fourth authors), PREFERED (second, third and fourth authors) and URTI-CLIM (second and fourth authors). The third author is also indebted to the Alexander von Humboldt Foundation for its support. The authors would like to thank the three reviewers for giving valuable comments and references.

Quatrième partie

Les modèles intégro-différentiels

Chapitre 6

Accelerating solutions in integro-differential equations

Ce travail est publié dans le *SIAM Journal on Mathematical Analysis* [Ga11]

Sommaire

6.1 Introduction and main assumptions

In this chapter we study the large-time behavior of the solutions of integro-differential equations with slowly decaying dispersal kernels. Namely, we consider the Cauchy problem :

$$\begin{cases} u_t = J \star u - u + f(u), \ t > 0, \ x \in \mathbb{R} \\ u(0,x) = u_0(x), \ x \in \mathbb{R} \end{cases} \tag{6.1}$$

where $J(x)$ is the dispersal kernel and

$$(J \star u)(t,x) = \int_{\mathbb{R}} J(x-y)u(t,y)dy.$$

We assume that the nonlinearity f is monostable and that the initial condition u_0 is compactly supported.

The equation (6.1) arises in population dynamics [70, 129] where the unknown quantity u typically stands for a population density. One of the most interesting features of this model, compared to reaction-diffusion equations, is that it can take rare long-distance dispersal events into account. Therefore, equation (6.1) and other closely related equations have been used to explain some rapid propagation phenomena that could hardly be explained with reaction-diffusion models, at least with compactly supported initial conditions. A classical example is Reid's paradox of rapid plant migration [43, 44, 169] which is usually explained using integro-differential equations with slowly decaying kernels or with reaction-diffusion equations with slowly decaying – and therefore noncompact – initial conditions [157]. As we shall see in this chapter, the use of slowly decaying dispersal kernels is the key assumption that leads to qualitative behavior of the solution of (6.1) very different from what is expected with reaction-diffusion equations.

Let us make our assumptions more precise. We assume that the initial condition $u_0 : \mathbb{R} \to [0,1]$ is continuous, compactly supported and not identically equal to 0.

The reaction term $f : [0,1] \to \mathbb{R}$ is of class $\mathcal{C}^1$ and satisfies :

$$f(0) = f(1) = 0, \ \ f(s) > 0 \ \text{ for all } \ s \in (0,1), \ \text{ and } f'(0) > 0. \tag{6.2}$$

A particular class of such reaction term is that of Fisher-KPP type [72, 112]. For this class, the growth rate $f(s)/s$ is maximal at $s = 0$. Furthermore, we assume that there exist $\delta > 0$, $s_0 \in (0,1)$ and $M \geq 0$ such that

$$f(s) \geq f'(0)s - Ms^{1+\delta} \text{ for all } s \in [0, s_0]. \tag{6.3}$$

This last assumption is readily satisfied if f is of class $C^{1,\delta}$.

We assume that the kernel $J : \mathbb{R} \to \mathbb{R}$ is a nonnegative even function of mass one and with finite first moment :

$$J \in \mathcal{C}^0(\mathbb{R}), \ \ J > 0, \ \ J(x) = J(-x), \ \ \int_{\mathbb{R}} J(x)dx = 1 \text{ and } \int_{\mathbb{R}} |x|J(x)dx < \infty. \tag{6.4}$$

Furthermore, we assume that $J(x)$ is decreasing for all $x \geq 0$, J is a $\mathcal{C}^1$ function for large x and

$$J'(x) = o(J(x)) \text{ as } |x| \to +\infty. \tag{6.5}$$

This last condition implies that J decays more slowly than any exponentially decaying functions as $|x| \to \infty$, in the sense that

$$\forall \eta > 0, \ \ \exists \ x_\eta \in \mathbb{R}, \ \ J(x) \geq e^{-\eta x} \ \text{ in } \ [x_\eta, \infty), \tag{6.6}$$

or, equivalently, $J(x)e^{\eta|x|} \to \infty$ as $|x| \to \infty$ for all $\eta > 0$. We shall refer to functions J satisfying the above assumptions (6.4), (6.5) as *exponentially unbounded kernels*.

The assumption (6.5) is in contrast with the large mathematical literature on integro-differential equations [8, 47, 54, 173, 185, 186] as well as integro-difference equations [122, 123], where the dispersal kernels J are generally assumed to be exponentially bounded as $|x| \to \infty$, *i.e.* :

$$\exists\, \eta > 0 \text{ such that } \int_{\mathbb{R}} J(x)e^{\eta|x|} < \infty. \tag{6.7}$$

In this "exponentially bounded case", it follows from the results in [185] that, under our assumptions on u_0 and f, the solution of (6.1) admits a *finite* spreading speed c^*. Thus, for any c_1, c_2 with $0 < c_1 < c^* < c_2 < \infty$ the solution u to (6.1) tends to zero uniformly in the region $|x| \geq c_2 t$, whereas it is bounded away from zero uniformly in the region $|x| \leq c_1 t$ for t large enough. Thus, the spreading properties of the solution of (6.1) when J is exponentially bounded are quite similar to that of the solution of the reaction-diffusion equation $u_t = u_{xx} + f(u)$ with $u(0, \cdot) = u_0$ [9, 10, 72, 112]. The existence of such a finite spreading speed is also true for other integro-differential equations with exponentially bounded dispersal kernels [8, 54, 173, 185].

Let us come back to problem (6.1) with an exponentially unbounded kernel J. In this case, it is known that equation (6.1) does not admit any traveling wave solution with constant speed and constant (or periodic) profile [191]. Moreover, numerical results and formal analytic computations carried out for linear integro-difference equations [113] and linear integro-differential equations [129] indicate that exponentially unbounded dispersal kernels lead to accelerating propagation phenomena and infinite spreading speeds. In this chapter, we prove rigorously such results for the solution u of (6.1) when the kernel J is exponentially unbounded *i.e.* J satisfies (6.4) and (6.5).

Our approach is inspired from [88], where it was shown for a reaction-diffusion equation $u_t = u_{xx} + f(u)$ that exponentially unbounded initial conditions lead to solutions which accelerate and have infinite spreading speed. Here, we get comparable results starting from compactly supported initial data and with exponentially unbounded dispersal kernels. However, the interpretation of our results as well as their proofs are very different from those in [88, 157]. These differences are mostly due to the nonlocal nature of the operator $u \mapsto J \star u - u$, and to its lack of regularization properties.

6.2 Main results

Before stating our main results, we recall that from the maximum principle [185, 191] and from the assumptions on u_0, the solution u of (6.1) satisfies

$$0 < u(t, x) < 1 \text{ for all } t > 0 \text{ and } x \in \mathbb{R}.$$

For any $\lambda \in (0, 1)$ and $t \geq 0$ we denote by

$$E_\lambda(t) = \{x \in \mathbb{R},\ u(t, x) = \lambda\},$$

the level set of u of value λ at time t. For any subset $A \subset (0, J(0))$, we set

$$J^{-1}\{A\} = \{x \in \mathbb{R},\ J(x) \in A\},$$

the inverse image of A by J.

Our first result says that the level sets $E_\lambda(t)$ of all level values $\lambda \in (0, 1)$ (namely, the time-dependent sets of real numbers x such that $u(t, x) = \lambda$) move infinitely fast as $t \to \infty$.

Theorem 6. *Let u be the solution of* (6.1) *with a continuous and compactly supported initial condition $u_0 : \mathbb{R} \to [0,1]$ ($u_0 \not\equiv 0$). Assume that J is an exponentially unbounded kernel satisfying* (6.4) *and* (6.5). *Then,*

$$\forall c \geq 0, \ \min_{|x| \leq ct} u(t,x) \to 1 \text{ as } t \to \infty \tag{6.8}$$

and for any given $\lambda \in (0,1)$, there is a real number $t_\lambda \geq 0$ such that $E_\lambda(t)$ is non-empty for all $t \geq t_\lambda$, and

$$\lim_{t \to +\infty} \frac{\min\{E_\lambda(t) \cap [0,+\infty)\}}{t} = \lim_{t \to +\infty} \frac{-\max\{E_\lambda(t) \cap (-\infty,0]\}}{t} = +\infty. \tag{6.9}$$

Our next result gives a "lower bound" for the level sets $E_\lambda(t)$ in terms of the behavior of J at ∞.

Theorem 7. *Under the same asumptions as in Theorem 6, for any $\lambda \in (0,1)$ and $\varepsilon \in (0, f'(0))$ there exists $T_{\lambda,\varepsilon} \geq t_\lambda$ such that*

$$\forall\, t \geq T_{\lambda,\varepsilon}, \ E_\lambda(t) \subset J^{-1}\left\{\left(0, e^{-(f'(0)-\varepsilon)t}\right]\right\}. \tag{6.10}$$

In our next result, we will either assume :

Hypothesis 1. *An exponentially unbounded kernel J satisfies Hypothesis 1 if and only if there exists $\sigma > 0$ such that $|J'(x)/J(x)|$ is nonincreasing for all $x \geq \sigma$ and there exists $\varepsilon_0 \in (0,1)$ such that*

$$\int_{\mathbb{R}} J(z)^{\varepsilon_0} dz < \infty. \tag{6.11}$$

or

Hypothesis 2. *An exponentially unbounded kernel J satisfies Hypothesis 2 if and only if*

$$\left|\frac{J'(x)}{J(x)}\right| = O\left(\frac{1}{|x|}\right) \text{ as } |x| \to \infty. \tag{6.12}$$

Under these additional assumptions on the kernel J, we are able to establish an "upper bound" for the level sets $E_\lambda(t)$.

Theorem 8. *Let u be the solution of* (6.1) *with a continuous and compactly supported initial condition $u_0 : \mathbb{R} \to [0,1]$ ($u_0 \not\equiv 0$). Assume that J satisfies either Hypothesis 1 or Hypothesis 2. Then, there exists $\rho > f'(0)$ such that for any $\lambda \in (0,1)$ there is $T_\lambda \geq t_\lambda$ such that*

$$\forall t \geq T_\lambda, \ E_\lambda(t) \subset J^{-1}\left\{\left[e^{-\rho t}, J(0)\right]\right\}. \tag{6.13}$$

Theorem 7 together with Theorem 8 provide an estimation of the position of the level sets $E_\lambda(t)$ for large time t. In particular the inclusions (6.10) and (6.13) mean that, for any $\lambda \in (0,1)$ and any element $x_\lambda(t) \in E_\lambda(t)$, we have

$$\min\left(J^{-1}\left(e^{-(f'(0)-\varepsilon)t}\right) \cap [0,+\infty)\right) \leq \ |x_\lambda(t)| \ \leq \max\left(J^{-1}\left(e^{-\rho t}\right) \cap [0,+\infty)\right), \tag{6.14}$$

for large t.

6.3 Case studies

Let us apply the results of section 6.2 to several examples of exponentially unbounded kernels :

- Functions J which are logarithmically sublinear as $|x| \to \infty$, that is

$$J(x) = Ce^{-\alpha|x|/\ln(|x|)} \text{ for large } |x|, \tag{6.15}$$

  with $\alpha > 0$, $C > 0$;
- Functions J which are logarithmically power-like and sublinear as $|x| \to \infty$, that is

$$J(x) = Ce^{-\beta|x|^\alpha} \text{ for large } |x|, \tag{6.16}$$

  with $\alpha \in (0,1)$, β, $C > 0$;
- Functions J which decay algebraically as $|x| \to \infty$, that is

$$J(x) = C|x|^{-\alpha} \text{ for large } |x|, \tag{6.17}$$

  with $\alpha > 2$, $C > 0$. .

First, if J satisfies (6.4) and (6.15) then J satisfies hypothesis 1 (but not hypothesis 2). Theorem 7 and 8 then imply that for any level value $\lambda \in (0,1)$ and any $\varepsilon > 0$, it exists $\rho > f'(0)$ such that every element $x_\lambda(t)$ in the level set $E_\lambda(t)$ satisfies :

$$\frac{f'(0)-\varepsilon}{\alpha}\, t\ln(t) \;\le\; |x_\lambda(t)| \;\le\; \frac{\rho}{\alpha} t\ln(t) \quad \text{for large } t. \tag{6.18}$$

Now, if J satisfies (6.4) and (6.16) then J satisfies hypothesis 1 (but not hypothesis 2) and it follows from Theorems 7 and 8 that the positions of the level sets $E_\lambda(t)$ are asymptotically algebraic and superlinear as $t \to +\infty$, in the sense that for $\varepsilon > 0$, there is $\rho > f'(0)$ such that

$$\left(\frac{f'(0)-\varepsilon}{\beta}\right)^{1/\alpha} t^{1/\alpha} \le |x_\lambda(t)| \le \left(\frac{\rho}{\beta}\right)^{1/\alpha} t^{1/\alpha} \quad \text{for large } t, \tag{6.19}$$

where $x_\lambda(t)$ is any element of the level set $E_\lambda(t)$ (see Fig. 6.1).

Next, if J satisfies (6.4) and decays algebraically for large x as in (6.17), then J satisfies both hypothesis 1 and 2 and it follows from Theorems 7 and 8 that the position of the level sets $E_\lambda(t)$ move exponentially fast as $t \to +\infty$ in the sense that, for any $\lambda \in (0,1)$ and $\varepsilon > 0$, there is $\rho > f'(0)$ such that

$$\frac{f'(0)-\varepsilon}{\alpha}\, t \;\le\; \ln\left(|x_\lambda(t)|\right) \;\le\; \frac{\rho}{\alpha}\, t \quad \text{for large } t, \tag{6.20}$$

for any $x_\lambda(t)$ in the level set $E_\lambda(t)$. The profile of the solution $u(t,x)$ of (6.1) with an algebraically decreasing kernel is illustrated in Fig. 6.2 (a).

We can observe that the result of Theorem 8 does not enable us to obtain a ratio close to 1 between the upper and the lower bound in (6.18)-(6.20). Indeed, as we shall see in the proof of the Theorem 8, the constant ρ in the upper bound verifies $\rho = \max_{s\in[0,1]} f(s)/s + K(J)$ for some positive constant $K(J)$ which only depends on the kernel J. Therefore, if the function f is not of the KPP type, we have $\max_{s\in[0,1]} f(s)/s > f'(0)$ which in turns implies that $\rho > f'(0)$. Moreover, even when f satisfies the KPP assumption, we are not able to take ρ close to $f'(0)$, since the constant $K(J)$ cannot be taken as small as we want independently of J. It seems reasonable to conjecture from Fig. 6.1 that the upper bound in (6.14) is not optimal.

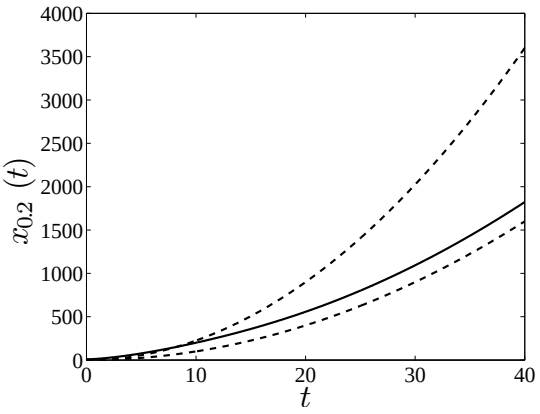

FIGURE 6.1 – Plain line : position $x_{0.2}(t)$ of the level set $E_{0.2}(t)$ of the solution of (6.1) with $f(u) = u(1-u)$, $u_0(x) = \max((1-(x/10)^2), 0)$ and the exponentially unbounded kernel $J(x) = (1/4)e^{-\sqrt{|x|}}$. Observe that $x_{0.2}(t)$ remains bounded by $t \mapsto J^{-1}(e^{-f'(0)t}) = (t - \ln(4))^2$ and $J^{-1}(e^{-(f'(0)+1/2)t}) = (3t/2 - \ln(4))^2$ (dashed lines) for large t.

In another framework, Cabré and Roquejoffre [37] were able to derive upper bound sharper than that of (6.20) for the level sets of the solutions u of equations of the type $u_t = Au + f(u)$, where f is concave and therefore satisfies the KPP assumption, u_0 is compactly supported or monotone one-sided compactly supported, and the operator A is the generator of a Feller semi-group. A typical example is the fractional Laplacian $A = -(-\Delta)^\alpha$ with $0 < \alpha < 1$: if u is smooth and decays slowly to 0 at infinity,

$$(-\Delta)^\alpha u(x) = c_\alpha \int_{\mathbb{R}} \frac{u(x) - u(y)}{|x-y|^{1+2\alpha}} dy, \quad \text{for all } x \in \mathbb{R},$$

where c_α is chosen such that the symbol of $(-\Delta)^\alpha$ is $|\xi|^{2\alpha}$. In this case, the asymptotic exponential spreading of the level sets also follows from the algebraic decay of the kernel $J_\alpha(x) = |x|^{-(1+2\alpha)}$ associated with the operator A. For instance, if $\alpha = 1/2$, $N = 1$, $f(u) = u(1-u)$ and the initial condition $u(0,\cdot) \not\equiv 0$ is compactly supported, then for $\lambda \in (0,1)$, the functions $x_\lambda^-(t) = \inf\{x : u(t,x) = \lambda\}$ and $x_\lambda^+(t) = \sup\{x : u(t,x) = \lambda\}$ satisfy for some constant $C_\lambda > 1$ and for t large enough :

$$-C_\lambda e^{t/2} \le x_\lambda^-(t) \le -\frac{1}{C_\lambda} e^{t/2} \quad \text{and} \quad \frac{1}{C_\lambda} e^{t/2} \le x_\lambda^+(t) \le C_\lambda e^{t/2}.$$

This bounds which are sharper than those in (6.20), could be derived because of the almost explicit nature of the heat kernel $p(t,x)$ associated with A and satisfying $p_t = Ap$. This allowed the authors of [37] to construct accurate supersolutions of $u_t = Au + f(u)$. Note that the kernel J_α is singular at $x = 0$ and does not satisfy the hypotheses of Theorems 7 and 8.

Lastly, let us consider the example of a function J satisfying (6.4),(6.5) and such that $|J'/J|$ is not monotone as $|x| \to \infty$, e.g.

$$J(x) = C|x - \sin(x)|^{-\alpha} \text{ for large } |x| \text{ (with } \alpha > 2).$$

Then J does not satisfies hypothesis 1, but still satisfies hypothesis 2. Thus, we can apply Theorems 7 and 8 which lead to the same estimates as (6.20).

In all above examples the positions of the level sets increase super-linearly with time. This illustrates the accelerating behavior of the solution of (6.1) for exponentially unbounded kernels. Coming

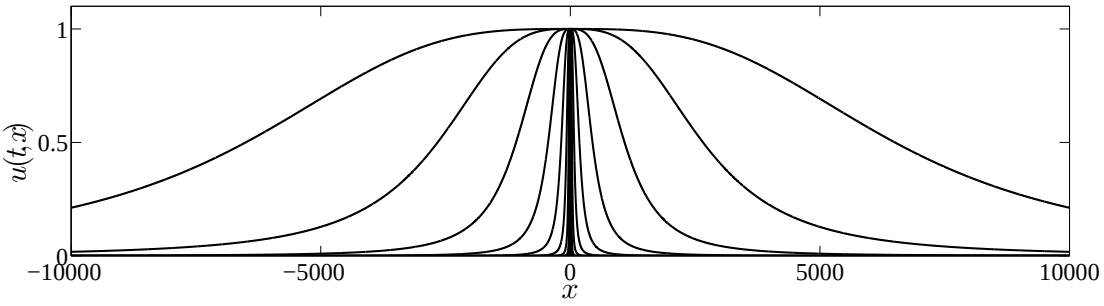

(a) Accelerated propagation

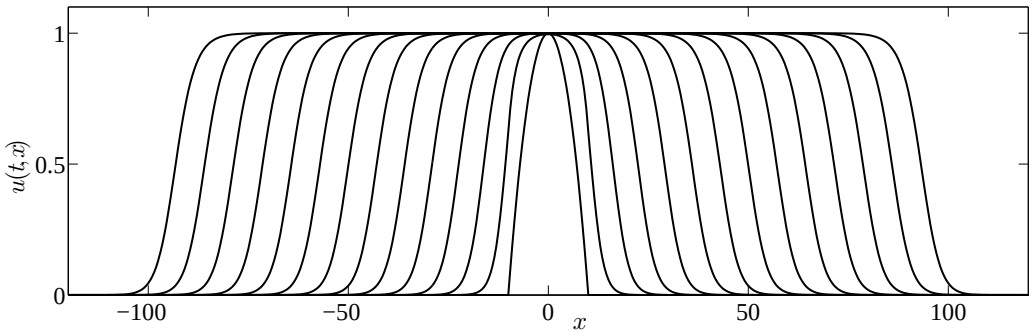

(b) Finite speed of propagation

FIGURE 6.2 – The solution $u(t,x)$ of problem (6.1) at successive times $t = 0, 3, \ldots, 30$, with $f(u) = u(1-u)$ and $u_0(x) = \max((1-(x/10)^2), 0)$: (a) with an exponentially unbounded kernel $J(x) = (1+|x|)^{-3}$; (b) with an exponentially bounded kernel $J(x) = (1/2)e^{-|x|}$.

back to Fig. 6.2 (a), we indeed observe that the distance between level sets of the same level tends to increase with time when time growths as $t_n = an$ with $a > 0$ and when J is exponentially unbounded, whereas it remains constant in the exponentially bounded case (Fig. 6.2 (b)). Moreover, in Fig. 6.2 (a), the solution tends to flatten as $t \to \infty$ *i.e.* the lower the level λ, the faster the level sets $E_\lambda(t)$ propagate. In particular, this implies that the solution does not converge to a traveling wave solution. This is coherent with the fact that (6.1) does not admit traveling wave solutions when the kernel J is exponentially unbounded [191].

6.4 Proofs of the Theorems

4.1 Proof of Theorem 6

We begin with proving that for any $t \geq 0$, $\liminf_{x\to\pm\infty} u(t,x) = 0$. Let us define $\overline{v}(t,x) = v(t,x)e^{rt}$ for all $(t,x) \in [0,\infty) \times \mathbb{R}$, where $r = \sup_{s\in(0,1]} (f(s)/s) \geq f'(0) > 0$ and v satisfies the following problem :

$$\begin{cases} v_t = J \star v - v, \ t > 0, \ x \in \mathbb{R}, \\ v(0,x) = u_0(x), \ x \in \mathbb{R}. \end{cases} \tag{6.21}$$

Then $\overline{v}$ verifies $\overline{v}_t = J\star\overline{v} - \overline{v} + r\overline{v}$ on $(0,\infty)\times\mathbb{R}$ and $\overline{v}(0,x) = u_0(x)$. From the maximum principle [185, 191], we get $0 < u(t,x) \leq \overline{v}(t,x)$ for all $(t,x) \in (0,\infty)\times\mathbb{R}$.

Moreover, since u_0 is compactly supported and the operator $u \mapsto J \star u - u$ is Lipschitz-continuous on $L^\infty(\mathbb{R}) \cap L^1(\mathbb{R})$, the Cauchy-Lipschitz theorem implies that the solution $t \mapsto v(t,\cdot)$ of problem (6.21) belongs to $\mathcal{C}^1([0,\infty), L^\infty(\mathbb{R}) \cap L^1(\mathbb{R}))$. Integrating (6.21) over $\mathbb{R}$ and using (6.4), we get $\|v(t)\|_{L^1(\mathbb{R})} = \|u_0\|_{L^1(\mathbb{R})}$. This implies that $u(t)$ belongs to $L^1(\mathbb{R})$ for all $t > 0$. Since $u(t,x) > 0$ for any $t > 0$ and $x \in \mathbb{R}$, we have :

$$\liminf_{x \to -\infty} u(t,x) = 0 \text{ and } \liminf_{x \to +\infty} u(t,x) = 0 \text{ for each } t \geq 0. \tag{6.22}$$

Let us now prove that $u(t,0) \to 1$ as $t \to \infty$. Let $\tilde{f}$ satisfy (6.2), (6.3) and such that $\tilde{f} \leq f$ in $[0,1]$, $\tilde{f}(s) \leq \tilde{f}'(0)s$ for all $s \in [0,1]$ and $\tilde{f}$ is a nonincreasing function in a neighborhood of 1. We denote by $\tilde{u}$ the solution of the Cauchy problem (6.1) with the nonlinearity $\tilde{f}$. From the maximum principle $u \geq \tilde{u}$ on $[0,\infty) \times \mathbb{R}$.

Then, let us set $g_\varepsilon(s) = \tilde{f}(s) - \varepsilon s$ in $[0,1]$, where $\varepsilon \in (0,1)$ is small enough such that $g'_\varepsilon(0) > 0$. Set

$$\lambda_\varepsilon = \sup\{s > 0 \mid g_\varepsilon > 0 \text{ in } (0,s]\} < 1.$$

One can choose $\varepsilon > 0$ small enough so that $g_\varepsilon < 0$ on $(\lambda_\varepsilon, 1]$. From (6.4) we know that there exists $A_\varepsilon > 0$ such that

$$D_\varepsilon = \int_{-A_\varepsilon}^{A_\varepsilon} J(y)dy = 1 - \varepsilon.$$

Let $\underline{v}$ be the solution of the following Cauchy problem :

$$\begin{cases} \partial_t \underline{v} = D_\varepsilon (J_\varepsilon \star \underline{v} - \underline{v}) + g_\varepsilon(\underline{v}), \ t > 0, \ x \in \mathbb{R}, \\ \underline{v}(0,x) = u_0(x), \ x \in \mathbb{R}, \end{cases} \tag{6.23}$$

where J_ε is a compactly supported kernel defined by :

$$J_\varepsilon(x) = \frac{J(x)}{\displaystyle\int_{-A_\varepsilon}^{A_\varepsilon} J(y)dy} \mathbb{1}_{[-A_\varepsilon, A_\varepsilon]}(x).$$

We have

$$\partial_t \underline{v} = (J \times \mathbb{1}_{[-A_\varepsilon, A_\varepsilon]}) \star \underline{v} - \underline{v} + \tilde{f}(\underline{v}) \leq J \star \underline{v} - \underline{v} + \tilde{f}(\underline{v}).$$

The maximum principle implies that $0 \leq \underline{v}(t,x) \leq \tilde{u}(t,x) \leq u(t,x)$ (≤ 1) for all $t \geq 0$ and $x \in \mathbb{R}$. From Theorem 3.2 in [124], we know that $\underline{v}$ propagates with a finite speed $c^*_\varepsilon > 0$ *i.e.* for all $c \in (0, c^*_\varepsilon)$,

$$\sup_{|x| \leq ct} |\underline{v}(t,x) - \lambda_\varepsilon| \to 0 \text{ as } t \to +\infty. \tag{6.24}$$

In particular, we have :

$$\lim_{t \to \infty} \underline{v}(t,0) = \lambda_\varepsilon \leq \lim_{t \to \infty} u(t,0) \leq 1.$$

Since $\lambda_\varepsilon \to 1$ as $\varepsilon \to 0$, we get

$$u(t,0) \to 1 \text{ as } t \to \infty.$$

It then follows that for any $\lambda \in (0,1)$ there exists a time $t_\lambda \geq 0$ such that

$$u(t,0) > \lambda \text{ for all } t \geq t_\lambda. \tag{6.25}$$

Since the functions $x \mapsto u(t,x)$ are continuous for all $t > 0$, one concludes from (6.22) and (6.25) that $E_\lambda(t)$ is a non-empty set for all $t \geq t_\lambda$.

Let us now prove (6.9). From [124], we know that the propagation speed c^*_ε is the minimal speed of traveling wave solutions of problem (6.23). This speed verifies [38, 166] :

$$c^*_\varepsilon = \min_{\eta>0} \left\{ \frac{1}{\eta} \left(D_\varepsilon \int_{\mathbb{R}} J_\varepsilon(z) e^{\eta z} dz - 1 + \tilde{f}'(0) \right) \right\}. \tag{6.26}$$

Let $A > 0$, $\lambda \in (0,1)$, $t \geq t_\lambda$ and $x_\lambda(t) \in E_\lambda(t)$. Since J is exponentially unbounded in the sense of (6.6), $c^*_\varepsilon \to \infty$ as $\varepsilon \to 0$. Let us choose $\varepsilon > 0$ small enough such that $\lambda_\varepsilon > \lambda$ and $c^*_\varepsilon > A$. Then, it follows from (6.24) that $|x_\lambda(t)| \geq At$ for t large enough. Since this is true for any $A > 0$ and any $x_\lambda(t) \in E_\lambda(t)$ we get (6.8) and (6.9). □

4.2 Proof of Theorem 7

This section is devoted to the proof of a lower bound for $\min\{E_\lambda(t) \cap (0,+\infty)\}$ (resp. $-\max\{E_\lambda(t) \cap (-\infty,0)\}$). The proof is divided into three parts. We begin with showing that the solution of (6.1) at time $t = 1$ is larger than some multiple of J. Then, we construct an appropriate subsolution of (6.1) which enables us to prove the lower bound for small values of λ. Lastly, we show that the lower bound remains true for any value of $\lambda \in (0,1)$.

More precisely, let us fix $\lambda \in (0,1)$ and $\varepsilon \in (0, f'(0))$. We claim that

$$E_\lambda(t) \subset J^{-1} \left\{ \left(0, e^{-(f'(0)-\varepsilon)t} \right] \right\} \tag{6.27}$$

for t large enough.

Step 1 : $u(1,\cdot)$ *is bounded from below by a multiple of* $J(\cdot)$

Let us define

$$v(t,x) = (u_0(x) + t(J \star u_0)(x)) e^{-t}.$$

Then it is easy to see that v is a subsolution of the following linear Cauchy problem :

$$\begin{cases} \underline{u}_t = J \star \underline{u} - \underline{u}, \ t > 0, \ x \in \mathbb{R}, \\ \underline{u}(0,x) = u_0(x), \ x \in \mathbb{R}. \end{cases} \tag{6.28}$$

Indeed, $v(0,x) = u_0(x)$ and for all $(t,x) \in [0,\infty) \times \mathbb{R}$:

$$v_t - J \star v + v = -te^{-t} \left(J \star (J \star u_0) \right)(x) \leq 0.$$

Since $\underline{u}$ is also a subsolution of the equation (6.1) verified by u, we get :

$$u(t,x) \geq v(t,x) \text{ for all } (t,x) \in [0,\infty) \times \mathbb{R}.$$

Moreover, $v(1,x) = (u_0(x) + (J \star u_0)(x)) e^{-1}$ for all $x \in \mathbb{R}$ which implies that is exists $C \in (0,1)$ such that $v(1,x) \geq CJ(x)$ for all $x \in \mathbb{R}$. Finally,

$$u(1,x) \geq v(1,x) \geq CJ(x) \text{ for all } x \in \mathbb{R}. \tag{6.29}$$

Step 2 : Proof of (6.27) *for small values of* λ

We recall that there exist $\delta > 0$, $s_0 \in (0,1)$ and $M \geq 0$ such that $f(s) \geq f'(0)s - Ms^{1+\delta}$ for all $s \in [0, s_0]$.

Define $\rho_1 > 0$ by

$$\rho_1 = f'(0) - \varepsilon/2. \tag{6.30}$$

Since J satisfies (6.4) and (6.5), we can choose $\xi_1 > 0$ such that for all $|x| \geq \xi_1$,

$$|J'(x)| \leq (\varepsilon'/2) \times J(x), \tag{6.31}$$

where $\varepsilon' > 0$ satisfies

$$\varepsilon' \int_0^\infty J(z) z dz \leq \varepsilon/2.$$

Let us set :

$$\kappa = \inf_{(-\xi_1, \xi_1)} CJ = CJ(\xi_1) > 0, \ s_1 = \min(s_0, \kappa), \tag{6.32}$$

and

$$B = \max\left(s_1^{-\delta}, \frac{M}{\rho_1 \delta}, \frac{M\left(\frac{\delta}{1+\delta}\right)^\delta}{(1+\delta)(f'(0) - \varepsilon/2)} \right) > 0. \tag{6.33}$$

Let g be the function defined in $[0, \infty)$ by

$$g(s) = s - Bs^{1+\delta}.$$

We observe that

$$g(s) \leq 0 \text{ for all } s \geq s_1 \text{ and } g(s) \leq s_1 \text{ for all } s \geq 0.$$

Moreover, let $0 < s_2 < s_1$ be such that $g'(s_2) = 0$ and

$$\lambda_2 = g(s_2) = \max_{s \in [0, s_0]} g(s) = \frac{\delta}{1+\delta} \left((1+\delta)B\right)^{-1/\delta}. \tag{6.34}$$

Let $\xi_0(t) > 0$ be such that :

$$C\, J(\xi_0(t)) e^{\rho_1 t} = s_2 \text{ for all } t \geq 0. \tag{6.35}$$

We can notice that for all $t \geq 0$, $\xi_0(t) \geq \xi_1$ and that $\xi_0(t)$ is continuous and increasing in $t \geq 0$, since J is continuous and decreasing in $[0, \infty)$.

Then, let us define $\underline{u}$ as follows :

$$\underline{u}(t,x) = \begin{cases} g(CJ(x)e^{\rho_1 t}) & \text{for all } |x| > \xi_0(t) \\ \lambda_2 = g(s_2) = g(CJ(\xi_0(t))e^{\rho_1 t}) & \text{for all } |x| \leq \xi_0(t) \end{cases} \quad \text{for all } t \geq 0. \tag{6.36}$$

Observe that $0 < CJ(x)e^{\rho_1 t} \leq CJ(\xi_0(t))e^{\rho_1 t} = s_2 < s_1$ when $|x| \geq \xi_0(t)$, whence $\underline{u}(t,x) > 0$ for all $t \geq 0$ and $x \in \mathbb{R}$. Let us check that $\underline{u}$ is a sub-solution of (6.1). Since $J(x)$ is nonincreasing with respect to $|x|$ and u satisfies (6.29), we have

$$\begin{array}{l} \underline{u}(0,x) = CJ(x) - B(CJ(x))^{1+\delta} \leq CJ(x) \leq u(1,x) \text{ for all } |x| > \xi_0(0) \\ \underline{u}(0,x) = \lambda_2 = g(CJ(\xi_0(0))) \leq CJ(x) \leq u(1,x) \text{ for all } |x| \leq \xi_0(0). \end{array} \tag{6.37}$$

Then, let us check that $\underline{u}$ is a subsolution of the equation satisfied by u in the region where $\underline{u} < \lambda_2$. Let (t,x) be any point in $[0,\infty) \times \mathbb{R}$ such that $\underline{u}(t,x) < \lambda_2$.As already emphasized, one has $0 < CJ(x)e^{\rho_1 t} < s_1$, whence $CJ(x) < s_1$ and $|x| \geq \xi_1$ from (6.32). Furthermore,

$$0 < \underline{u}(t,x) < CJ(x)e^{\rho_1 t} < s_1 \leq s_0 < 1. \tag{6.38}$$

Thus, since f satisfies (6.3), we get

$$f(\underline{u}(t,x)) \geq f'(0)\left(CJ(x)e^{\rho_1 t} - B(CJ(x))^{1+\delta} e^{\rho_1(1+\delta)t}\right) - M(CJ(x))^{1+\delta} e^{\rho_1(1+\delta)t}. \tag{6.39}$$

Let us now show that $J \star \underline{u} - \underline{u} \geq -(\varepsilon/2)\underline{u}$, for all $t \in [0,\infty)$ and $|x| > \xi_0(t)$. Let $t \in [0,\infty)$ and

$$x > \xi_0(t) > 0.$$

Remember that J is decreasing on $[0,+\infty)$ and that g is decreasing in $[0,s_2]$ (which implies that $\underline{u}(t,y)$ is nonincreasing with respect to $|y|$). Then

$$\begin{aligned}
(J \star \underline{u})(t,x) - \underline{u}(t,x) &= \int_{\mathbb{R}} J(x-y)(\underline{u}(t,y) - \underline{u}(t,x))dy \\
&\geq \int_{|y|>x} J(x-y)(\underline{u}(t,y) - \underline{u}(t,x))dy \\
&\geq \int_{-\infty}^{-x} J(x-y)(\underline{u}(t,y) - \underline{u}(t,x))dy + \int_{x}^{\infty} J(x-y)(\underline{u}(t,y) - \underline{u}(t,x))dy \\
&\geq \int_{x}^{\infty} (J(x-y) + J(x+y))(\underline{u}(t,y) - \underline{u}(t,x))dy.
\end{aligned} \tag{6.40}$$

Observe that for all $y > x$,

$$0 \geq \underline{u}(t,y) - \underline{u}(t,x) = \int_x^y \partial_x \underline{u}(t,s)ds.$$

Furthermore, for all $t > 0$ and $s > \xi_0(t)$

$$\partial_x \underline{u}(t,s) = CJ'(s)e^{\rho_1 t} g'\left(CJ(s)e^{\rho_1 t}\right) = CJ'(s)e^{\rho_1 t}\left(1 - (1+\delta)B(CJ(s))^{\delta} e^{\rho_1 \delta t}\right).$$

Since $s > \xi_0(t) \geq \xi_1$:

$$\begin{aligned}
|\partial_x \underline{u}(t,s)| &\leq (\varepsilon'/2)CJ(s)e^{\rho_1 t} g'\left(CJ(s)e^{\rho_1 t}\right) \\
&\leq (\varepsilon'/2)CJ(s)e^{\rho_1 t}\left(1 - B(CJ(s))^{\delta} e^{\rho_1 \delta t}\right) = (\varepsilon'/2)\underline{u}(t,s) \\
&\leq (\varepsilon'/2)\underline{u}(t,x).
\end{aligned}$$

Finally, for all $y \geq x > \xi_0(t)$

$$\underline{u}(t,y) - \underline{u}(t,x) \geq -(\varepsilon'/2)(y-x)\underline{u}(t,x). \tag{6.41}$$

Then, from equation (6.40) and (6.41), we get

$$\begin{aligned}
(J \star \underline{u})(t,x) - \underline{u}(t,x) &\geq \int_x^{\infty} (J(x-y) + J(x+y))(\underline{u}(t,y) - \underline{u}(t,x))dy \\
&\geq -(\varepsilon'/2)\left(\int_x^{\infty} J(y-x)(y-x)dy + \int_x^{\infty} J(x+y)(y-x)dy\right)\underline{u}(t,x) \\
&\geq -(\varepsilon'/2)\left(\int_0^{\infty} J(z)zdz + \int_0^{\infty} J(2x+z)zdz\right)\underline{u}(t,x) \\
&\geq -\varepsilon'\left(\int_0^{\infty} J(z)zdz\right)\ \underline{u}(t,x) \\
&\geq -(\varepsilon/2)\,\underline{u}(t,x).
\end{aligned} \tag{6.42}$$

The same property holds for $x < -\xi_0(t)$ by symmetry of J and $\underline{u}$ with respect to x. It follows from (6.30), (6.33), (6.39) and (6.42) that, for all $t \geq 0$ and $|x| \geq \xi_0(t)$

$$\begin{aligned}
&\underline{u}_t(t,x) - (J \star \underline{u}(t,x) - \underline{u}(t,x)) - f(\underline{u}(t,x)) \\
&\leq \rho_1 CJ(x)e^{\rho_1 t} - \rho_1(1+\delta)B(CJ(x))^{1+\delta}e^{\rho_1(1+\delta)t} + \varepsilon/2\,\underline{u}(t,x) \\
&\quad -f'(0)\left(CJ(x)e^{\rho_1 t} - B(CJ(x))^{1+\delta}e^{\rho_1(1+\delta)t}\right) + M(CJ(x))^{1+\delta}e^{\rho_1(1+\delta)t} \\
&\leq (\rho_1 - f'(0) + \varepsilon/2)\,CJ(x)e^{\rho_1 t} + (M - B[\rho_1(1+\delta) - f'(0) + \varepsilon/2])\,(CJ(x))^{1+\delta}e^{\rho_1(1+\delta)t} \\
&\leq (M - B\,\delta\,\rho_1)(CJ(x))^{1+\delta}e^{\rho_1(1+\delta)t} \\
&\leq 0.
\end{aligned} \tag{6.43}$$

Let us now check that $\underline{u}$ is a subsolution of the equation satisfied by u, in the region where $\underline{u} = \lambda_2$. Let (t,x) be any point in $[0,\infty)\times\mathbb{R}$ such that $\underline{u}(t,x) = \lambda_2$. The same arguments as above imply that for any point (t,x) satisfying $\underline{u}(t,x) = \lambda_2$, *i.e.* for all $(t,x) \in [0,\infty)\times[-\xi_0(t),\xi_0(t)]$, we get

$$\begin{aligned}
(J\star\underline{u})(t,x) - \underline{u}(t,x) &= \int_{\mathbb{R}} J(x-y)(\underline{u}(t,y)-\lambda_2)dy \\
&= \int_{|y|\geq\xi_0(t)} J(x-y)(\underline{u}(t,y)-\lambda_2)dy \\
&= \int_{\xi_0(t)}^{\infty} (J(x-y)+J(x+y))(\underline{u}(t,y)-\underline{u}(t,\xi_0(t)))dy \\
&\geq -(\varepsilon'/2)\left(\int_{\xi_0(t)}^{\infty} J(y-x)(y-\xi_0(t))dy + \int_{\xi_0(t)}^{\infty} J(x+y)(y-\xi_0(t))dy\right)\lambda_2 \\
&\geq -(\varepsilon'/2)\left(\int_0^{\infty} J(z+\xi_0(t)-x)zdz + \int_0^{\infty} J(z+x+\xi_0(t))zdz\right)\lambda_2 \\
&\geq -\varepsilon'\left(\int_0^{\infty} J(z)zdz\right)\lambda_2 \\
&\geq -(\varepsilon/2)\,\lambda_2.
\end{aligned} \tag{6.44}$$

For all $x \in [0,\xi_0(t))$ it follows from (6.36) that $\underline{u}_t(t,x) = 0$. Let us show that this is also true when $x = \xi_0(t)$. As already noticed, $\xi_0(t)$ is an increasing function of t. Thus, for all $h > 0$ $\xi_0(t) < \xi_0(t+h)$, which implies that $\underline{u}(t+h,\xi_0(t)) = \lambda_2 = \underline{u}(t,\xi_0(t))$. As a consequence,

$$\lim_{h\to 0, h>0} \frac{\underline{u}(t+h,\xi_0(t)) - \underline{u}(t,\xi_0(t))}{h} = 0.$$

Moreover,

$$\lim_{h\to 0, h>0} \frac{\underline{u}(t,\xi_0(t)) - \underline{u}(t-h,\xi_0(t))}{h} = \lim_{h\to 0, h>0} \frac{\lambda_2 - g(CJ(\xi_0(t))e^{\rho_1(t-h)})}{h}.$$

For all $h > 0$ small enough and using the definition (6.35) of $\xi_0(t)$, we obtain :

$$g(CJ(\xi_0(t))e^{\rho_1(t-h)}) = \lambda_2 - \rho_1 CJ(\xi_0(t))g'(s_2)h + o(h) = \lambda_2 + o(h).$$

This implies that

$$\underline{u}_t(t,\xi_0(t)) = \lim_{h\to 0} \frac{\underline{u}(t,\xi_0(t)) - \underline{u}(t-h,\xi_0(t))}{h} = 0. \tag{6.45}$$

Since $\underline{u}_t(t,x) = 0$ for all $x \in [0,\xi_0(t))$, the above equality and the symmetry of the problem imply that :

$$\underline{u}_t(t,x) = 0 \text{ for all } |x| \leq \xi_0(t). \tag{6.46}$$

It follows from (6.33), (6.44) and (6.46) that for all $t \geq 0$ and $|x| \leq \xi_0(t)$,

$$\begin{aligned}
&\underline{u}_t(t,x) - (J\star\underline{u}(t,x) - \underline{u}(t,x)) - f(\underline{u}(t,x)) \\
&\leq (\varepsilon/2)\,\lambda_2 - \left(f'(0)\lambda_2 - M\lambda_2^{1+\delta}\right) \\
&\leq -\lambda_2(f'(0)-\varepsilon/2)\left(1 - \frac{M}{(1+\delta)B(f'(0)-\varepsilon/2)}\left(\frac{\delta}{1+\delta}\right)^{\delta}\right) \\
&\leq 0.
\end{aligned} \tag{6.47}$$

Using the above inequality together with (6.37) and (6.43), the maximum principle implies that

$$\underline{u}(t-1,x) \leq u(t,x) \text{ for all } t \geq 1 \text{ and } x \in \mathbb{R}. \tag{6.48}$$

Fix now any real number ω small enough so that :

$$0 < \omega < s_2$$

This real number ω does not depends on λ but depends on ε, as well as on J and f. Remember that $t_\omega \geq 0$ is such that $E_\omega(t)$ is a non-empty set for all $t \geq t_\omega$. Since J is continuous and decreasing on $[0, +\infty)$, there exists then a time $\overline{t}_\omega \geq \max(t_\omega, 1)$ such that for all $t \geq \overline{t}_\omega$, there exists $y_\omega(t) \in (\xi_1, \infty)$ such that

$$CJ(y_\omega(t))e^{\rho_1(t-1)} = \omega.$$

Furthermore, the function $y_\omega(t) : [\overline{t}_\omega, \infty) \to [\xi_1, \infty)$ is increasing and continuous.

Lastly, let Ω be the open set defined by

$$\Omega = \{(t, x) \in (\overline{t}_\omega, +\infty) \times \mathbb{R},\ |x| < y_\omega(t)\}.$$

We claim that

$$\underline{u}(t-1, x) > g(\omega) > 0 \ \text{ for all } (t, x) \in \Omega.$$

Indeed, if $(t, x) \in \Omega$ is such that $CJ(x)e^{\rho_1(t-1)} \geq s_2$, then $|x| \leq \xi_0(t-1)$ and

$$\underline{u}(t-1, x) = \lambda_2 = g(s_2) > g(\omega) > 0.$$

Otherwise, (t, x) is such that $\omega < CJ(x)e^{\rho_1(t-1)} < s_2$, whence $|x| > \xi_0(t-1)$ and

$$\underline{u}(t-1, x) = g(CJ(x)e^{\rho_1(t_1)}) \geq g(\omega) > 0.$$

Finally equation (6.48) implies that

$$u(t, x) \geq g(\omega) > 0 \text{ for all } (t, x) \in \Omega. \tag{6.49}$$

Thus, setting $\theta = g(\omega)$, we get that if $\lambda \in (0, \theta)$ and if $x \in E_\lambda(t)$ for $t \geq \max(t_\lambda, \overline{t}_\omega)$, then

$$|x| \geq y_\omega(t) \geq \xi_1 \geq \xi_0(0)$$

Since $\rho_1 = f'(0) - \varepsilon/2 > f'(0) - \varepsilon$, there exists then a time $T_{\lambda,\varepsilon} \geq \max(t_\lambda, \overline{t}_\omega)$ such that,

$$\forall t > T_{\lambda,\varepsilon},\ \forall x \in E_\lambda(t),\ J(x) \leq J(y_\omega(t)) = \frac{\omega e^{\rho_1}}{C} e^{-\rho_1 t} \leq e^{-(f'(0)-\varepsilon)t}. \tag{6.50}$$

This proves (6.27) for $\lambda \in (0, \theta)$.

Step 3 : Proof of (6.27) *for any* $\lambda \in (0, 1)$

Assume that $\lambda \in (0, 1)$. Let $\underline{u}_{\theta,0}$ be the function defined by

$$\underline{u}_{\theta,0}(x) = \begin{cases} \theta(1 - |x|) & \text{if } |x| \leq 1, \\ 0 & \text{if } |x| > 1, \end{cases}$$

where $\theta = g(\omega)$ is given in Step 2. Let us set $\tilde{f}(s) = f(s) - (1 - D_\lambda)s$ for all $s \in [0, 1]$ with

$$D_\lambda = \int_{-\xi_1}^{\xi_1} J(y)dy \in (0, 1),$$

where ξ_1 is chosen large enough such that $\tilde{f}'(0) > 0$ and $\tilde{f}(s) > 0$ in $(0, \lambda]$.

We consider the solution $\underline{u}_\theta$ of the Cauchy problem :

$$\begin{cases} \partial_t \underline{u}_\theta = D_\lambda \left(J_\lambda \star \underline{u}_\theta - \underline{u}_\theta \right) + \tilde{f}(\underline{u}_\theta), \ t > 0, \ x \in \mathbb{R}, \\ \underline{u}_\theta(0,x) = \underline{u}_{\theta,0}(x), \ x \in \mathbb{R}, \end{cases} \tag{6.51}$$

where J_λ is a compactly supported kernel defined by :

$$J_\lambda(x) = \frac{J(x)}{\displaystyle\int_{-\xi_1}^{\xi_1} J(y)dy} \mathbb{1}_{[-\xi_1,\xi_1]}(x), \ x \in \mathbb{R}.$$

It follows from (6.49) and the definition of y_ω that for any time $T \geq \overline{t}_\omega$ and any small shift X in the sense that $|X| \leq y_\omega(T) - 1$, the solution u satisfies

$$u(T,x) \geq \underline{u}_{\theta,0}(x - X), \quad \text{for all } x \in \mathbb{R}.$$

Moreover, we have for all $(t,x) \in (0,\infty) \times \mathbb{R}$:

$$\begin{aligned} &\partial_t \underline{u}_\theta(t,x) - (J \star \underline{u}_\theta(t,x) - \underline{u}_\theta(t,x)) - f(\underline{u}_\theta(t,x)) \\ &\leq \ \partial_t \underline{u}_\theta(t,x) - D_\lambda J_\lambda \star \underline{u}_\theta(t,x) + \underline{u}_\theta(t,x) - f(\underline{u}_\theta(t,x)) \\ &\leq \ \partial_t \underline{u}_\theta(t,x) - D_\lambda \left(J_\lambda \star \underline{u}_\theta(t,x) - \underline{u}_\theta(t,x) \right) - \tilde{f}(\underline{u}_\theta(t,x)) \\ &\leq \ 0. \end{aligned}$$

The maximum principle implies that for any time $T \geq \overline{t}_\omega$ and any small shift X in the sense that $|X| \leq y_\omega(T) - 1$,

$$u(T+t,x) \geq \underline{u}_\theta(t, x - X), \quad \text{for all } t \geq 0, \text{ and } x \in \mathbb{R}. \tag{6.52}$$

Moreover, we know from Theorem 3.2 in [124] that there exists $c_\lambda^* > 0$ such that

$$\liminf_{t\to\infty} \inf_{|x|<c_\lambda^* t} \underline{u}_\theta(t,x) = \sup \{ s > 0 \mid \tilde{f} > 0 \text{ in } (0,s) \} > \lambda.$$

In particular, there exists $T_\lambda \geq 0$ such that $\underline{u}_\theta(T_\lambda, x) > \lambda$ for all $|x| < c_\lambda^* T_\lambda$. Therefore, taking in particular $x = X$ in equation (6.52), we get that for any $T \geq \overline{t}_\omega$ and $|X| \leq y_\omega(T) - 1$,

$$u(T + T_\lambda, X) \geq \underline{u}_\theta(T + T_\lambda, 0) > \lambda.$$

As a consequence, there exists $\underline{T}_{\lambda,\varepsilon} \geq \max\left(\overline{t}_\omega + T_\lambda, t_\lambda\right)$ such that for all $t \geq \underline{T}_{\lambda,\varepsilon}$ and for all $x \in E_\lambda(t)$, one has $|x| > y_\omega(t - T_\lambda) - 1$ and

$$J(x) \leq J\left(y_\omega\left(t - T_\lambda\right) - 1\right) = \frac{\omega e^{\rho_1}}{C} e^{-\rho_1 (t - T_\lambda)} \times \frac{J\left(y_\omega\left(t - T_\lambda\right) - 1\right)}{J\left(y_\omega\left(t - T_\lambda\right)\right)} \leq e^{-(f'(0)-\varepsilon)t}, \tag{6.53}$$

since $y_\omega(t - T_\lambda) \to \infty$ as $t \to \infty$ and $\dfrac{J(s-1)}{J(s)} \to 1$ as $s \to \infty$, from (6.5). This implies (6.27) and completes the proof of Theorem 7. □

4.3 Proof of Theorem 8

In this section, we prove an upper bound for $\max\{E_\lambda(t) \cap (0,+\infty)\}$ (resp. $-\min\{E_\lambda(t) \cap (-\infty,0)\}$). The proof of this upper bound is based on the construction of suitable supersolutions of (6.1). The construction of such supersolutions strongly relies on Hypotheses 1 and 2.

We shall prove that there exists $\rho > 0$ such that, for any $\lambda \in (0,1)$,

$$E_\lambda(t) \subset J^{-1}\left\{[e^{-\rho t}, J(0)]\right\} \text{ for large } t. \tag{6.54}$$

Since $f \in \mathcal{C}^1([0,1])$, the "per capita growth rate" $f(s)/s$ is bounded from above by $r = \sup_{s\in(0,1]} (f(s)/s) > 0$.

Proof of (6.54) *under Hypothesis 1*

Assume that J satisfies hypothesis 1. Then J'/J is negative and nondecreasing on $[\sigma, +\infty)$. Therefore $\ln(J)$ is a nonincreasing convex function on $[\sigma, +\infty)$. It is then possible to define a function $\varphi : [0,\infty) \to [0,\infty)$ and $\tau \in [0,\sigma]$ such that φ is nondecreasing and concave and

$$\varphi(0) = 0,\ \varphi(+\infty) = +\infty, \text{ and } \varphi(x) = (\varepsilon_0 - 1)\ln(J(x+\tau)) \text{ on } [\sigma - \tau, +\infty). \tag{6.55}$$

By concavity, we have the following property, for all $y \geq x \geq 0$:

$$\varphi(y) - \varphi(x) \leq \varphi(y - x). \tag{6.56}$$

Thus, we claim that :

$$\forall\, x \geq 0, \forall\, y \in \mathbb{R},\ \varphi(x) - \varphi(|x-y|) \leq \varphi(|y|). \tag{6.57}$$

Even if it means increasing σ, one can assume without loss of generality, that $J < 1$ on $[\sigma, \infty)$. Indeed, if $y \leq 0$ then $\varphi(x) - \varphi(|x-y|) \leq 0 \leq \varphi(|y|)$. If $y > 0$, since φ is nondecreasing and from (6.56), we have $\varphi(|y-x|) \geq \varphi(\max(x,y)) - \varphi(\min(x,y)) \geq \varphi(x) - \varphi(y)$. Notice that (6.57) implies immediately that

$$\forall x \in \mathbb{R},\ \forall y \in \mathbb{R},\ \varphi(|x|) - \varphi(|x-y|) \leq \varphi(|y|). \tag{6.58}$$

Let us define

$$\phi(x) = e^{-\varphi(|x|)} \text{ for all } x \in \mathbb{R}.$$

Using (6.58), we get :

$$\begin{aligned} \frac{(J \star \phi)(x)}{\phi(x)} &= \int_{\mathbb{R}} \frac{\phi(x-y)}{\phi(x)} J(y)dy \\ &= \int_{\mathbb{R}} J(y) e^{\varphi(|x|) - \varphi(|x-y|)} dy \\ &\leq \int_{\mathbb{R}} J(y) e^{\varphi(|y|)} dy = \int_{\mathbb{R}} J(y)/\phi(y) dy. \end{aligned} \tag{6.59}$$

Moreover,

$$\begin{aligned} \int_{\mathbb{R}} J(y)/\phi(y)dy = \int_{\mathbb{R}} J(y)e^{\varphi(|y|)}dy &= \int_{|y|<\sigma} J(y)e^{\varphi(|y|)}dy + \int_{|y|\geq\sigma} J(y)e^{\varphi(|y|)}dy \\ &= \int_{|y|<\sigma} J(y)e^{\varphi(|y|)}dy + \int_{|y|\geq\sigma} \left(\frac{J(y+\tau)}{J(y)}\right)^{\varepsilon_0 - 1} J(y)^{\varepsilon_0} dy < \infty, \end{aligned} \tag{6.60}$$

from hypothesis 1 and since $\dfrac{J(y+\tau)}{J(y)} \to 1$ as $y \to \pm\infty$ from (6.5).

Since u_0 is compactly supported, there exists $\sigma_1 > 0$ such that $\phi(x) \geq u_0(x)$, for all $|x| \geq \sigma_1$. Finally, set

$$\rho_0 = \max\left\{\int_{\mathbb{R}} J(y)e^{\varphi(|y|)}dy, 1\right\} - 1 + r,$$

and define $\overline{u}$ as follows :

$$\forall (t,x) \in [0,+\infty) \times \mathbb{R},\ \overline{u}(t,x) = \min\left(\frac{\phi(x)}{\phi(\sigma_1)} e^{\rho_0 t}, 1\right).$$

Observe that $u_0(x) \leq \overline{u}(0,x)$ for all $x \in \mathbb{R}$. Let us now check that $\overline{u}$ is a supersolution of the equation (6.1) satisfied by u. Since $u \leq 1$,it is enough to check that $\overline{u}$ is a supersolution of (6.1) whenever $\overline{u} < 1$. Note that since $\phi(x)$ is nonincreasing with respect to $|x|$, $\overline{u}(t,x) < 1$ implies that $|x| > \sigma_1$. Assume that $(t,x) \in [0,+\infty) \times [\sigma_1, \infty)$ and $\overline{u}(t,x) < 1$, then it follows from (6.59) that

$$\begin{aligned}
(J \star \overline{u})(t,x) &\leq (J \star \phi)(x) \frac{e^{\rho_0 t}}{\phi(\sigma_1)} \\
&\leq \frac{\phi(x)}{\phi(\sigma_1)} e^{\rho_0 t} \int_{\mathbb{R}} J(y)/\phi(y) dy \ \cdot \\
&= \overline{u}(t,x) \int_{\mathbb{R}} J(y)/\phi(y) dy.
\end{aligned}$$

This implies that for all (t,x) such that $\overline{u}(t,x) < 1$

$$\begin{aligned}
&\overline{u}_t(t,x) - (J \star \overline{u})(t,x) + \overline{u}(t,x) - f(\overline{u}(t,x)) \\
&\geq \rho_0 \overline{u}(t,x) - (J \star \overline{u})(t,x) + \overline{u}(t,x) - r\overline{u}(t,x) \\
&\geq (\rho_0 - \int_{\mathbb{R}} J(y)/\phi(y) dy + 1 - r)\overline{u}(t,x) \\
&\geq 0,
\end{aligned} \tag{6.61}$$

from the definition of ρ_0. The parabolic maximum principle [185, 191] then implies that :

$$u(t,x) \leq \overline{u}(t,x) \leq (\phi(x)/\phi(\sigma_1)) e^{\rho_0 t}, \text{ for all } (t,x) \in [0,\infty) \times \mathbb{R}.$$

For all $t \geq t_\lambda$ (so that $E_\lambda(t)$ is not empty) and for all $x \in E_\lambda(t)$, there holds

$$(|x| < \sigma_1) \text{ or } \left(|x| \geq \sigma_1 \text{ and } \lambda = u(t,x) \leq (\phi(x)/\phi(\sigma_1)) e^{\rho_0 t}\right).$$

In all cases, we get that

$$\forall t \geq t_\lambda, \forall x \in E_\lambda(t), \phi(x) \geq \min\left(\phi(\sigma_1), \lambda \phi(\sigma_1) e^{-\rho_0 t}\right).$$

Then, from the definition of ϕ for large x, and since $J(s+\tau)/J(s) \to 1$ as $s \to \pm\infty$ for any $\rho > \rho_0/(1-\varepsilon_0)$, there exists a time $\overline{T}_\lambda \geq t_\lambda$ such that

$$\forall t \geq \overline{T}_\lambda,\ \forall x \in E_\lambda(t),\ \ J(x) \geq e^{-\rho t}, \tag{6.62}$$

which gives (6.54).

Proof of (6.54) *under Hypothesis 2* Assume that J is satisfies hypothesis 2. Since $J(x)$ is decreasing with respect to $|x|$, we get the following inequality for any $x \geq 0$:

$$\begin{aligned}
\frac{(J \star J)(x)}{J(x)} &= \int_{-\infty}^{0} \frac{J(x-y)}{J(x)} J(y) dy + \int_0^x \frac{J(x-y)J(y)}{J(x)} dy + \int_x^{+\infty} \frac{J(y)}{J(x)} J(x-y) dy \\
&\leq 1 + \int_0^{x/2} \frac{J(x-y)}{J(x)} J(y) dy + \int_{x/2}^{x} \frac{J(x-y)}{J(x)} J(y) dy \\
&\leq 1 + \frac{J(x/2)}{J(x)}.
\end{aligned} \tag{6.63}$$

From the symmetry of J, the inequality also holds for $x \leq 0$. Moreover, since J satisfies (6.12), there exists $x_0 > 0$, and $C_0 > 0$ such that

$$\ln\left(\frac{J(x/2)}{J(x)}\right) = \int_{|x|/2}^{|x|} \left|\frac{J'(s)}{J(s)}\right| ds \leq \int_{|x|/2}^{|x|} \frac{C_0}{s} ds = C_0 \ln(2) \text{ for all } |x| \geq x_0.$$

This implies that there exists $K > 0$ such that for all $x \in \mathbb{R}$,

$$\frac{(J \star J)(x)}{J(x)} \leq 1 + K. \tag{6.64}$$

Since u_0 is compactly supported, there exists $\sigma_1 > 0$ such that $J(\sigma_1) \leq 1$ and $J(x) \geq u_0(x)$, for all $|x| \geq \sigma_1$. Then, set $\rho_0 = r + K$ and for all $(t, x) \in [0, +\infty) \times \mathbb{R}$:

$$\overline{u}(t, x) = \min\left(\frac{J(x)}{J(\sigma_1)} e^{\rho_0 t}, 1\right).$$

Observe that $u_0(x) \leq \overline{u}(0, x)$ for all $x \in \mathbb{R}$. Let us now check that $\overline{u}$ is a supersolution of the equation (6.1) satisfied by u. In the region (t, x) such that $\overline{u}(t, x) = 1$, the same arguments as in section 4.3 lead to :

$$\overline{u}_t(t, x) - J \star \overline{u}(t, x) + \overline{u}(t, x) - f(\overline{u}(t, x)) \geq 1 - J \star \overline{u}(t, x) \geq 0.$$

Let us check that $\overline{u}$ is also a supersolution of (6.1) when $\overline{u} < 1$. If $t \geq 0$, $|x| \geq \sigma_1$ and $\overline{u}(t, x) < 1$ then it follows from (6.64) that

$$\begin{aligned}
(J \star \overline{u})(t, x) &\leq (J \star J)(x) \frac{e^{\rho_0 t}}{J(\sigma_1)} \\
&\leq (1 + K) \frac{J(x)}{J(\sigma_1)} e^{\rho_0 t} \\
&\leq (1 + K) \overline{u}(t, x).
\end{aligned}$$

This implies that

$$\begin{aligned}
\overline{u}_t(t, x) - (J \star \overline{u})(t, x) + \overline{u}(t, x) - f(\overline{u}(t, x)) &\geq \rho_0 \overline{u}(t, x) - (J \star \overline{u})(t, x) + \overline{u}(t, x) - r\overline{u}(t, x) \\
&\geq (\rho_0 - (1 + K) + 1 - r)\overline{u}(t, x) \\
&\geq 0.
\end{aligned} \tag{6.65}$$

The parabolic maximum principle [185, 191] implies that :

$$u(t, x) \leq \overline{u}(t, x) \leq \frac{J(x)}{J(\sigma_1)} e^{\rho_0 t}, \text{ for all } (t, x) \in [0, \infty) \times \mathbb{R}.$$

For all $t \geq t_\lambda$ (so that $E_\lambda(t)$ is not empty) and all $x \in E_\lambda(t)$, there holds

$$(|x| < \sigma_1) \text{ or } \left(|x| \geq \sigma_1 \text{ and } \lambda = u(t, x) \leq \frac{J(x)}{J(\sigma_1)} e^{\rho_0 t}\right).$$

In all cases, one gets that

$$\forall t \geq t_\lambda, \forall x \in E_\lambda(t), J(x) \geq \min\left(J(\sigma_1), \lambda J(\sigma_1) e^{-\rho_0 t}\right),$$

Then, for any $\rho > \rho_0 \geq f'(0) > 0$, there exists a time $\overline{T}_\lambda \geq t_\lambda$ such that

$$\forall t \geq \overline{T}_\lambda, \ \forall x \in E_\lambda(t), \ \ J(x) \geq e^{-\rho t}, \tag{6.66}$$

which proves (6.54). □

6.5 Discussion

We have analyzed the spreading properties of an integro-differential equation with exponentially unbounded or "fat-tailed" kernels. Since the pioneering work of Kot et al. [113], there have been few mathematical papers on integral equations with exponentially unbounded kernels. However, such slowly decaying kernels are highly relevant in the context of population dynamics with long distance dispersal events [43, 44].

We proved that for kernels J which decrease to 0 slower than any exponentially decaying function the level sets of the solution u of the problem (6.1) propagate with an infinite asymptotic speed. This first result, which could also be derived from the results in the recent paper of Weinberger and Zhao [187], shows the qualitative difference between dispersal operators with exponentially unbounded kernels and dispersal operators with exponentially bounded kernel which are known to lead to finite spreading speed [8, 54, 173, 185]. This result supports the use of "fat-tailed" dispersal kernels to model accelerating propagation or fast propagation phenomena [43, 44, 169].

Moreover, we obtained lower and upper bounds for the position of any level set of u. These bounds allowed us to estimate how the solution accelerates, depending on the kernel J : the slower the kernel decays, the faster the level sets propagate. Through several examples, we have seen in section 6.2 that the level sets of the solution of problem (6.1) move almost linearly when J is close to an exponentially bounded kernel (see example (6.15), $J(x) = Ce^{-|x|/\ln(|x|)}$ for $|x| \gg 1$) while the level sets move exponentially fast when the kernel J has a very fat-tail (see example (6.17), $J(x) = C|x|^{-\alpha}$ for $|x| \gg 1$).

It is noteworthy that our results have been derived under assumptions more general than the KPP assumption $f(s) < f'(0)s$. Indeed, results of Theorems 6, 7 and 8 hold with nonlinearities f which may take a weak Allee effect into account : the maximum of the "per capita growth rate" $f(s)/s$ is not necessarily reached at $s = 0$. In ecological models, the Allee effect can occur for various reasons [7]. For instance, at low densities individuals may have trouble finding mates. Our spreading properties in the case with a weak Allee effect are in agreement with the numerical results in [183] which show that exponentially unbounded dispersal kernels can lead to infinite spreading speeds. The conclusion is very different when the nonlinearity f takes a strong Allee effect into accounts, that is if $f(s) < 0$ for small value of s. Indeed it is proved in this case that problem (6.1) admits traveling wave solutions with constant speed [14, 41, 46]. Thus the solutions of problem (6.1) with such nonlinearities have a finite speed of propagation.

One could wonder whether the solution of problem (6.1) with exponentially unbounded kernel converges to some kind of "accelerated traveling wave solution", that is a solution $u(t, x) = \phi(x - c(t))$ where c is a superlinear function. Our numerical computations suggest that the answer is no (see Fig. 6.2 (a)) since the solutions u becomes flat at large time. The computations also suggest that the solution $u(t, x)$ is not a generalized transition wave in the sense of [21, 20]. Such a result has been proved by Hamel and Roques [88] for the solution of a reaction-diffusion problem with an exponentially unbounded initial condition. In our case, the proof seems to be more involved since the operator $u \mapsto J \star u - u$ is not a differential operator.

Bibliographie

Publications personnelles

[CGHR12] M Cristofol, J Garnier, F Hamel et L Roques : Uniqueness from pointwise observations in a multi-parameter inverse problem. *Comm. Pure Appl. Anal.*, 11:173–188, 2012.

[Ga11] J Garnier : Accelerating solutions in integro-differential equations. *SIAM J. Math. Anal.*, 43:1955–1974, 2011.

[GGHR12] J Garnier, T Giletti, F Hamel et L Roques : Inside dynamics of pulled and pushed fronts. *J. Math. Pures Appl.*, 11:173–188, 2012.

[GGN12] J Garnier, T Giletti et G Nadin : Maximal and minimal spreading speeds for reaction diffusion equations in nonperiodic slowly varying media. *J. Dyn. Differ. Equ.,* à paraître.

[GHR12] J Garnier, F Hamel et L Roques : Success rate of a biological invasion and the spatial distribution of the founding population. *Bull. Math. Bio.*, 74:453–473, 2012.

[RGHK12] L Roques, J Garnier, F Hamel et E Klein : Allee effect promotes diversity in traveling waves of colonization. *Proc. Natl. Acad. Sci. USA,* doi : 10.1073/pnas.1201695109.

Autres références

[7] W C Allee : *The Social Life of Animals.* Norton, 1938.

[8] H G Aronson : The asymptotic speed of propagation of a simple epidemic. *In Nonlinear Diffusion*, 1977.

[9] H G Aronson et D G Weinberger : Nonlinear diffusion in population genetics, combustion and nerve propagation. *In Partial Differential Equations and Related Topics*, 1975.

[10] H G Aronson et D G Weinberger : Multidimensional non-linear diffusion arising in population-genetics. *Adv. Math.*, 30(1):33–76, 1978.

[11] F Austerlitz et P H Garnier-Géré : Modelling the impact of colonisation on genetic diversity and differentiation of forest trees : interaction of life cycle, pollen flow and seed long-distance dispersal. *Heredity*, 90:282–290, 2003.

[12] F Austerlitz, S Mariette, N Machon, P H Gouyon et B Godelle : Effects of colonization processes on genetic diversity : differences between annual plants and tree species. *Genetics*, 154 (3):1309–1321, 2000.

[13] N H Barton et M Turelli : Spatial waves of advance with bistable dynamics : cytoplasmic and genetic analogues of allee effects. *Am. Nat.*, 178(3):E48–E75, 2011.

[14] P W Bates, P C Fife, X Ren et X Wang : Traveling waves in a convolution model for phase transitions. *Arch. Ration. Mech. Anal.*, 138:105–136, 1997.

[15] M Belassoued et M Yamamoto : Inverse source problem for a transmission problem for a parabolic equation. *J. Inverse Ill-Posed Probl.*, 14(1):47–56, 2006.

[16] L Berec, E Angulo et F Courchamp : Multiple allee effects and population management. *Trends Ecol. Evol.*, 22:185–191, 2007.

[17] H Berestycki, O Diekmann, C J Nagelkerke et P A Zegeling : Can a species keep pace with a shifting climate ? *Bull. Math. Bio.*, 71(2):399–429, 2009.

[18] H Berestycki et F Hamel : *Reaction-Diffusion Equations and Propagation Phenomena*. Springer, *à paraître*.

[19] H Berestycki et F Hamel : Front propagation in periodic excitable media. *Comm. Pure Appl. Math.*, 55(8):949–1032, 2002.

[20] H Berestycki et F Hamel : Generalized travelling waves for reaction-diffusion equations. *In Perspectives in Nonlinear Partial Differential Equations : in Honor of Haim Brezis*, 2007.

[21] H Berestycki et F Hamel : Generalized transition waves and their properties. *Comm. Pure Appl. Math.*, 65:592–648, 2012.

[22] H Berestycki, F Hamel et G Nadin : Asymptotic spreading in heterogeneous diffusive excitable media. *Journal of Functional Analysis*, 255(9):2146–2189, 2008.

[23] H Berestycki, F Hamel et N Nadirashvili : The speed of propagation for KPP type problems. I : Periodic framework. *J. Eur. Math. Soc.*, 7(2):173–213, 2005.

[24] H Berestycki, F Hamel et L Roques : Analysis of the periodically fragmented environment model : I - species persistence. *J. Math. Biol.*, 51(1):75–113, 2005.

[25] H Berestycki, F Hamel et L Roques : Analysis of the periodically fragmented environment model : II - biological invasions and pulsating travelling fronts. *J. Math. Pures Appl.*, 84(8):1101–1146, 2005.

[26] H Berestycki, F Hamel et L Rossi : Liouville-type results for semilinear elliptic equations in unbounded domains. *Ann. Mat. Pura Appl.*, 186(3):469–507, 2007.

[27] H Berestycki et B Larrouturou : Quelques aspects mathematiques de la propagation des flammes premelangees. *Pitman. Res.*, 220:65–129, 1991.

[28] H Berestycki et G Nadin : Spreading speeds for one-dimensional monostable reaction-diffusion equations. *preprint*.

[29] H Berestycki, B Nicolaenko et B Scheurer : Traveling wave solutions to combustion models and their singular limits. *SIAM J. Math. Anal.*, 16:1207–1242, 1985.

[30] H Berestycki et L Rossi : Reaction-diffusion equations for population dynamics with forced speed I - the case of the whole space. *Discrete Contin. Dyn. Syst.*, 21(1):41–67, 2008.

[31] R Bialozyt, B Ziegenhagen et R J Petit : Contrasting effects of long distance seed dispersal on genetic diversity during range expansion. *J. Evol. Biol.*, 19(1):12–20, 2006.

[32] J Billingham et D J Needham : The development of traveling waves in quadratic and cubic autocatalysis with unequal diffusion rates. I. Permanent form of traveling waves. *Philos. Trans. R. Soc. Lond. Ser. A*, 334:1–24, 1991.

[33] M Bramson : Convergence of solutions of the Kolmogorov equation to travelling waves. *Mem. Amer. Math. Soc.*, 44, 1983.

[34] N F Britton : *Reaction-Diffusion Equations and their Applications to Biology.* Academic Press, 1986.

[35] A L Bukhgeim et M V Klibanov : Global uniqueness of a class of multidimensional inverse problems. *Sov. Math.*, 24:244–247, 1981.

[36] X Cabré et J M Roquejoffre : The influence of fractional diffusion on Fisher-KPP equations. *preprint.*

[37] X Cabré et J M Roquejoffre : Propagation de fronts dans les équations de Fisher-KPP avec diffusion fractionnaire. *C. R. Math. Acad. Sci. Paris*, 347(23–24):1361–1366, 2009.

[38] A Carr et J Chmaj : Uniqueness of travelling waves for nonlocal monostable equations. *Proc. Amer. Math. Soc.*, 132(8):2433–2439, 2004.

[39] G Chapuisat et E Grenier : Existence and nonexistence of traveling wave solutions for a bistable reaction-diffusion equation in an infinite cylinder whose diameter is suddenly increased. *Commun. Partial Differ. Equations*, 30:1805–1816, 2005.

[40] E Chasseigne, M Chaves et J D Rossi : Asymptotic behavior for nonlocal diffusion equations. *J. Math. Pures Appl.*, 86:271–291, 2006.

[41] X Chen : Existence, uniqueness, and asymptotic stability of traveling waves in nonlocal evolution equations. *Adv. Diff. Equations*, 2:125–160, 1997.

[42] M Choulli, E M Ouhabaz et M Yamamoto : Stable determination of a semilinear term in a parabolic equation. *Comm. Pure Appl. Anal.*, 5:447–462, 2006.

[43] J S Clark : Why trees migrate so fast : Confronting theory with dispersal biology and the paleorecord. *Am. Nat.*, 152:204–224, 1998.

[44] J S Clark, C Fastie, G Hurtt, S T Jackson, C Johnson, G A King, M Lewis, J Lynch, S Pacala, C Prentice, E W Schupp, T Webb III et P Wyckoff : Reid's paradox of rapid plant migration. *BioScience*, 48:13–24, 1998.

[45] R S Cosner et C Cantrell : *Spatial Ecology via Reaction-Diffusion Equations.* John Wiley & Sons Ltd, 2003.

[46] J Coville : Travelling fronts in asymmetric nonlocal reaction diffusion equation : the bistable and ignition case. *Preprint*, 2007.

[47] J Coville et L Dupaigne : On a nonlocal reaction diffusion equation arising in population dynamics. *Proc. Roy. Soc. Edinburgh Sect. A*, 137:1–29, 2007.

[48] A Cristofol, M Gaitan, P et Yamamoto M Benabdallah : Inverse problem for a parabolic system with two components by measurements of one component. *Appl. Anal.*, 88(5):683–710, 2009.

[49] M Cristofol et L Roques : Biological invasions : Deriving the regions at risk from partial measurements. *Math. Biosci.*, 215(2):158–166, 2008.

[50] DAISIE : *Handbook of Alien Species in Europe*. Springer, 2009.

[51] DAISIE : *Alien Terrestrial Arthropods of Europe*. BioRisk 4, Volume 1 and 2. Pensoft, 2010.

[52] M B Davis et R G Shaw : Range shifts and adaptive responses to quaternary climate change. *Science*, 292(5517):673–9, 2001.

[53] B Dennis : Allee effects : population growth, critical density, and the chance of extinction. *Nat. Resour. Model.*, 3:481–538, 1989.

[54] O Diekmann : Run for your life. A note on the asymptotic speed of propagation of an epidemic. *J. Diff. Equations*, 33:58–73, 1979.

[55] A P Dobson et R M May : Patterns of invasions by pathogens and parasites. *In Ecology of Biological Invasions of North America and Hawaii*, 1986.

[56] J M Drake : Allee effects and the risk of biological invasion. *Risk Anal.*, 24:795–802, 2004.

[57] K L S Drury, J M Drake, D M Lodge et G Dwyer : Immigration events dispersed in space and time : Factors affecting invasion success. *Ecol. Model.*, 206:63–78, 2007.

[58] Y Du et H Matano : Convergence and sharp thresholds for propagation in nonlinear diffusion problems. *J. Eur. Math. Soc.*, 12:279–312.

[59] P DuChateau et W Rundell : Unicity in an inverse problem for an unknown reaction term in a reaction-diffusion equation. *J. Diff. Equations*, 59:155–164, 1985.

[60] R Durrett : Ten lectures on particle systems.

[61] J P Eckmann et C E Wayne : The nonlinear stability of front solutions for parabolic differential equations. *Comm. Math. Phys.*, 161:323–334, 1994.

[62] C A Edmonds, A S Lillie et L L Cavalli-Sforza : Mutations arising in the wave front of an expanding population. *Proc. Natl. Acad. Sci. USA.*, 101(4):975–979, 2004.

[63] H Egger, H W Engl et M Klibanov : Global uniqueness and Hölder stability for recovering a nonlinear source term in a parabolic equation. *Inverse Problems*, 21:271–290, 2005.

[64] M El Smaily, F Hamel et L Roques : Homogenization and influence of fragmentation in a biological invasion model. *Discrete Contin. Dyn. Syst.*, 25:321–342, 2009.

[65] L Excoffier, M Foll et R J Petit : Genetic consequences of range expansions. *Annu. Rev. Ecol. Evol. Syst.*, 40(1):481–501, 2009.

[66] L Excoffier et N Ray : Surfing during population expansions promotes genetic revolutions and structuration. *Trends Ecol. Evol.*, 23(7):347–351, 2008.

[67] L Fahrig : Effects of habitat fragmentation on biodiversity. *Annu. Rev. Ecol. Evol. Syst.*, 34:487–515, 2003.

[68] J Fayard, E K Klein et F Lefèvre : Long distance dispersal and the fate of a gene from the colonization front. *J. Evol. Biol.*, 22(11):2171–2182, 2009.

[69] P C Fife : Long-time behavior of solutions of bistable non-linear diffusion equations. *Arch. Ration. Mech. Anal.*, 70(1):31–46, 1979.

[70] P C Fife : *Mathematical Aspects of Reacting and Diffusing Systems.* Springer-Verlag, 1979.

[71] P C Fife et J McLeod : The approach of solutions of nonlinear diffusion equations to traveling front solutions. *Arch. Ration. Mech. Anal.*, 65:335–361, 1977.

[72] R A Fisher : The wave of advance of advantageous genes. *Ann. Eugenics*, 7:335–369, 1937.

[73] M Freidlin : On wave front propagation in periodic media. *In Stochastic analysis and applications.* Adavances in Probability and related topics, 1984.

[74] M Freidlin et J Gärtner : On the propagation of concentration waves in periodic and random media. *Sov. Math.*, 20:1282–1286, 1979.

[75] A Friedman : *Partial Differential Equations of Parabolic Type.* Prentice-Hall, 1964.

[76] M Gaitan, P Ramoul et M Cristofol : Inverse problems for a two by two reaction-diffusion system using a carleman estimate with one observation. *Inverse Problems*, 22:1561–1573, 2006.

[77] T Gallay : Ondes progressives dans les sytèmes de reaction-diffusion. *Cours École d'été de l'Institut Fourier*, 2005.

[78] R H Gardner, B T Milne, M G Turner et R V O'Neill : Neutral models for the analysis of broad-scale landscape pattern. *Landscape Ecol.*, 1:19–28, 1987.

[79] P Grindrod : *Theory and Applications of Reaction-Diffusion Equations.* Clarendon Press, 1996.

[80] K Hadeler et F Rothe : Travelling fronts in nonlinear diffusion equations. *J. Math. Biol.*, 2:251–263, 1975.

[81] O Hallatschek, P Hersen, S Ramanathan et D R Nelson : Genetic drift at expanding frontiers promotes gene segregation. *Proc. Natl. Acad. Sci. USA*, 104(50):19926–19930, 2007.

[82] O Hallatschek et D R Nelson : Gene surfing in expanding populations. *Theor. Popul. Biol.*, 73:158–170, 2008.

[83] O Hallatschek et D R Nelson : Life at the front of an expanding population. *Evolution*, 64-1:193–206, 2009.

[84] F Hamel : Reaction-diffusion problems in cylinders with no invariance by translation. Part I : Small perturbations. *Ann. Inst. H. Poincaré, Anal. Non Linéaire*, 14(4):457–498, 1997.

[85] F Hamel : Reaction-diffusion problems in cylinders with no invariance by translation. Part II : Monotone preturbations. *Ann. Inst. H. Poincaré, Anal. Non Linéaire*, 14(5):555–596, 1997.

[86] F Hamel, J Fayard et L Roques : Spreading speeds in slowly oscillating environments. *Bull. Math. Bio.*, 72:1166–1191, .

[87] F Hamel et G Nadin : Spreading properties and complex dynamics for monostable reaction-diffusion equations. *Comm. Part. Diff. Equations*.

[88] F Hamel et L Roques : Fast propagation for KPP equations with slowly decaying initial conditions. *J. Diff. Equations*, 249:1726–1745, 2010.

[89] F Hamel, L Roques et G Nadin : A viscosity solution method for the spreading speed formula in slowly varying media. *Indiana Univ. Math. J.,* à paraître, .

[90] F Harary et H Harborth : Extremal animals. *J. Comb. Inf. Syst. Sci.*, 1:1–8, 1976.

[91] D L Hartl et A G Clark : *Principles of Population Genetics*. Sinauer, 2006.

[92] A Hastings, K Cuddington, K F Davies, C J Dugaw, S Elmendorf, A Freestone, S Harrison, M Holland, J Lambrinos, U Malvadkar, B A Melbourne, K Moore, C Taylor et D Thomson : The spatial spread of invasions : new developments in theory and evidence. *Ecol. Lett.*, 8(1):91–101, 2005.

[93] D Henry : *Geometric Theory of Semilinear Parabolic Equations*. Lecture Notes in Mathematics. Springer, 1981.

[94] G M Hewitt : The genetic legacy of the quarternary ice ages. *Nature*, 405:907–913, 2000.

[95] G E Hutchinson : Circular causal systems in ecology. *Ann. NY Acad. Sci.*, 50:221–246, 1948.

[96] K M Ibrahim, R A Nichols et G M Hewitt : Spatial patterns of genetic variation generated by different forms of dispersal during range expansion. *Heredity*, 77(3):282–291, 1996.

[97] O Y Immanuvilov et M Yamamoto : Lipschitz stability in inverse parabolic problems by the Carleman estimate. *Inverse Problems*, 14:1229–1245, 1998.

[98] IUCN : *Guidelines for the Prevention of Biodiversity Loss Caused by Alien Invasive Species prepared by the Species Survival Commission (SSC) Invasive Species Specialist Group*. Approved by the 51st Meeting of the IUCN Council, Gland, 2000.

[99] IUCN : *Policy recommendations papers for sixth meeting of the Conference of the Parties to the Convention on Biological Diversity (COP6)*. The Hague, Netherlands, 2002.

[100] A R Kanarek et C T Webb : Allee effects, adaptive evolution, and invasion success. *Evol. Appl.*, 3:122–135, 2010.

[101] Ja I Kanel : Certain problem of burning-theory equations. *Dokl. Akad. Nauk SSSR*, 136:277–280, 1961.

[102] Ja I Kanel : Stabilization of solutions of the equations of combustion theory with finite initial functions. *Matematicheskii Sbornik*, 65:398–413, 1964.

[103] N Kawasaki et K Shigesada : *Biological Invasions : Theory and Practice*. Oxford University Press, 1997.

[104] T H Keitt : Spectral representation of neutral landscapes. *Landscape Ecol.*, 15:479–494, 2000.

[105] T H Keitt, M A Lewis et R D Holt : Allee effects, invasion pinning, and species' borders. *Am. Nat.*, 157:203–216, 2001.

[106] M Kenis : Insects-insecta. *In Invasive alien species in Switzerland. An inventory of alien species and their threat to biodiversity and economy in Switzerland*. Swiss Confederation - Federal Office for the Environment Environmental Studies, 2006.

[107] M Kenis, M A Auger-Rozenberg, A Roques, L Timms, C Péré, M J W Cock, J Settele, S Augustin et C Lopez-Vaamonde : Ecological effects of invasive alien insects. *Biol. Invasions*, 11(1):21–45, 2009.

[108] M Kirkpatrick et N H Barton : Evolution of a species' range. *Am. Nat.*, 150:1–23, 1997.

[109] M V Klibanov et A A Timonov : *Carleman Estimates for Coefficient Inverse Problems and Numerical Applications*. VSP, 2004.

[110] S Klopfstein, M Currat et L Excoffier : The fate of mutations surfing on the wave of a range expansion. *Mol. Biol. Evol.*, 23(3):482–490, 2006.

[111] K Kobayashi : On the semilinear heat equations with time-lag. *Hiroshima Math. J.*, 7:459–472, 1977.

[112] N S Kolmogorov, N Petrovsky et I G Piskunov : Étude de l'équation de la diffusion avec croissance de la quantité de matière et son application à un problème biologique. *Bull. Univ. Moscou, Sér A*, 1:1–26, 1937.

[113] M Kot, M Lewis et P Van den Driessche : Dispersal data and the spread of invading organisms. *Ecology*, 77:2027–2042, 1996.

[114] A M Kramer, B Dennis, A M Liebhold et J M Drake : The evidence for Allee effects. *Popul. Ecol.*, 51:341–354, 2009.

[115] D A Larson : Demographic stochasticity and allee effect on a scale with isotrophic noise. *Oikos*, 83:353–358, 1998.

[116] K S Lau : On the nonlinear diffusion equation of Kolmogorov, Petrovsky and Piscounov. *J. Diff. Equations*, 59:44–70, 1985.

[117] B Leung, J M Drake et D M Lodge : Predicting invasions : propagule pressure and the gravity of allee effects. *Ecology*, 85:1651–1660, 2004.

[118] M A Lewis et P Kareiva : Allee dynamics and the speed of invading organisms. *Theor. Popul. Biol.*, 43:141–158, 1993.

[119] M A Lewis et P Van Den Driessche : Waves of extinction from sterile insect release. *Math. Biosci.*, 116(2):221–247, 1993.

[120] A Lorenzi : An inverse problem for a semilinear parabolic equation. *Ann. Mat. Pura Appl.*, 131:145–166, 1982.

[121] M. Lucia, C B Muratov et M Novaga : Linear vs. nonlinear selection for the propagation speed of the solutions of scalar reaction-diffusion equations invading an unstable equilibrium. *Comm. Pure Appl. Math*, 57:616–636, 2004.

[122] F Lutscher : A short note on short dispersal events. *Bull. Math. Bio.*, 69:1615–1630, 2007.

[123] F Lutscher : Density-dependent dispersal in integrodifference equations. *J. Math. Biol.*, 56:499–524, 2008.

[124] F Lutscher, E Pachepsky et M Lewis : The effect of dispersal patterns on stream population. *SIAM J. Appl. Math.*, 65(4):1305–1327, 2005.

[125] J F Mallordy et J M Roquejoffre : A parabolic equation of the KPP type in higher dimensions. *SIAM J. Math. Anal.*, 26(1):1–20, 1995.

[126] H Matano, K I Nakamura et B Lou : Periodic traveling waves in a two-dimensional cylinder with saw-toothed boundary and their homogenization limit. *Netw. Heterog. Media*, 1:537–568, 206.

[127] E Mayr : *Systematics and the Origin of Species from the Viewpoint of a Zoologist*. Columbia University Press, 1942.

[128] M A McCarthy : The allee effect, finding mates and theoretical models. *Ecol. Model.*, 103 (1):99–102, 1997.

[129] J Medlock et M Kot : Spreading disease : Integro-differential equations old and new. *Math. Biosci.*, 184(2):201–222, 2003.

[130] A Mellet, J-M Roquejoffre et Y Sire : Generalized fronts for one-dimensional reaction-diffusion equations. *Discrete And Continuous Dynamical Systems*, 26(1):303–312, 2009.

[131] D Mollison : Long-distance dispersal of wind-borne organisms. *manuscript*, 1977.

[132] D Mollison : Spatial contact models for ecological and epidemic spread. *J. R. Stat. Ser. B Stat. Methodol.*, 39:283–326, 1977.

[133] D Mollison : Markovian contact process. *Adv. Appl. Prob.*, 10:85–108, 1978.

[134] C B Muratov et M Novaga : Front propagation in infinite cylinders. I. A variational approach. *Comm. Math. Sci.*, 6:799–826, 2008.

[135] J D Murray : *Mathematical Biology*. Springer-Verlag, 2002.

[136] G Nadin et L Rossi : Propagation phenomena for time heterogeneous KPP reaction-diffusion equations. *J. Math. Pures Appl.*, 2012.

[137] S I Nakamura : A note on uniqueness in an inverse problem for a semilinear parabolic equation. *Nihonkai Math. J*, 12:71–73, 2001.

[138] C Neuhauser : Mathematical challenges in spatial ecology. *Not. AMS*, 48:1304–1314, 2001.

[139] J Nolen, J-M Roquejoffre, L Ryzhik et A Zlatoš : Existence and non-existence of Fisher-KPP transition fronts. *Arch. Ration. Mech. Anal.*, 203:217–246, 2012.

[140] J Nolen et J Xin : Asymptotic spreading of KPP reactive fronts in incompressible space-time random flows. *Ann. Inst. H. Poincaré, Anal. Non Linéaire*, 26(3):815–839, 2008.

[141] C V Pao : *Nonlinear Parabolic and Elliptic Equations*. Plenum Press, 1992.

[142] A Pazy : *Semigroup of Linear Operators and Applications to Partial Differential Equations*. Springer-Verlag, 1983.

[143] C P Pease, R Lande et J J Bull : A model of population growth, dispersal and evolution in a changing environment. *Ecology*, 70:1657–1664, 1989.

[144] M S Pilant et W Rundell : An inverse problem for a nonlinear parabolic equation. *Comm. Partial Diff. Equations*, 11:445–457, 1986.

[145] A R Pluess : Pursuing glacier retreat : genetic structure of a rapidly expanding larix decidua population. *Mol. Ecol.*, 20(3):473–485, 2011.

[146] P Poláčik : Threshold solutions and sharp transitions for nonautonomous parabolic equations on r^n. *Arch. Ration. Mech. Anal.*, 199(1):69–97, 2011.

[147] M H Protter et H F Weinberger : *Maximum Principles in Differential Equations*. Prentice-Hall, 1967.

[148] S Ramachandran, O Deshpande, C C Roseman, N A Rosenberg, M W Feldman et L L Cavalli-Sforza : Support from the relationship of genetic and geographic distance in human populations for a serial founder effect originating in africa. *Proc. Natl. Acad. Sci. USA*, 102 (44):15942–15947, 2005.

[149] C Reid : *The Origin of the British Flora*. Dulau & Co, 1899.

[150] D M Richardson, P Pŷsek, M Rejmánek, M G Barbour, F Dane Panetta et C J West : Naturalization and invasion of alien plants : concepts and definitions. *Diversity Distrib.*, 6:93–107, 2000.

[151] A Roques, W Rabitsch, J Y Rasplus, C Lopez-Vaamonde, W Nentwig et M Kenis : *Alien terrestrial invertebrates of Europe*. Springer, 2009.

[152] L Roques : Study of the premixed flame model with heat losses the existence of two solutions. *European J. Appl. Math.*, 16(Part 6):741–765, 2005.

[153] L Roques et M D Chekroun : On population resilience to external perturbations. *SIAM J. Appl. Math.*, 68(1):133–153, 2007.

[154] L Roques et M D Chekroun : Does reaction-diffusion support the duality of fragmentation effect ? *Ecol. Complex.*, in press, 2010.

[155] L Roques et M Cristofol : On the determination of the nonlinearity from localized measurements in a reaction-diffusion equation. *Nonlinearity*, 23:675–686, 2010.

[156] L Roques et F Hamel : Mathematical analysis of the optimal habitat configurations for species persistence. *Math. Biosci.*, 210(1):34–59, 2007.

[157] L Roques, F Hamel, J Fayard, B Fady et E K Klein : Recolonisation by diffusion can generate increasing rates of spread. *Theor. Popul. Biol.*, 77:205–212, 2010.

[158] L Roques, A Roques, H Berestycki et A Kretzschmar : A population facing climate change : joint influences of allee effects and environmental boundary geometry. *Popul. Ecol.*, 50 (2):215–225, 2008.

[159] L Roques et R S Stoica : Species persistence decreases with habitat fragmentation : an analysis in periodic stochastic environments. *J. Math. Biol.*, 55(2):189–205, 2007.

[160] N A Rosenberg, J K Pritchard, J L Weber, H M Cann, K K Kidd, L A Zhivotovsky et M W Feldman : Genetic structure of human populations. *Science*, 298(5602):2381–2385, 2002.

[161] F Rothe : Convergence to pushed fronts. *Rocky Mountain J. Math.*, 11:617–634, 1981.

[162] J Rousselet, R Zhao, D Argal, M Simonato, A Battisti, A Roques et C Kerdelhué : The role of topography in structuring the demographic history of the pine processionary moth, *Thaumetopoea pityocampa* (lepidoptera : Notodontidae). *J. Biogeogr.*, 37:1478–1490, 2010.

[163] D H Sattinger : On the stability of waves of nonlinear parabolic systems. *Adv. Math.*, 22:312–355, 1976.

[164] D H Sattinger : Weighted norms for the stability of traveling waves. *J. Diff. Equations*, 25:130–144, 1977.

[165] K W Schaaf : Asymptotic behavior and traveling wave solutions for parabolic functional differential equations. *Trans. Amer Math Soc.*, 302:587–615, 1987.

[166] K Schumacher : Travelling-front solutions for integro-differential equations. I. *J. Reine Angew. Math.*, 316:54–70, 1980.

[167] W Shen : Traveling waves in diffusive random media. *J. Dynamics and Diff. Eqns.*, 16:1011–1060, 2004.

[168] E Shigesada, N Kawasaki et K Teramoto : Traveling periodic-waves in heterogeneous environments. *Theor. Popul. Biol.*, 30(1):143–160, 1986.

[169] J G Skellam : Random dispersal in theoretical populations. *Biometrika*, 38:196–218, 1951.

[170] S Soubeyrand, L Held, M Hohle et I Sache : Modelling the spread in space and time of an airborne plant disease. *J. R. Stat. Ser. C Appl. Stat.*, 57:253–272, 2008.

[171] S Soubeyrand, S Neuvonen et A Penttinen : Mechanical-statistical modeling in ecology : from outbreak detections to pest dynamics. *Bull. Math. Bio.*, 71:318–338, 2009.

[172] A N Stokes : On two types of moving front in quasilinear diffusion. *Math. Biosci.*, 31:307–315, 1976.

[173] H R Thieme : Density-dependent regulation of spatially distributed populations and their asymptotic speed of spread. *J. Math. Biol.*, 8:173–187, 1979.

[174] J M J Travis, T Münkemüller, O J Burton, A Best, C Dytham et K Johst : Deleterious mutations can surf to high densities on the wave front of an expanding population. *Mol. Biol. Evol.*, 24(10):2334–2343, 2007.

[175] P Turchin : *Quantitative Analysis of Movement : Measuring and Modeling Population Redistribution in Animals and Plants*. Sinauer Associates, 1998.

[176] A M Turing : The chemical basis of morphogenesis. *Phil. Trans. R. Soc. B*, 237:37–72, 1952.

[177] K Uchiyama : The behaviour of solutions of some non-linear diffusion equations for large time. *J. Math. Kyoto Univ.*, 18(3):453–508, 1978.

[178] W van Saarloos : Front propagation into unstable states. *Phys. Rep.*, 386:29–222, 2003.

[179] R R Veit et M A Lewis : Dispersal, population growth, and the Allee effect : dynamics of the house finch invasion of eastern north america. *Am. Nat.*, 148:255–274, 1996.

[180] M Vilà, C Basnou, P Pyšek, M Josefsson, P Genovesi, S Gollasch, W Nentwig, S Olenin, A Roques, D Roy, P E Hulme et DAISIE partners : How well do we understand the impacts of alien species on ecosystem services ? A pan-European cross-taxa assessment. *Front. Ecol. Environ.*, 2009.

[181] M O Vlad, L L Cavalli-Sforza et J Ross : Enhanced (hydrodynamic) transport induced by population growth in reaction-diffusion systems with application to population genetics. *Proc. Natl. Acad. Sci. USA*, 101(28):10249–10253, 2004.

[182] G-R Walther, A Roques, P E Hulme, M T Sykes, P Pyšek, I Kűhn, M Zobel, S Bacher, Z Botta-Dukát, H Bugmann, B Czúcz, J Dauber, T Hickler, V Jarošík, M Kenis, S Klotz, D Minchin, M Moora, W Nentwig, J Ott, V E Panov, B Reineking, C Robinet, V Semenchenko, W Solarz, W Thuiller, M Vilà, K Vohland et J Settele : Alien species in a warmer world : risks and opportunities. *Trends Ecol. Evol.*, 24(12):686–693, 2009.

[183] M-H Wang, M Kot et M G Neubert : Integrodifference equations, allee effects and invasions. *J. Math. Biol.*, 44:150–168, 2002.

[184] D Wegmann, M Currat et L Excoffier : Molecular diversity after a range expansion in heterogeneous environments. *Genetics*, 174(4):2009–2020, 2006.

[185] H F Weinberger : Long-time behavior of a class of biological models. *SIAM J. Math. Anal.*, 13(3):353–396, 1982.

[186] H F Weinberger : On spreading speeds and traveling waves for growth and migration in periodic habitat. *J. Math. Biol.*, 45:511–548, 2002.

[187] H F Weinberger et X Q Zhao : An extension of the formula for spreading speeds. *Math. Biosci. Eng.*, 7(1):187–194, 2010.

[188] C K Wikle : Hierarchical models in environmental science. *International Statistical Review*, 71:181–199, 2003.

[189] F A Williams : *Combustion Theory*. Benjamin Cummings, 1985.

[190] J Xin : Front propagation in heterogeneous media. *SIAM Review*, 42:161–230, 2000.

[191] H Yagisita : Existence and nonexistence of travelling waves for a nonlocal monostable equation. *Publ. RIMS, Kyoto Univ.*, 45:925–953, 2009.

[192] M Yamamoto et J Zou : Simultaneous reconstruction of the initial temperature and heat radiative coefficient. *Inverse Problems*, 17:1181–1202, 2001.

[193] T Yamanaka et A M Liebhold : Mate-location failure, the allee effect, and the establishment of invading populations. *Popul. Ecol.*, 51:337–340, 2009.

[194] Ya. B. Zel'dovich, G I Barenblatt, V B Librovich et G M Makhviladze : *The Mathematical Theory of Combustion and Explosions*. Consultants Bureau, 1985.

[195] A Zlatŏs : Sharp transition between extinction and propagation of reaction. *J. Amer. Math. Soc.*, 19:251–263, 2006.

Résumé

Cette thèse porte sur l'analyse mathématique de modèles de réaction-dispersion de la forme $\partial_t u = \mathcal{D}(u) + f(x,u)$. L'objectif est de comprendre l'influence du terme de réaction f, de l'opérateur de dispersion $\mathcal{D}$, et de la donnée initiale u_0 sur la propagation des solutions de ces équations. Nous nous sommes intéressés principalement à deux types d'équations de réaction-dispersion : les équations de réaction-diffusion où l'opérateur de dispersion différentielle est $\mathcal{D} = \partial_x^2$ et les équations intégro-différentielles pour lesquelles $\mathcal{D}$ est un opérateur de convolution, $\mathcal{D}(u) = J \star u - u$. Dans le cadre des équations de réaction-diffusion en milieu homogène, nous proposons une nouvelle approche plus intuitive concernant les notions de fronts progressifs tirés et poussés. Cette nouvelle caractérisation nous a permis de mieux comprendre d'une part les mécanismes de propagation des fronts et d'autre part l'influence de l'effet Allee, correspondant à une diminution de la fertilité à faible densité, lors d'une colonisation. Ces résultats ont des conséquences importantes en génétique des populations. Dans le cadre des équations de réaction-diffusion en milieu hétérogène, nous avons montré sur un exemple précis comment la fragmentation du milieu modifie la vitesse de propagation des solutions. Enfin, dans le cadre des équations intégro-différentielles, nous avons montré que la nature sur- ou sous-exponentielle du noyau de dispersion J modifie totalement la vitesse de propagation. Plus précisément, la présence de noyaux de dispersion à queue lourde ou à décroissance sous-exponentielle entraîne l'accélération des lignes de niveaux de la solution u.

Mots-clés : réaction-diffusion ; fronts ; problèmes inverses ; milieu hétérogène ; intégro-diférentielles ; dispersion à longue distance ; noyau de dispersion ; fragmentation ; monostable ; bistable

Abstract

This thesis deals with the mathematical analysis of reaction-dispersion models of the form $\partial_t u = \mathcal{D}(u) + f(x,u)$. We investigate the influence of the reaction term f, the dispersal operator $\mathcal{D}$ and the initial datum u_0 on the propagation of the solutions of these reaction-dispersion equations. We mainly focus on two types of equations : reaction-diffusion equations ($\mathcal{D} = \partial_x^2$) and integro-differential equations ($\mathcal{D}$ is a convolution operator, $\mathcal{D}(u) = J \star u - u$). We first investigate the homogeneous reaction-diffusion equations. We provide a new and intuitive explanation of the notions of pushed and pulled traveling waves. This approach allows us to understand the inside dynamics the traveling fronts and the impact of the Allee effect, that is a low fertility at low density, during a colonisation. Our results also have important consequences in population genetics. In the more general and realistic framework of heterogeneous reaction-diffusion equations, we exhibit examples where the fragmentation of the media modifies the spreading speed of the solution. Finally, we investigate integro-differential equations and prove that *fat-tailed* dispersal kernels J, that is kernels which decay slower than any exponentially decaying function at infinity, lead to acceleration of the level sets of the solution u.

Keywords : reaction-diffusion ; traveling waves ; inverse problems ; heterogeneous media ; integro-differential equations ; long distance dispersal ; dispersal kernels ; fragmentation ; monostable ; bistable